

FINAL REPORT

Friction Bearing Design of Steel H-Piles

Project IA-H3, FY 94

Report No. ITRC FR 94-5

Prepared by

James H. Long
and

Massimo Maniaci
Department of Civil Engineering
University of Illinois at Urbana-Champaign
Urbana, Illinois

December 2000

Illinois Transportation Research Center
Illinois Department of Transportation

ILLINOIS TRANSPORTATION RESEARCH CENTER

This research project was sponsored by the State of Illinois, acting by and through its Department of Transportation, according to the terms of the Memorandum of Understanding established with the Illinois Transportation Research Center. The Illinois Transportation Research Center is a joint Public-Private-University cooperative transportation research unit underwritten by the Illinois Department of Transportation. The purpose of the Center is the conduct of research in all modes of transportation to provide the knowledge and technology base to improve the capacity to meet the present and future mobility needs of individuals, industry and commerce of the State of Illinois.

Research reports are published throughout the year as research projects are completed. The contents of these reports reflect the views of the authors who are responsible for the facts and the accuracy of the data presented herein. The contents do not necessarily reflect the official views or policies of the Illinois Transportation Research Center or the Illinois Department of Transportation. This report does not constitute a standard, specification, or regulation.

Neither the United States Government nor the State of Illinois endorses products or manufacturers. Trade or manufacturers' names appear in the reports solely because they are considered essential to the object of the reports.

Illinois Transportation Research Center Members

**Bradley University
DePaul University
Eastern Illinois University
Illinois Department of Transportation
Illinois Institute of Technology
Lewis University
Northern Illinois University
Northwestern University
Southern Illinois University Carbondale
Southern Illinois University Edwardsville
University of Illinois at Chicago
University of Illinois at Urbana-Champaign
Western Illinois University**

Reports may be obtained by writing to the administrative offices of the Illinois Transportation Research Center at Southern Illinois University Edwardsville, Campus Box 1803, Edwardsville, IL 62026 [telephone (618) 650-2972], or you may contact the Engineer of Physical Research, Illinois Department of Transportation, at (217) 782-6732.

IDOT ITRC 1-5-38911

**FRICTION BEARING DESIGN OF
STEEL H-PILES**

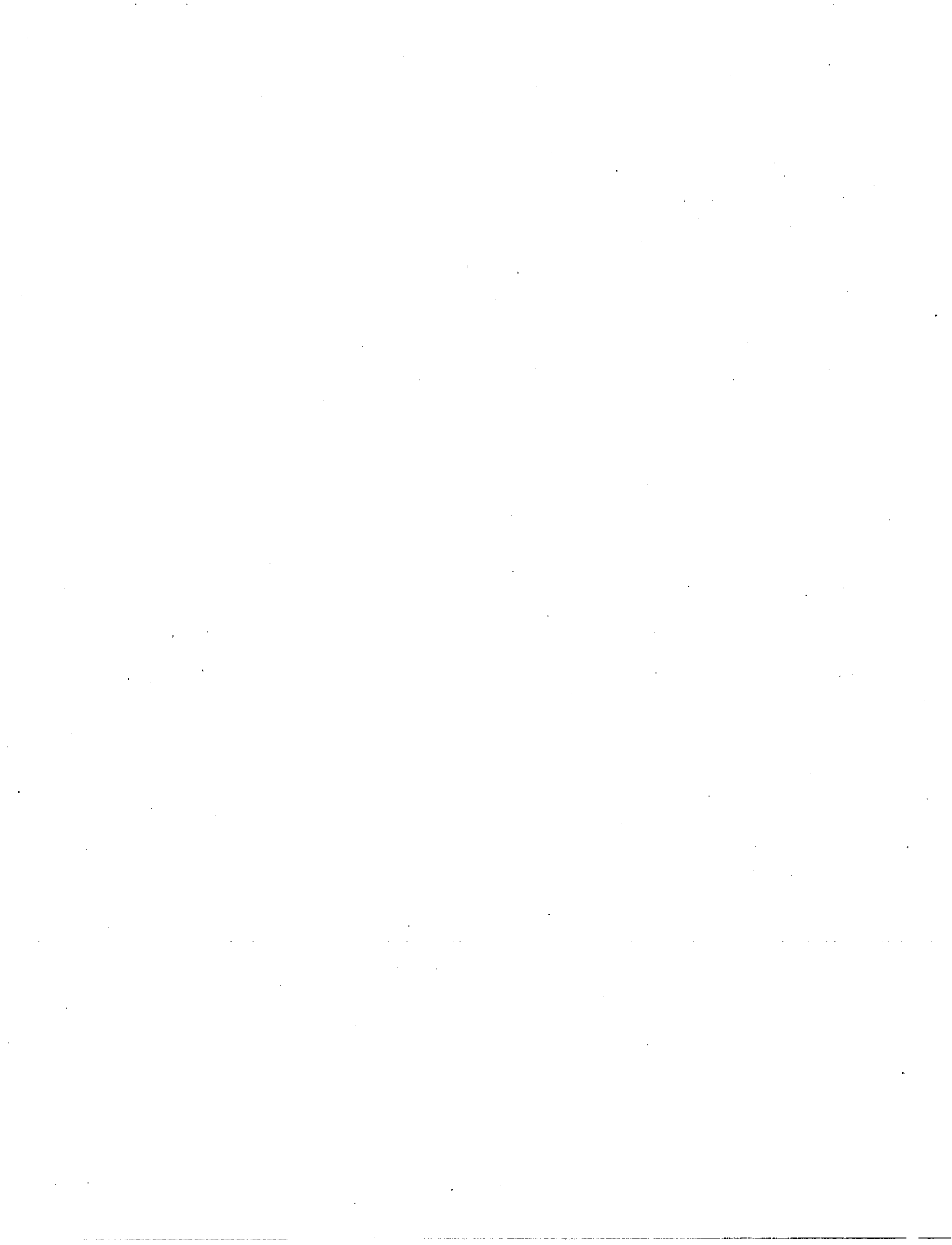
Final Project Report submitted by:
Associate Professor James H. Long
Graduate Research Assistant Massimo Maniaci
Department of Civil and Environmental Engineering
University of Illinois at Urbana-Champaign
205 North Mathews
Urbana, Illinois 61801-2352

Final Report submitted:
Illinois Transportation Research Center
Engineering Building, Room 3026
Southern Illinois University at Edwardsville
Edwardsville, IL 62026-1803

December 2000



1. Report No. ITRC FR 94-5	2. Government Accession No.	3. Recipient's Catalog No.	
4. Title and Subtitle Friction Bearing Design of Steel H-Piles		5. Report Date December 2000	6. Performing Organization Code
7. Author(s) James H. Long and Massimo Maniaci		8. Performing Organization Report No.	
9. Performing Organization Name and Address Department of Civil and Environmental Engineering University of Illinois at Urbana-Champaign 205 N. Mathews Ave. Urbana, IL 61801		10. Work Unit No. (TRAIIS)	
12. Sponsoring Agency Name and Address Illinois Transportation Research Center, Administrative Office Southern Illinois University at Edwardsville Engineering Building, Room 3026, Edwardsville, IL 62026		11. Contract or Grant No. IA-H3, FY94	13. Type of Report and Period Covered Final Report August 1995 through June 2000
15. Supplementary Notes		14. Sponsoring Agency Code	
16. Abstract <p>Improved methods for the design and construction of pile foundations can reduce significantly the cost of installation and materials by requiring fewer or shorter piles, and by providing better information on the resistance of the pile during driving. However, some of these methods may require greater computational effort, expense, and time to determine pile capacities more accurately. There are additional concerns that steel H-piles that act primarily in friction may exhibit different behavior than other piles.</p> <p>The objective of this study is to develop better procedures for predicting the axial capacity of driven piles in general, with an additional objective to determine if H-piles require special consideration. This objective was addressed by: 1) collecting, studying, and analyzing data collected on pile driving, and 2) comparing several methods for predicting the axial capacity of piles with several predictive methods such as the Engineering News formula, the Gates formula, WEAP, the Measured Energy (ME) approach, PDA, and CAPWAP. Methods for predicting the axial capacity of piles are compared with results of full-scale load tests from database collections and from load tests conducted in Jacksonville, Illinois</p> <p>The purpose of this project was to collect and analyze information on axial capacity of piles, to provide a means to assess the methods' accuracy, and to determine factors of safety appropriate for each predictive method. The predictive methods are ranked in terms of accuracy and efficiency for determining pile capacity.</p>			
17. Key Words Axial capacity, database, dynamic formulae, dynamic monitoring, factor of safety, H-pile, load test, piles capacity, pile driving, reliability, time effects, wave equation		18. Distribution Statement No restriction. This document is available to the public through the National Technical Information Services (NTIS), Springfield, Virginia 22161.	
19. Security Classification (of this report) Unclassified	20. Security Classification (of this page) Unclassified	21. No. of Pages 284	22. Price



ABSTRACT

The Illinois Department of Transportation is active in the design and the review of design of piles. Current design procedures employed by IDOT are under review. Improved methods for the design and construction of pile foundations can reduce significantly the cost of installation and materials by requiring fewer or shorter piles, and by providing better information on the resistance of the pile during driving. However, some of these methods may require greater computational effort, expense, and time to determine pile capacities more accurately. There are also concerns that current methods may not be suitable for driving steel H-piles that act primarily in friction.

The objective of this study is to develop better procedures for predicting the axial capacity of driven piles in general, with an additional objective to determine if H-piles require special consideration. This objective was addressed by: 1) collecting, studying, and analyzing data collected on pile driving, and 2) comparing several methods for predicting the axial capacity of piles with several predictive methods such as the Engineering News formula, the Gates formula, WEAP, the Measured Energy (ME) approach, PDA, and CAPWAP. Methods for predicting the axial capacity of piles are compared with results of full-scale load tests from database collections and from load tests conducted in Jacksonville, Illinois.

The purpose of this project was to collect and analyze information on axial capacity of piles, to provide a means to assess the methods' accuracy, and to determine factors of safety appropriate for each predictive method. The predictive methods are ranked in terms of accuracy and efficiency for determining pile capacity.

TABLE OF CONTENTS

<u>Chapter/Appendix</u>	<u>Page</u>
LIST OF TABLES	vii
LIST OF FIGURES	ix
EXECUTIVE SUMMARY	xiii
ACKNOWLEDGEMENTS	xvi
1.0 INTRODUCTION	1
2.0 METHODS FOR PREDICTING AXIAL PILE CAPACITY	3
INTRODUCTION	3
ESTIMATES USING STATIC METHODS	4
<i>SPILE</i>	4
Point Resistance	5
Shaft Resistance	6
ESTIMATES USING DYNAMIC FORMULAE	9
<i>The Engineering News (EN) Formula</i>	9
<i>Gates Formula</i>	10
<i>Wave Equation Analysis</i>	11
ESTIMATES USING PILE DRIVING ANALYZER	12
<i>PDA (Pile Driving Analyzer)</i>	12
<i>The Measured Energy Method</i>	13
<i>CAPWAP (CASE Pile Wave Analysis Program)</i>	15
SUMMARY	15
3.0 COLLECTION OF LOAD TESTS	32
INTRODUCTION	32
DATABASE FROM OLSON AND DENNIS	32
<i>Cohesionless Soils</i>	33
<i>Cohesive Soils</i>	34
FLAATE, 1964	35
OLSON AND FLAATE, 1967	35
<i>Original Gates Equation</i>	36
<i>Modified Gates Equation (Olson and Flaate)</i>	36
<i>Modified Gates Equation (USDOT)</i>	36
FRAGASZY ET AL. 1988, 1989	37
PAIKOWSKY ET AL., 1994	37
DAVIDSON ET AL, 1996	38
ESLAMI, 1996	38
DATABASE FROM FHWA	38
SUMMARY	39
4.0 METHODS TO COMPARE PREDICTED AND MEASURED CAPACITY	57

INTRODUCTION	57
DETAILS OF DATASET	57
PREDICTED VERSUS MEASURED PLOTS	58
STATISTICAL INTERPRETATION FOR PREDICTIVE METHODS	59
<i>Definition of Bias and Precision</i>	59
<i>Bias and Precision for Load Test Data</i>	60
<i>Cumulative Distribution</i>	61
SUMMARY	62
5.0 LOAD TEST DATABASES – PREDICTED VS. MEASURED BEHAVIOR	68
INTRODUCTION	68
FLAATE, 1964	68
<i>EN formula</i>	68
Details of EN formula used by Flaate	69
Statistics for EN method	69
<i>Hiley and Janbu methods</i>	70
<i>Gates method</i>	70
<i>Important Details of the Pile Load Test Database</i>	70
OLSON AND FLAATE, 1967	72
FRAGASZY ET AL. 1988, 1989	73
PAIKOWSKY ET AL. 1994	74
DAVIDSON ET AL., 1996	76
ESLAMI, 1996	77
DATABASE FROM FHWA	78
<i>EOD conditions</i>	78
<i>BOR conditions</i>	78
<i>Static formulas</i>	79
SUMMARY	79
6.0 ANALYSES OF LOAD TEST DATABASES	98
INTRODUCTION	98
EFFECT OF USING BOR VERSUS EOD	98
OBSERVATIONS OF BIAS AND SCATTER FOR SPECIFIC METHODS	100
<i>EN Formula</i>	101
<i>Gates Formula</i>	102
<i>WEAP Method of Analysis</i>	102
<i>Measured Energy (ME) Method</i>	103
<i>PDA Method</i>	104
<i>CAPWAP Method</i>	105
<i>Static Method</i>	106
MODIFIED GATES	107
<i>Dataset Created for Study of Gates Method</i>	108
<i>Modified Gates (with Linear Correction Factor)</i>	108
<i>Modified Gates (with Power Function for Correction Factor)</i>	110
H-PILES	111
<i>Flaate Database</i>	111

<i>Fragaszy Database</i>	112
<i>FHWA Database</i>	113
AGREEMENT OF JACKSONVILLE RESULTS WITH DATABASES	114
SUMMARY: BIAS AND SCATTER	114
<i>EN formula</i>	115
<i>Gates and Modified Gates</i>	115
<i>WEAP</i>	116
<i>ME Approach</i>	116
<i>PDA Method</i>	116
<i>CAPWAP Method</i>	117
EOD	121
7.0 SAFETY FACTORS AND WASTED CAPACITY	146
INTRODUCTION	146
GLOBAL FACTOR OF SAFETY AND PILE RELIABILITY	146
CUMULATIVE DISTRIBUTION TO ASSESS LEVELS OF RELIABILITY	147
DETERMINING FACTOR OF SAFETY	147
<i>Illustration of Methodology with EN Formula</i>	148
<i>Back-calculation of FS required for Load Test</i>	148
<i>Factors of Safety for Predictive Methods using EOD</i>	148
<i>Factors of Safety for Predictive Methods using BOR</i>	151
EFFICIENCY OF PREDICTIVE METHODS	152
SUMMARY	154
8.0 SUMMARY AND CONCLUSIONS	159
SUMMARY	159
CONCLUSIONS OVERALL OBSERVATIONS OF BIAS AND SCATTER	160
<i>EN formula</i>	160
<i>Gates and Modified Gates</i>	161
<i>WEAP</i>	161
<i>ME Approach</i>	161
<i>PDA Method</i>	162
<i>CAPWAP Method</i>	162
DISCUSSION AND LIMITATIONS	162
9.0 REFERENCES	164
APP. A DETAILS OF JACKSONVILLE SITE	169
INTRODUCTION	169
SITE LOCATION	169
SITE CHARACTERIZATION	169
<i>Subsurface Investigation Program</i>	169
<i>Soil Profile</i>	170
<i>Soil Exploration Results</i>	171
PILE DRIVING	172
<i>Installation & Equipment</i>	172

Pile Driving Criteria	173
<i>Driving Schedule & Results</i>	173
PILE TESTING PROGRAM	175
<i>Static Load Test</i>	175
Equipment & Setup	175
Procedure	176
Results	176
<i>Dynamic Load Test</i>	176
PDA Results	177
CAPWAP Results	177
OTHER LOAD CAPACITY PREDICTIONS	178
<i>Dynamic Formulae</i>	178
Engineering News (EN) formula	179
Gates formula	180
<i>WEAP (Wave Equation Analysis of Pile Driving)</i>	180
Input Parameters	181
Results	182
APP. B MEASURED TIME EFFECTS FOR AXIAL CAPACITY OF DRIVEN PILING	230
INTRODUCTION	230
LITERATURE REVIEW	230
<i>Dissipation of Excess Pore Pressure</i>	231
Clays	231
Sands	232
<i>Aging</i>	233
<i>Empirical Relationships</i>	233
<i>Other Observations</i>	234
SUMMARY RELATIONSHIPS FOR DATABASE	234
<i>Some Specific Observations</i>	235
<i>Summary Relationships for Piles in each Soil Type</i>	235
Clay	236
Sand	236
Mixed Soil Profile	237
DISCUSSION	238
SUMMARY AND CONCLUSIONS	239
ACKNOWLEDGMENTS	239
REFERENCES	240
APP. C STATISTICS FOR INTERPRETING Q_p/Q_M DATA	253
INTRODUCTION	253
<i>Definitions</i>	253
ESTIMATING THE POPULATION MEAN	254
<i>Theory</i>	254
<i>Example Problem</i>	255
SIGNIFICANT DIFFERENCE BETWEEN TWO MEANS	256
<i>Theory</i>	256

<i>Example Problem</i>	257
ESTIMATING THE POPULATION VARIANCE	258
<i>Theory</i>	258
<i>Example Problem</i>	260
SIGNIFICANT DIFFERENCE BETWEEN TWO VARIANCES	261
<i>Theory</i>	261
<i>Example Problem</i>	262
REFERENCES	263

LIST OF TABLES

<u>Table</u>	<u>Page</u>
3.1 Load Test Data used by Flaate (1964) and by Olson and Flaate (1967)	40
3.2 Load Test Data used from Fragaszy (1988)	42
3.3 Load Test Data from Paikowsky et al. (1994)	43
3.4 Load Test Data from Florida DOT (Davidson et al., 1996)	46
3.5 Load Test Data from Eslami (1996)	47
3.6 Load Test Data using EOD information, from Rausche et al. (1996)	49
3.7 Load Test Data using BOR information, from Rauschce et al. (1996)	53
4.1 Fictitious Load Test Data used for illustration	47
4.2 Statistical parameters for Q_p/Q_m values from Table 4.1	63
4.3 Load Test Data for cumulative distribution plot for method A	64
5.1 Statistical parameters for Q_p/Q_m values for all Load Test Data from Flaate (data shown in Fig. 5.1)	81
5.2 Statistical parameters for Q_p/Q_m values from Fragaszy (load test data shown in Fig. 5.2)	81
5.3 Statistical parameters for Q_p/Q_m values from Paikowsky et al. (1994) (load test data shown in Fig. 5.3)	81
5.4 Statistical parameters for Q_p/Q_m values from Davidson et al. (1996) (load test data shown in Fig. 5.4)	82
5.5 Statistical parameters for Q_p/Q_m values from Eslami (1996) (load test data shown in Fig. 5.5)	82
5.6 Statistical parameters for Q_p/Q_m values from Fig. 5.6a – 5.6f (1994) (from FHWA database)	83
6.1 Statistical parameters for Q_p/Q_m values from FHWA database for comparison of EOD versus BOR	118
6.2 Statistical parameters for Q_p/Q_m values using FHWA database. Load tests are filtered so that all tests are able to be predicted for either EOD or BOR	118
6.3 Statistical parameters for Q_p/Q_m values for EOD and BOR conditions for all databases in which statistical values for EN formula could be determined	119
6.4 Statistical parameters for Q_p/Q_m values for EOD and BOR conditions for all databases in which statistical values for Gates formula could be determined	119
6.5 Statistical parameters for Q_p/Q_m values for EOD and BOR conditions for all databases in which statistical values for WEAP could be determined	120
6.6 Statistical parameters for Q_p/Q_m values for EOD and BOR conditions for all databases in which statistical values for ME could be determined	120
6.7 Statistical parameters for Q_p/Q_m values for EOD and BOR conditions for all databases in which statistical values for PDA could be determined	121
6.8 Statistical parameters for Q_p/Q_m values for EOD and BOR conditions for all databases in which statistical values for CAPWAP could be determined	121

6.9	Statistical parameters for Q_p/Q_m values for static methods using cone results and other static methods	122
6.10	Statistical parameters for Q_p/Q_m values for Original Gates method and the two modified Gates methods	122
6.11	Statistical parameters for all piles compared with only H-piles using Olson and Flaate data	123
6.12	Statistical parameters for all piles compared with only H-piles using load test data from Fragaszy	123
6.13	Statistical parameters for all piles compared with only H-piles using FHWA data	124
7.1	Global factors of safety calculated for predictive methods using EOD	155
7.2	Global factors of safety calculated for predictive methods using BOR	156
7.3	Summary of representative factors of safety	157
7.4	Summary of representative factors of safety and wasted capacity index	157
A.1	Pile Driving Record, Pile DTP-1	183
A.2	Pile Driving Record, Pile DTP-2	185
A.3	Pile Driving Record, Pile SLTP	187
A.4	Load-displacement data for test 1 (SLT-1)	189
A.5	Load-displacement data for test 2 (SLT-2)	191
A.6	Summary of Dynamic Testing Field Results Jacksonville Load Test Program, Jacksonville, Illinois	194
A.7	Summary of CAPWAP Analysis Results, Jacksonville Load Test Program, Jacksonville, Illinois	195
A.8	Dynamic load test results	196
A.9	Summary of WEAP input variables used in this study	197
A.10	WEAP Output Data for test pile SLTP-1	199
A.11	WEAP Output Data for test pile SLTP-2	201
B.1	Empirical formulae for predicting pile capacities with time	243
B.2	Load test database used for time-dependent capacity	244
C.1	Student's t-distribution	262
C.2a	Chi-squared (χ^2) table for upper-bound estimates	263
C.2b	Chi-squared (χ^2) table for lower-bound estimates	264
C.3a	F-distribution values for the upper 10 percent	265
C.3b	F-distribution values for the upper 5 percent	266
C.3c	F-distribution values for the upper 2.5 percent	267
C.3d	F-distribution values for the upper 1 percent	268

LIST OF FIGURES

<u>Figure</u>	<u>Page</u>
2.1 Chart for estimating alpha coefficient, α , and bearing capacity factor, N_q (modified from Bowles, 1977)	17
2.2 Relationship between maximum and minimum unit pile point resistance and friction angle for cohesionless soils (from Meyerhof, 1976)	18
2.3 Adhesion values for piles in cohesive soils	19
2.4 Adhesion factors for driven piles in clay (alpha method) (form Tomlinson, 1980)	20
2.5 Design curves for evaluating K_d for piles when $\phi' = 25^\circ$ (form Nordlund, 1979)	21
2.6 Design curves for evaluating K_d for piles when $\phi' = 30^\circ$ (form Nordlund, 1979)	22
2.7 Design curves for evaluating K_d for piles when $\phi' = 35^\circ$ (form Nordlund, 1979)	23
2.8 Design curves for evaluating K_d for piles when $\phi' = 40^\circ$ (form Nordlund, 1979)	24
2.9 Correction factor for K_d when $\delta \neq \phi'$ (from Nordlund, 1979)	25
2.10 Relation of δ/ϕ' and pile displacement, ζ , for various types of piles (from Nordlund, 1979)	26
2.11 Chart for correction of N-values in sand for influence of effective overburden pressure	27
2.12 Relationship between standard penetration test values and f or relative density (from Peck, Hanson, and Thornburn)	28
2.13 Model simulating the hammer-pile-soil system for one-dimensional wave equation (from Smith, 1960)	29
2.14 Force and velocity traces showing two impact peaks indicative of driving in soils capable of large deformations (from Paikowsky, 1994)	30
2.15 Elastic-plastic soil resistance-displacement relationship (from Smith, 1960)	31
4.1 Predicted vs measured capacity for fictitious dataset	66
4.2 Cumulative distribution plot for method A	67
5.1 Predicted vs measured capacity for Flaate (1964)	84
5.2 Predicted vs measured capacity for Fragaszy (1988)	86
5.3 <u>Predicted vs measured capacity (adapted from Paikowsky et al, 1994)</u>	88
5.4 Predicted vs measured capacity for Florida DOT (adapted from Davidson et al, 1996)	90
5.5 Predicted vs measured capacity from Eslami (1996)	93
5.6 Predicted vs measured capacity for FHWA database using EOD	96
5.7 Predicted vs measured capacity for FHWA database using BOR data	97

6.1	Average and standard deviation for all predictive methods in which each method could only be used to predict capacity from both EOD and BOR results	125
6.2	Average and standard deviation for all predictive methods in which each method could only be used to predict capacity from EOD results	126
6.3	Average and standard deviation for all predictive methods in which each method could only be used to predict capacity from BOR results	127
6.4	Average and standard deviation for datasets in which the EN formula could be used to predict capacity from EOD and BOR results	128
6.5	Average and standard deviation for datasets in which the Gates formula could be used to predict capacity from EOD and BOR results	129
6.6	Average and standard deviation for datasets in which the WEAP could be used to predict capacity from EOD and BOR results	130
6.7	Average and standard deviation for datasets in which the ME method could be used to predict capacity from EOD and BOR results	131
6.8	Average and standard deviation for datasets in which the PDA method could be used to predict capacity from EOD and BOR results	132
6.9	Average and standard deviation for datasets in which the CAPWAP method could be used to predict capacity from EOD and BOR results	133
6.10	Average and standard deviation for datasets in which static formulae could be used to predict capacity from EOD and BOR results	134
6.11	Predicted vs measured capacity for Gates for the following databases: Flaate, Fragaszy, FHWA (unfiltered, filtered, and filtered for only cases where the hammer energies could be determined as W*H)	135
6.12	Ratio of Q_p/Q_m vs measured capacity for Gates method for the following databases: Flaate, Fragaszy, and FHWA (filtered and unfiltered)	136
6.13	Predicted vs measured and Q_p/Q_m vs measured for Flaate, Fragaszy, and FHWA datasets using original Gates formula	137
6.14	Predicted vs measured and Q_p/Q_m vs measured for Flaate, Fragaszy, and FHWA datasets using modified Gates formula (corrected with linear function)	138
6.15	Predicted vs measured and Q_p/Q_m vs measured for Flaate, Fragaszy, and FHWA datasets using modified Gates formula (corrected with a power function)	139
6.16	Comparison of predicted vs measured capacity for H-piles vs all piles (Flaate database)	140
6.17	Comparison of predicted vs measured capacity for H-piles vs all piles (Fragaszy database)	141
6.18	Comparison of predicted vs measured capacity for H-piles vs all piles (EOD-FHWA database)	142
6.19	Comparison of predicted vs measured capacity for H-piles vs all piles (BOR-FHWA database)	143
6.20	Comparison of predicted vs measured capacity for all piles (EOD-FHWA database) with emphasis on Jacksonville load test	144
6.21	Comparison of predicted vs measured capacity for all piles (BOR-FHWA database) with emphasis on Jacksonville load test	145

7.1	Cumulative distribution for EN formula for EOD conditions and using FHWA database with all piles	158
A.1	General location map for Jacksonville load test site	202
A.2	Location map for load test site near Jacksonville, IL	203
A.3	Plan and profile views of overpass at Jacksonville load test site	204
A.4	Boring locations for Jacksonville load test site	205
A.5	Soil profile for Jacksonville load test site	206
A.6	Variation in water content with depth for soil profile at Jacksonville load test site	207
A.7	Variation in Standard Penetration Resistance (blowcount) with depth for soil profile at Jacksonville load test site	208
A.8	Variation with depth of ½ the unconfined compressive strength for soil profile at Jacksonville load test site	209
A.9	Summary of water content, standard penetration resistance, and strength for Jacksonville load test site	210
A.10	Plan view of test and reaction piles at Jacksonville load test site	211
A.11	Delmag D19-32 single acting diesel hammer used at the Jacksonville load test site	212
A.12	Driving resistance of pile DTP-1 at Jacksonville load test site	213
A.13	Driving resistance of pile DTP-2 at Jacksonville load test site	214
A.14	Driving resistance of pile SLTP at Jacksonville load test site	215
A.15	Schematic view of hydraulic jack and load cell	215
A.16	Photograph of hydraulic jack and load cell	217
A.17	Schematic view of hydraulic jack, electric pump, and hand pump for static load test	218
A.18	Photograph of hydraulic jack, electric pump, and hand pump for static load test	219
A.19	Schematic view of reaction beam and two anchor piles	220
A.20	Photograph of reaction frame for load test. Two anchor piles are located on each end of the reaction frame. Test pile and hydraulic jack are in the center.	221
A.21	Setup of dial gages and wireless mirror and scale system for measuring displacement during load test	222
A.22	Load-displacement relationship for the first static load test (SLT-1)	223
A.23	Load-displacement relationship for the second static load test (SLT-2)	224
A.24	Relationship between pile capacity and driving resistance based on penetration resistance at End-of-Driving (EOD) for comparison with first load test on pile SLT	225
A.25	Relationship between pile capacity and driving resistance based on penetration resistance at Beginning-of-Restrike (BOR) for comparison with first load test on pile SLT	226
A.26	Relationship between pile capacity and driving resistance based on penetration resistance at End-of-Driving (EOD) for comparison with second load test on pile SLT	227

A.27	Relationship between pile capacity and driving resistance based on penetration resistance at Beginning-of-Restrike (BOR) for comparison with second load test on pile SLT	228
B.1	Time dependent increase in pile capacity	245
B.2	Gain in capacity after dissipation of excess pore pressures	246
B.3	Axial capacity for piles in clay	247
B.4	Normalized capacity for piles in clay	248
B.5	Normalized capacity for piles in sand	249
B.6	Normalized capacity for piles in mixed soil profile	250
B.7	Normalized capacity for sand with upper/lower bound	251

EXECUTIVE SUMMARY

The Illinois Department of Transportation uses driven piling for the support of bridges and other transportation-related structures. Current procedures for estimating the axial load capacity for a driven pile are reviewed and evaluated in terms of accuracy. Improved methods for the design and construction of pile foundations can reduce significantly the cost of installation and materials by requiring fewer or shorter piles, and by providing better information on the resistance of the pile during driving. There are concerns that current methods may not be suitable for driven steel H-piles that act primarily in friction, however, based on a review of the information collected and reviewed in this study, it is concluded the same predictive formulae can be used for H-piles.

While methods exhibiting good accuracy can result in improved design of pile foundations and reduce significantly the cost of these foundations, some methods require greater computational effort, expense, and time to determine pile capacities more accurately. This report ranks several predictive methods for determining axial pile capacity and discusses the effort required for each predictive method.

Several loadtests on piles were collected and organized and interpreted. The databases include those developed originally by Flaate, Olson and Flaate, Fragaszy, Paikowski, Davidson, and by the Federal Highway Administration (FHWA). An additional database reporting cone penetration tests (Eslami) was also investigated. Evaluations of predicted capacity were quantified for the following methods: the Engineering New Formula (EN), the Gates Method (Gates), the Modified Gates (mod. Gates), a Wave Equation Analysis Program (WEAP), a measured energy approach (ME), estimates from a pile driving analyzer (PDA), and the CASE Pile Wave Analysis Program (CAPWAP). The accuracy for all these predictive methods were compared for both end of driving (EOD) and beginning of re-strike (BOR) conditions.

The ability of EN, Gates, and ME methods to predict pile capacity accurately benefits little from using BOR data. WEAP, PDA, and especially CAPWAP benefit from the use of BOR data. Pile capacity using EOD data is shown to predict with about the same precision with WEAP, PDA, and CAPWAP. The ME and modified Gates methods appear to provide more precise measurements when only EOD data are used. Use of CAPWAP with BOR data results in the greatest precision of all predictive methods investigated. For non-monitored methods, BOR results generally exhibited slightly less scatter than when using EOD data. Based on the results of this study, representative values for the factor of safety are given below for each method.

EOD/BOR	Predictive Method	Factor of Safety	Index for Wasted Capacity
EOD	EN	9.8	1.00
	Gates	1.4	0.66
	Modified Gates	2.4	0.65
	WEAP	2	0.72
	ME	2.5	0.66
	PDA	2.1	0.69
	CAPWAP	2.1	0.78
BOR	WEAP	2.8	0.69
	ME	3.2	0.66
	PDA	2.3	0.61
	CAPWAP	2.0	0.60

These factors of safety result in the same level of reliability as currently used for driven piling by the Illinois Department of Transportation. It should be emphasized however, that all the methods above exhibit a tendency to overpredict or underpredict capacity (bias) by various amounts. The Factors of Safety shown above account for the bias exhibited by each method.

The “cost” for using a method is expressed as an “Index for Wasted Capacity (WCI).” In the table above, it is normalized to a value of 1.0 for the Engineering News formula. As can be seen, all the other methods have an index value less than the EN formula. For example, the WCI is 0.65 for the modified Gates method using EOD data. This means the modified Gates method would waste only 65% as much pile

capacity as the EN formula for the same reliability. All methods exhibit less wasted capacity than the EN formula (currently used by IDOT), meaning the EN formula is the most wasteful method for use in design. The modified Gates method could offer a more efficient formula with no change in data collection efforts used by IDOT.

Use of more sophisticated methods such as WEAP, ME, PDA, and CAPWAP to predict pile capacity using EOD conditions did not result in significantly better economy (lower WCI) than the modified Gates method. However, WEAP, ME, PDA, and CAPWAP did perform consistently well when BOR data were used, with the least wasted capacity using CAPWAP.

In summary, IDOT could benefit by using the modified Gates formula rather than the EN formula. The modified Gates formula requires the same information already collected in the field for evaluating capacity using the EN formula (only the formula is different).

It is important to explain why a simple empirical method can predict axial pile capacity with accuracy similar to the more sophisticated methods. One would expect the more sophisticated methods to perform significantly better (than empirical methods) because the soil, pile, and pile driving system are modeled. Indeed, the more sophisticated methods provide the engineer with critical information on pile stresses and pile drivability that the simpler methods (EN formula, Gates, and modified Gates) cannot provide. However, unknowns such as hammer efficiency, cannot be determined accurately without using pile dynamic monitoring. Other unknowns, such as the change in pile capacity with time can also make it difficult to predict pile. All these factors are important variables that influence pile capacity.

ACKNOWLEDGMENTS

The research described in this report was performed as a part of Illinois Transportation Research Center (ITRC) contract IDOT ITRC 1-5-38911. The ITRC is a public-private-university joint cooperative transportation research unit underwritten by the Illinois Department of Transportation (IDOT). Steven J. Hanna of Southern Illinois University at Edwardsville is the director of the ITRC. His excellent administration and support of this project is gratefully acknowledged.

The research was conducted by the Department of Civil and Environmental Engineering at the University of Illinois at Urbana-Champaign. Associate Professor James H. Long was the principal investigator of the research project. Several graduate students contributed to the project. The graduate students include Mr. Mike Wysockey, Mr. John Kerrigan, Mr. Diyar Bozkurt, and Mr. Massimo Maniaci.

Outstanding assistance was provided to the researchers by a number of IDOT personnel. Mr. Tom Domagalski of the Bureau of Bridges and Structures and Mr. Emile Samara, formerly of the Bureau of Bridges and Structures, were instrumental in developing the research plan and monitoring research progress. Mr. Bill Kramer, and Mr. Alan Goodfield from the Bureau of Bridges and Structures, and Mr. Riyad Wahab from the Bureau of Materials and Physical Research served on the technical review committee and provided several excellent suggestions during the project. Mr. John Stestak, resident engineer for IDOT, was instrumental in the success of the axial pile load tests in Jacksonville, Illinois.

Appreciation is also extended to Mr. Carl Ealy of the Federal Highway Administration for providing the authors with a copy of the FHWA loadtest database.

Chapter 1

INTRODUCTION

Approximately 300 bridges are built or contracted to be built in Illinois each year with many of these bridges supported on pile foundations. The Illinois Department of Transportation is active in the design (and the review of design) of piles. Current design procedures employed by IDOT are based upon studies performed over 20 years ago and improved methods for the design of pile foundations can reduce significantly the cost of these foundations. However, some of these methods may require greater computational effort, expense, and time to determine pile capacities more accurately. Thus it is useful to rank the predictive methods available for accuracy and effort required to determine capacity.

Improved methods for the design and construction of pile foundations can reduce significantly the cost of installation and materials by requiring fewer or shorter piles, and by providing better information on the resistance of the pile during driving. There are concerns that current methods may not be suitable for driven steel H-piles that act primarily in friction.

The objective of this study is to develop better procedures for predicting the behavior of piles during and after pile driving. This objective will be obtained by: 1) collecting, studying, and analyzing data collected on pile driving, and 2) comparing several methods for predicting the axial capacity of piles with the dynamic methods used currently by IDOT. Methods for predicting the axial capacity of piles are compared with results of full-scale load tests conducted in Jacksonville, Illinois.

It is the purpose of this project to collect and analyze information on axial capacity of piles, to provide a means to assess the methods accuracy, and to recommend factors of safety appropriate to each predictive method.

Chapter 2 introduces and discusses the methods used for predicting pile capacity. The emphasis of this report is placed on predictive methods that determine pile capacity based on their resistance during pile driving. Chapter 3 identifies several collections of load tests. These load tests contain information collected during pile driving that allow the predictive methods to calculate capacity and then be compared with the capacity measured with a static load test.

Chapter 4 identifies techniques that are used to compare predicted and measured axial pile capacity. There are three important techniques which are: 1) visual plotting of predicted versus measured capacity, 2) statistical treatment of the data to quantify how well the predictive method works, and 3) using the collection of data to establish a relationship between a capacity factor and the reliability of the pile foundation. Chapter 5 presents the data for predicted versus measured load and develops basic statistics to quantify how well predicted and measured capacities agree.

Chapter 6 further analyzes the load test databases to determine if there is benefit to using pile driving data at the end of driving versus beginning of re-strike. Further studies are also conducted to determine if similar trends are observed with different load test databases. Chapter 7 attempts to draw a relationship between reliability and factor of safety needed for each predictive method. Chapter 7 also identifies the efficiency of each method. Chapter 8 summarizes the finding in each of the chapters. Chapter 9 presents a list of references used in the report.

Two H-piles were driven and load tested in Jacksonville as part of this research effort. Appendix A provides information on the Jacksonville load tests. Appendix B is a report on the change in axial capacity with time that driven pile undergo. Appendix C is a tutorial on statistical techniques used in this report.

METHODS FOR PREDICTING AXIAL PILE CAPACITY

INTRODUCTION

Several methods are available for predicting pile capacity based upon the resistance of the pile during driving or during retapping. This chapter introduces both static methods for predicting capacity and methods that use the behavior during driving to determine capacity. However, the report will focus on the six methods that use driving resistance to predict capacity: the Engineering News (EN) formula, the Gates formula, the Wave Equation Analysis Program (WEAP), the Pile Driving Analyzer (PDA), the Measured Energy method, and the CASE Pile Wave Analysis Program (CAPWAP).

The first three predictive methods may be used to estimate pile capacity based on simple field measurements of driving resistance. The EN and Gates methods are simple dynamic formulae that require only the hammer energy and pile set (or blow count). WEAP requires numerical modeling the pile hammer, the pile, and the soil, and develops a relationship between capacity and driving resistance. The remaining three methods (PDA, Measured Energy Method, CAPWAP) require detailed measurements of the temporal variation of pile force and velocity during driving.

Each method can use results of pile behavior at the end of driving (EOD) or beginning of restrike (BOR). When it is possible and practical, restriking the pile is a prudent procedure since time effects can influence significantly the final capacity for a pile. Because of tight construction schedules, it may be common to restrike after 24 hours; however, a longer time may be required for fine-grained soils to allow development of full set-up conditions (FHWA, 1995).

ESTIMATES USING STATIC METHODS

The ultimate capacity, Q_u , of a pile under axial load is generally accepted to be equal to the sum of the pile tip capacity, Q_p , and the shaft capacity, Q_s :

$$Q_u = Q_p + Q_s \quad (2.1)$$

These terms can be further broken down and defined as follows:

$$Q_p = q_p \cdot A_p - W \quad (2.2)$$

and

$$Q_s = \sum_{i=1}^n f_{si} C_i l_i \quad (2.3)$$

where q_p = bearing capacity of pile tip, A_p = area of pile tip, W = weight of pile, f_{si} = ultimate skin resistance per unit area of pile shaft segment i , C_i = perimeter of pile segment i , l_i = length of pile segment i , and n = number of pile segments.

Thus, evaluating the ultimate pile capacity, Q_u , reduces to estimating the magnitude of f_{si} for each pile segment and q_p at the pile tip. A number of methods are available for evaluating the ultimate pile capacity, most of which are based on empirical methods, derived from correlations of measured pile capacity with soil data. One method is described in the following section.

SPILE

The SPILE computer program was developed by the Federal Highway Administration (FHWA) for determining the ultimate capacity of piles. The purpose of this section is to present the equations, analytical procedures, and empirical curves utilized by the program, with the intent of providing the reader with some insight into the workings of the program.

The basis of SPILE is the methods and equations presented by Nordlund (1963,1979), Thurman (1964), Meyerhof (1976), Cheney and Chassie (1982), Tomlinson (1970, 1985), and the FHWA Pile Manual.

Point Resistance

The point bearing capacity is obtained from bearing capacity theory:

$$q_p = cN_c + qN_q + \frac{1}{2}B\gamma N_\gamma \quad (2.4)$$

where N_c , N_q , N_γ = bearing capacity factors , c = cohesion of soil, q = vertical stress at pile base, γ = unit weight of soil, and B = pile diameter (or width).

Combining Eqns. 2.2 and 2.4, the following equation applies for calculating the pile tip capacity:

$$Q_p = (cN_c + qN_q + \frac{1}{2}B\gamma N_\gamma) \cdot A_p - W \quad (2.5)$$

The soil strength parameters c and ϕ , the unit weight of the soil γ , and the vertical stress q are evaluated according to the conditions under which the soil may fail (i.e., undrained vs drained).

For an undrained analysis, c , ϕ , and γ are values appropriate to undrained conditions and q is in terms of total stresses. In saturated soils, $\phi = 0$ and c = undrained shear strength, s_u . With $\phi = 0$, $N_\gamma = 0$ and $N_q = 1$. Substituting these values into Eqn. (2.5) yields:

$$Q_p = (s_u N_c + q) A_p - W \quad (2.6)$$

The weight of the pile is assumed equal to the second term (i.e., $A_p \cdot q \approx W$) and a value of $N_c = 9$ is usually used. Thus, for an *undrained analysis*, the pile tip capacity is approximated as follows:

$$Q_p = 9 \cdot s_u \cdot A_p \quad (2.7)$$

For a drained analysis, the soil strength parameters are drained values and q is in terms of effective stresses. For these conditions, Eqn. 2.5 becomes:

$$Q_p = (c' N_c + q' N_q + \frac{1}{2} \gamma B N_\gamma) A_p - W \quad (2.8)$$

The first and third terms in brackets and the pile weight are negligible when compared to the second term. Thus, the pile tip capacity for a *drained analysis* is approximated as follows:

$$Q_p = A_p q' N_q \quad (2.9)$$

where $q' = \sigma'_{vo}$ = initial vertical effective stress at the pile tip.

The program uses a modification of Eqn. 2.9:

$$Q_p = A_p q' \alpha N_q \quad (2.10)$$

where α = a dimensional factor dependent on the depth-to-width (D/B) ratio of the pile (Fig. 2.1).

The program checks the calculated pile tip capacity (Eqn. 2.10) with limiting values proposed by Meyerhof (Fig. 2.2) and if they are exceeded, the latter value is reported.

Shaft Resistance

The ultimate skin resistance per unit area of shaft is calculated as follows:

$$f_s = c_a + \sigma_h \tan \delta_s \quad (2.11)$$

where c_a = pile-soil adhesion, σ_h = normal stress at pile-soil interface, and δ_s = pile-soil friction angle. The normal stress, σ_h , is related to the vertical stress, σ_v , as

$$\sigma_h = K \cdot \sigma_v \quad (2.12)$$

where K = coefficient of lateral stress. Thus,

$$f_s = c_a + K\sigma_v \tan \delta_s \quad (2.13)$$

Combining Eqns. 2.3 and 2.13, the following equation applies for calculating the shaft capacity:

$$Q_s = \sum_{i=1}^n (c_a + K\sigma_v \tan \delta_s)_i C_i l_i \quad (2.14)$$

As with the pile tip capacity, the pile-soil parameters c_a and δ_s and the vertical stress σ_v in Eqn. 2.14 are evaluated according to the conditions under which the soil may fail (i.e., undrained vs drained).

For an undrained analysis, δ_s may be taken as zero, so that Eqn. 2.14 reduces to

$$Q_s = \sum_{i=1}^n (c_a)_i C_i l_i \quad (2.15)$$

where c_a = undrained pile-soil adhesion.

The undrained pile-soil adhesion, c_a , varies considerably with many factors, including pile type, soil type, and method of installation (driven versus drilled or augered). It is usually correlated with the undrained shear strength s_u as follows:

$$c_a = \alpha \cdot s_u \quad (2.16)$$

where α = empirical coefficient that depends on the aforementioned factors.

Substituting Eqn. 2.16 into Eqn. 2.15 yields the equation for calculating the shaft capacity for *undrained conditions*:

$$Q_s = \sum_{i=1}^n (\alpha \cdot s_u)_i C_i l_i \quad (2.17)$$

Figures 2.3 and 2.4 present the α -values used by the program.

For a drained analysis, the pile-soil adhesion parameter is a drained value and σ_v is in terms of effective stresses. Thus, Eqn. 2.14 can be written as:

$$Q_s = \sum_{i=1}^n (c'_a + K\sigma'_v \tan \delta_s)_i C_i l_i \quad (2.18)$$

The first term in brackets is assumed negligible when compared to the second term, in which case:

$$Q_s = \sum_{i=1}^n (K\sigma'_v \tan \delta_s)_i C_i l_i \quad (2.19)$$

The program uses a modification of Eqn. 2.19, which is based on the method developed by Nordlund (1963,1979) and takes into account pile taper and different pile materials. For tapered piles:

$$Q_s = \sum_{i=1}^n [K_\delta C_f \sigma'_v (\sin\{w + \delta_s\} / \cos w)]_i C_i l_i \quad (2.20)$$

where K_δ = coefficient of lateral stress, C_f = correction factor for K_δ when $\delta_s \neq \phi$, and w = angle of pile taper (measured in degrees). For non-tapered piles ($w = 0$), Eqn. 2.20 simplifies to:

$$Q_s = \sum_{i=1}^n [K_\delta C_f \sigma'_v \sin \delta_s]_i C_i l_i \quad (2.21)$$

Figs. (2.5-2.8) present the values of K_δ versus w for various values of ϕ when $\delta_s = \phi$. Fig. (2.9) gives the correction factor, C_f , for K_δ when $\delta \neq \phi$. Fig. (2.10) gives δ/ϕ values for different pile types and sizes. Using these figures and Eqns. 2.19 or 2.20, the shaft capacity for a *drained analysis* is calculated.

ESTIMATES USING DYNAMIC FORMULAE

The dynamic formula is an energy balance equation. The equation relates energy delivered by the pile hammer to energy absorbed during pile penetration. Dynamic formulae are expressed generally in the form of the following equation:

$$eWH = Rs \quad (2.22)$$

where e = efficiency of hammer system, W = ram weight, H = ram stroke, R = pile resistance, and s = pile set (permanent pile displacement per blow of hammer). The pile resistance, R , is assumed to be related directly to the ultimate static pile capacity, Q_u .

Dynamic formulae provide a simple means to estimate pile capacity; however, there are several shortcomings associated with their simplified approach (FHWA, 1995):

- dynamic formulae focus only on the kinetic energy of driving, not on the driving system,
- dynamic formulae assume constant soil resistance rather than a velocity dependent resistance, and
- the length and axial stiffness of the pile are ignored.

Although hundreds of dynamic formulae have been proposed, only a few of them are used commonly (Fragaszy, 1989). An extensive study of all dynamic formulae is beyond the scope of this study; however, the EN formula and the Gates formula are included herein as examples of the performance of these methods.

The Engineering News (EN) Formula

The EN formula, developed by Wellington (1892) is expressed as :

$$Q_u = \frac{WH}{s + c} \quad (2.23)$$

where Q_u = the ultimate static pile capacity, W = weight of hammer, H = drop of hammer, s = pile penetration for the last blow and c is a constant (with units of length). Specific values for c depend on the hammer type and may also depend upon the ratio of the weight of pile to the weight of hammer ram. The Department of Transportation in the State of Illinois uses a value of c according to the following rules:

- $c = 1.0$ (inch) for gravity hammers
- $c = 0.1$ (inch) for air/steam hammers
- $c = 0.1 W_p/W$ (inch) for air/steam hammers in the case of very heavy steel and concrete piles, where W_p = weight of pile, and W = weight of hammer ram.

It is often recommended that the EN formula be used with $FS = 6$, and in fact, many formulae found in the published literature and design guidelines express Eqn. 2.23 with a factor of 6 in the formula. A FS equal to 9 is used by the Department of Transportation in the State of Illinois. The reader should be aware that various forms of this equation exist and should inspect carefully the equation and units for the formula and the FS implicit in the formula. A FS equal to 1 is used for the EN formula in this study.

Gates Formula

The dynamic formula (Gates, 1957) originally proposed by Gates is:

$$Q_u = (3/7)\sqrt{eE} \log\left(\frac{10}{s}\right) \quad (2.24)$$

where Q_u = ultimate capacity (tons), E = energy of pile driving hammer (ft-lb), e = efficiency of hammer (0.75 for drop hammers, and 0.85 for all other hammers, or efficiency given by manufacturer), s = pile set per blow (inches). A factor of safety equal to 3 is recommended by Gates (Gates, 1957) to achieve the allowable bearing capacity. Adjustments to the original Gates equations were proposed by Olson and Flaate (1967) and are discussed further in Chapter 3.

Wave Equation Analysis

Wave equation analyses use the one-dimensional wave equation to estimate pile stresses and pile capacity during driving (Goble and Rausche, 1986). Isaacs (1931) first suggested that the one-dimensional wave equation analyses can model the hammer-pile-soil system more accurately than dynamic formulae based on Newtonian mechanics.

Wave equation analyses model the pile hammer, pile, and soil resistance as a discrete set of masses, springs, and viscous dashpots. Smith's discrete model for the hammer-pile-soil system is shown in Fig. 2.13.

A finite difference method is used to model the stress-wave through the hammer-pile-soil system. The basic wave equation is:

$$E_p \frac{\partial^2 u}{\partial x^2} - \frac{S_p}{A_p} f_s = \rho_b \frac{\partial^2 u}{\partial t^2} \quad (2.25)$$

where E_p = modulus of elasticity, u = axial displacement of the pile, x = distance along axis of pile, S_p = pile circumference, A_p = pile area, f_s = frictional stress along the pile, ρ_b = unit density of the pile material, and t = time.

Wave equation analyses may be conducted before piles are driven to assess the behavior expected for the hammer-pile selection. Wave equation analyses provide a rational means to evaluate the effect of change in pile properties or pile driving systems on pile driving behavior and driving stresses (FHWA, 1995). Furthermore, better estimates of pile capacity and pile behavior have been reported if the field measurement of energy delivered to the pile is used as direct input into the analyses (FHWA, 1995).

ESTIMATES USING PILE DRIVING ANALYZER

PDA (Pile Driving Analyzer)

The PDA method refers to a procedure for determining pile capacity based on the temporal variation of pile head force and velocity. The PDA monitors instrumentation attached to the pile head, and measurements of strain and acceleration are recorded versus time. Strain measurements are converted to pile force, and acceleration measurements are converted to velocities. A simple dynamic model (CASE model) is applied to estimate the pile capacity. The calculations for the CASE model are simple enough for static pile capacity to be estimated during pile driving operations. Several versions of the CASE method exist, and each method will yield a different static capacity. A more detailed presentation of CASE methods are presented by Hannigan (1990).

PDA measurements are used to estimate total pile capacity as:

$$R_{TL} = \frac{F_{T1} + F_{T1+2L/c}}{2} + [V_{T1} - V_{T1+2L/c}] \frac{Mc}{2L} \quad (2.26)$$

where R_{TL} = total pile resistance, F_{T1} = measured force at the time $T1$, $F_{T1+2L/c}$ = measured force at the time $T1$ plus $2L/c$, V_{T1} = measured velocity at the time $T1$, $V_{T1+2L/c}$ = measured velocity at the time $T1$ plus $2L/c$, L = length of the pile, c = speed of wave propagation in the pile, and M is the pile mass per unit length. The value, $2L/c$ is the time required for a wave to travel to the pile tip and back. Terms for force and velocity are illustrated in Fig. 2.14.

The total pile resistance, R_{TL} , includes a static and dynamic component of resistance. Therefore, the total pile resistance is:

$$R_{TL} = R_{static} + R_{dynamic} \quad (2.27)$$

where R_{static} is the static resistance and $R_{dynamic}$ is the dynamic resistance. The dynamic resistance is assumed viscous and therefore is velocity dependent. The dynamic resistance is estimated as:

$$R_{dynamic} = J \frac{Mc}{L} V_{toe} \quad (2.28)$$

where J is the CASE damping constant and V_{toe} is the velocity at the toe of the pile. The velocity at the toe of the pile can be estimated from PDA measurements of force and velocity as:

$$V_{toe} = V_{T1} + \frac{F_{T1} - R_{TL}}{\frac{Mc}{L}} \quad (2.29)$$

Substituting Eqns. 2.28 and 2.29 into Eqn. 2.27 and rearranging terms results in the expression for static load capacity of the pile as:

$$R_{static} = R_{TL} - J \left[V_{T1} \frac{Mc}{L} + F_{T1} - R_{TL} \right] \quad (2.30)$$

The calculated value of R_{TL} can vary depending on the selection of T1. T1 can occur at some time after initial impact:

$$T1 = TP + \delta \quad (2.31)$$

where TP = time of impact peak, and δ = time delay. The two most common CASE methods are the RSP method and the RMX method. The RSP method uses the time of impact as T1 (corresponds to $\delta = 0$ in Eqn. 2.31). The RMX method varies δ to obtain the maximum value of R_{static} .

The Measured Energy Method

The Measured Energy method (Paikowsky et al, 1994) provides a simple means to calculate capacity based upon measurements from a PDA. Accordingly, as in the CASE method, it is possible to estimate pile capacity during driving. This method estimates pile capacity with a dynamic formula similar to Eqn. 2.23; however, energy delivered to the pile and pile displacement are determined from dynamic measurements during driving.

Maximum pile displacement (D_{\max}) and transferred energy (E_n) are calculated from the variation of pile head force and velocity during (and immediately following) hammer impact. Two terms are calculated, and along with field blow counts, are used to determine axial capacity as follows:

$$R_u = \frac{E_n}{s + \frac{D_{\max} - s}{2}} \quad (2.32)$$

where R_u = axial capacity of the pile, E_n = delivered energy, D_{\max} = maximum displacement, s = pile set. D_{\max} and E_n are determined from dynamic measurements of acceleration and strain. E_n is determined as:

$$E_n = \int V(t)F(t)dt \quad (2.33)$$

where $V(t)$ = velocity at the pile top for the analyzed blow and $F(t)$ = force at the pile top for the analyzed blow. The energy in Eqns. 2.32 and 2.33 is equal to the total area under the curve OAB (Fig. 2.15). The velocity is determined by integrating the acceleration:

$$V(t) = \int a(t)dt \quad (2.34)$$

where $a(t)$ is the measured acceleration over the duration of the analyzed blow.

The force at the pile head is simply the measured strain multiplied by the axial stiffness of the pile:

$$F(t) = \varepsilon(t)E_p A_p \quad (2.35)$$

where ε = strain measured, E_p = modulus of elasticity of the pile material, and A_p = cross-sectional area of the pile.

The value of D_{\max} is obtained by integrating the velocity:

$$D_{\max} = \int V(t)dt \quad (2.36)$$

CAPWAP (CASE Pile Wave Analysis Program)

CAPWAP employs PDA measurements obtained during driving with the more realistic modeling capabilities of WEAP to estimate ultimate capacity. The method uses the acceleration history measured at the top of the pile as a boundary condition for WEAP analyses. The result of the analyses is a predicted force versus time response at the top of the pile. Comparison of predicted and measured force response allows the user to determine the accuracy of the wave equation model, and model parameters are modified until the measured and predicted force versus time plots are in close agreement.

This approach requires more time because iterations with operator intervention are necessary. Accordingly, CAPWAP analyses are usually conducted in the office and are currently (2000) unsuitable for obtaining field estimates during driving operations.

SUMMARY

Several methods for predicting axial pile capacity have been presented and discussed. Although static methods are presented, their driving performance out in the field is often used to confirm final pile capacities. Accordingly, more emphasis is placed on the methods that use driving behavior to determine capacity.

Predictions of pile capacity can be made with visual observation for the EN formula, Gates formula, and WEAP method of analysis. However, the ME, PDA, and CAPWAP methods require the pile head accelerations and strains to be monitored during driving. The simple dynamic formulae, such as EN and Gates, are simple to use, however, they do not model the mechanics of pile driving well. Furthermore, energy delivered by the pile hammer (an important parameter that effects the prediction of pile capacity) is based on estimates rather than measurements. WEAP models the pile driving components, but relies on estimates for energy delivered to the pile. The remaining three methods, ME, PDA, and CAPWAP use pile dynamic

monitoring to determine energy delivered to the pile head and displacements of the pile. The ME method uses a very simple model to predict pile capacity, the PDA uses a slightly more complicated model, and CAPWAP uses a more complete model for the pile driving system.

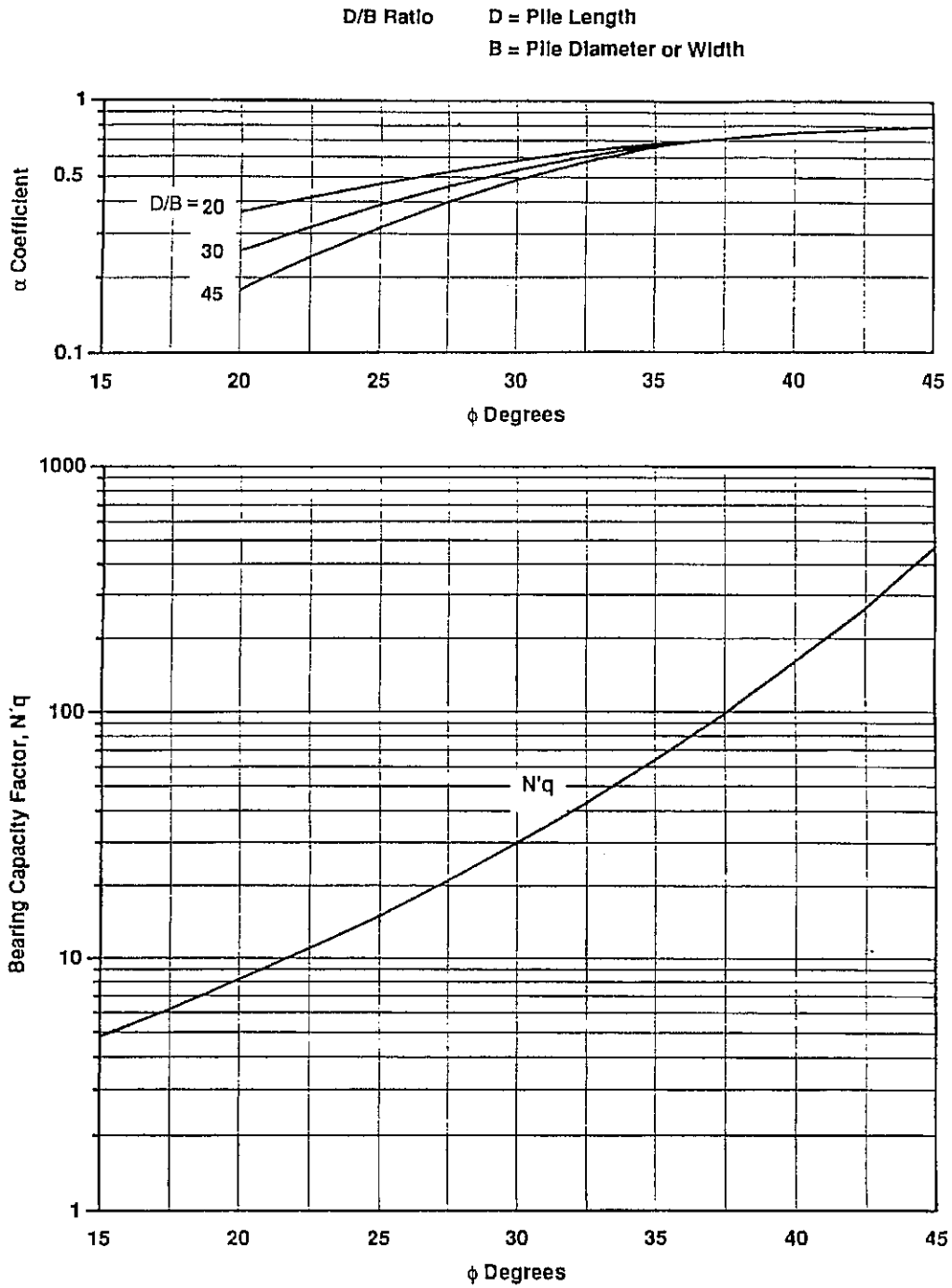


Figure 2.1 Chart for estimating alpha coefficient and bearing capacity factor $N'q$ (chart modified from Bowles 1977)

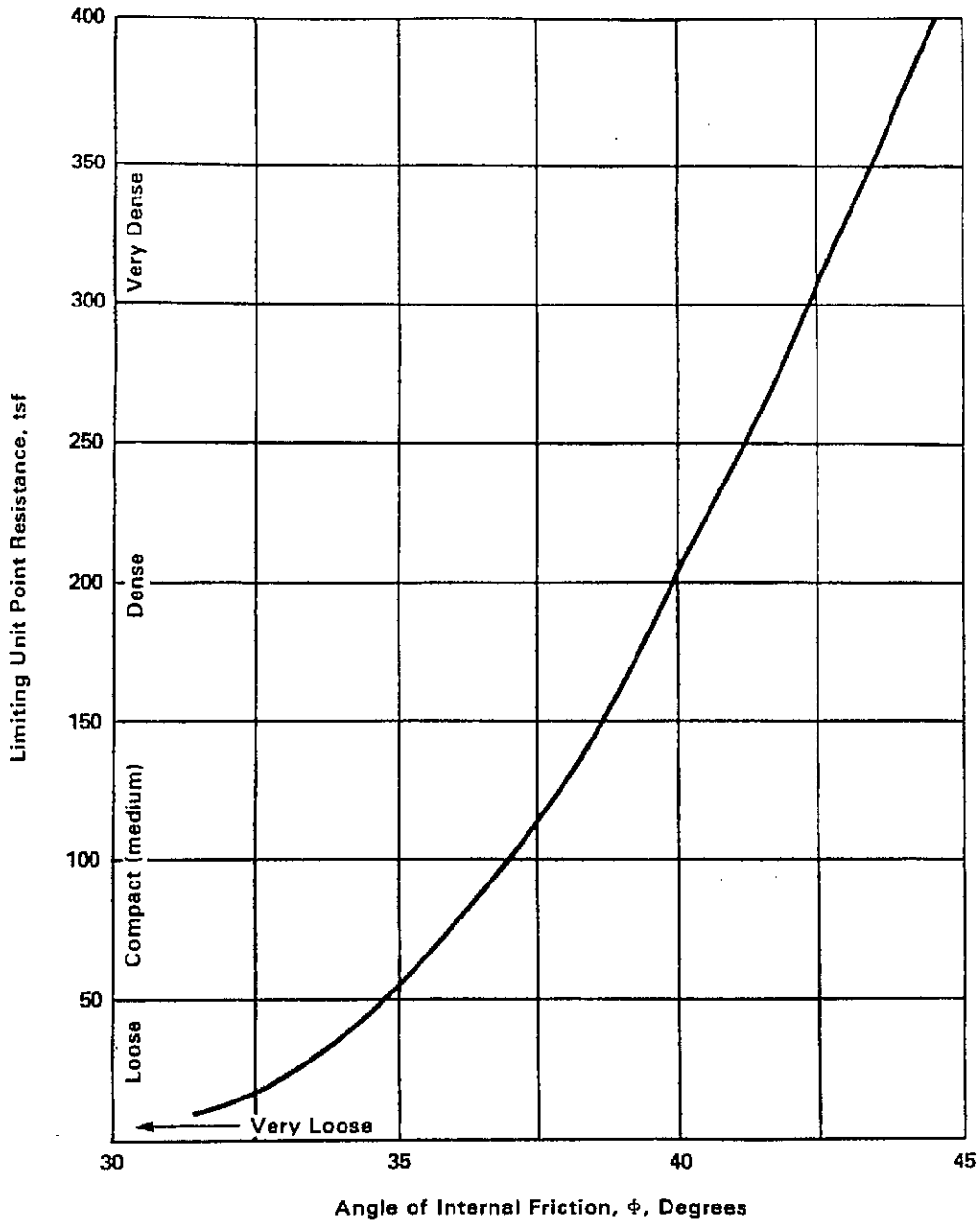
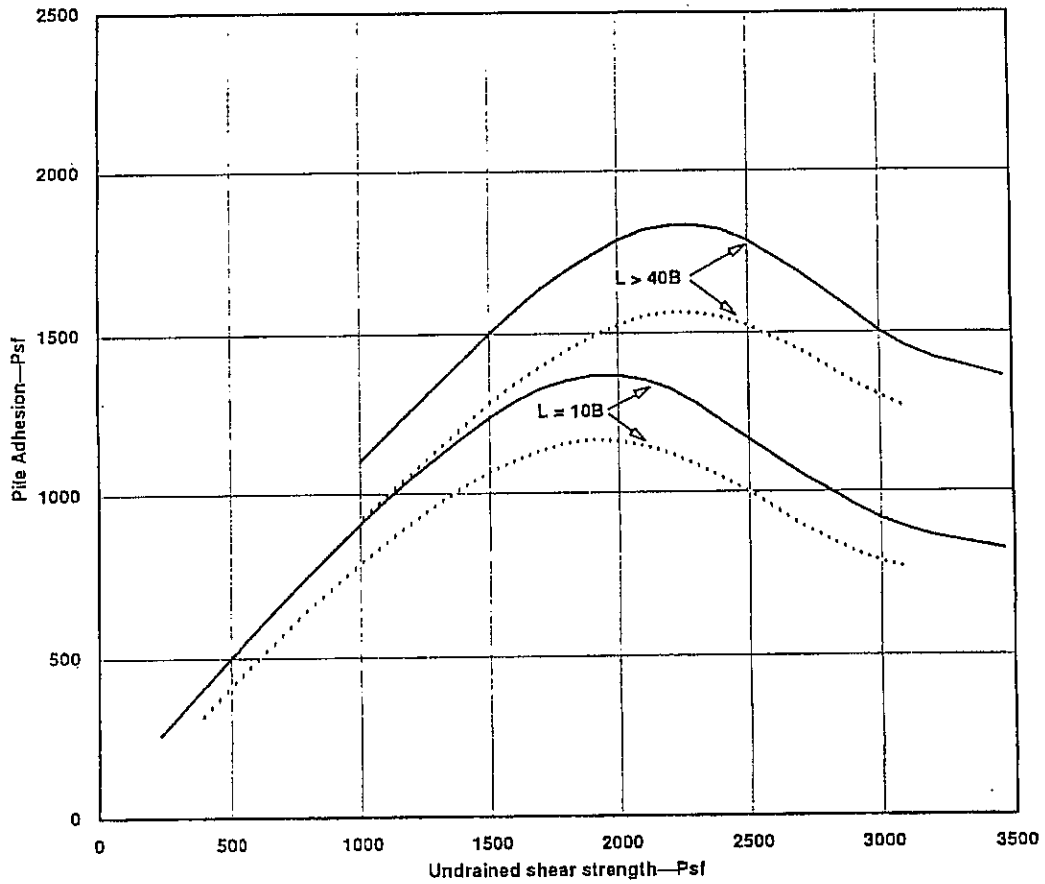


Figure 2.2 Relationship between maximum and minimum unit pile point resistance and friction angle for cohesionless soils (after Meyerhof 1976).



Legend

L = Distance from Ground Surface to Bottom of Clay Layer

B = Pile Diameter

———— Concrete Timber, Corrugated Steel Piles

..... Smooth Steel Piles

Reference: Based on Tomlinson 1979

Figure 2.3 Adhesion values for piles in cohesive soils.

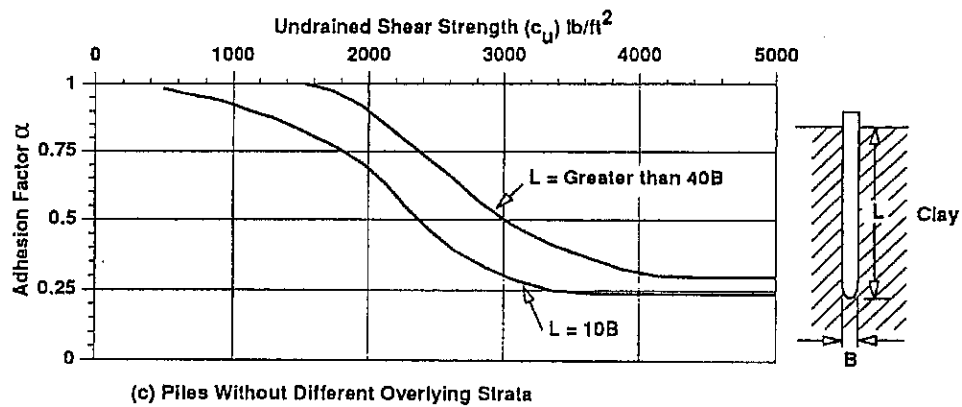
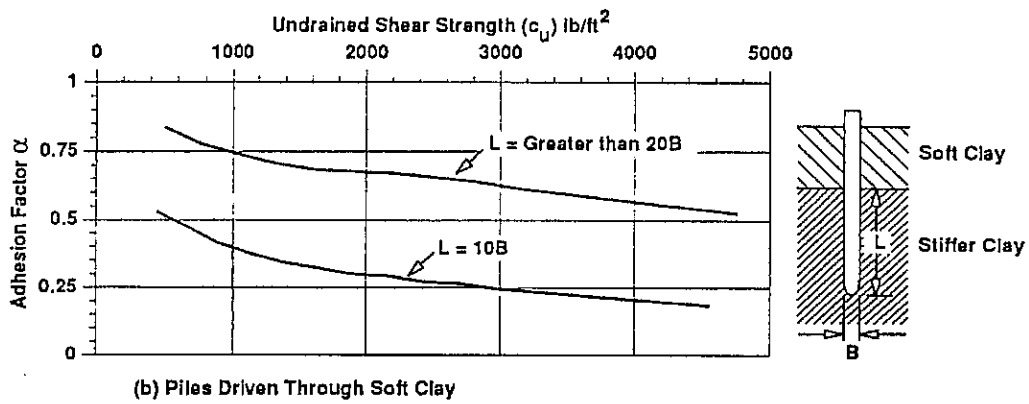
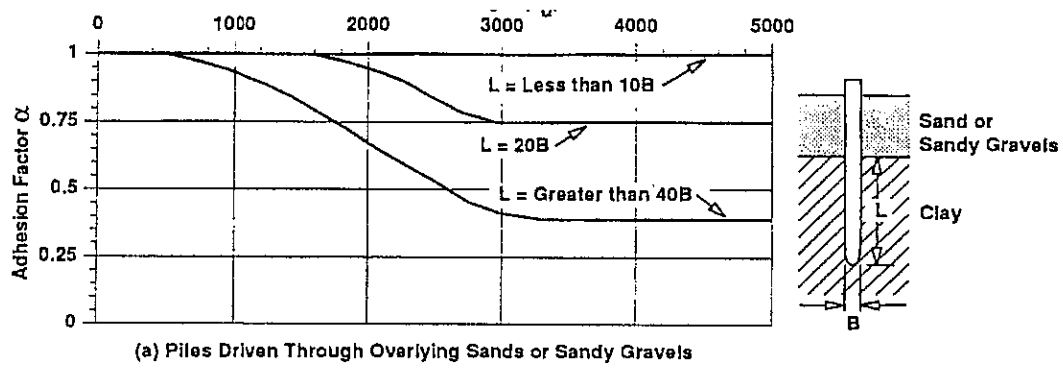


Figure 2.4 Adhesion factors for driven piles in clay (alpha method) (after Tomlinson 1980).

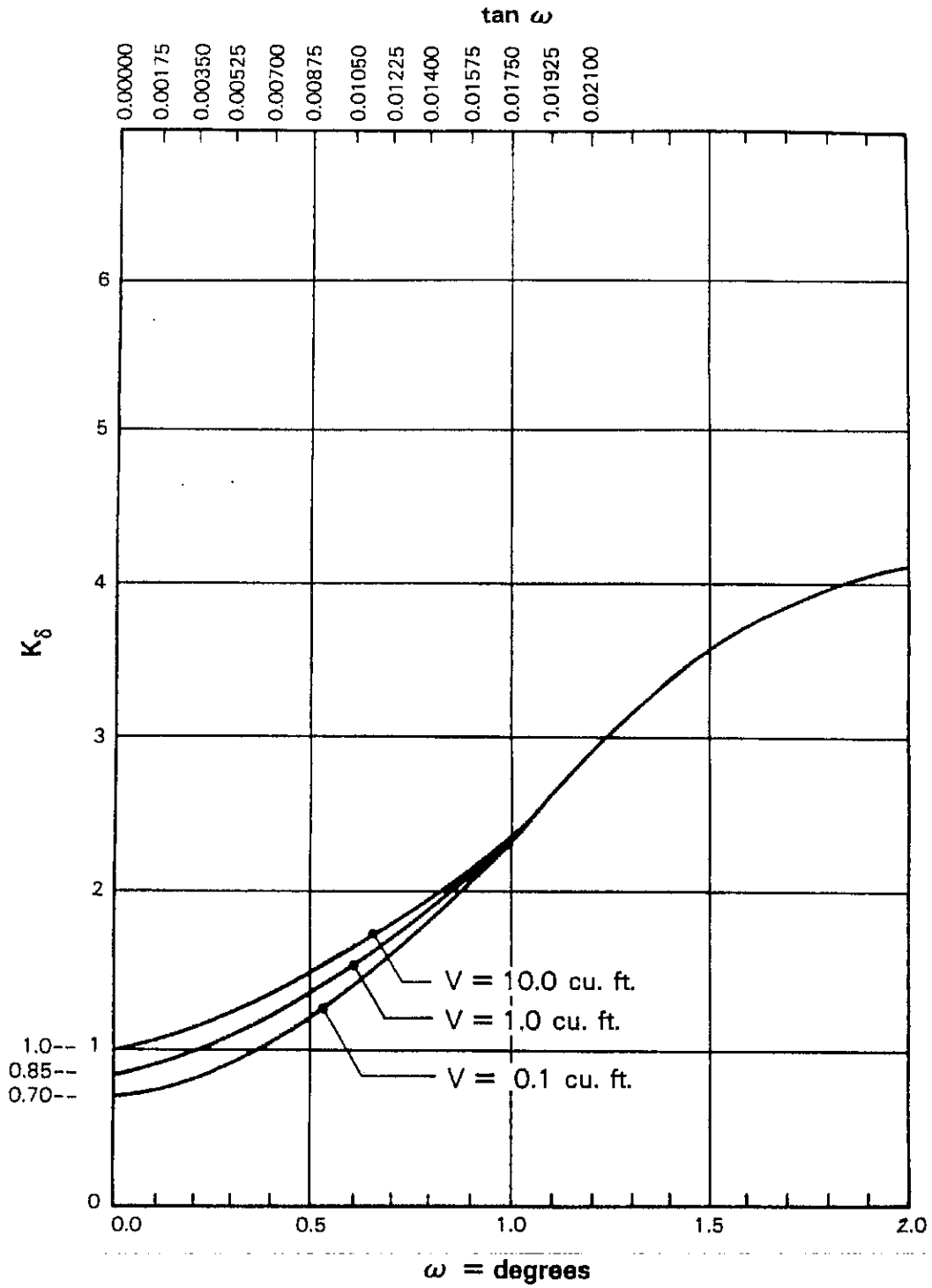


Figure 2.5 Design Curves for evaluating K_δ for piles when $\phi=25^\circ$ (after Nordlund 1979).

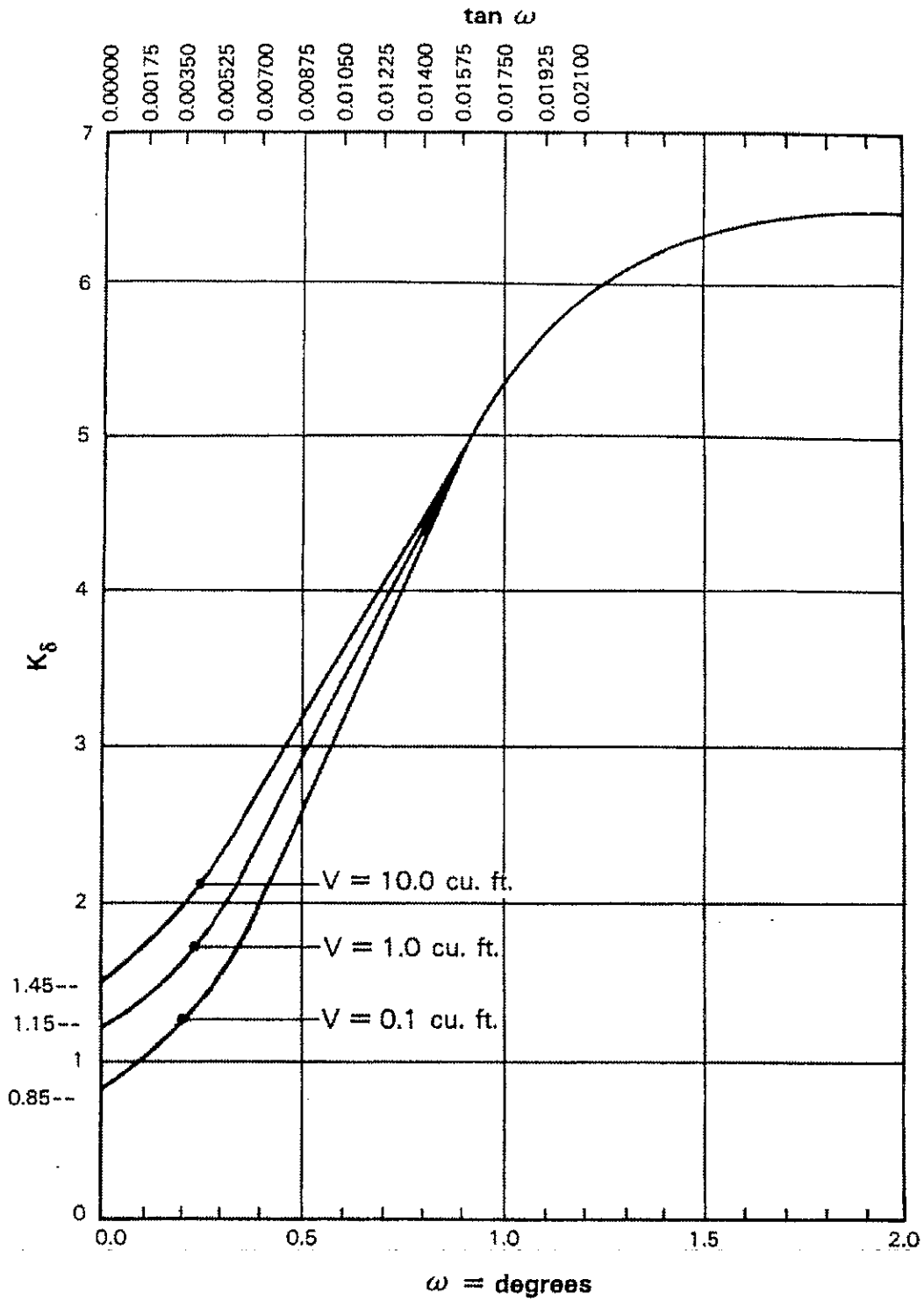


Figure 2.6 Design curves for evaluating K_δ for piles when $\phi=30^\circ$ (after Nordlund 1979).

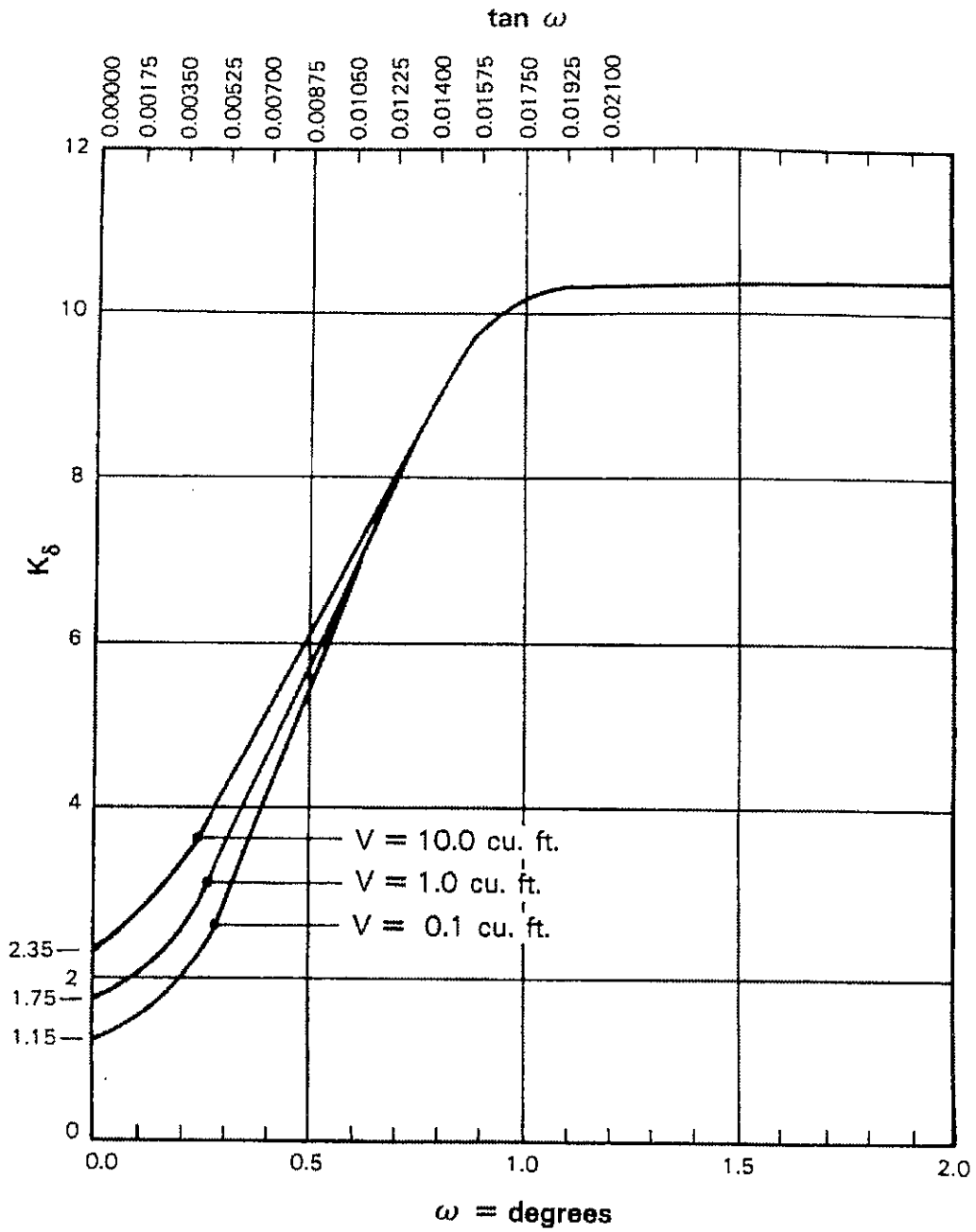


Figure 2.7 Design curves for evaluating K_s for piles when $\phi=35^\circ$ (after Nordlund 1979).

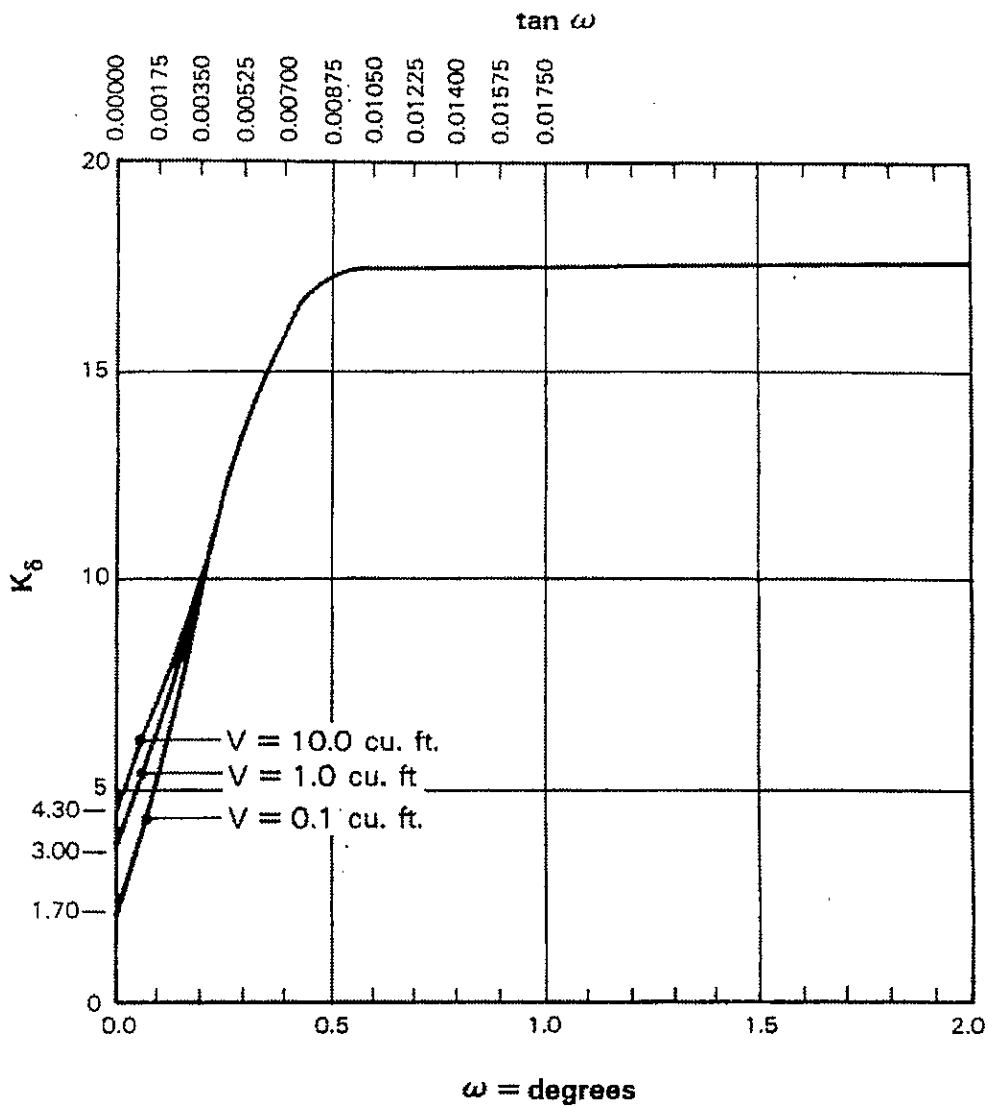


Figure 2.8 Design curves for evaluating K_δ for piles when $\phi=40^\circ$ (after Nordlund 1979).

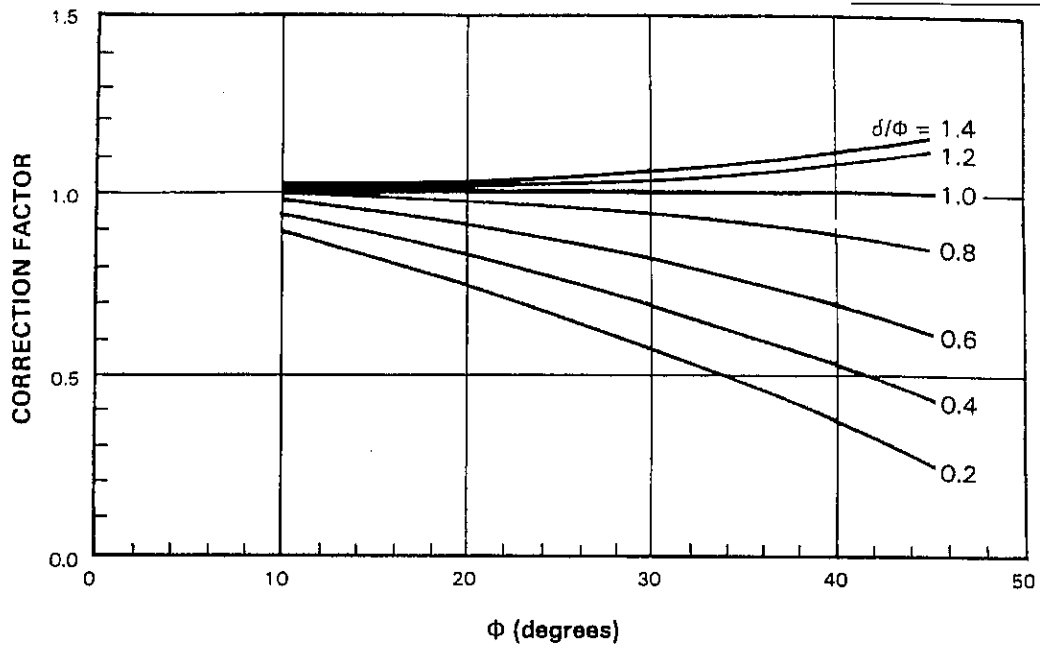
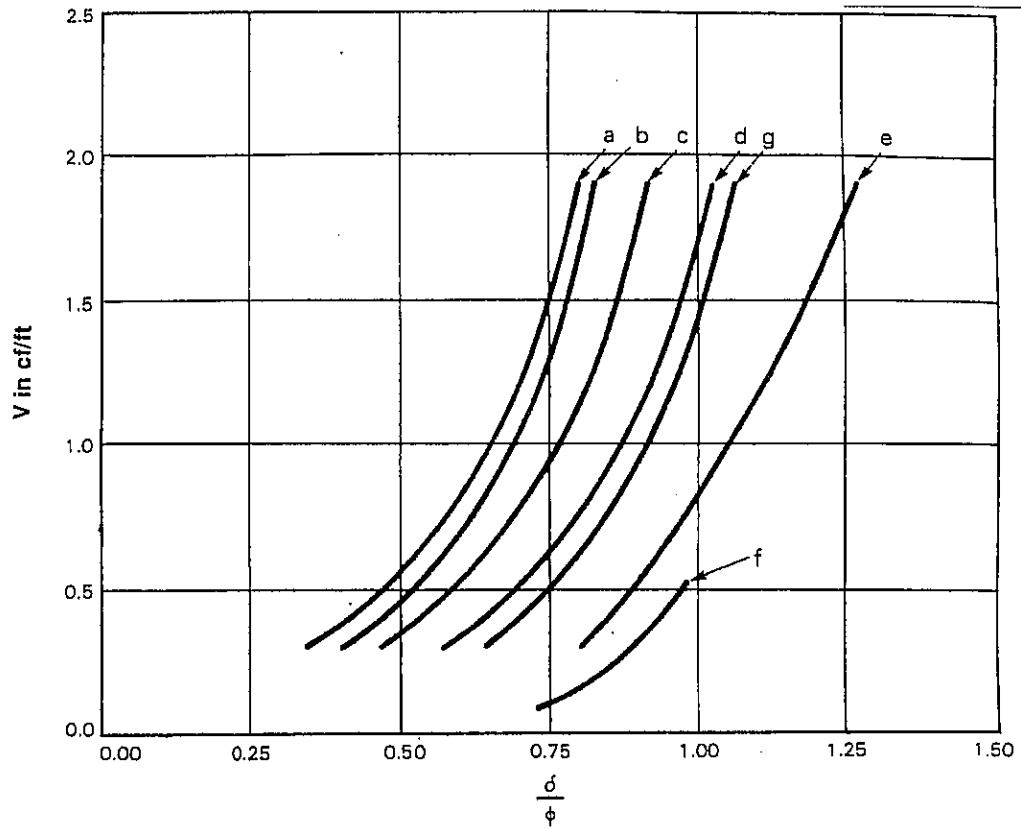


Figure 2.9 Correction factor for K_s when $\delta \neq \phi$
 (after Nordlund 1979).



- a. Pipe piles and non-tapered portion of monotube piles
- b. Timber piles
- c. Precast concrete piles
- d. Raymond step-taper Piles
- e. Raymond uniform taper piles
- f. H-piles and augercast piles
- g. Tapered portion of monotube piles

Figure 2.10 Relation of δ/ϕ and pile displacement, V , for various types of piles (after Nordlund 1979).

$$\text{Correction Factor } C_N = \frac{\text{Corrected "N"''}}{\text{Field "N"''}}$$

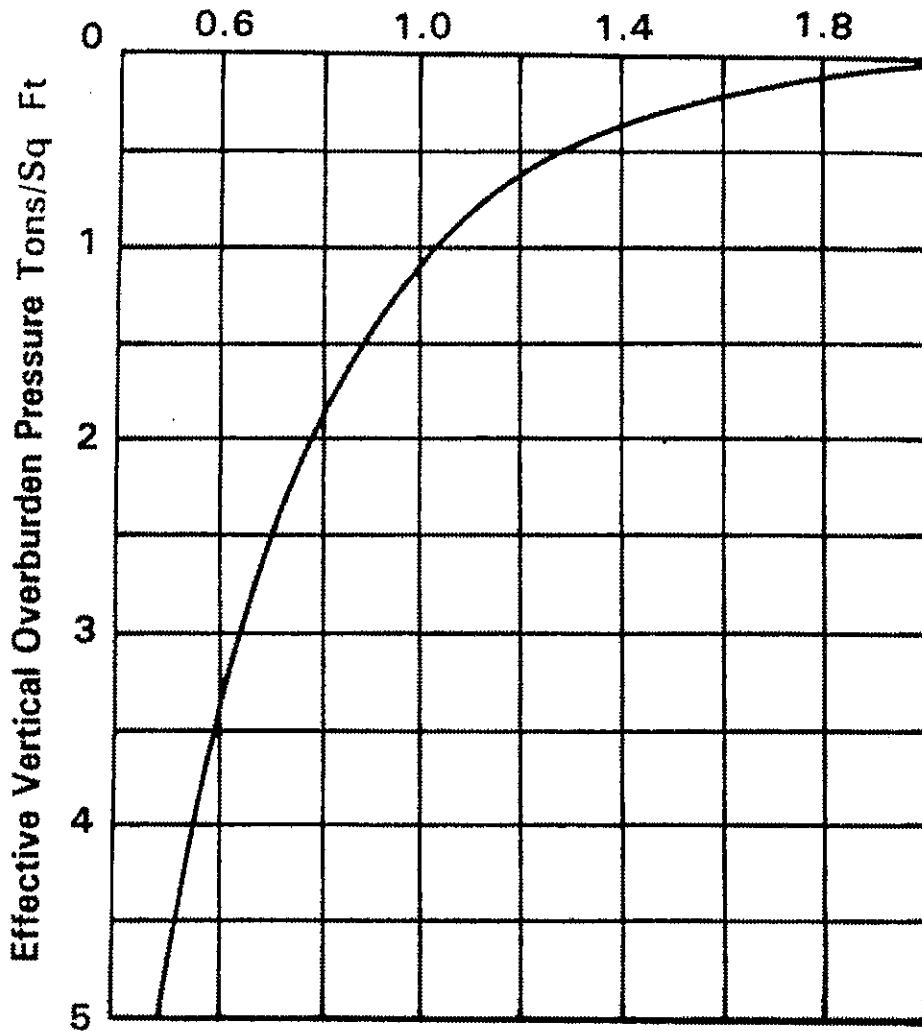


Figure 2.11 Chart for correction of N-value in sand for influence of effective overburden pressure.

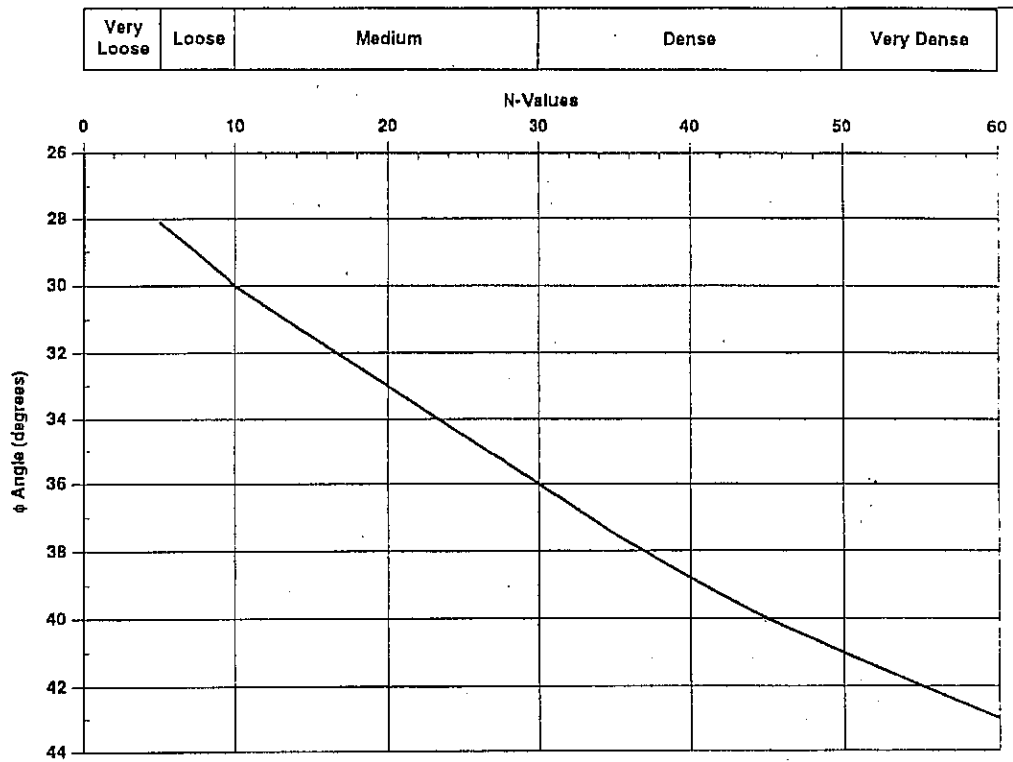


Figure 2.12 Relationship between standard penetration test values and ϕ or relative density descriptions (replotted after Peck, Hanson, and Thornburn).

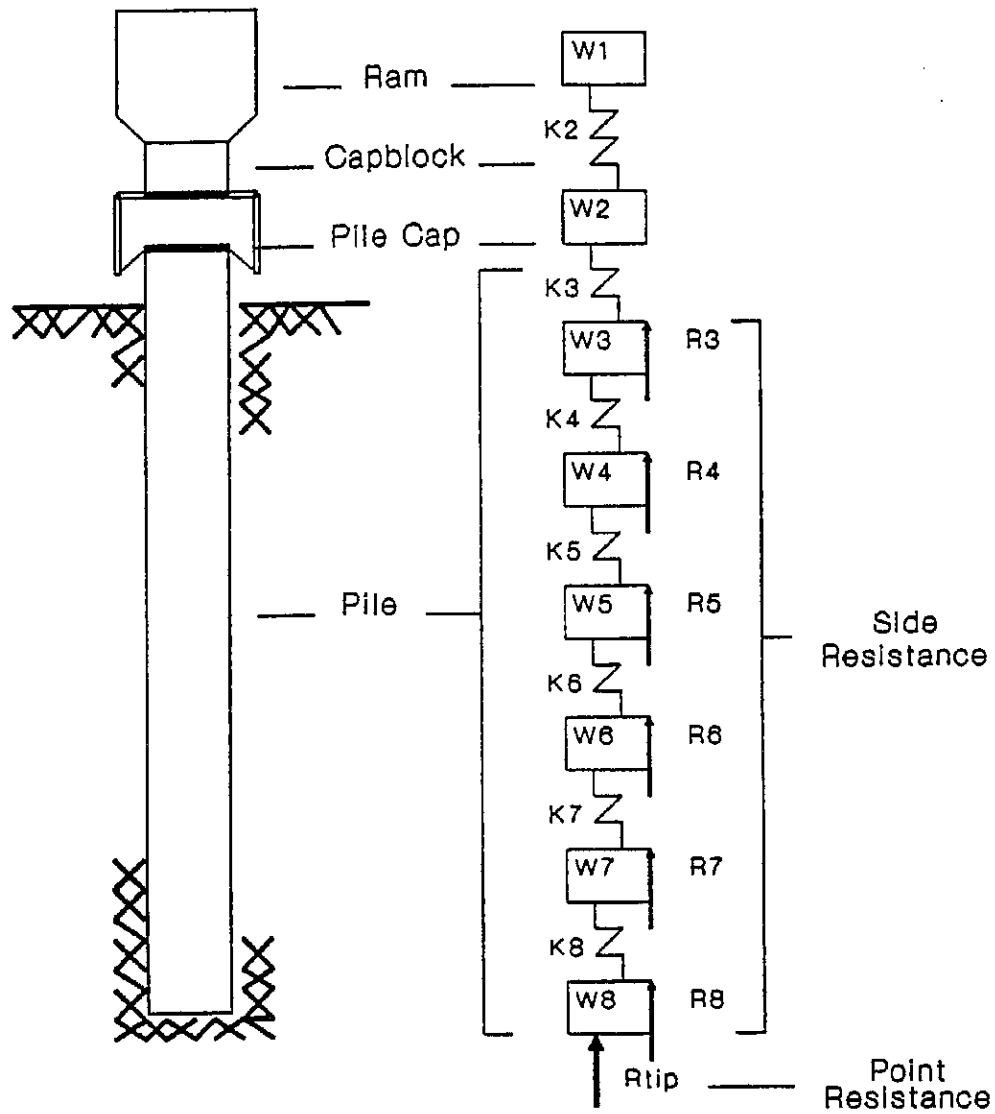


Figure 2.13 Model simulating the hammer-pile-soil system for one-dimensional wave equation (after Smith, 1960).

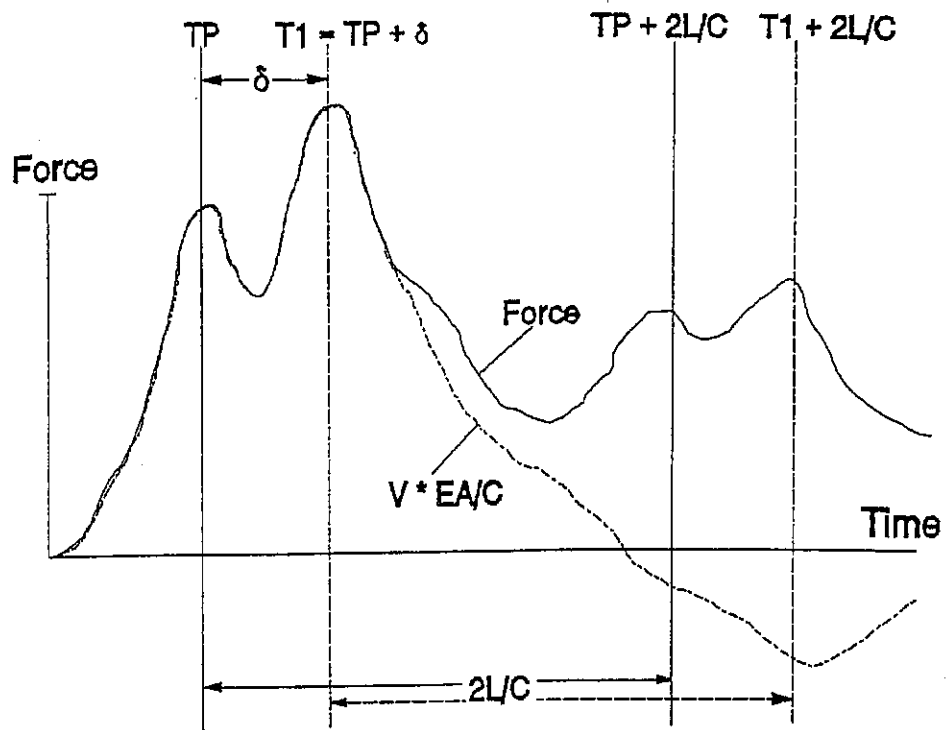


Figure 2.14 Force and velocity traces showing two impact peaks indicative of driving in soils capable of large deformations (after Paikowsky et al. 1994)

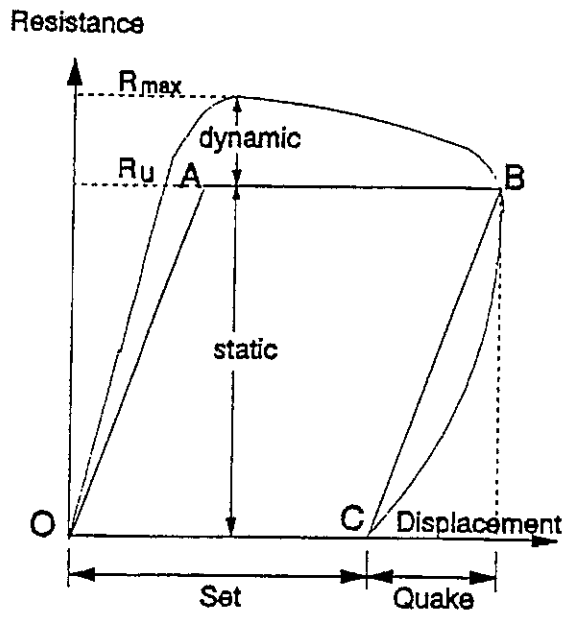


Figure 2.15 Elasto-plastic soil resistance-displacement relationship (after Smith, 1960)

COLLECTION OF LOAD TESTS

INTRODUCTION

Several datasets have been collected to investigate how well methods predict axial capacity of piles. This chapter presents a discussion of some of these collections. Some collections (Dennis and Olson, 1983) conducted studies for predicting how well pile capacities could be determined using static formulas. Their results are presented, but their database is not used in this study because their database focuses on static methods and the focus of this report is on predictions based on driving behavior. Similarly, a database of load tests is also presented that use cone penetration tests to predict capacity. These results are used to provide perspective and precedent for accuracy of methods that can be obtained from methods other than those that use driving behavior.

Several databases were collected and interpreted that contained information on the driving behavior during driving. These methods include dynamic formulae, methods that model the mechanics of the pile and pile driving system, and methods that require measurements of acceleration and strain at the pile head during driving. This chapter introduces the databases and the data from these collections.

DATABASE FROM OLSON AND DENNIS

This method investigates the ability to predict capacity based on Static formulas, and a number of formulas are investigated. Dynamic formulas are not investigated in this method Dennis and Olson (1983) investigated some of the design methods for predicting the axial compressive and tensile load capacities of driven piles. The study followed the empirical approach with the major objective being to assemble a sufficiently large database with which to reevaluate these methods. Through a series

of direct comparisons and indirect correlations, empirical coefficients and correction factors were developed to modify the existing methods and improve their accuracy.

The original database consisted of 1004 tests obtained from literature and unpublished data from government agencies, oil companies, and consulting firms. The final data set used in the investigation was obtained by deleting all tests for piles other than steel pipe piles, piles with oversized cover plates, piles in pre-bored or jetted holes, tests where the quality of the data was questionable, tests where a load-settlement curve was unavailable, and tests where insitu vertical effective stresses could not be estimated with acceptable accuracy. In addition, only data for tests carried to plunging failure were used.

Each soil type (i.e., cohesionless and cohesive) was individually analyzed by the methods; they are discussed separately below.

Cohesionless Soils

Only 66 load tests met the soil type requirements in addition to those mentioned above. One method was used to predict the pile capacities. It was a slightly amplified version of the method recommended by the American Petroleum Institute (API) and was referred to as the APIS method. This method was chosen because of its widespread use for predicting pile capacities in cohesionless soils based on visual soil classification.

Measured (Q_m) and computed (Q_c) pile capacities were plotted and their mean value and standard deviation calculated. The results indicated that, on average, the APIS method led to about a 20% overprediction of pile capacities and the scatter (as measured by the standard deviation of Q_c/Q_m) was large.

A revised method of analysis, termed method NSA1, was introduced to better correlate the computed versus measured capacities. Data were obtained for 21 tests on instrumented piles, six of which were tested in both compression and tension and 15 in compression only, and 30 tests on non-instrumented piles in tension. A separate analysis for steel H-piles, where the side capacity was calculated using the area of the

enclosing rectangle, indicated that K should be taken as 0.8 if the same values of d are to be used.

When the revised method was applied to the original data set used to evaluate the APIS method, a 10% reduction (on average) in overprediction of capacity was observed, but, more importantly, a large reduction in scatter of the ratio of calculated to measured pile capacities resulted.

Cohesive Soils

The final data set reduced to 84 load tests after considering the soil type and above mentioned requirements and rejecting tests if either the pile tip was in sand or a major part of the side capacity came from sand (usually >30%). Of these, 27 were loaded in tension and 57 were in compression.

Five methods were used to predict pile capacities: the ALP1 (Tomlinson, 1957), ALP2 (Tomlinson, 1971), APIC (1980 RP2A Recommended Practice), LAM1 (Vijayvergiya and Focht, 1972), and LAM2 (Kraft et al. 1981) methods. Measured pile capacities were compared with values predicted using these methods. Mean values and standard deviations were also calculated.

The two lamda methods had the least scatter but tended to overpredict capacities by about 20% (on average). The APIC method had slightly more scatter but overpredicted capacities by only about 13% (on average). The two alpha methods had the largest scatter and the greatest differences between measured and predicted capacities. The scatter in all of the methods tended to correlate with sampling and testing quality.

To reduce the scatter, the analyses utilized a standard strength which was taken as the unconsolidated-undrained triaxial compressive shearing strength measured on samples of high quality, preferably samples taken from a pushed thin walled sampler of three inches in diameter or more.

FLAATE, 1964

Flaate's work includes 116 load tests on timber, steel, and precast concrete piles driven into sandy soils. All driving resistance values were obtained at end of driving (EOD). Hiley, Janbu, and Engineering News formulas were selected for evaluation. Flaate reported the Janbu, Hiley, and Engineering News formulas give very good, good, and poor predictions of static capacity, respectively. Flaate suggested that a Factor of Safety equal to 12 may be required for the EN formula. The measured and predicted pile capacities are given in Table 3.1.

OLSON AND FLAATE, 1967

The load tests used by Olson and Flaate are similar to those presented in Flaate's (1964) work, but only 93 of the 116 load tests were used. Olson and Flaate eliminated load tests exceeding 100 tons for timber piles and 250 tons for concrete and steel piles because it is common practice for load tests to be conducted when pile capacities greater than 250 tons are required. However, the exclusion of these load tests has minimal effects on the conclusions. An additional column is added in the summary table (table 3.1) to identify hammer type (gravity hammer versus other types of hammers). It will be shown later that the two types of hammers (gravity hammer versus other) need to be considered separately when comparing predicted versus measured.

Olson and Flaate compared seven different dynamic pile-driving formulas: Engineering News, Gow, Hiley, Pacific Coast Uniform Building Code, Janbu, Danish and Gates. Janbu was found to be the most accurate of the seven formulas for timber and steel piles. However, it was concluded that no formula was clearly superior. Danish, Janbu, and Gates exhibited the highest average correlation factors; however, since the Gates formula was simpler than the other formulas, Gates was recommended as the most reasonable formula.

Original Gates Equation

Gates originally developed his pile driving formula in 1957. The empirical solution is as follows:

$$R_u = \frac{6}{7} \sqrt{eE_r} \log(10N_b) \quad (3.1)$$

where R_u is the predicted capacity (in kips), e is efficiency, E_r is rated or observed hammer energy (in ft-lbs), and N_b is the number of hammer blows to penetrate the pile one inch.

Modified Gates Equation (Olson and Flaate)

Olson and Flaate offered a modified version of the original Gates equation. The modifications were based on a statistical fit through the predicted versus measured data. Their modifications are as follows:

$$R_u = 1.11 \sqrt{eE_r} \log(10N_b) - 34 : \text{for timber piles} \quad (3.2)$$

$$R_u = 1.39 \sqrt{eE_r} \log(10N_b) - 54 : \text{for concrete piles} \quad (3.3)$$

$$R_u = 2.01 \sqrt{eE_r} \log(10N_b) - 166 : \text{for steel piles} \quad (3.4)$$

$$R_u = 1.55 \sqrt{eE_r} \log(10N_b) - 96 : \text{for all piles} \quad (3.5)$$

As before, units of R_u are in kips, E_r is in units of ft-lbs, and N_b is in blows per inch.

Modified Gates Equation (USDOT)

The FHWA pile manual recommends a modified Gates formula. Their equation is as follows:

$$R_u = 1.75 \sqrt{eE_r} \log(10N_b) - 100 \quad (3.6)$$

A similar equation can be obtained by averaging the equations for steel and concrete piles proposed by Olson and Flaate.

FRAGASZY et al. 1988, 1989

The purpose of the study by Fragaszy et al. was to clarify whether the Engineering News formula should be used in western Washington and northwest Oregon. Fragaszy et al. collected 103 individual pile load tests which were driven into a variety of soil types. Thirty-eight of these piles had incomplete data, while 2 of them were damaged during driving. The remaining 63 piles were used. Only 4 of the 63 piles have details that would allow wave equation analyses to be conducted, thus only dynamic formulas are compared. The data are believed to be representative of driving resistances at the end of initial driving (EOD). As a result of the study, the following conclusions were drawn: (1) the EN formula with a factor of safety 6 may not provide a desirable level of safety, (2) other formulas provide more reliable estimates of capacity than the Engineering News formula, (3) no dynamic formula is clearly superior although the Gates method preformed well, and (4) the pile type and soil conditions can influence the accuracy of the formulas.

PAIKOWSKY et al., 1994

Two large data sets were collected and interpreted in this study. One set of pile data (labeled as PD/LT) had 208 dynamic measurements on 120 piles and had static load tests for each pile. The other data set (labeled as PD) contained 403 piles monitored during driving but did not contain results of static load tests.

The PD/LT data set contained information on results of static load tests, PDA measurements and CASE interpretations of axial capacity, interpretations of capacity based on CAPWAP analysis, CASE damping coefficients, and the measured energy method. The PD dataset contained information from CAPWAP analyses and from the Measured Energy method and a summary table of predicted and measured capacity is given in Table 3.3.

This effort identifies the Measured Energy method as an excellent method for predicting axial capacity of piles using EOD behavior. Paikowsky et al concluded that for EOD measurements, the Measured Energy method gives, on the average,

more accurate results than CAPWAP or PDA and therefore should be used as an additional method for predicting pile capacity.

DAVIDSON et al, 1996

Davidson et al. (1996) and his co-workers collected information on 101 driven concrete piles and compared the measured capacity with predictions using static formulas (SPT94), PDA, and CAPWAP. The database is given in Table 3.4. They report that the SPT94 method under-predicts capacity. The best method was reported to be CAPWAP using driving information at the beginning of restrike (BOR). On the average, using EOD information resulted in under-prediction of pile capacity for both PDA and CAPWAP predictions.

ESLAMI, 1996

Eslami investigated the use of the static cone penetrometer to predict pile capacity. Although the use of the static cone penetrometer is beyond the scope of this study, it is included to present the reader with a perspective of the accuracy of pile prediction that can be obtained from methods that do not use pile driving resistance to predict capacity. Eslami investigated several cone methods including those proposed by Schmertmann (1978), DeRuiter (1971), Meyerhof (1976), and Tumay (1981). Predicted and measured capacities are given in Table 3.5.

DATABASE FROM FHWA

The Federal Highway Administration (FHWA) made available their database on driven piling as developed and described in Rausche et al. (1996). Although the database includes details for 200 piles, only 123 load tests (out of the 200) present enough information to be useful for this study.

The database includes several pile types, lengths, soil conditions, and pile driving hammers. Unique features of this database include the predictions based on several methods such as WEAP, PDA, and CAPWAP. The database provides enough

information that additional capacities can be predicted using methods such as Engineering News Formula, Gates Formula, and the Measured Energy approach.

Measured capacity, along with predicted capacity using six methods are given in Table 3.6 for the driving resistance at the end of driving (EOD). The six predictive methods are the Engineering News Formula (EN), the Gates Method, the Wave Equation Analysis Package (WEAP), the Measured Energy Approach (ME), the Pile Driving Analyzer (PDA), and CAPWAP. The first three methods allow capacities to be predicted based on the estimates of energy and visual measurement of pile penetration during driving. The last three methods (ME, PDA, and CAPWAP) require instrumentation to measure the dynamic change of stress and displacement in the pile. Specific details for each method are given elsewhere; however, Table 3.6 lists these six predictive methods in the six columns (EN, GATES, WEAP, ME, PDA, CAPWAP).

The columns are arranged from left to right in increasing levels of effort and resources to predict capacity, thus, Gates requires (slightly) more effort to predict capacity than the EN formula, but WEAP requires more than both EN and Gates. CAPWAP requires the greatest effort of the six methods.

Another unique and important feature of this database is that there are several piles which were re-driven (or re-struck) at some time after initial driving. Pile capacity, along with capacity predicted using the driving information at the beginning of restrike (BOR) is given in Table 3.7. The column headings for this table are identical to the previous table (Table 3.7), but estimates of capacity can differ significantly.

SUMMARY

Loadtest results and background have been presented for several collections of load test databases. The databases include those developed by Flaate (1964), Olson and Flaate (1967), Fragaszy et al. (1988), Paikowski et al. (1994), Davidson et al. (1996), and by the FHWA (Rausche et al. 1996). An additional database reporting cone penetration tests (Eslami) was also presented.

Table 3.1 Load test data used by Flaate (1964), and by Olson and Flaate (1967)

LTN	Pile Type	Measured Capacity (kips)	Hammer Type	Predicted Capacities			
				Q _{EN} (kips)	Q _{Hiley} (kips)	Q _{Janbu} (kips)	Q _{Gates} (kips)
1. c01	Precast Conc.	154	gravity	106	146	164	115
2. c02	Precast Conc.	154	gravity	78	134	166	109
3. c03	Precast Conc.	198	gravity	82	128	198	117
4. c04	Precast Conc.	264	gravity	84	120	198	122
5. c05	Precast Conc.	242	gravity	84	120	228	122
6. c06	Precast Conc.	276	gravity	84	110	210	122
7. c07	Precast Conc.	140	steam/single	390	136	262	135
8. c08	Concrete	68	gravity	58	36	62	78
9. c09	Concrete	70	gravity	52	34	52	71
10. c10	Concrete	160	gravity	74	110	172	125
11. c11	Concrete	146	gravity	74	108	166	122
12. c12	Concrete	242	gravity	150	170	258	194
13. c13	Concrete	264	gravity	180	132	304	166
14. c14	Concrete	592	steam/single	910	240	416	246
15. c15	Precast Concrete	190	steam/single	796	316	432	243
16. c16	Precast Concrete	580	steam/single	632	260	496	328
17. c17	Precast Concrete	276	steam/single	490	186	318	208
18. s01	HP 24	112	gravity	74	92	90	86
19. s02	HP 24	88	gravity	74	92	90	86
20. s03	HP 24	90	gravity	80	102	102	91
21. s04	HP 24	110	gravity	80	106	106	93
22. s05	HP 24	134	gravity	84	118	118	97
23. s06	HP 24	90	gravity	90	132	134	102
24. s07	HP 24	158	gravity	90	132	134	102
25. s08	HP 24	90	gravity	90	152	142	104
26. s09	HP 24	134	gravity	90	152	142	104
27. s10	HP 24	178	gravity	98	160	160	112
28. s11	HP 24	158	gravity	102	214	202	118
29. s12	HP 24	220	gravity	102	180	184	118
30. s13	Steel	310	gravity	348	426	386	199
31. s14	Steel	248	gravity	238	300	294	167
32. s15	Steel	440	gravity	268	420	364	189
33. s16	Steel	236	gravity	126	220	268	135
34. s17	Steel	214	gravity	122	214	236	129
35. s18	Steel	406	gravity	228	330	444	183
36. s19	Steel	488	gravity	280	482	578	223
37. s20	Steel	674	gravity	230	418	400	186
38. s21	Steel	466	gravity	148	290	326	180
39. s22	Steel	594	gravity	254	614	464	225
40. s23	Steel	610	gravity	258	654	474	233
41. s24	Steel	592	gravity	258	634	508	233
42. s25	Steel	620	gravity	262	654	514	243
43. s26	H	280	steam/double	1200	258	290	221
44. s27	H	300	steam/double	1410	270	292	240
45. s28	H	280	steam/double	1450	270	292	243
46. s29	H	180	steam/double	900	226	258	196
47. s30	H	160	steam/double	940	230	260	200
48. s31	Pipe	300	steam/single	936	238	232	196
49. s32	Pipe	240	steam/single	900	238	226	193
50. s33	HP	198	steam/single	394	110	200	129
51. s34	HP	48	gravity	52	38	52	70
52. s35	HP	16	gravity	8	12	18	34
53. s36	H	580	steam/single	756	200	342	194
54. s37	pipe	570	steam/single	908	236	412	208
55. s38	H	270	steam/single	518	230	282	167
56. s39	pipe	700	steam/single	1580	252	478	258
57. s40	pipe	630	steam/single	1250	274	456	236
58. s41	pipe	600	steam/single	934	248	520	250
59. s42	pipe	720	steam/single	2790	286	534	345

Table 3.1 (cont'd) Load test data from Flaate (1964) , and by Olson and Flaate (1967)

LTN	Pile Type	Measured Capacity (kips)	Hammer Type	Predicted Capacity			
				Q _{EN} (kips)	Q _{Hiley} (kips)	Q _{Janbu} (kips)	Q _{Gates} (kips)
60. s43	monotube	340	Steam/single	1286	104	192	231
61. s44	monotube	286	steam/single	1386	110	182	243
62. s45	pipe	516	steam/single	1000	118	300	243
63. s46	pipe	614	steam/single	2790	286	532	345
64. s47	pipe	346	steam/single	604	216	306	178
65. s48	pipe	924	steam/single	2340	264	578	345
66. s49	H	88	steam/single	514	286	310	154
67. s50	H	126	steam/single	530	270	294	156
68. s51	H	110	steam/single	300	148	180	125
69. s52	H	84	steam/single	256	76	154	118
70. s53	H	54	steam/single	200	82	118	106
71. s54	H	108	steam/single	360	136	198	135
72. s55	H	120	steam/single	372	120	188	139
73. w01	wood	76	gravity	60	58	74	79
74. w02	wood	76	gravity	66	70	92	88
75. w03	wood	70	gravity	52	52	58	70
76. w04	wood	68	gravity	56	58	66	74
77. w05	wood	46	gravity	42	44	40	58
78. w06	wood	44	gravity	50	60	54	69
79. w07	wood	214	gravity	180	216	190	145
80. w08	wood	234	gravity	180	410	264	190
81. w09	wood	80	steam/double	154	52	72	90
82. w10	wood	80	steam/double	124	46	62	82
83. w11	wood	80	steam/double	136	48	68	85
84. w12	wood	80	steam/double	304	96	90	116
85. w13	wood	86	steam/double	172	54	88	94
86. w14	wood	50	steam/single	80	40	48	65
87. w15	wood	52	steam/single	86	50	56	67
88. w16	wood	142	steam/single	310	136	146	127
89. w17	wood	74	steam/single	170	78	90	91
90. w18	wood	90	steam/single	226	82	102	104
91. w19	wood	374	gravity	400	368	406	232
92. w20	wood	246	gravity	348	496	418	266
93. w21	wood	242	gravity	252	248	280	177
94. w22	wood	324	gravity	276	318	312	197
95. w23	wood	196	gravity	76	128	172	134
96. w24	wood	192	gravity	76	114	178	134
97. w25	wood	100	gravity	98	60	90	94
98. w26	wood	106	gravity	126	94	110	112
99. w27	wood	90	steam/single	24	8	108	32
100. w28	wood	56	steam/single	78	28	42	61
101. w29	wood	88	steam/single	164	66	86	96
102. w30	wood	80	steam/single	184	70	96	102
103. w31	wood	136	gravity	148	210	132	121
104. w32	wood	186	gravity	180	288	198	146
105. w33	wood	136	gravity	126	176	114	105
106. w34	wood	210	gravity	168	262	188	137
107. w35	wood	136	gravity	110	166	118	106
108. w36	wood	148	gravity	170	188	148	129
109. w37	wood	106	gravity	128	92	104	112
110. w38	wood (oak)	86	steam/single	202	82	112	99
111. w39	wood (oak)	98	steam/single	146	68	84	87
112. w40	wood (oak)	74	steam/single	182	76	98	95
113. w41	wood (cypress)	94	steam/single	202	80	112	99
114. w42	wood	108	steam/single	322	166	178	129
115. w43	wood	136	steam/single	322	156	168	129
116. w44	wood	132	steam/single	376	202	222	137

Table 3.2 Load test data from Fragaszy et al. (1988)

LTN	Pile Type	Measured Capacity (kips)	Predicted Capacities			
			Q _{EN} (kips)	Q _{Hiley} (kips)	Q _{Janbu} (kips)	Q _{Gates} (kips)
1. HP-3	Steel H Pile	284	732	400	280	194
2. HP-4	Steel H Pile	158	130	124	90	94
3. HP-5	Steel H Pile	244	612	372	268	186
4. HP-6	Steel H Pile	364	494	224	200	166
5. HP-7	Steel H Pile	298	462	294	232	162
6. CP-4	Closed Steel Pipe Pile	494	2140	780	600	324
7. CP-6	Closed Steel Pipe Pile	246	952	672	394	220
8. OP-3	Open Steel Pipe Pile	424	896	500	428	230
9. OP-4	Open Steel Pipe Pile	450	1772	590	352	308
10. FP-1	Concrete Filled Steel Pipe Pile	290	858	524	430	212
11. FP-2	Concrete Filled Steel Pipe Pile	158	226	154	134	124
12. FP-3	Concrete Filled Steel Pipe Pile	600	1548	682	508	274
13. FP-6	Concrete Filled Steel Pipe Pile	244	736	350	226	200
14. FP-7	Concrete Filled Steel Pipe Pile	442	1234	556	264	270
15. FP-8	Concrete Filled Steel Pipe Pile	522	3072	860	288	386
16. FP-9	Concrete Filled Steel Pipe Pile	338	1264	624	268	272
17. SC-3	Square Prestressed Concrete Pile	210	842	452	436	210
18. SC-4	Square Prestressed Concrete Pile	204	318	168	156	144
19. SC-5	Square Prestressed Concrete Pile	176	196	108	110	114
20. SC-6	Square Prestressed Concrete Pile	110	196	122	108	114
21. SC-8	Square Prestressed Concrete Pile	280	416	230	224	164
22. SC10	Square Prestressed Concrete Pile	260	218	140	122	120
23. SC-13	Square Prestressed Concrete Pile	376	534	240	286	170
24. SC-14	Square Prestressed Concrete Pile	482	612	346	316	202
25. SC-15	Square Prestressed Concrete Pile	510	724	366	334	216
26. SC-16	Square Prestressed Concrete Pile	170	534	272	266	188
27. SC-17	Square Prestressed Concrete Pile	390	1676	564	492	302
28. OC-1	Octagonal Prestressed Concrete Pile	1036	5580	724	742	518
29. OC-2	Octagonal Prestressed Concrete Pile	900	3266	606	722	410
30. OC-3	Octagonal Prestressed Concrete Pile	1240	7460	1044	1120	626
31. OC-6	Octagonal Prestressed Concrete Pile	486	1624	188	234	284
32. OC-9	Octagonal Prestressed Concrete Pile	496	872	262	242	230
33. OC10	Octagonal Prestressed Concrete Pile	254	3710	604	692	434
34. OC11	Octagonal Prestressed Concrete Pile	248	3642	404	546	428
35. OC14	Octagonal Prestressed Concrete Pile	304	388	194	208	158
36. OC16	Octagonal Prestressed Concrete Pile	170	196	118	106	114
37. HC-1	Hollow Concrete	512	2998	428	588	386
38. HC-2	Hollow Concrete	592	2172	404	468	324
39. HC-4	Hollow Concrete	600	2560	1018	732	352
40. HC-5	Hollow Concrete	600	2304	706	688	342
41. HC-6	Hollow Concrete	620	3600	884	888	416
42. ST-1	Raymond Step Taper Pile	302	914	286	486	212
43. ST-2	Raymond Step Taper Pile	296	796	470	540	200
44. ST-3	Raymond Step Taper Pile	310	720	320	420	192
45. ST-4	Raymond Step Taper Pile	284	732	216	322	194
46. ST-5	Raymond Step Taper Pile	280	796	340	446	200
47. ST-6	Raymond Step Taper Pile	288	664	252	342	186
48. ST-7	Raymond Step Taper Pile	480	856	482	416	212
49. ST-8	Raymond Step Taper Pile	326	688	320	274	194
50. ST-9	Raymond Step Taper Pile	600	1680	462	256	284
51. ST-10	Raymond Step Taper Pile	580	1710	812	330	288
52. ST-11	Raymond Step Taper Pile	426	376	196	212	150
53. ST-12	Raymond Step Taper Pile	418	684	348	396	190
54. ST-15	Raymond Step Taper Pile	338	1044	688	640	228
55. ST-17	Raymond Step Taper Pile	324	940	638	602	220
56. ST-22	Raymond Step Taper Pile	310	576	350	306	182
57. ST-23	Raymond Step Taper Pile	336	602	276	322	174
58. T-1	Timber Pile	336	604	320	154	176
59. T-6	Timber Pile	140	280	158	134	130
60. T-7	Timber Pile	132	206	146	114	114
61. T-8	Timber Pile	98	90	84	58	78
62. T-10	Timber Pile	96	224	144	112	118
63. T-11	Timber Pile	114	36	34	2	38

Table 3.3 Load test data from Pakowski et al. (1994)

LTN	Pile Type	Measured Capacity (kips)	Predicted Capacities			
			Q_{EN} (kips)	Q_{Hiley} (kips)	Q_{Janbu} (kips)	Q_{Gates} (kips)
1	HP10x42	304	230	362	375	484
3	HP10x42	304			431	535
4	PSC12"sq	358	226	418	305	487
6	PSC14"sq	378	179	480	297	621
8	CEP12.75"	284	244	401	288	582
10	HP14x89	926	367	569	731	689
12	CEP 14"	650	511	708	521	696
14	CEP 26"	598	496	716	700	1169
16	PSC24"oct	760	530	646	731	1158
18	HP114x117	776	566	584		
19	RC24"sq	1700	658	763	767	1269
21	PSC20"sq	1360	559	839	729	1207
23	CEP 18"	440	346	357	499	734
25	CEP 18"	408	424	524	526	781
27	CEP 18"	342	323	412	340	426
29	CEP12.75"	316	270	342	265	363
31	CEP12.75"	368	375	402	340	353
33	CEP 14"	330	285	246	319	306
35	CEP 14"	209	184	179	217	279
37	CEP 48"	1300	295	1145	652	1154
39	CEP 48"	1000		1708		1280
41	PSC 18"sq	370	205	302	257	462
43	PSC 18"sq	370			382	840
44	PSC 18"sq	550	428	568	489	950
46	PSC 18"sq	550			599	896
47	PSC 24"sq	625	340	547	307	744
49	PSC 24"sq	625			587	826
50	PSC 24"sq	817	446	772	604	1062
52	PSC 24"sq	817			852	1448
53	PSC 36"sq	1140	662	1543	945	2238
55	HP14x73	315	194	336	198	389
57	HP14x73	345	159	305	179	285
59	HP14x73	765	342	476	652	831
61	Monotube	243	210	211	239	280
63	PSC14"sq	366	288	392	295	403
65	PSC24"sq	400	136	258	272	598
67	PSC24"sq	400			350	893
68	CEP 9.6"	540	410	444	500	433
70	CEP 9.6"	366			342	430
71	CEP 11.73"	468			409	540
72	CEP 11.73"	468			489	543
73	CEP 10.24"	189			241	369
74	CEP 12.75"	242			207	408
75	CEP 12.75"	660			610	782
76	CEP 12.75"	660			584	742
77	CEP 12.75"	660	558	704		
78	PSC24"sq	610	509	751	506	781
80	PSC24"sq	610			536	777
81	PSC24"sq	453	450	597	480	713
83	PSC24"sq	453			443	772

Table 3.3 (cont'd) Load test data from Pakowski et al. (1994)

LTN	Pile Type	Measured Capacity (kips)	Predicted Capacity			
			Q_{EN} (kips)	Q_{Hiley} (kips)	Q_{Janbu} (kips)	Q_{Gates} (kips)
84	PSC30"sq	900			941	1769
85	PSC30"sq	820			805	1448
86	OEP 60"	1984	1775	2729		
87	OEP 60"	1984	1800	2870		
88	OEP 60"	2866	2366	3042		
89	OEP 48"	1345	1252	1872		
90	OEP 48"	3285	2778	2964		
91	HP12x74	322			260	274
92	CEP12.75"	330			360	468
93	HP12x74	612			650	618
94	CEP12.75"	600			580	526
95	T. Timber	122			139	183
96	PSC 12"sq	402			334	425
97	PSC 12"sq	415			420	732
98	HP12x53	284			279	320
99	PSC 20"sq	380			361	519
100	PSC 20"sq	580			474	813
101	PSC 20"sq	620			612	1169
102	PSC 20"sq	600			582	985
103	PSC 10"sq	250			197	241
104	PSC 10"sq	270			232	274
105	PSC 18"sq	344			505	630
106	PSC 18"sq	510			616	665
107	PSC 54"sq	920			807	1927
109	CEP 13.38"	440	365	424		
110	CEP 9.75"	256	293	339		
111	CEP 9.75"	188	275	281		
112	CEP 10"	440	413	453		
113	CEP 13.38"	280	317	302		
114	CEP 13.38"	380	341	413		
115	CEP 14"	464	214	557		
116	CEP 14"	480	205	511		
117	CEP 14"	450	492	599		
118	CEP 14"	640	267	566		
119	CEP 14"	390	305	570		
120	CEP 14"	250	239	399		
121	CEP 14"	500	520	674		
122	OEP 36"	1120	1109	1357		
123	CP 12.75"	360	250	357		
124	RC 10.8"sq	652	383	464		
125	RC 10.8"sq	652	611	698		
126	RC 10.8"sq	558	259	339	564	653
128	HP10x42	330	398	434		
129	HP12x74	500	457	605		
130	HP12x74	580	512	623		
132	HP12x74	340	405	483		
133	HP10x57	334	446	532		
134	HP12x74	240	455	530		
135	HP10x57	300	426	491		
136	HP10x57	360	524	630		

Table 3.3 (cont'd) Load test data from Pakowski et al. (1994)

LTN	Pile Type	Measured Capacity (kips)	Predicted Capacity			
			Q_{EN} (kips)	Q_{Hiley} (kips)	Q_{Janbu} (kips)	Q_{Gates} (kips)
137	HP12x74	460	561	599		
138	CP 9.625"	502	522	636		
139	CP 9.625"	271			479	625
140	VC 24"sq	958	472	629	538	660
142	VC 24"sq	958	368	545	462	612
144	VC 24"sq	958			925	1421
149	VC 24"sq	715	459	549	555	665
151	VC 24"sq	715			452	970
152	VC 24"sq	715			442	930
153	PSC 18"sq	315	224	303	282	415
155	PSC 18"sq	315			296	505
156	VC 24"sq	524	431	624	503	715
158	VC 24"sq	524			565	834
159	VC 24"sq	812	517	474	669	722
161	VC 24"sq	812			803	881
162	VC 24"sq	808	311	513	780	996
164	VC 24"sq	976	353	549	641	745
166	VC 24"sq	976			761	918
167	PSC 24"sq	500			564	978
168	PSC 24"sq	500			502	998
169	VC 30"sq	1250			568	1008
170	VC 30"sq	1250			584	1167
171	VC 30"sq	1435			814	1803
172	VC 30"sq	1435	639	1827		
173	VC 30"sq	1515			820	1776
174	VC 30"sq	1515			749	1824
175	VC 30"sq	1515			683	1501
176	VC 30"sq	1515	845	1641		
177	VC 30"sq	643			619	864
178	VC 30"sq	643			444	1306
179	VC 30"sq	917			776	855
180	VC 30"sq	917	449	1069		
181	VC 30"sq	1463			812	1001
182	VC 30"sq	1463			949	1422
183	VC 30"sq	1463			909	1289
184	VC 30"sq	1410	857	1238	850	1225
186	VC 30"sq	1410			485	1162
187	PSC 24"sq	960	488	555	619	788
189	PSC 24"sq	960	716	957	563	1113
191	HP 12x74	800	439	657	715	898
193	HP 12x74	800	650	923		
194	CP 12.75"	490	290	418	355	520
196	CP 12.75"	490	401	546		
197	PSC 12"sq	466	400	625		
198	#14 Timber	164	143	248		
199	HP 12x74	354	432	553	294	504
201	HP 12x74	556	575	720	616	707
203	HP 12x53	410	484	506	395	490
205	CP 7.063"	140			166	169
206	HP12x89	730	218	564		
207	HP12x89	325			100	266
208	CP 12.75"	340	248	306		

Table 3.4 Load test data from Florida DOT (Davidson et al. 1996)

LTN	Measured Capacity (kips)	Predicted Capacities				
		Q _{PDA-EOD} (kips)	Q _{PDA-BOR} (kips)	Q _{CAPWAP-EOD} (kips)	Q _{CAPWAP-BOR} (kips)	Q _{SPT94} (kips)
1. 1	997	1025	970	574	846	893
2. 2	1549	1225		1301		976
3. 3	1542	1500		1409		240
4. 4	740	750	1080	706	914	
5. 5	922	500	996	367	925	567
6. 7	672	612	680	459	442	245
7. 8	308	318	410	224	296	8
8. 9	498	620	636	431	565	124
9. 10	739	664	920	517	803	184
10. 11	734	480	884	311	779	445
11. 12	955	712	884	353	761	
12. 13	425	266	520	198	524	110
13. 14	579		538		474	761
14. 15	369		362		361	503
15. 16	835			255	445	443
16. 23	497	232	724		502	177
17. 24	1231	1044	732	568	584	527
18. 25	1405	964	1384		814	635
19. 26	1481	832	900		683	474
20. 27	626		800		444	693
21. 28	910	312	832		776	694
22. 29	1453	960	1048		909	557
23. 30	1368	908		857	485	369
24. 31	940	736	688	716	563	167
25. 32	794		601		850	865
26. 33	450	245		234	544	510
27. 34	309	360			320	463
28. 35	396	260			407	313
29. 36	355	305			425	287
30. 39	632	490	480	509	536	194
31. 42	468	430	420	450	443	259
32. 45	754	464	848	377	781	508
33. 46	1090	860	1164		1085	591
34. 47	563	876	892	808	920	471
35. 48	919	580	1000		941	
36. 49	832	500	890		805	584
37. 50	869	596	568	658	587	513
38. 52	910	880	1000		830	919
39. 53	786	820	840		725	551
40. 54	974	774	1080	700	901	817
41. 55	1089	1082	1268	1049	1464	1053
42. 56	1110	1280	1492	1300	1403	757
43. 57	1103	1048	1178	1030	1150	927
44. 86	200					119
45. 93	768	1000	1330		1220	754
46. 94	567	630	860		799	583
47. 95	1047	1040	1400		1347	762
48. 96	1116	1020	1560		1400	720
49. 97	600	850	1070		899	361
50. 98	679	1040	950		950	831
51. 100	199			245	235	158
52. 101	275			264	281	244

Table 3.5 Load test data from Eslami (1996)

LTN	Pile Type	Meas Cap (kips)	Predicted Capacity (kips)					
			Q _{Schmertmann}	Q _{DeRuiter}	Q _{French}	Q _{Meyerhof}	Q _{Tumay}	Q _{Eslami}
1	P, St.	61	32	57	49		146	55
2	P, St.	121	97	126	142		224	142
3	P, St.	236	185	196	237	225		255
4	P, St.	1574	1509	1127	1552	1515		2138
5	P, St.	180	210	271	203		188	210
6	HP, St.	182	218	272	203		185	210
7	P, St.	81	73	76	95	120		113
8	Sq., Conc	202	123	85	149	133		235
9	Sq., Conc	281	234	164	276	240		346
10	Oct., Conc	1147	1183	1027	976	1106		1342
12	P, St.	922	746	815	1006	901		1157
15	P, St.	967	812	827	709	855		1077
17	P, St.	375	767	830	765	941		976
18	Sq., Conc	180	251	125	232	236		198
20	Sq., Conc	663	331	701	464		739	685
21	P, St.	585	237	510	265		532	495
22	Tr., Conc	486	219	404	267		505	412
23	P, St.	384	187	312	193		389	330
27	Sq., Conc	587	536	583	492		622	662
35	Sq., Conc	106	61	115	89		98	178
36	P, St.	135	113	152	121		101	157
37	P, Conc.	776	624	596	947	984		940
43	P, St.	236	347	292	237	342		368
58	HP, St.	697	348	773	597	432		611
59	HP, St.	450	288	503	249		302	392
63	Sq., Conc	944	649	501	630	739		898
64	Sq., Conc	247	300	249	279	317		359
71	Sq., Conc	225	233	220	199	203		230
72	Sq., Conc	178	128	108	243	237		220
77	P, St.	337	324	268	250	332		362
79	Sq., Conc	303	300	231	503	510		393
80	P, St.	19	30	18	13			20
81	P, St.	175	112	183	95		123	146
83	P, St.	180	116	215	97		128	171
101	P, St.	261	147	199	142		231	215
102	P, St.	380	218	320	294		317	355
13	P, St.	742	653	677	897	745		893
14	P, St.	629	653	677	897	745		893
26	Sq., Conc	455	404	444	375		465	496
28	Sq., Conc	259	367	269	445	324		365
29	Sq., Conc	410	416	502	719	648		671
30	Sq., Conc	283	204	172	369	228		258
34	P, St.	379	273	653	187		296	340
38	P, St.	641	676	686	801	1072		1094
39	HP, St.	450	715	571	597	658		572
41	HP, St.	450	705	606	484	730		800
42	HP, St.	719	697	598	462	711		774
44	P, St.	196	440	379	309	452		470
45	P, St.	292	507	441	391	578		588
46	HP, St.	135	187	132	277	233		316
48	HP, St.	196	185	226	469	339		405
56	Rd., Conc	73	154	80	80			87
57	Rd., Conc	126	271	176	141			179
69	Rd., Conc	1147	1109	913	963	1186		1353

Table 3.5 (cont'd) Load test data from Eslami (1996)

LTN	Pile Type	Meas Cap. (kips)	Predicted Capacity (kips)					
			Q _{Schmertmann}	Q _{DeRuiter}	Q _{French}	Q _{Meyerhof}	Q _{Tumay}	Q _{Eslami}
70	Rd., Conc	1349	1073	947	831			1098
73	Sq., Conc	360	509	455	595	392		640
74	Sq., Conc	157	185	134	284	240		234
75	Sq., Conc	303	230	206	324	278		341
76	P, St.	133	119	90	145	172		206
85	P, St.	43	46	45	29			51
86	P, St.	103	47	48	31			94
87	P, St.	90	79	103	54			98
88	P, St.	91	79	103	54			98
89	P, St.	85	79	103	54			98
90	P, St.	88	79	103	54			98
91	P, St.	70	54	69	36			66
92	P, St.	79	54	69	36			66
93	P, St.	65	54	69	36			66
94	P, St.	63	54	69	36			66
95	P, St.	79	54	69	36			66
96	P, St.	24	34	13	20			22
97	P, St.	84	124	47	74			84
98	P, St.	18	35	14	22			19
99	P, St.	19	36	18	24			12
100	P, St.	100	127	53	80			69
103	Sq., Conc	279	269	454	230		462	325
104	Sq., Conc	162	100	158	91		201	117
105	Sq., Conc	324	192	317	171		287	245
106	Sq., Conc	216	269	453	222		433	358
107	Sq., Conc	205	188	412	205		268	293
108	HP, St.	121	56	42	66	67		105
109	HP, St.	223	239	118	103	138		209
110	Sq., Conc	209	269	505	318		408	337
111	Sq., Conc	281	261	554	347		407	372
112	HP, St.	85	95	251	123		173	112
113	Sq., Conc	207	190	268	251	433		293
114	Sq., Conc	247	399	305	363	440		351
115	Sq., Conc	121	138	102	189	319		232
116	Sq., Conc	311	50	291	446	466		500
117	Sq., Conc	202	220	396	186		371	239
121	Sq., Conc	247	256	396	207		384	297
123	Sq., Conc	173	406	266	381	222		298
124	HP, St.	247	189	159	202	217		323
125	Sq., Conc	211	360	246	429	466		313
126	HP, St.	83	113	106	126	146		109
127	Sq., Conc	232	375	405	281	422		379
128	Sq., Conc	211	331	230	424	418		362
129	Sq., Conc	110	193	121	219	220		203
130	Sq., Conc	247	268	166	290	269		231
131	Sq., Conc	337	447	420	559	612		423
132	Sq., Conc	382	195	237	209	388		391
134	HP, St.	472	405	201	268	258		442
136	Sq., Conc	126	147	219	154		219	168
137	Sq., Conc	259	348	489	333		497	421
138	HP, St.	279	127	235	124		226	262
139	HP, St.	283	134	277	132		226	303
140	HP, St.	270	158	283	208		234	309
141	Sq., Conc	214	246	199	331	388		351

Table 3.6 Load test data using EOD information, from Rausche et al. (1996)

LTN	Pile Type	Meas. Cap. (kips)	EOD - Predicted Capacity (kips)					
			Q _{EN}	Q _{Gates}	Q _{WEAP}	Q _{ME}	Q _{PDA}	Q _{CAPWAP}
1	PSC	950	1361	297	300			368
2	PSC	953	1933	358				
3	PSC	710	1548	329	400			459
4	PSC	520	1503	310	320			431
5	PSC	800	1275	284	360			517
6	PSC	800	1385	330	400			311
7	PSC	980	1456	344	620			353
8	PSC	508	574	204	100			
9	PSC	520	2037	442	596	492		250
10	PSC	925	2149	403	750			550
11	PSC	835	1984	361	640			580
12	PSC	381	758	221	116			500
13	PSC	572	1369	305	460	301		213
14	PSC	650	1230	307	440	567		462
15	PSC	850	1533	379	547	548		382
16	PSC	1100	2804	575	1120	773		437
17	H	306	1014	225	185	1545		662
18	PSC	380	1184	249	380	377		774
19	PSC	383	1328	287	363	473		378
20	CEP	287	903	214	180	480		290
22	CEP	446	1381	277	240	451		229
23	CEP	440	1381	277	270	480		229
24	CEP	353	1309	271	270	431		179
25	PSC	1450	1593	460	1100	412		244
26	HT	330	800	193	200	767		351
27	HT	388	608	175	240	524		387
28	PSC	388	566	193	70	467		424
29	OEP	270	605	168		397		323
30	OEP	760	2557	357	580			559
31	H	284	605	183	150	576		194
								194
								159
								136
								474

Table 3. 6 Load test data using EOD information, from Rausche et al. (1996)

LTN	Pile Type	Meas. Cap. (kips)	EOD - Predicted Capacity (kips)					
			Q_{EN}	Q_{Gates}	Q_{WEAP}	Q_{ME}	Q_{PDA}	Q_{CAPWAP}
32	PSC	807	2178	474	1200	1107	1238	295
33	CEP/H	1262	7160	544	450	328		255
34	PSC	842	624	217	180	153		152
35	CEP	497	539	167	1479	426	366	351
36	CEP	784	1479	248	550	570		367
37	H	932	1157	236	580	708		511
38	CEP	660	1583	264	370			
39	H	509	1047	223	360			
40	CEP	375	1264	242	596	703	570	569
41	H	576	5400	479	660	902	676	676
42	OEP	732	4320	421	215	396	311	294
43	H	308	1179	233				
44	H	153	901	206	380	477	336	342
45	CSWP	757	1606	293				
46	H	498	575	194				
47	PSC	1410	1401	325				
48	PSC	1491	2965	551				
49	PSC	632	1783	369				
50	PSC	900	1689	374				
51	PSC	1447	2586	482				
-52	PSC	1376	2962	557				
-53	PSC	938	1648	336				
54	H	500	1174	240				
55	CEP	600	2489	337	420	687	500	496
56	PSC	792	1672	348	500	646	580	530
57	H	770	5362	469		575	579	566
58	RC	1620	2229	508	325	760	640	658
59	CEP	325	930	214	120	282	278	285
60	CEP	246	482	164	210	179	184	184
61	PSC	267	920	255		278	253	254

Table 3.6 Load test data using EOD information, from Rausche et al. (1996)

LTN	Pile Type	Meas. Cap. (kips)	EOD - Predicted Capacity (kips)					
			Q_{EN}	Q_{Gates}	Q_{WEAP}	Q_{ME}	Q_{PDA}	Q_{CAPWAP}
62	PSC	650	3172	510	800	751	490	509
63	PSC	472	2812	440	320	597	440	450
64	OEP	1514	1785	294	680	764	652	581
65	PSC	987	1382	302	500		230	
66	M	240	661	172	190	211	111	210
67	PSC	395	2092	397	335	498		275
68	PSC	1060	1989	369	350		280	
69	PSC	590	1245	267	140		152	
70	H	618	571	175	100		118	
71	H	313	893	223	110	279	222	215
72	OEP	600	1964	305	350	745	458	460
73	PSC	1095	4556	570			1060	
74	PSC	360	793	225				
75	PSC/H	503	1553	279	650	789	607	600
76	PSC/H	1045	4500	444	880		1150	
77	HT	1460	4793	445				
78	HT	1281	5133	464	660	691	548	554
79	CEP/C	740	6191	543	545	654	509	508
80	CEP/C	689	5536	489				
81	PSC	956	4647	460				
82	PSC	1000	4360	530	960	1133	669	529
83	PSC	967	1880	368	960	1199	859	574
84	PSC	820	2044	398	565	1012	594	706
85	PSC	1020	2627	594	770	932	550	555
86	CEP	659	3786	395	540			390
87	CEP	656	2943	354	623			
88	CEP	470	2515	322	410			
89	CEP	580	489	167	300	325	324	
90	CEP	380	186	100	66			
91	CEP	600	327	137	180			155

Table 3.6 Load test data using EOD information, from Rausche et al. (1996)

LTN	Pile Type	Meas. Cap. (kips)	EOD - Predicted Capacity (kips)						
			Q_{EN}	Q_{Gates}	Q_{WEAP}	Q_{ME}	Q_{PDA}	Q_{CAPWAP}	
92	CEP	657	300	131	120				187
93	CEP	380	300	131	175				150
94	H	580	4431	478	844		720	537	512
95	H	305	1894	279	260		538	423	405
96	H	340	1894	279	340		510	466	446
97	H	240	2512	332	330		580	447	455
98	H	310	2512	332	400		558	456	428
99	H	367	4034	427	390		613	513	524
100	H	480	3397	376	430		585	564	561
101	PSC	363	920	304	373		391	287	288
102	H	374	1980	291	300		466	447	428
103	H	521	2310	310	521			462	
104	H	378	2582	326	350			426	
105	H	635	2424	323	600			430	
117	H	1378	6745	537	1244		1446	1411	
118	H	474	1945	308			941	394	
119	H	296	1762	295			694	320	
120	H	575	3109	372			1187	425	
122	PSC	148	966	236			132	64	65
185	OEP	425	1385	276	400		345	300	304
187	CEP	109	111	77				61	
188	T	130	111	77				61	
189	PSC	119	136	91					
190	CEP	114	111	77				37	
191	PSC	644	1997	372					
192	G	158	659	176	107		229	91	
193	CEP	347	628	173	194		204	163	
194	M	383	726	182	75		260	239	60
196	PSC	414	494	187			211		45
197	PSC	511	566	216			262		59
198	PSC	555	688	250			173		91
199	PSC	541	648	223			193		
200	PSC	541	1701	389			211		103

Table 3.7 Load test data using BOR information, from Rausche et al. (1996)

LTN	Pile Type	Meas. Cap. (kips)	BOR - Predicted Capacity (kips)						
			Q_{EN}	Q_{Gates}	Q_{WEAP}	Q_{ME}	Q_{PDA}	Q_{CAPWAP}	
1	PSC	950	2789	479	1015				925
2	PSC	953	4955	598	1420				962
3	PSC	710	3432	445	980				452
4	PSC	520	2468	368	770				565
5	PSC	800	3444	547	990				803
6	PSC	800	2287	538	980				779
7	PSC	980	2295	519	1075				761
8	PSC	508	1661	473	810		522	280	518
9	PSC	520	2020	437	621		1797	540	580
10	PSC	925	3977	558	1380		1448	1038	941
11	PSC	835	4051	520	1230		839	853	805
12	PSC	381	2857	433	890		896	408	382
13	PSC	572	2268	397	705		1016	681	599
14	PSC	650	2302	456	900		1446	503	587
15	PSC	850	2930	591	1135		2402	893	852
16	PSC	1100	2678	545	1000			707	945
17	H	306			370			469	431
18	PSC	380	1458	276	345		497	389	305
19	PSC	383	1378	289	375		621	310	297
20	CEP	287	1716	278	350		582	413	288
22	CEP	446	2568	355	590		734	387	499
23	CEP	440	2568	355	570		781	659	526
24	CEP	353	1855	313	450		426	352	341
25	PSC	1450	1861	689	1800		1207		729
26	HT	330	1408	241	306		399	222	198
27	HT	388	481	154	170		333	169	179
28	PSC	388	1627	346	990		891	338	350
29	OEP	270	1257	233	270		295	181	261
30	OEP	760	2950	377	600		674	521	506
31	H	284	1513	263	370		381	369	279

Table 3.7 Load test data using BOR information, from Rausche et al. (1996)

LTN	Pile Type	Meas. Cap. (kips)	BOR - Predicted Capacity (kips)					
			Q _{EN}	Q _{Gates}	Q _{WEAP}	Q _{ME}	Q _{PDA}	Q _{CAPWAP}
32	PSC	807	2970	655	1380	1833	601	850
33	CEP/H	1262	7425	555	1050	1389	1009	975
34	PSC	842	1004	238	440	579		519
35	CEP	497	1114	228	265	344		277
36	CEP	784			365			351
37	H	932			570			731
38	CEP	660	3091	359	516	697		521
39	H	509	2928	351	565			
40	CEP	375	2748	341	475			
41	H	576	4950	453	662	819	527	543
42	OEP	732	5600	492	727	836	512	494
43	H	308	2600	328	370	437	321	300
44	CSWP	153	1219	231	215	249	231	179
45	H	757	6943	539	690	829	710	652
46	PSC	498	2047	387	850	992	491	475
47	PSC	1410	3214	632	1570	1918	889	818
48	PSC	1491	3236	639	1570			683
49	PSC	632	3154	602	1240	1602	598	567
50	PSC	900	3103	603	1370	844	765	772
51	PSC	1447	3156	614	1650	1528	821	843
52	PSC	1376	2495	442	1100			485
53	PSC	938	2480	402	915			
54	H	500	1908	289	445	774	517	524
55	CEP	600	2520	345	870	1113	820	700
56	PSC	792	2038	390	1005	1221	790	731
57	H	770			960			566
58	RC	1620	2548	605	1190	1446	830	767
59	CEP	325	798	198	315	348		319
60	CEP	246	864	206	330	280	217	217
61	PSC	267	1020	279	425	397	254	264

Table 3.7 Load test data using BOR information, from Rausche et al. (1996)

LTN	Pile Type	Meas. Cap. (kips)	BOR - Predicted Capacity (kips)					
			Q_{EN}	Q_{Gates}	Q_{WEAP}	Q_{ME}	Q_{PDA}	Q_{CAPWAP}
62	PSC	650	3326	472	680	776	490	536
63	PSC	472	3892	472	680	763	1000	443
64	OEP	1514	6815	640	990	1134	750	1035
65	PSC	987	2012	449	948		700	
66	M	240	1231	225	273	280	121	239
67	PSC	395	2161	407	750	655		395
68	PSC	1060	4255	730	1495	2101	1030	1015
69	PSC	590	4154	421	662	922	780	720
70	H	618	6429	565	902	833	627	629
71	H	313	3200	368	570	617	346	341
72	OEP	600	4000	406	915	1099	634	596
73	PSC	1095	5376	730	1530	1585	846	850
74	PSC	360	1709	357	480	536	384	379
75	PSC/H	503	2000	325	540	688	544	550
76	PSC/H	1045	4000	425	975	1348	1133	1125
77	HT	1460	5492	486	636	1099	660	662
78	HT	1281	4909	452	670	1128	661	636
79	CEP/C	740	4528	432	580	855	640	630
80	CEP/C	689	5202	468	590	800	610	618
81	PSC	956	4856	475	675	873	568	541
82	PSC	1000	3114	401	555	967	638	620
83	PSC	967	2019	387	900	1244	1177	846
84	PSC	820	2308	432	810	1676	898	914
85	PSC	1020	2600	583	1200	1487	659	631
86	CEP	659	5355	514	355	1025	642	518
87	CEP	656	4917	470	620	932		635
88	CEP	470	3500	379	558	528		528
89	CEP	580	2320	311	345	524	506	530
90	CEP	380	2072	293	384	475		400
91	CEP	600			323		450	454

Table 3.7 Load test data using BOR information, from Rausche et al. (1996)

LTN	Pile Type	Meas. Cap. (kips)	BOR - Predicted Capacity (kips)					
			Q _{EN}	Q _{Grtcs}	Q _{WEAP}	Q _{ME}	Q _{PPDA}	Q _{CAPWAP}
92	CEP	657	3252	385	396			575
93	CEP	380	1300	242	288			340
94	H	580	4147	439	585			
95	H	305	2325	314	425			
96	H	340	2592	341	412			
97	H	240	3302	370	516			
98	H	310	3000	351	473			
99	H	480	4062	430	620			
100	H	480	4739	564	691			
101	PSC	363	778	269	465	401	292	295
102	H	374	2843	342	490	552	495	491
103	H	521	3465	384	595	511	511	522
104	H	378	3080	357	480	495	434	431
105	H	635	4155	417	520	663	587	582
117	H	1378	7837	632	1000	1316	1236	1221
118	H	474	2760	353		1137	481	472
119	H	296	2572	341		1036	441	308
120	H	575	3669	397		1485	468	473
122	PSC	148	4159	489	377	641	200	156
185	OEP	425	3540	399		478	423	427
187	CEP	109	540	163		213	167	99
188	T	130	669	177		213	136	140
189	PSC	119	707	216		203	111	96
190	CEP	114	540	163		194	124	70
191	PSC	644	2468	368	760	943	670	660
192	G	158	862	195	255	327	250	250
193	CEP	347	970	204	160	233	209	205
194	M	383	1585	256		274	213	250
196	PSC	414	1896	527	980	1098		377
197	PSC	511			1075			360
198	PSC	555		485	1225			394
199	PSC	541	2200	538	890	1179		517
200	PSC	541	2390		990	1080		508

Chapter 4

METHODS TO COMPARE PREDICTED AND MEASURED CAPACITY

INTRODUCTION

This chapter identifies methods used in the following chapters to compare the accuracy of each predictive method. Two techniques identify how well predicted pile capacity agrees with measured pile capacity. The first technique is the most straightforward. The agreement is illustrated by plotting predicted capacity versus measured capacity. This plot can be used to visually determine trends for the method such as its tendency to over- or under-predict capacity. In addition, the scatter exhibited by the plot is an indication of how reliably the method predicts capacity.

The second method is to use statistical methods to quantify the agreement between predicted and measured capacity for a specific predictive method. A quantitative measure of agreement is important for two purposes: to objectively allow comparison of accuracy of several predictive methods, and to assess the reliability of the method.

Davisson's method (Davisson, 1973) is used to define the failure load from static load test results.

DETAILS OF DATASET

A summary of 100 load tests is given in Table 4.1. The table includes the load test number, the measured capacity, and the predicted capacity using method A and method B. The load test data are fictitious, but are used in this chapter to illustrate the techniques for visualizing and quantifying load test information. Real load test data will be introduced and analyzed in following chapters.

PREDICTED VERSUS MEASURED PLOTS

A plot of Q_p vs Q_m for the two predictive methods is shown (Fig. 4.1a and 4.1b) to illustrate the agreement between predicted capacity and measured capacity. Each graph includes three 45 degree lines. The solid line identifies the relationship where predicted and measured pile capacities are equal ($Q_p = Q_m$). The upper dashed line represents the boundary where predicted capacity is twice the measured capacity ($Q_p = 2 Q_m$) and lower dashed line represents a predicted capacity one-half the measured capacity ($Q_p = 0.5 Q_m$).

Data points plotting close to the 45 degree solid line ($Q_p = Q_m$) indicate a method that predicts capacity well. Data points that plot above the $Q_p = Q_m$ line indicate over-prediction. Data points plotting below the $Q_p = Q_m$ line indicate under-prediction.

Inspection of Figs 4.1a and 4.1b provides the reader with a subjective assessment of the accuracy for each of the methods. These plots can be used to visually determine trends for the method such as a method's tendency to over- or under-predict capacity, and a method's tendency to exhibit scatter. For example, the load test data plotted for method A (Fig. 4.1a) show most of the data plotting above the $Q_p = Q_m$ line. Therefore, it can be seen that method A tends to overpredict capacity of the pile. On the other hand, most of the data for method B (Fig. 4.1b) plots below the $Q_p = Q_m$ line, and therefore, method B tends to underpredict capacity.

The scatter exhibited by the plot of Q_p versus Q_m allows assessment of the precision of a method. For example, a plot exhibiting considerable scatter indicates an imprecise method. When comparing the precision of two methods, the method that exhibits smaller scatter also exhibits greater precision. For example, considerable less scatter is exhibited by method A (Fig 4.1a) than method B (Fig. 4.1b). Most of the load test data for method A plot within a narrow band (between the lines $Q_p = Q_m$ and $Q_p = 2Q_m$). However, a much larger band is required to capture most of the data for method B. Accordingly, method A predicts capacity with greater precision than method B, and is a more reliable method than method B.

The Q_p versus Q_m plot provides a very useful tool to compare methods for prediction. It allows one to determine visually how accurately and how precisely the method predicts capacity. In summary, the two plots (Figs. 4.1a and 4.1b) show that, on the average, method A overpredicts capacity, while method B, on the average, underpredicts the capacity. Furthermore, method A predicts capacity more precisely as exhibited by the smaller degree of scatter about the $Q_p = Q_m$ line.

Visual inspection of the Q_p versus Q_m plot provides a powerful tool to compare the accuracy and precision of predictive methods. However, there is also a need to quantify the accuracy and precision of a method to allow comparisons to be made objectively. Means to quantify accuracy and precision are discussed in the following section.

STATISTICAL INTERPRETATION FOR PREDICTIVE METHODS

In the previous section, a plot of Q_p versus Q_m was used to assess (visually) the accuracy and precision of a method. Accuracy was defined as how well (on the average) the method predicts capacity. In statistics, this is defined as the bias of a method. The scatter in the plot is a measure of how precise the method is, and in statistics, this is referred to as precision.

Definition of Bias and Precision

Bias and precision will be used herein as two simple statistical parameters for defining a method's ability to predict capacity. Bias is a systematic error between the average ratio of Q_p/Q_m and the ideal ratio of Q_p/Q_m (which is unity). Statistically, the bias can be estimated with a sample mean. Precision is the scatter or "variability of a large group of individual test results obtained under similar conditions" (ASTM C670-90a, 1990). Statistically, precision can be estimated with a sample standard deviation. The two terms, mean and standard deviation, are defined in detail below. The distribution of Q_p/Q_m is log-normal (Cornell, 1969). A log-normal distribution means that the values of $\ln(Q_p/Q_m)$ are normally distributed. Accordingly, we can estimate the mean and standard deviation for the $\ln(Q_p/Q_m)$ for the predictive

measures as a means to assess the bias and precision. The mean value (μ_{ln}) of $\ln(Q_p/Q_m)$ is calculated as

$$\mu_{ln} = \frac{1}{n} \sum_{i=1}^n \ln\left(\frac{Q_p}{Q_m}\right) \quad (4.1)$$

where n is the number of observations. A mean value equal to zero ($\mu_{ln} = 0$) represent that, on the average, predicted capacity equals measured capacity. For $\mu_{ln} < 0$, the method, on the average, underpredicts capacity, and the method, on the average, overpredicts capacity if $\mu_{ln} > 0$. The mean can be converted to an arithmetic equivalent (μ) by the following:

$$\mu = e^{\mu_{ln}} \quad (4.2)$$

A measure for scatter exhibited by a predictive method can be quantified with a standard deviation (σ_{ln}). The equation for standard deviation for the $\ln(Q_p/Q_m)$ is as follows:

$$\sigma_{ln}^2 = \frac{1}{n-1} \sum_{i=1}^n \left(\ln\left(\frac{Q_p}{Q_m}\right)_i - \mu_{ln} \right)^2 \quad (4.3)$$

Values of the converted mean(μ) and standard deviation (σ_{ln}) are given for each of the predictive methods in Table 4.1.

Bias and Precision for Load Test Data

To illustrate the statistical methods, the bias and precision are compared for methods A and B. The fictitious load test data shown in Table 4.1 is used to determine the mean and standard deviation for each method. Equation 4.1 is used to determine the bias for method A. The average value for the $\ln(Q_p/Q_m)$ is $\mu_{ln} = 0.243$ which corresponds to the arithmetic equivalent, $\mu = 1.28$ (Eqn. 4.2). Therefore, method A, on the average, overpredicts capacity by a factor of 1.28. Equation 4.3 is used to assess the precision of method A. The standard deviation for the ratio of $\ln(Q_p/Q_m)$

is calculated to be $\sigma_{in} = 0.227$. Thus we now have two parameters with which we can quantify and compare the accuracy and precision of method A.

Using the same equations to calculate accuracy and precision for method B, we determine that for method B, the descriptive parameters are $\mu_{in} = -0.223$, $\mu = 0.80$, and $\sigma_{in} = 0.562$.

A summary Table of parameters is given in Table 4.2. Method A tends to overpredict by a factor of 1.28 ($\mu = 1.28$) while method B tends to underpredict ($\mu = 0.8$). The standard deviation (σ_{in}) for method A is significantly less (0.227) than for method B (0.562). Accordingly, method A is significantly more precise than method B. These numerical results confirm and quantify the observations of the Q_p versus Q_m plots shown in Fig. 4.1.

Cumulative Distribution

A cumulative distribution plot is used to compare and quantify the ability of a method to predict capacity. The plot provides a link between the value of Q_p/Q_m and probability. This relationship will be used in later chapters to determine a partial factors of safety for a given requirement for reliability.

The plot is constructed for each predictive method by sorting the Q_p/Q_m data from smallest ratio to largest ratio and numbering each Q_p/Q_m value from $I = 1$ to n , where n is equal to the number of load tests in the dataset. A cumulative probability value (CP_i) for each Q_p/Q_m ratio is calculated as

$$CP_i = \frac{i}{n+1} \quad (4.4)$$

Values of Q_p/Q_m versus cumulative probability are plotted (Fig. 4.2) for method A. The data follow approximately a straight line which indicate a log-normal distribution. The plot illustrates the relationship between Q_p/Q_m and reliability. For example, it can be seen that a cumulative probability of 50 percent corresponds to a

Q_p/Q_m of 1.28. This means 50 percent of the time the predictive formula underpredicts capacity by a factor of 1.28 or less.

The distribution shown in Fig. 4.2 can also be used to draw a relationship between reliability and Q_p/Q_m . An example is given to illustrate what is necessary to attain a 90 percent reliability for a pile to carry a given load. A pile with a 90 percent reliability will carry a known load without failing 90 percent of the time. As shown in Fig. 4.2, a cumulative probability of 90 percent corresponds to a Q_p/Q_m equal to 1.74. Thus, if we use method A to predict a pile capacity equal to 300 kips, then we can say the pile will be able to carry a load of 172 kips ($=300/1.74$) 90 percent of the time.

The cumulative distribution curve can be used for other reliabilities as well and the reader can repeat the above exercise for reliabilities such as 70 percent, 80 percent, 95 percent. However, the cumulative distribution relationship cannot be used for reliabilities greater than 99 percent without extrapolation because there are only 100 load tests that create the dataset. Higher degrees of reliability such as 99.9 percent would require 1000 load tests.

Practically, the number of load tests in a dataset are usually less than 100, and therefore, extrapolation is required to attain reliabilities greater than 99 percent.

SUMMARY

Methodology for treating the load test data is introduced and explained. The mean (μ) and standard deviation (σ_n) for the ratio of predicted capacity divided by the measured capacity (Q_p/Q_m) are used as the fundamental parameters to identify the agreement between measured and predicted capacity. The two terms provide a simple and convenient way to quantify the accuracy and precision of a method.

The cumulative distribution provides a link between the ratio of Q_p/Q_m and the reliability of a method. This relationship allows different predictive methods to be compared by comparing the ratio of Q_p/Q_m required for a prescribed reliability.

Table 4.1 Fictitious load test data used for illustration

LTN	Measured Capacity	Predicted Capacity		LTN	Measured Capacity	Predicted Capacity	
		Method A	Method B			Method A	Method B
1	117	172	94	51	201	258	228
2	136	200	44	52	57	77	49
3	213	270	67	53	220	368	189
4	271	402	663	54	264	348	214
5	63	48	31	55	88	87	18
6	273	290	89	56	69	100	32
7	218	170	226	57	108	147	107
8	201	271	76	58	250	266	744
9	82	66	66	59	299	323	211
10	252	396	158	60	80	121	37
11	136	162	128	61	152	246	220
12	292	529	187	62	75	113	34
13	94	123	81	63	172	200	92
14	233	409	362	64	117	139	60
15	244	385	588	65	208	266	280
16	277	492	399	66	286	479	287
17	58	69	35	67	192	204	184
18	120	149	72	68	254	318	76
19	265	382	202	69	236	418	279
20	248	415	282	70	119	128	42
21	170	247	235	71	137	157	54
22	161	178	115	72	277	470	193
23	176	180	316	73	73	77	33
24	86	95	168	74	280	381	84
25	152	189	180	75	160	278	69
26	229	299	147	76	191	214	121
27	73	83	117	77	238	352	279
28	79	135	44	78	115	142	139
29	184	339	187	79	300	340	164
30	83	101	23	80	214	228	111
31	121	175	41	81	174	204	214
32	279	295	188	82	80	73	55
33	148	209	150	83	160	236	164
34	135	188	94	84	161	193	113
35	238	275	188	85	127	135	255
36	261	358	232	86	93	92	63
37	277	230	328	87	88	101	54
38	109	99	81	88	236	347	382
39	285	449	349	89	113	108	149
40	107	173	108	90	105	186	184
41	130	280	129	91	285	407	454
42	58	47	82	92	201	378	626
43	188	270	318	93	274	324	183
44	158	227	44	94	171	153	60
45	296	522	193	95	290	215	243
46	184	221	103	96	96	108	70
47	298	291	396	97	212	298	277
48	157	196	76	98	217	263	174
49	155	234	104	99	226	271	171
50	217	185	129	100	224	365	203

Table 4.2 Statistical parameters for Q_p/Q_m values from Table 4.1

Method	μ_{in}	μ	σ_{in}
A	0.243	1.28	0.227
B	-0.223	0.80	0.562

Table 4.3 Load test data for cumulative distribution plot for method A

i	CP_i $i/(n+1), \%$	Q_p/Q_m Method A	i	CP_i $i/(n+1), \%$	Q_p/Q_m Method A
1	0.99	0.741	51	50.50	1.275
2	1.98	0.756	52	51.49	1.285
3	2.97	0.780	53	52.48	1.307
4	3.96	0.806	54	53.47	1.315
5	4.95	0.814	55	54.46	1.320
6	5.94	0.831	56	55.45	1.353
7	6.93	0.851	57	56.44	1.354
8	7.92	0.897	58	57.43	1.361
9	8.91	0.905	59	58.42	1.367
10	9.90	0.908	60	59.41	1.374
11	10.89	0.954	61	60.40	1.393
12	11.88	0.978	62	61.39	1.409
13	12.87	0.984	63	62.38	1.410
14	13.86	0.989	64	63.37	1.427
15	14.85	1.023	65	64.36	1.435
16	15.84	1.045	66	65.35	1.438
17	16.83	1.059	67	66.34	1.439
18	17.82	1.061	68	67.33	1.444
19	18.81	1.061	69	68.32	1.446
20	19.80	1.063	70	69.31	1.448
21	20.79	1.065	71	70.30	1.464
22	21.78	1.066	72	71.29	1.466
23	22.77	1.073	73	72.28	1.473
24	23.76	1.080	74	73.27	1.473
25	24.75	1.101	75	74.26	1.478
26	25.74	1.106	76	75.25	1.485
27	26.73	1.119	77	76.24	1.510
28	27.72	1.121	78	77.23	1.512
29	28.71	1.133	79	78.22	1.513
30	29.70	1.134	80	79.21	1.568
31	30.69	1.144	81	80.20	1.573
32	31.68	1.149	82	81.19	1.574
33	32.67	1.153	83	82.18	1.616
34	33.66	1.165	84	83.17	1.623
35	34.65	1.171	85	84.16	1.635
36	35.64	1.183	86	85.15	1.672
37	36.63	1.188	87	86.14	1.672
38	37.62	1.189	88	87.13	1.673
39	38.61	1.191	89	88.12	1.694
40	39.60	1.199	90	89.11	1.705
41	40.59	1.200	91	90.10	1.733
42	41.58	1.202	92	91.09	1.754
43	42.57	1.216	93	92.08	1.764
44	43.56	1.221	94	93.07	1.774
45	44.55	1.230	95	94.06	1.776
46	45.54	1.234	96	95.05	1.776
47	46.53	1.242	97	96.04	1.815
48	47.52	1.248	98	97.03	1.838
49	48.51	1.250	99	98.02	1.880
50	49.50	1.269	100	99.01	2.157

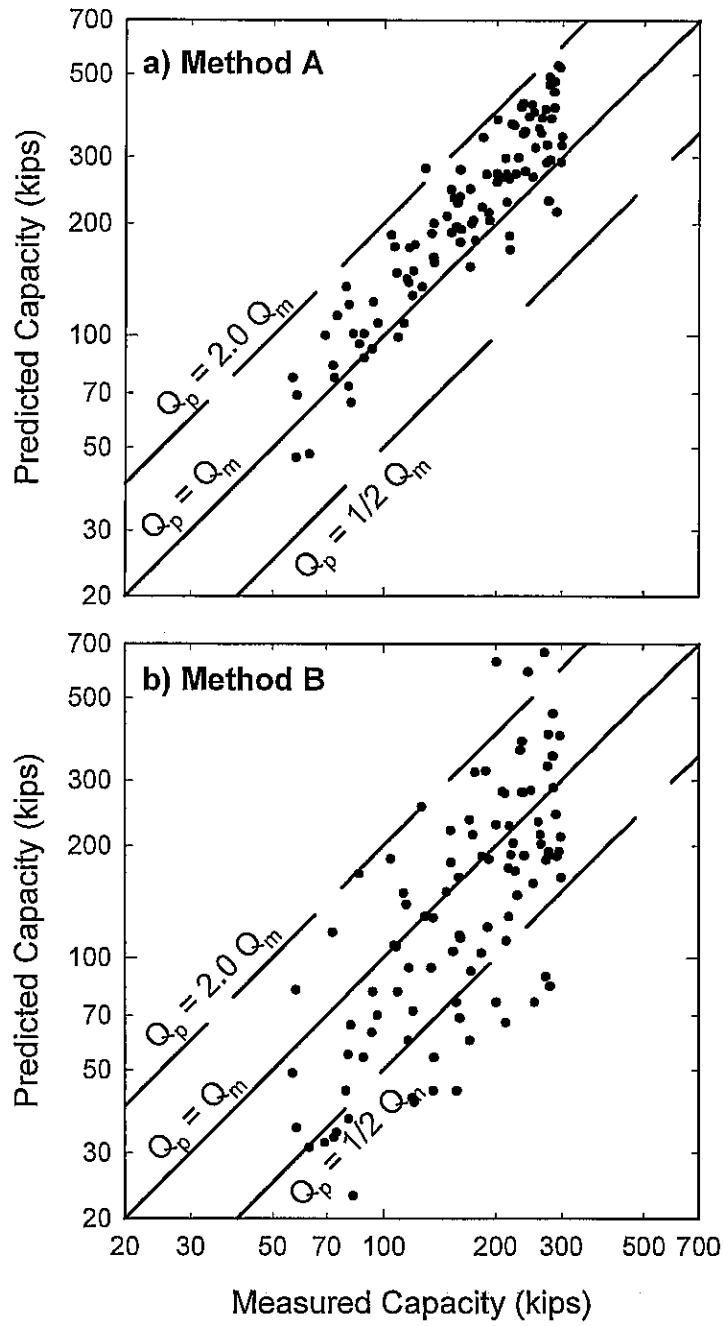


Figure 4.1 Predicted versus measured capacity for fictitious dataset

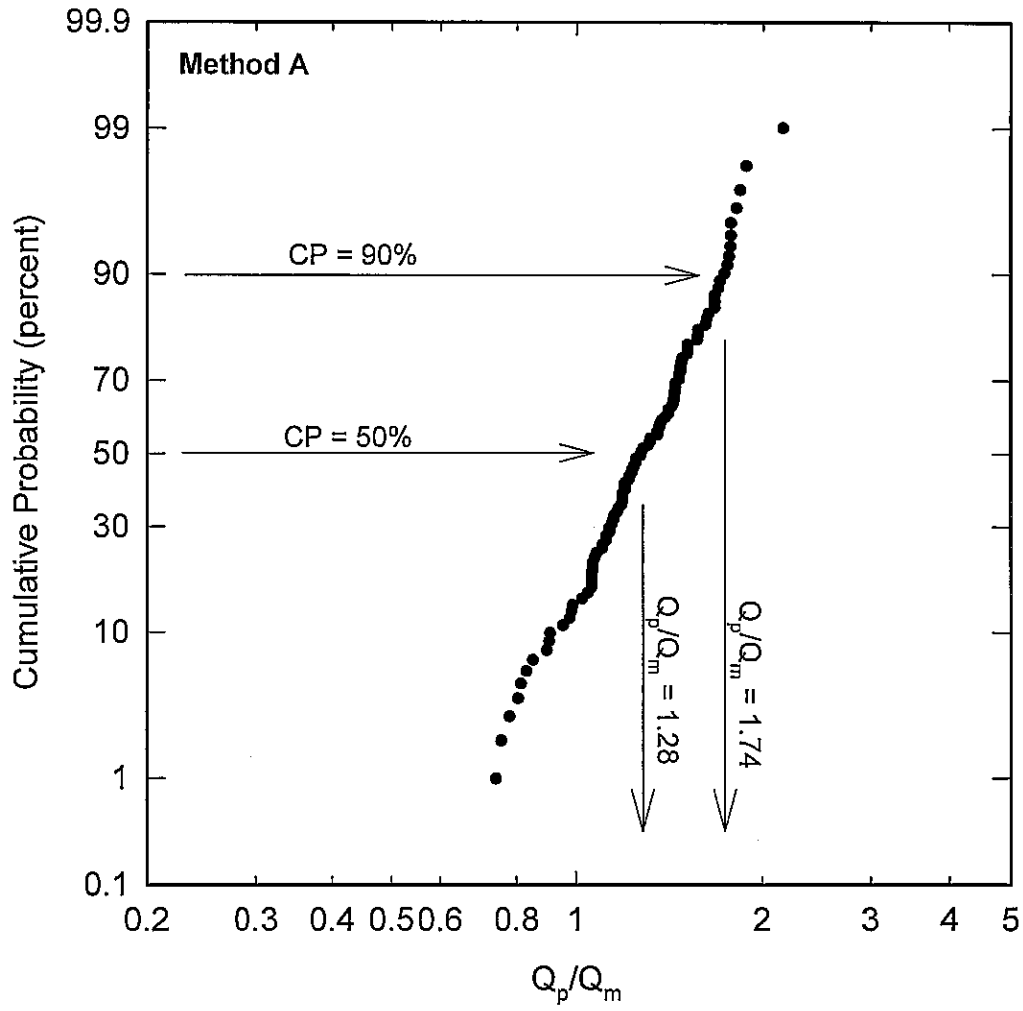


Figure 4.2 Cumulative distribution plot for method A

LOAD TEST DATABASES – PREDICTED vs. MEASURED BEHAVIOR

INTRODUCTION

Predicted and measured capacities for several databases are compared. Specifically, the databases are as follows: Flaate, Olson and Flaate, Frigaszy, Paikowski, Davidson, Eslami, and FHWA. Several methods for predicting capacity are investigated for each database and the accompanying statistics (mean and standard deviation) are provided for each method. Plots of predicted versus measured capacity provide a visual means to assess the accuracy of the methods, while the statistical values, presented in tables, provide a quantitative measure of bias and precision.

FLAATE, 1964

The measured and predicted capacities reported by Flaate's pile load test database are given in Chapter 3. A plot of predicted versus measured capacity for the Engineering News formula is given in Fig. 5.1a and plots for the Hiley method, the Janbu method and the original Gates method are presented in Figs. 5.1b, 5.1c, and 5.1d, respectively.

EN formula

The agreement between measured and predicted capacity using the Engineering News (EN) formula (Fig. 5.1a) is quite poor. It is apparent that the EN formula overpredicts capacity for the piles collected by Flaate. The plot also exhibits considerable scatter, meaning the EN method is inconsistent, and can significantly underpredict capacity and overpredict capacity.

Details of EN formula used by Flaate

It is important to note that Flaate used an unfactored prediction for pile capacity (R_u) using the EN formula. Flaate used the following EN formula to predict capacity:

$$R_u = \frac{WH}{s + c} \quad (5.1)$$

where W is in kips, and the terms H , s , and c are in inches. For comparison, the Illinois DOT uses a similar equation:

$$R_u = \frac{2WH}{s + c} \quad (5.2)$$

where W is in kips, H is in feet, and s and c are in units of inches. The result of mixing will cause R_u in equation 5.2 to have a value 1/6 that of equation 5.1. Accordingly, it is the purpose of equation 5.2 to provide a safe bearing value, whereas equation 5.1 provides a prediction of ultimate capacity.

Statistics for EN method

Average (or mean) and standard deviation values were obtained for value of Q_p/Q_m for each load test in which the EN formula was used to predict pile capacity. The equation used to obtain the average value (μ) and the standard deviation (σ_{in}) is described in detail in Chapter 4. Considering all pile load tests collected by Flaate, the EN formula (using Flaate's definition for pile capacity, eqn. 5.1) overpredicts measured capacity by an average (μ) of 1.23.

The standard deviation (σ_{in}) is a measure of scatter. The value of σ_{in} for the EN formula is very large ($\sigma_{in} = 0.790$) which reflects the large degree of scatter observed in Fig. 5.1.

A summary of the mean (μ) and standard deviation (σ_{in}) for the EN formula is given in Table 5.1 along with other methods for predicting capacity. The first group of

data is represented as “all hammer types.” A comparison of σ_m for this data shows that the EN formula exhibits the greatest scatter (σ_m) of all predictive methods.

Hiley and Janbu methods

Flatte also investigated the Hiley method and the Janbu method. Plots of predicted capacity versus measured capacity are shown in Figs 5.1b and 5.1c, respectively. The Hiley method shows a slight tendency to underpredict capacity but exhibits less scatter than the EN formula. The Janbu equation predicts capacity quite well. The plot (Fig. 5.1c) shows data plot near the $Q_p = Q_m$ line with very little scatter.

Statistics for the Hiley and Janbu methods are given in Table 5.1. Mean values of Q_p/Q_m are 0.82 and 1.03, and σ_m values are 0.499 and 0.307, respectively.

Gates method

A plot of predicted versus measured capacity using the Gates method is shown in Fig. 5.1d. Although Flaate (1964) did not consider the Gates method in his original work, later efforts with Olson (Olson and Flaate, 1967) did consider the Gates method. Accordingly, fundamental driving data reported by Flaate was used to determine capacity according to the original Gates formula (Eqn. 3.1). The plot indicates a tendency of the method to underpredict capacity and scatter is small.

The mean and standard deviation for Q_p/Q_m values for the Gates method are 0.78 and 0.429, respectively (Table 5.1). A mean value of 0.78 identifies the Gates method tends to underpredict capacity. The standard deviation is the second lowest value (only Janbu’s method exhibited a smaller σ_m).

Important Details of the Pile Load Test Database

The pile load test data used by Flaate represents pile types and installation methods used during the period of time that pre-dates 1964. Therefore, it is possible the database includes pile types or installation methods that are no longer common in today’s practice, but bias the results of the database. For example, several of the pile load tests in the Flaate database were conducted on timber piles. Timber piles are not

commonly used in current bridge construction in Illinois. Furthermore, more than half of the piles (62) in the Flaate database were driven with gravity hammers, while the remaining piles (54) were driven with diesel or steam hammers. Today, the gravity hammer is rarely used in driving piles for bridge foundations. Accordingly, the character of the Flaate database and its effect on relationships between predicted and measured is given in the following paragraphs.

Correlations between predicted and measured capacity were investigated with the Flaate database for pile type and type of hammer used for installation. Certainly, there are different correlations that result when the database is filtered for each pile type and each hammer type specifically; however, hammer type appeared to have the most significant effect in the Flaate database. There seems to be an important difference in agreement between measured and predicted capacity for piles driven with gravity hammers as opposed to piles driven with non-gravity hammers. For example, consider the mean value of Q_p/Q_m for the EN formula. When all piles are included, the mean value (μ) of Q_p/Q_m is 1.23; however, $\mu = 0.68$ if only piles driven with gravity hammers are considered, and $\mu = 2.45$ if only piles are considered that were driven with hammers other than gravity hammers. The difference between mean values indicates that relationships between predicted and measured values need to be distinguished separately for gravity hammers and non-gravity hammers. Accordingly, mean and standard deviation values for Q_p/Q_m are given separately in Table 5.1. Values for mean and standard deviation for piles installed with "all hammers types other than gravity" represent results more appropriate to installation methods in today's practice.

It can be seen in Table 5.1 that the standard deviation for the EN formula dropped significantly (from $\sigma_m = 0.790$ for "all hammers" to $\sigma_m = 0.523$ for "all hammers except gravity"). Statistics for the other methods changed, but not as significantly as for the EN formula.

Mean and standard deviation values for piles driven with "gravity hammer only" is shown on the last 4 rows in Table 5.1. It can be seen that for all predictive methods,

the scatter (as indicated by the standard deviation, σ_{ln}) is the least for this dataset. Since prediction of pile capacity requires an estimate of energy delivered to the pile, more accurate estimates of energy delivered to the pile will result in more consistent predictions. It is therefore possible that the reduced scatter observed for piles driven with gravity hammers is because energy delivered to the pile can be better estimated with a simple mechanism such as a gravity hammer rather than a more complicated mechanism, such as a steam hammer or double acting hammer.

OLSON AND FLAATE, 1967

Since the database used by Olson and Flaate (1967) is nearly identical to the database used by Flaate (1964), the predicted versus measured relationships, and the statistical parameters are similar to those determined for the Flaate database. However, Olson and Flaate suggested the Gates equation could be modified to provide a better statistical fit between predicted and measured. These modifications were presented in equations 3.2 – 3.5 and are of the form shown in the equation below.

$$\text{modified } R_u = A * (\text{original Gates prediction}) - B \quad (5.3)$$

A and B values are modified to minimize the error in the ratio of Q_p/Q_m .

However, the Flaate database (and accordingly, the Olson Flaate database) contains piles driven by gravity hammers and other types of hammers. As noted previously, the data for piles driven with gravity hammers need to be considered separately from the piles driven with other types of hammers. Olson and Flaate did not consider these data separately, so modifications to the Gates formula are given below based on piles driven with all hammer types other than gravity hammers. Statistics for concrete piles only are not presented because there were too few tests (5) to get a reliable fit.

$$R_u = 0.55\sqrt{eE_r} \log(10N_b) + 34: \text{ for timber piles} \quad (5.4)$$

$$R_u = 2.60\sqrt{eE_r} \log(10N_b) - 223 : \text{for steel piles} \quad (5.5)$$

$$R_u = 2.50\sqrt{eE_r} \log(10N_b) - 210 : \text{for concrete and steel piles} \quad (5.6)$$

$$R_u = 1.27\sqrt{eE_r} \log(10N_b) - 10 : \text{for all piles} \quad (5.7)$$

As before, units of R_u are in kips, E_r is in units of ft-lbs, and N_b is in blows per inch.

Equations 5.4 through 5.7 exhibit a considerable variation in factors depending on the type of pile. The results suggest there is a significant difference between concrete/steel piles and timber piles. Most likely, the difference in the equations is a result of the average capacity for the piles. For example, the average pile capacity for timber piles in the database is 88 kips, whereas the average capacity of the steel piles is 347 kips and the average capacity of the concrete piles is 356 kips. Thus, the different equations most likely represent the best fit for a range in capacity.

FRAGASZY et al. 1988, 1989

The measured and predicted capacities reported by Fragaszy et al, are plotted in Figs. 5.2a – 5.2d for the EN, Hiley, Janbu, and Gates method, respectively. The EN formula predicted capacity poorly. The EN method tends to overpredict and Fig. 5.2a exhibits a significant amount of scatter indicating an imprecise method. Numerical values for mean and standard deviation of the Q_p/Q_m values are 2.58 and 0.610, respectively (Table 5.2).

The plots of predicted versus measured relationships for the Hiley method (Fig. 5.2b) and the Janbu method (Fig. 5.2b) show similar degrees of scatter with the Hiley method slightly overpredicting ($\mu = 1.05$) measured capacity and with the Janbu method ($\mu = 0.94$) slightly underpredicting capacity. The statistics for the Hiley and Janbu methods are given in Table 5.2.

The smallest scatter was exhibited by the Gates method and predicted versus measured relationship is shown in Fig. 5.2d. The method tends to underpredict

capacity ($\mu = 0.63$) but the degree of scatter in the plot is small. Statistics for the Gates method are given in Table 5.2.

The timber piles in Fragaszy's database were small capacity piles with average capacities about $\frac{1}{4}$ that of the concrete and steel piles. Furthermore, since timber piles do not represent a common foundation selection in current bridge practice in Illinois, these piles were eliminated from consideration in determining the statistical parameters shown in Table 5.2.

A comparison of the four methods, EN, Hiley, Janbu, and Gates can be made using the statistical parameters presented in Table 5.2. The Engineering News formula overpredicts by a factor of 2.58, while the Hiley and Janbu methods are fairly neutral. The Gates method underpredicts capacity by a factor of 0.63 indicating that recalibration of the original Gates equation will be necessary. The scatter, as quantified by the magnitude of standard deviation reported in Table 5.2, shows the EN formula to have the greatest scatter ($\sigma_{in} = 0.610$) while the Gates method exhibits the least scatter ($\sigma_{in} = 0.307$). The Hiley and Janbu methods exhibit an intermediate amount of scatter ($\sigma_{in} = 0.438$, and $\sigma_{in} = 0.437$, respectively).

In the previous section, the Gates method was modified to develop a better statistical fit between measured and predicted capacity. Using the data provided by Olson and Flaate, modified Gates equations 5.4 through 5.7 were developed. Identical procedures were repeated to develop a modified Gates equation for Fragaszy's data. The equation is as follows:

$$R_u = 1.46\sqrt{eE_r} \log(10N_b) + 26 : \text{for all piles except timber} \quad (5.8)$$

As before, units of R_u are in kips, E_r is in units of ft-lbs, and N_b is in blows per inch.

PAIKOWSKY et al. 1994

The measured and predicted capacities reported by Paikowsky et al., 1994, are plotted in Figs. 5.3a – 5.3d for the Measured Energy approach and for CAPWAP. A more

detailed explanation of the Measured Energy approach and CAPWAP is given in Chapter 2.

A simplified explanation of the Measured Energy (ME) method is that it is similar to the EN formula; however, measurements of set and energy are obtained in a more precise manner by employing strain gages, accelerometers, and a pile dynamic monitor (PDM). This method was developed by Paikowsky et al. and results are plotted in Figs. 5.3a for predictions made from driving behavior recorded at the end of driving (EOD) and in Fig. 5.3b for predictions made by allowing the pile to set for several days and then recording the driving behavior at the beginning of restrike (BOR). The ME approach using EOD data appear to predict capacity well (Fig. 5.3a). The method appears to be clustered around the line of perfect agreement ($Q_p = Q_m$ line) and the degree of scatter is small. Estimates of capacity using BOR data overpredict capacity (Fig. 5.3b), but still exhibit a relatively small degree of scatter.

Statistics for the ME approach are given in Table 5.3 for both EOD and BOR conditions. The average value of Q_p/Q_m is 1.03 for EOD conditions and 1.25 for BOR conditions. Values of standard deviation are $\sigma_{ln} = 0.309$ for EOD conditions and $\sigma_{ln} = 0.303$ for BOR conditions. These values of σ_{ln} are relatively low, reflecting the small degree of scatter observed in Figs. 5.3a and 5.3b.

Plots of predicted capacity using CAPWAP versus measured capacity are shown in Figs. 5.3c and 5.3d for EOD and BOR conditions, respectively. CAPWAP predictions using EOD information underpredict capacity and exhibit a greater degree of scatter than the other methods shown in Figs. 5.3a, 5.3b, and 5.3d. However, when CAPWAP is used with BOR data, predictions are significantly improved. There is still a tendency to underpredict capacity, but the scatter decreases significantly. The mean values for Q_p/Q_m for CAPWAP are 0.73 and 0.83 for EOD and BOR conditions, respectively (Table 5.3). Values for standard deviation are 0.398 and 0.304 for EOD and BOR conditions, respectively.

This dataset provides insight into possible errors associated with the dynamic formulas investigated previously. For example, the EN formula has been shown to predict capacity poorly with a great degree of scatter. However, a very similar formula is used for the ME approach, but the correlations are much improved. A possible reason for improved accuracy may be because pile dynamic monitoring results in more reliable estimates for energy delivered to the pile and the set developed by the pile as compared to the more common use of visual observation of set, and rough estimates of hammer energy.

DAVIDSON et al., 1996

The measured and predicted capacities reported by Davidson et al., 1996, are plotted in Figs. 5.4a – 5.4e for the PDA, CAPWAP, and for a static method (SPT94). There are two estimates of capacity for PDA and CAPWAP which represent driving behavior at EOD and BOR. Details of the database are given in Chapter 3 but it is worthwhile to mention that all data are for concrete piles driven in Florida.

Predicted capacity versus measured capacity using PDA for EOD and BOR conditions are shown in Figs. 5.4a and 5.4b. The PDA is seen to underpredict capacity for EOD conditions (Fig. 5.4a) and overpredicts capacity for BOR conditions. Scatter is minimal. Statistics for Q_p/Q_m values are given in Table 5.4. The average value of Q_p/Q_m for EOD conditions is 0.84 and for BOR is 1.07. Scatter, as quantified by the standard deviation, is relatively low for both EOD and BOR conditions ($\sigma_{in} = 0.298$ for EOD and $\sigma_{in} = 0.266$ for BOR).

Predicted capacity versus measured capacity using CAPWAP for EOD and BOR conditions are shown in Figs. 5.4c and 5.4d. CAPWAP underpredicts capacity for EOD conditions (Fig. 5.4c) and slightly underpredicts capacity for BOR conditions. Scatter is greater for EOD conditions than for BOR conditions. Statistics for Q_p/Q_m values are given in Table 5.4. The average value of Q_p/Q_m for EOD conditions is 0.70 and for BOR is 0.95. Scatter, as quantified by the standard deviation, is relatively low

for BOR conditions, but higher for EOD conditions ($\sigma_{in} = 0.375$ for EOD and $\sigma_{in} = 0.317$ for BOR).

Predictions using a static method (SPT94) were also included in this study to compare the accuracy with methods that use dynamic driving behavior. Predicted capacity versus measured capacity using SPT94 is shown in Figs. 5.4e. SPT94 underpredicts capacity and exhibits considerable scatter. Statistics for Q_p/Q_m values are given in Table 5.4. The average value of Q_p/Q_m is 0.53. Scatter is significant ($\sigma_{in} = 0.734$).

ESLAMI, 1996

Eslami considered only methods that use results of cone penetration tests to predict the static capacity of piles. He investigated six methods and plots of predicted versus measured capacity are shown in Figs. 5.5a – 5.5f. The Schmertmann (Fig. 5.5a) and French (Fig. 5.5c) tend to underpredict capacity slightly while the Meyerhof, Tumay, and Eslami method tend to overpredict capacity. The Deruiter method has no tendency to over- or under-predict. An intermediate degree of scatter is observed in the plots of predicted versus measured relationships (Figs. 5.5a - 5.5f). The least amount of scatter is seen for the Eslami method.

Statistical parameters for Q_p/Q_m values are given in Table 5.5. The average value varies between 0.94 and 1.26 for all methods, which is a narrow range considering the details of predicting capacity are very different for each method. Likewise, the scatter is relatively small. Standard deviations ranged from the very small $\sigma_{in} = 0.28$ for the Eslami method to about $\sigma_{in} = 0.45$ for the French method. The predictions and the statistical parameters identify much better agreement between predicted and measured capacity using cone methods than using other static methods such as the SPT94 method reported by Davidson et al. 1994 (Fig. 5.4 and Table 5.4).

DATABASE FROM FHWA

The measured and predicted capacities for the EN formula, Gates, WEAP, ME, PDA, and CAPWAP are shown in Figs. 5.6a - 5.6f for EOD conditions and Figs. 5.7a - 5.7f for BOR conditions.

EOD conditions

The agreement between predicted and measured capacity is illustrated in Figs. 5.6a - 5.6f. Observations for the EN formula and Gates formula are similar to finding of the previous databases. The EN formula tends to overpredict and exhibits significant scatter. The Gates formula underpredicts capacity and exhibits considerably less scatter than the EN formula. Predictions made with WEAP slightly underpredict capacity and exhibit a fair amount of scatter. The measured energy approach seems to, on the average, predict capacity well. Both PDA and CAPWAP tend to underpredict capacity with a fair amount of scatter.

Statistics for Q_p/Q_m values for all these methods are given in Table 5.6. The table provides information on mean and standard deviation that allows the reader to compare values for each of the methods. In doing so, the least amount of scatter (smallest standard deviation) is shown for the Gates method and the greatest amount of scatter is exhibited by the EN formula. Methods arranged from the least amount of scatter to the greatest amount of scatter (in increasing magnitude of standard deviation): Gates (least scatter), PDA, ME, WEAP, CAPWAP, and EN (greatest scatter) formula. However, general conclusions cannot be drawn because each method uses a different subset of load test data to determine the statistics. Results with a more consistent subset of data will be given later.

BOR conditions

The agreement between predicted and measured capacity for beginning-of-restrike conditions is illustrated in Figs. 5.7a - 5.7f. EN formula (Fig. 5.7a) and Gates formula (Fig. 5.7b) provide similar results found in previous databases, except that with BOR data they tend to predict higher capacity than when using EOD data. Accordingly, the EN formula tends to overpredict capacity and exhibit significant scatter. The

Gates formula tends to underpredict capacity and exhibits considerably less scatter than the EN formula. Predictions made with WEAP slightly overpredict capacity and exhibit fair scatter. The scatter using WEAP with BOR conditions (Fig. 5.7c) is significantly less than with EOD (Fig. 5.6c) conditions. The measured energy (ME) approach tends to, on the average, overpredict capacity (Fig. 5.7d). Both PDA (Fig. 5.7e) and CAPWAP (Fig. 5.7f) tend to underpredict capacity slightly with a small degree of scatter. Significant reduction in scatter is seen for CAPWAP using BOR conditions (Fig. 5.7f) rather than EOD conditions (Fig. 5.6f).

Statistics quantifying the mean and standard deviation for the ratio Q_p/Q_m are given in Table 5.6. The least amount of scatter (smallest standard deviation) is shown for CAPWAP and the greatest amount of scatter is exhibited by the EN formula. Methods arranged from the least amount of scatter to the greatest amount of scatter (in increasing magnitude of standard deviation): CAPWAP (least scatter), PDA, ME, WEAP, Gates, and EN (greatest scatter) formula. General conclusions relating this sequence of methods to inherent variability for a predicted method cannot be drawn because the statistics for each method use a different subset of load test data. Results with a more consistent subset of data will be given later.

Static formulas

The FHWA database also includes a number of load tests on piles in which pile capacity was estimated with static formulas as recommended in SPILE (FHWA, 1993). Statistics for Q_p/Q_m (Table 5.6.) suggest the method tends to overpredict by 15 percent (average = 1.15) and exhibits a large degree of scatter ($\sigma_{in} = 0.556$).

SUMMARY

Predicted and measured capacities for several databases have been presented. Statistics for the EN, Gates, Modified Gates, WEAP, ME, PDA, and CAPWAP methods have been determined using databases by Flaate, Fragaszy, Davidson, and FHWA.

It has been emphasized that some of the data containing load tests are dated. Piles that were driven using gravity hammers seemed to develop capacities different from

those using more conventional hammers. Of the dynamic formulas investigated, the Gates method consistently predicted capacity as well or better than the other predictive methods. BOR data did not improve the precision of the Gates method significantly. The precision of WEAP, PDA, and CAPWAP improved when using BOR data.

Because the databases contain different piles in their datasets, estimates of accuracy and precision between databases do not agree. Accordingly, additional interpretations are necessary to use all the datasets in determining the ability of methods to predict pile capacity.

Table 5.1 Statistical parameters for Q_p/Q_m values for all load test data from Flaate (data shown in Figure 5.1)

Method	Hammer Type	n	μ	σ_{ln}
EN	All Hammer Types	116	1.23	0.790
Hiley		116	0.82	0.499
Janbu		116	1.03	0.307
Gates		116	0.78	0.429
EN	All hammer types except gravity	54	2.45	0.523
Hiley		54	0.74	0.614
Janbu		54	1.08	0.397
Gates		54	0.85	0.459
EN	Gravity hammer only	62	0.68	0.393
Hiley		62	0.91	0.346
Janbu		62	0.98	0.192
Gates		62	0.734	0.391

Table 5.2 Statistical parameters for Q_p/Q_m values from Fragaszy (loadtest data shown in Fig. 5.2)

Method	μ_{ln}	μ	σ_{ln}
EN	0.950	2.58	0.610
Hiley	0.045	1.05	0.438
Janbu	-0.060	0.94	0.437
Gates	-0.459	0.63	0.307

Table 5.3 Statistical parameters for Q_p/Q_m values from Paikowsky et al (1994) (loadtest data shown in Fig. 5.3)

Method	μ_{ln}	μ	σ_{ln}
ME – EOD	0.04	1.03	0.309
ME – BOR	0.22	1.25	0.303
CAPWAP - EOD	-0.31	0.73	0.398
CAPWAP - BOR	-0.184	0.83	0.304

Table 5.4 Statistical parameters for Q_p/Q_m values from Davidson et al, 1996 (loadtest data shown in Fig. 5.4)

Method	μ_m	μ	σ_m
PDA-EOD	-0.171	0.84	0.298
PDA-BOR	0.070	1.07	0.266
CAPWAP-EOD	-0.356	0.70	0.375
CAPWAP-BOR	-0.052	0.95	0.317
SPT94	-0.626	0.53	0.734

Table 5.5 Statistical parameters for Q_p/Q_m values from Eslami, 1996 (loadtest dataset shown in Fig. 5.5)

Cone Method	μ_m	μ	σ_m
Schmertmann	-0.058	0.944	0.443
DeRuiter	0.002	1.002	0.390
French	-0.063	0.939	0.447
Meyerhof	0.230	1.258	0.391
Tumay	0.142	1.153	0.374
Eslami	0.180	1.197	0.276

Table 5.6 Statistical parameters for Q_p/Q_m values from Fig 5.6a - 5.6f. (from FHWA dataset)

Method		n	μ	σ_{ln}
End of Driving (EOD)	EN	123	2.60	0.675
	Gates	123	0.53	0.410
	WEAP	88	0.64	0.501
	ME	73	0.93	0.462
	PDA	77	0.71	0.454
	CAPWAP	75	.58	0.591
Beginning of Restrike (BOR)	EN	116	4.62	0.514
	Gates	116	0.72	0.392
	WEAP	114	1.11	0.385
	ME	92	1.41	0.363
	PDA	85	0.91	0.319
	CAPWAP	112	0.86	0.269
Static Formula		112	1.15	0.556

*Note: All load tests are included in which a method could be used to compute capacity.

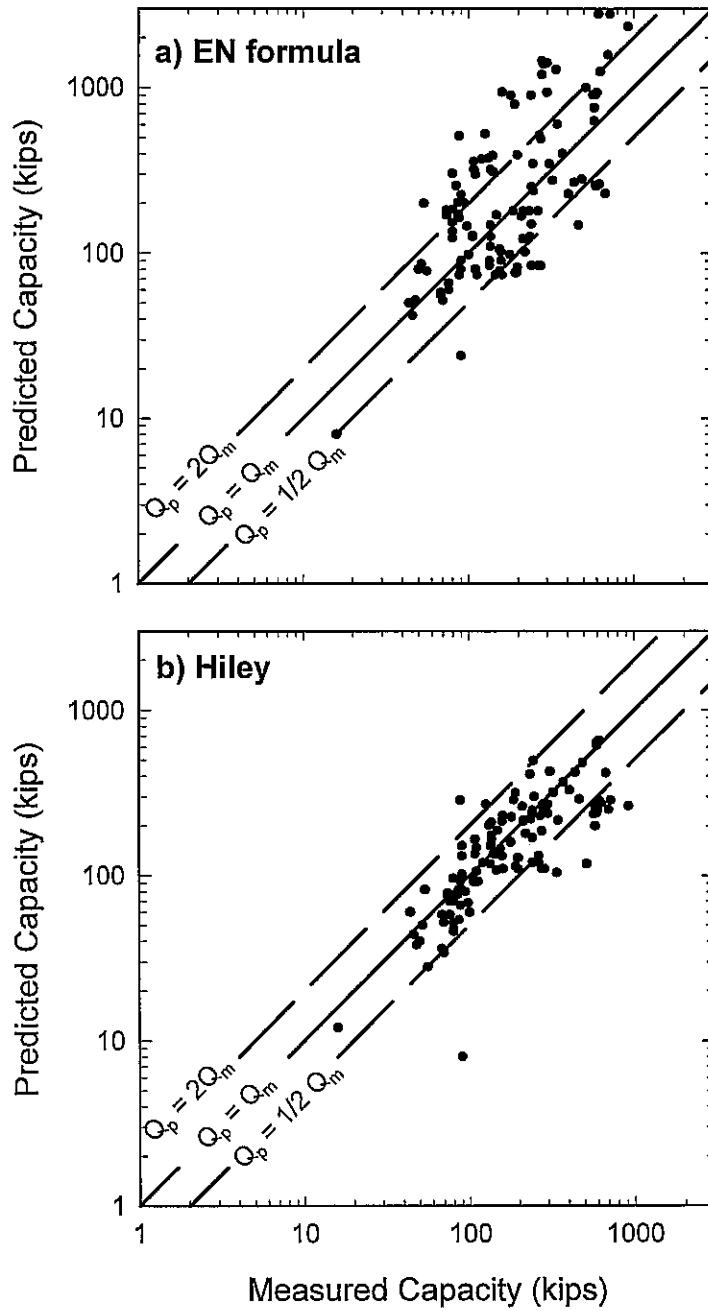


Figure 5.1 Predicted versus measured capacity for Flaate (1964)

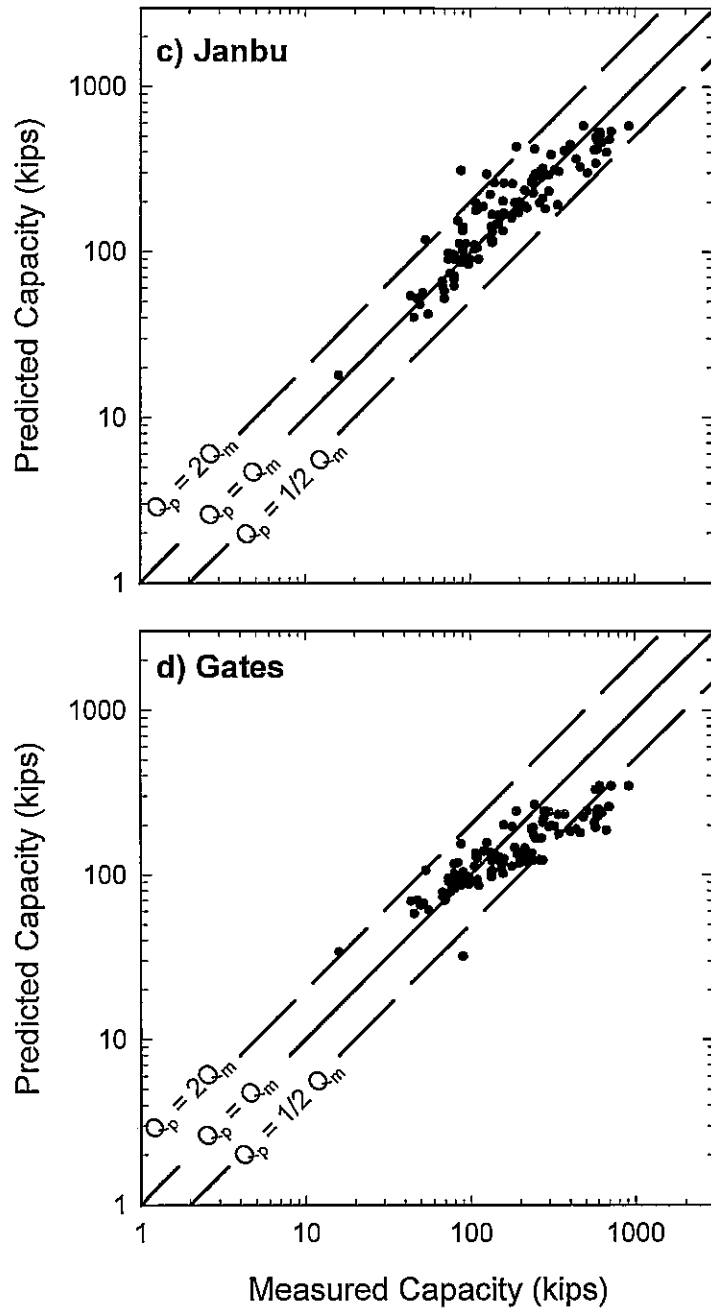


Figure 5.1 Predicted versus measured capacity for Flaate (1964) (cont'd)

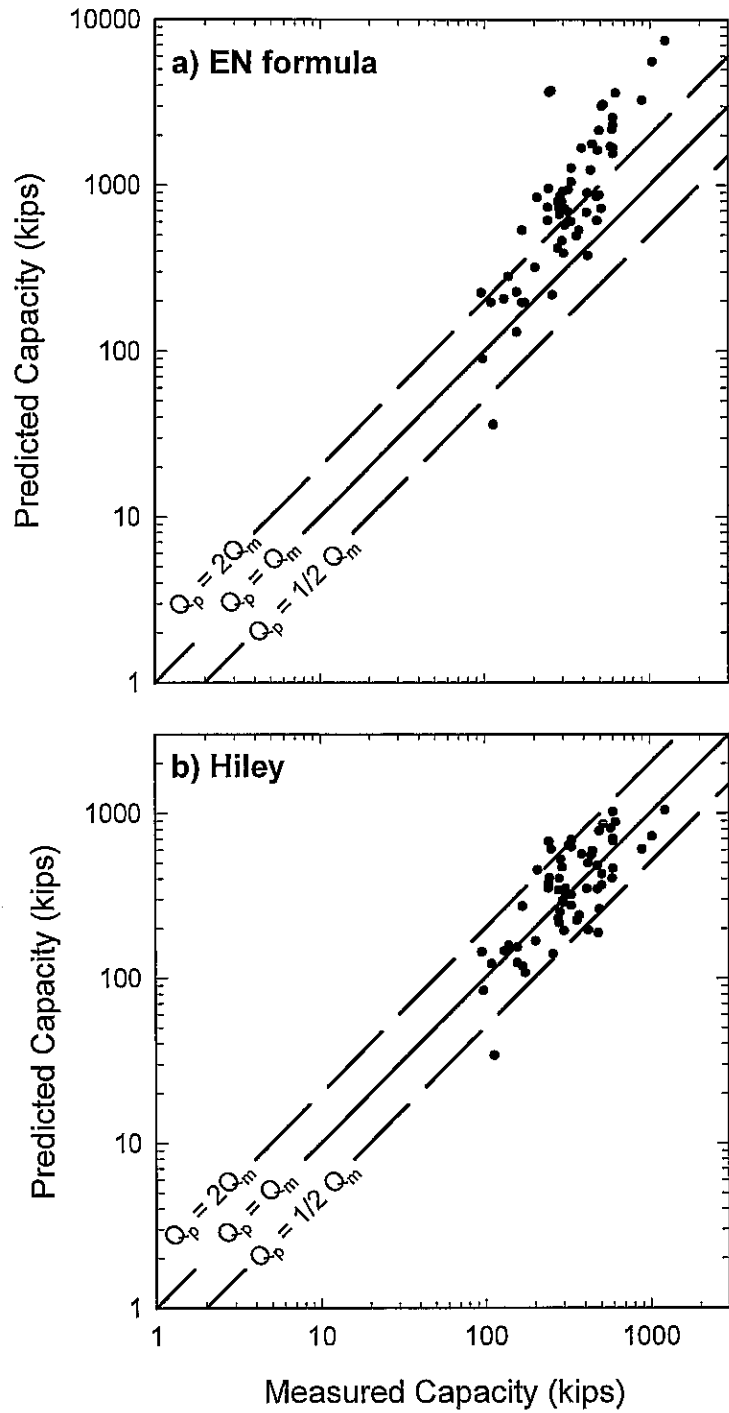


Figure 5.2 Predicted versus measured capacity for Frangos et al. (1988)

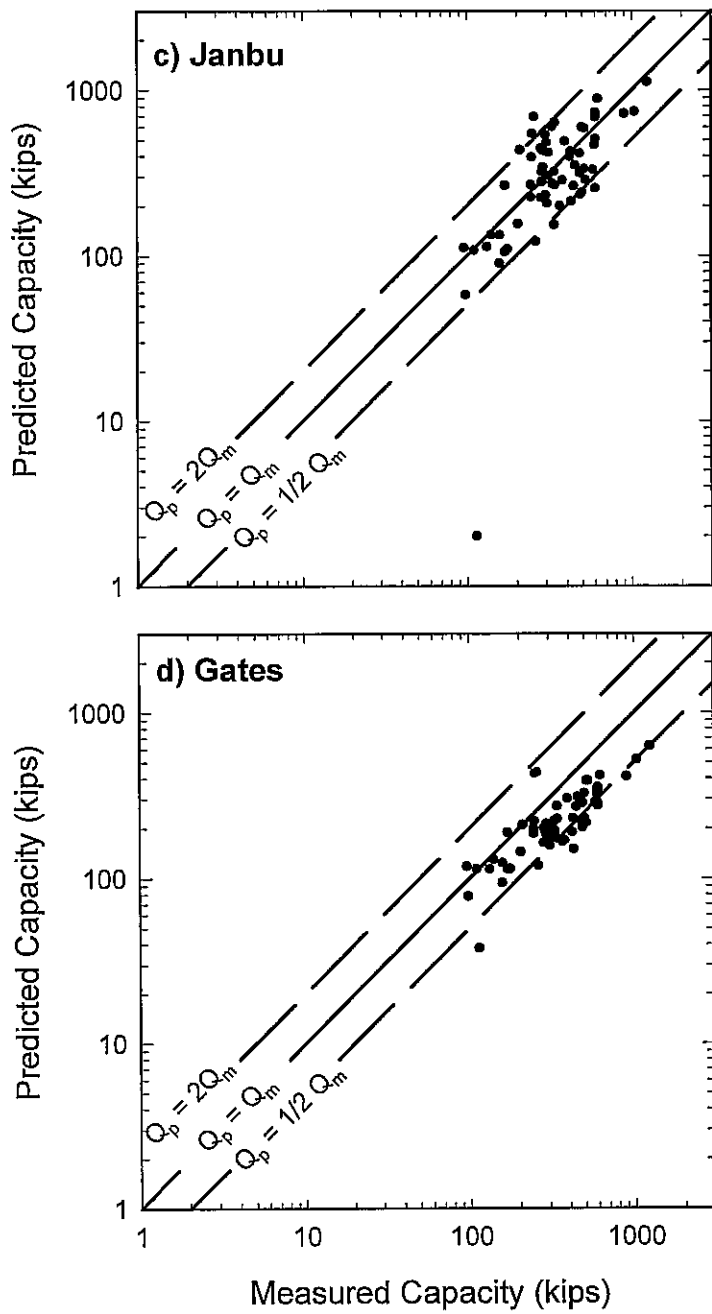


Figure 5.2 Predicted versus measured capacity for Fragaszy et al. (1988) (cont'd)

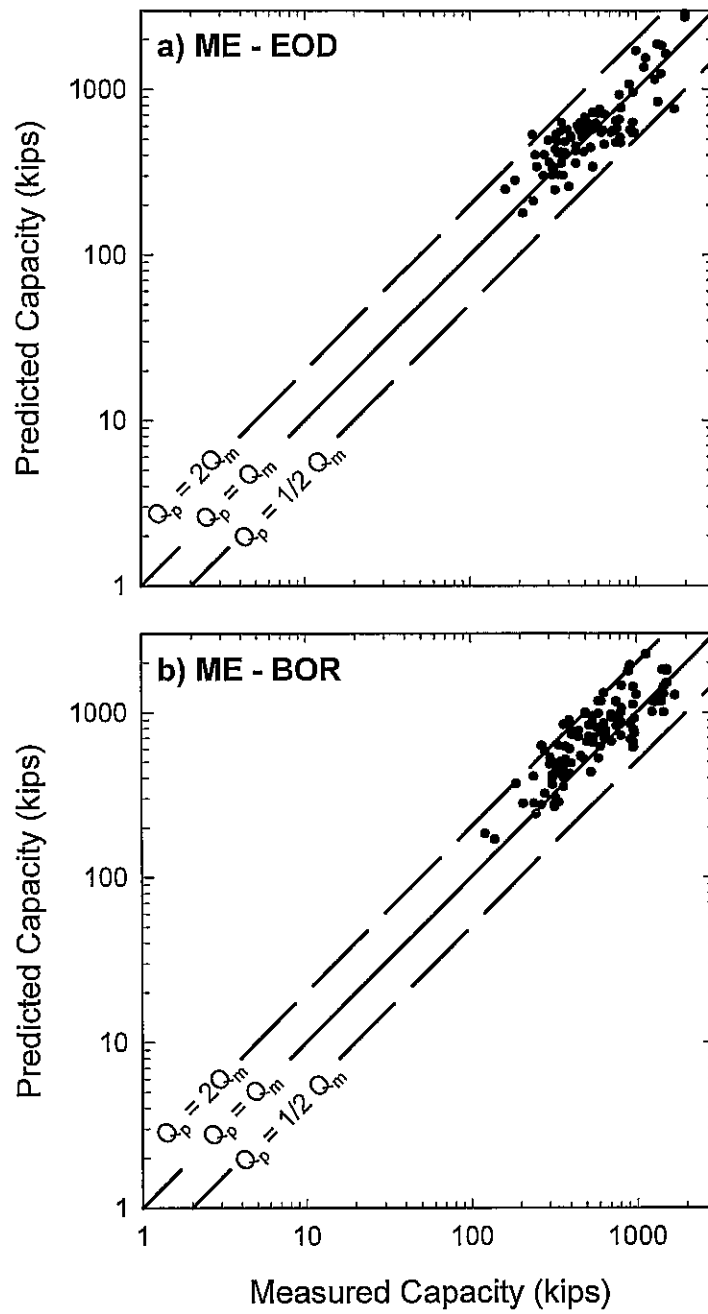


Figure 5.3 Predicted versus measured capacity (adapted from Pakowski et al. 1994)

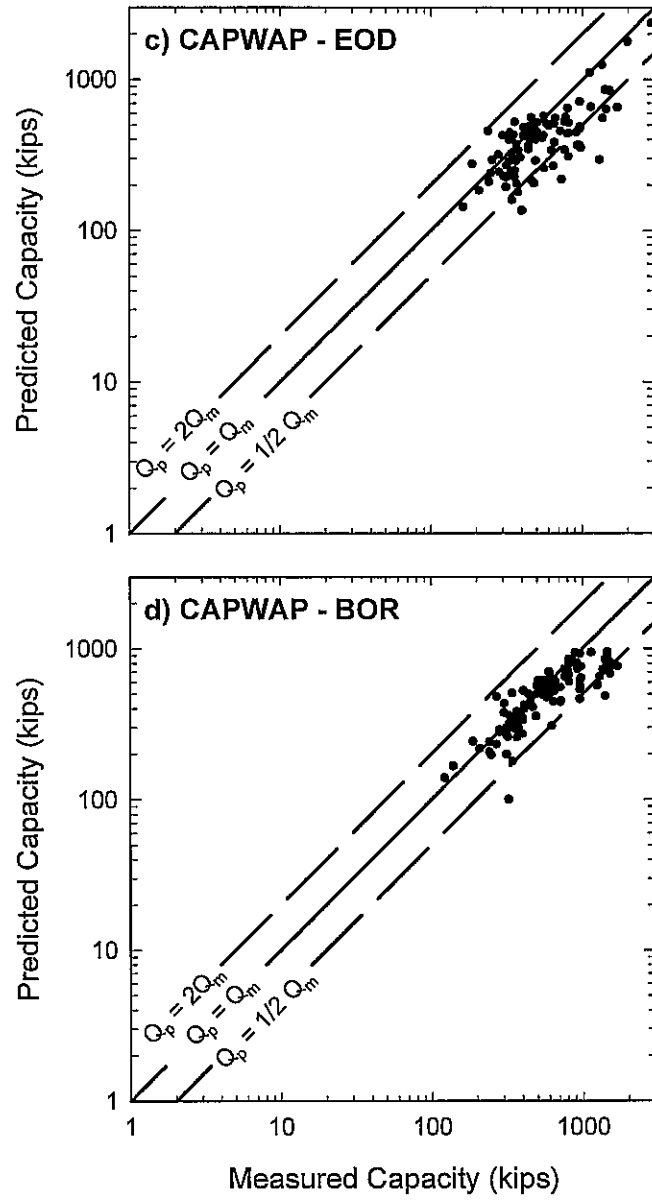


Figure 5.3 Predicted versus measured capacity (adapted from Pakowski et al. 1994) (cont'd)

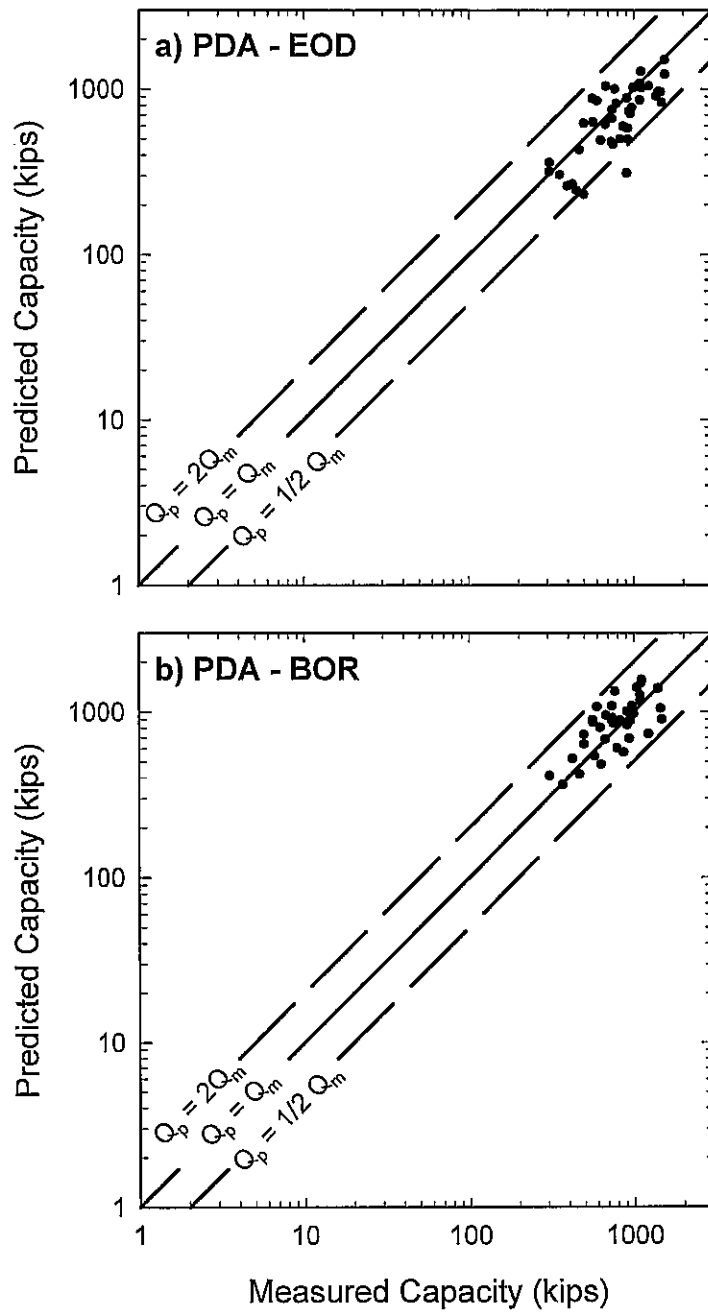


Figure 5.4 Predicted versus measured capacity for Florida DOT adapted from Davidson et al. (1996)

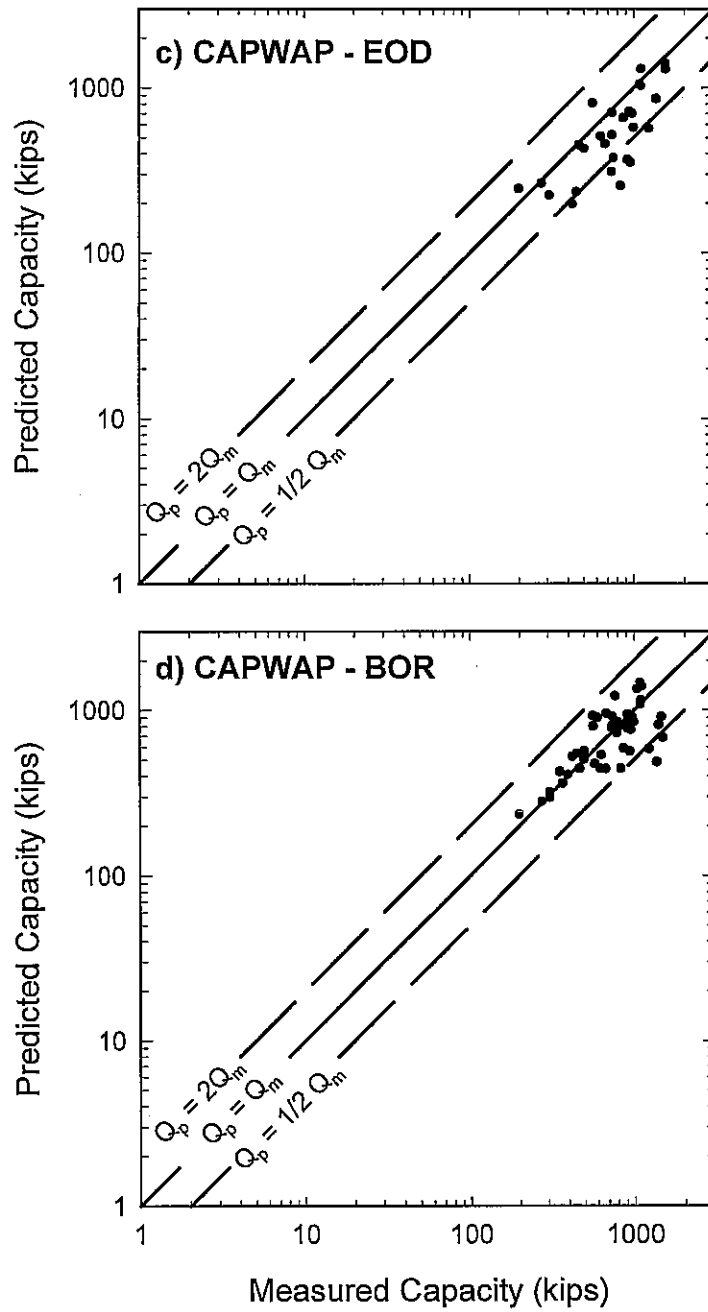


Figure 5.4 Predicted versus measured capacity for Florida DOT adapted from Davidson et al. (1996) (cont'd)

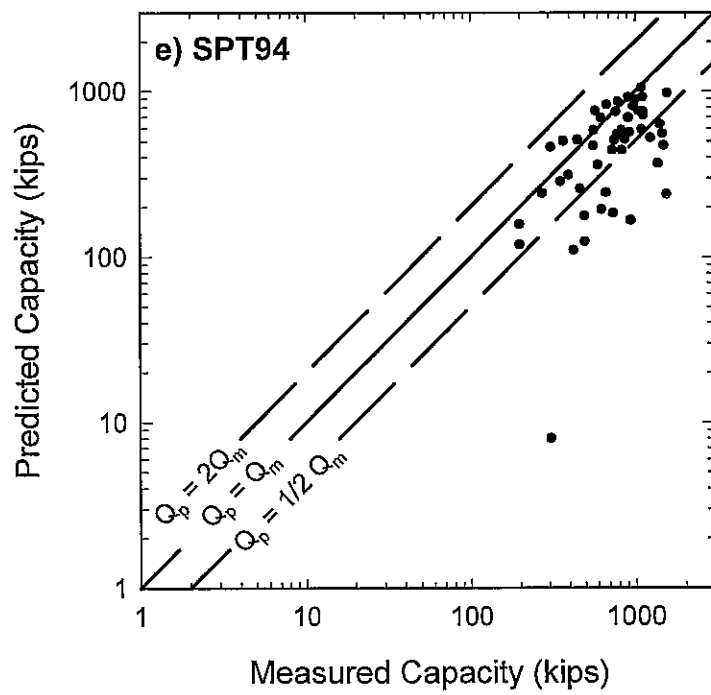


Figure 5.4 Predicted versus measured capacity for Florida DOT adapted from Davidson et al. (1996) (cont'd)

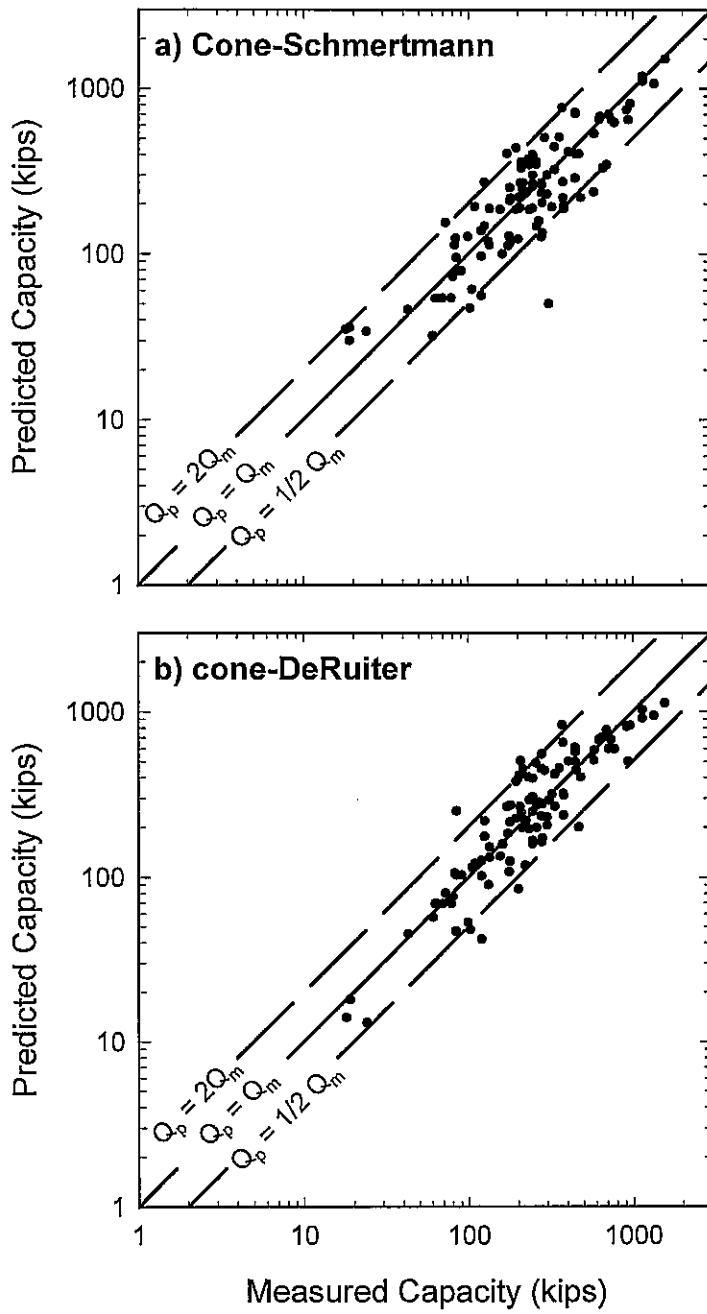


Figure 5.5 Predicted versus measured capacity from Eslami (1996)

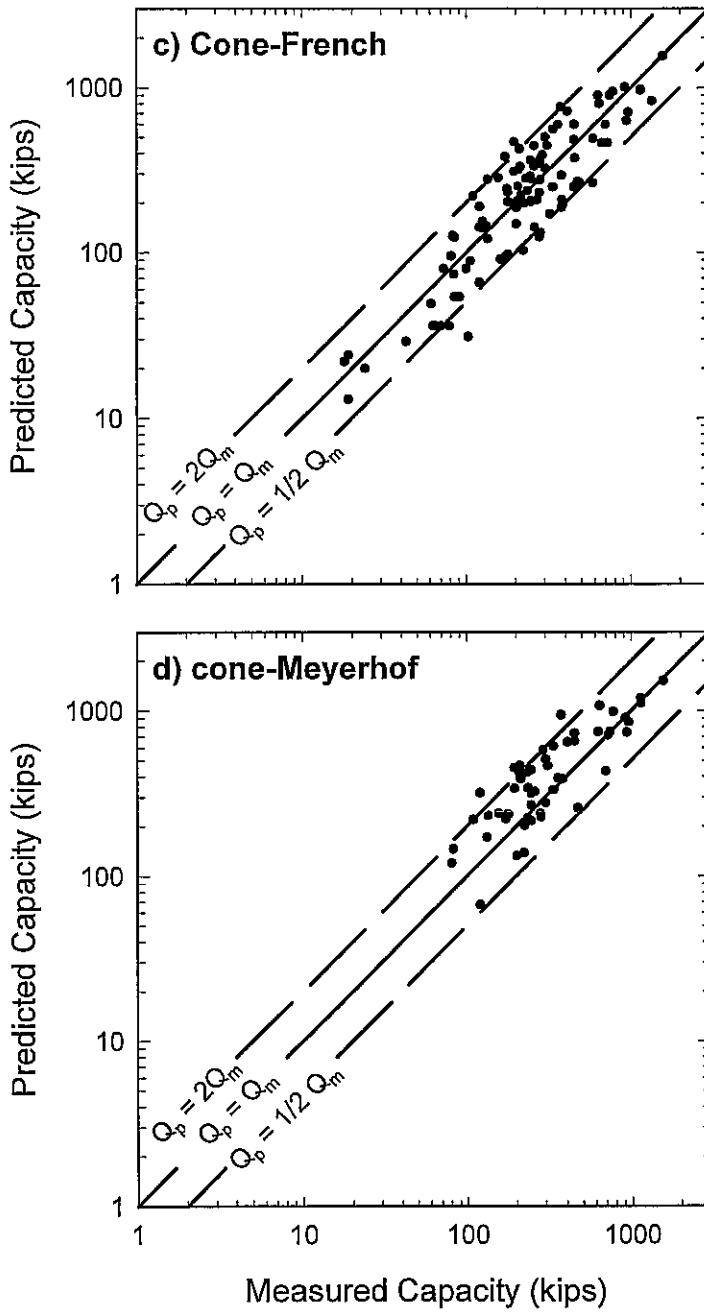


Figure 5.5 Predicted versus measured capacity from Eslami (1996) (cont'd)

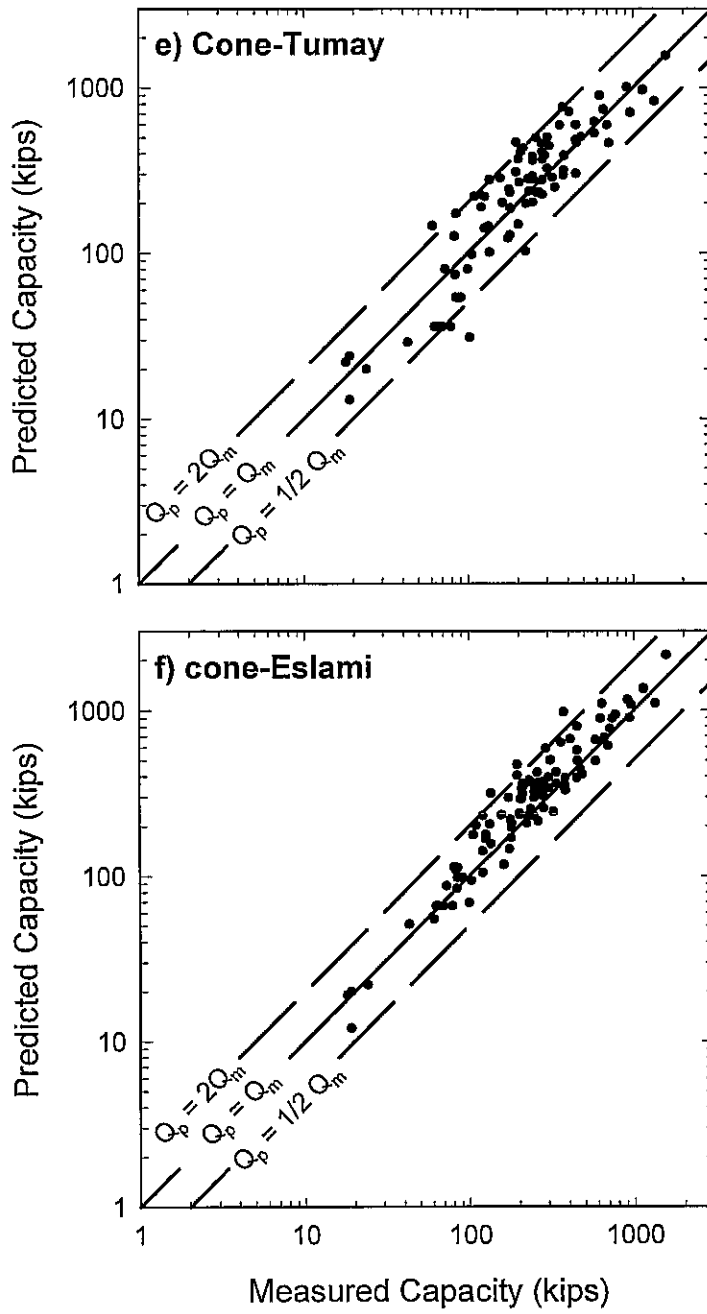


Figure 5.5 Predicted versus measured capacity from Eslami (1996) (cont'd)

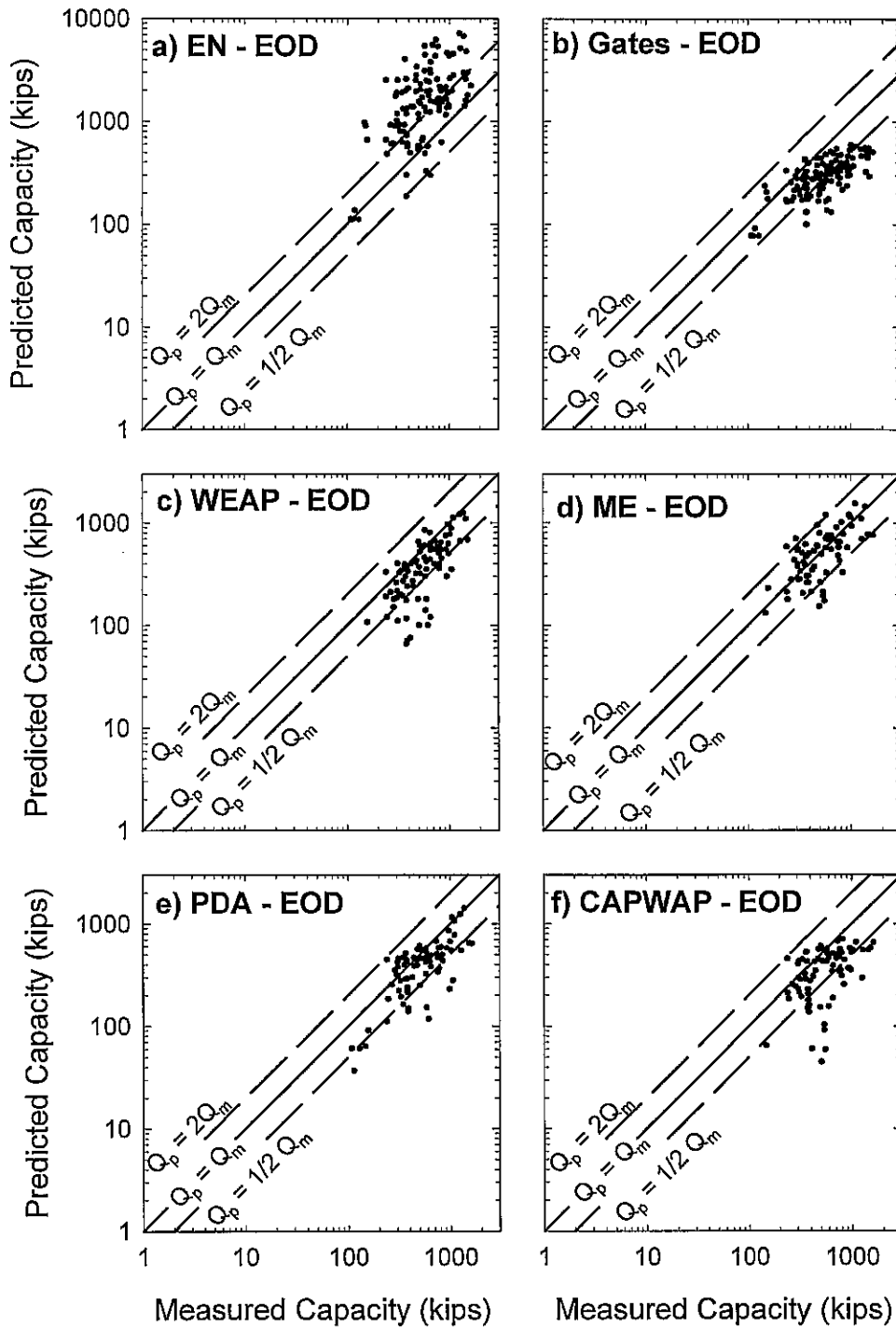


Figure 5.6 Predicted versus measured capacity for FHWA database using EOD data

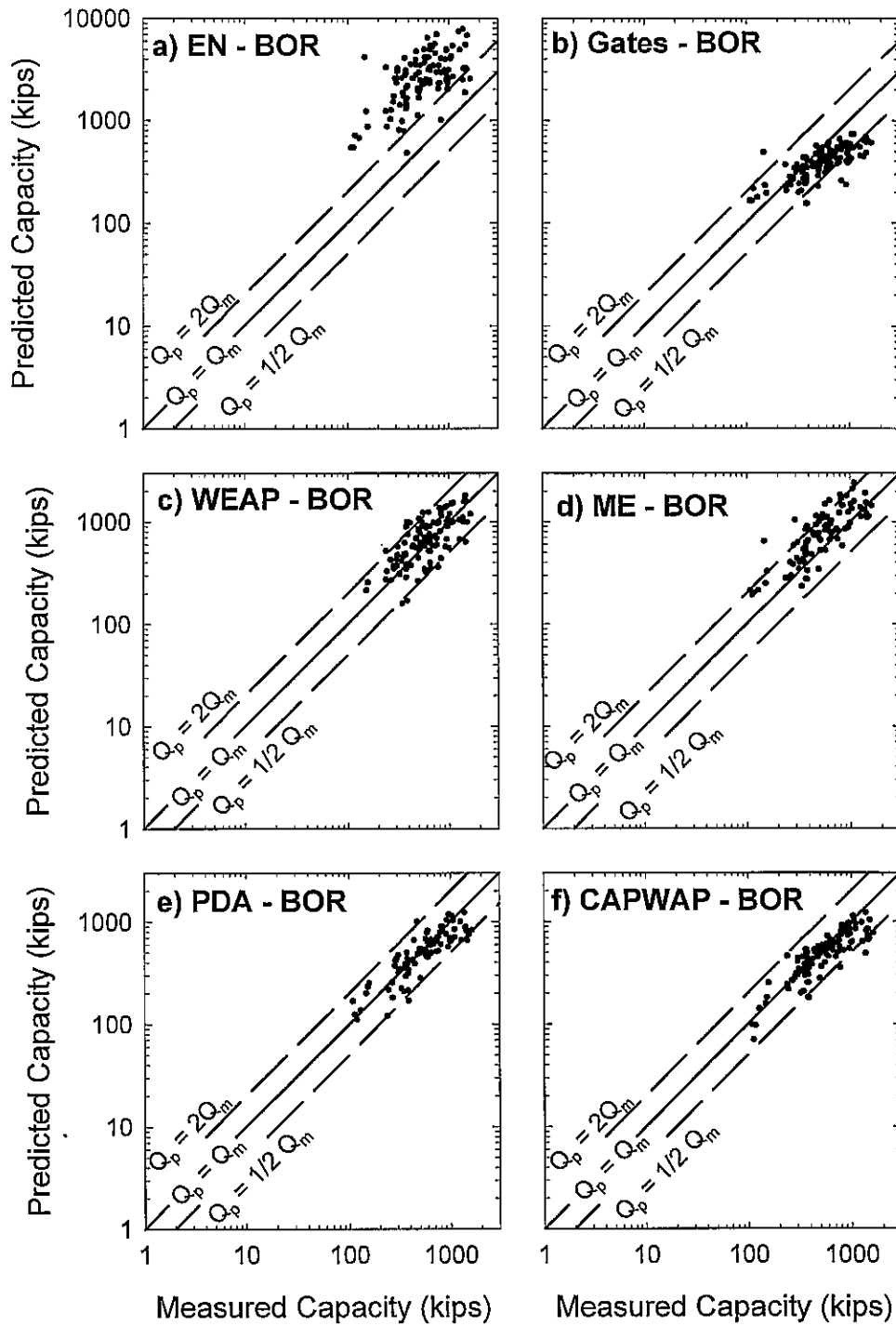


Figure 5.7 Predicted versus measured capacity for FHWA database using BOR data

ANALYSES OF LOAD TEST DATABASES

INTRODUCTION

The results from each of the databases are investigated separately and together to identify the effects using EOD versus BOR data to estimate capacity. Results from cone penetration methods are compared with those obtained using driving data. The Gates equation is investigated further and modifications to improve the equation are provided. H-piles are investigated as a subset of the larger databases to see if they behave differently, and results from the Jacksonville load test are compared with database results to determine if the load tests at Jacksonville are considered "typical."

EFFECT OF USING BOR VERSUS EOD

It is often recommended that BOR results should be used when WEAP, PDA, and CAPWAP are used to predict capacity (FHWA, 1995). Agreement between predicted and measured capacity using BOR results and EOD results are discussed herein.

The capacity of a pile may change with time after the pile is initially driven. An increase in pile capacity with time is called pile setup, whereas a decrease in pile capacity with time is called pile relaxation. It is more common for pile capacity to increase with time. Some pile capacities at 1 month after driving have been shown to increase to several times their capacity exhibited at the end of initial driving while other piles may exhibit little change in capacity. Piles driven into soft clays will usually exhibit a greater setup than piles driven into sands; however, piles driven into sands can also exhibit setup.

Several efforts to document and predict the magnitude of change in pile capacity with time are discussed in Appendix B. Most of the methods are empirical and

unreliable because the time dependent change in capacity depends on several factors including soil profile, pile type, and driving details. Accordingly, time effects are most reliably quantified on a site-by-site basis. Beginning of restrike (BOR) results provides the engineer with a way to assess the effect of time on the capacity of a pile.

The FHWA database is used to compare capacity predictions using BOR results with predictions using EOD results. Only load tests were included in which pile capacities could be predicted for both EOD and BOR. Results of the comparison are given in Table 6.1. For each predictive method, the mean (μ) and standard deviation (σ_{ln}) for the ratio of Q_p/Q_m (predicted capacity to measured capacity) is reported along with the number of load tests used to assess the statistics. The mean (μ) for BOR conditions is greater than the mean (μ) for EOD for all predictive methods. This result is due to the increase in pile driving resistance with time. A greater pile resistance for BOR conditions results in a prediction of greater capacity than for EOD conditions.

The standard deviations (σ_{ln}) for all methods decrease for BOR conditions. It is reasonable to expect Q_p/Q_m based on BOR conditions to exhibit less scatter since BOR conditions are more representative of pile resistance at some time after driving and closer to the time the static load test was conducted. It is interesting to note the change that occurs in the scatter associated with a predictive method for EOD and BOR conditions. The most empirical method (Gates) exhibits the least change in σ_{ln} while the most rigorous method (CAPWAP) exhibits the greatest change in σ_{ln} .

A graph is used to illustrate the changes that occur in mean and standard deviation from EOD conditions to BOR conditions (Fig. 6.1). The graph plots mean (μ) versus standard deviation (σ_{ln}) for each method (EN, Gates, WEAP, ME, PDA, and CAPWAP) for both EOD and BOR conditions. The graph does not imply there is a relationship between mean and standard deviation. The purpose of the graph is to allow the reader to visualize the changes in mean (bias) and standard deviation (scatter) that occur due to EOD and BOR conditions.

Mean (μ) and standard deviation (σ_{in}) for EOD conditions are plotted with a letter symbol identifying the method, and a “plus sign” represents the μ and σ_{in} for BOR conditions. A solid line joins the EOD and BOR symbols for each method. The path of the line drawn from EOD to BOR is upward (indicating an increase in μ) and to the left (indicating a decrease in σ_{in}). It can also be seen readily that the Gates method changes least, while the CAPWAP method changes the greatest.

The intent of the Fig. 6.1 is to illustrate the effect of using BOR as opposed to EOD results for a specific method. Accordingly, Fig. 6.1 should be used only to determine the advantage of using BOR results for each predictive method. The graph should not be used to compare between predictive methods because the same data are not used for each method. For example, the EN method uses 116 load tests to determine the mean and standard deviation for both EOD and BOR conditions; however, WEAP is evaluated using only 88 load tests.

OBSERVATIONS OF BIAS AND SCATTER FOR SPECIFIC METHODS

Several databases have been introduced and discussed in the previous chapters. The purpose of this section is to discuss overall observations of bias and scatter for predictive methods. By comparing results of several separate databases, we can determine the consistency of observed trends and assess the overall trends of predictive methods.

Bias and scatter will be discussed frequently in the following paragraphs. Equations to calculate bias and scatter and tables providing their values for each method have been presented earlier; however, this section will attempt to compare the bias and scatter among different databases. Accordingly, some guidelines are presented to assist the reader in evaluating the statistical parameters. For example, a mean value of 1.05 reflects a method that tends to overpredict capacity by an average of 5 percent. Predictive methods that overpredict or underpredict capacity by 5 percent are considered unbiased. Any mean value less than 0.95 and greater than 1.05 would benefit from recalibration to bring the average Q_p/Q_m to a value of unity.

Scatter exhibited by a predictive method is quantified with the standard deviation. The smaller values for standard deviation correspond to a method that predicts capacity consistently. Greater values for standard deviation reflect poor consistency. The scatter exhibited by a predictive method is placed into one of five categories according to its value of standard deviation. The five categories are very good, good, fair, poor, and very poor for standard deviation values between 0.0 – 0.3, 0.3 – 0.4, 0.4 – 0.5, 0.5 – 0.6, and greater than 0.6, respectively.

These categories are applied to the FHWA database for all methods (EN, Gates, WEAP, ME, PDA, and CAPWAP) for EOD and BOR conditions as shown in Figs. 6.2 and 6.3, respectively, and summarized in Table 6.2.

EN Formula

Predicted versus measured capacity has been determined for several databases including Flaate, Fragaszy, and the FHWA database. Results for the FHWA database are given as “unfiltered” and “filtered.” The unfiltered results represent all loadtest data in which the EN formula could be used to determine capacity. The “filtered” dataset represents a collection of load tests in which capacity could be predicted from several methods (such as EN, Gates, WEAP, ME, PDA, and CAPWAP). Table 6.3 lists the values of mean and standard deviation for Q_p/Q_m based on these datasets and the data are plotted in Figs. 6.4a and 6.4b.

The data shown in Fig. 6.4a are for EOD conditions. The mean values range from 2.5 to 3.5 meaning the method overpredicts capacity by a factor of 2.5 to 3.5. The standard deviations range from 0.52 to 0.68 which corresponds to a large degree of scatter, and therefore, the method’s precision is rated as poor to very poor.

The data shown in Fig. 6.4b are for BOR conditions. The mean value for BOR conditions is about 4.5, meaning the method overpredicts capacity by a factor of about 4.5. Use of BOR (instead of EOD) is seen to reduce the standard deviation; however, the precision for the method is not improved greatly (fair to poor).

In summary, the EN formula appears to overpredict capacity and exhibits poor precision. The method requires calibration to address the issue of overprediction. The precision for the EN method is poor and is slightly improved when using BOR results, however, the improvement is not enough to make this a precise method for predicting capacity.

Gates Formula

The datasets used for assessing the Gates and EN formulae are identical and described above. The datasets are those collected by Flaate, Fragaszy, and the FHWA. Table 6.4 lists the values of mean and standard deviation for Q_p/Q_m based on these datasets and the data are plotted in Figs. 6.5a and 6.5b.

The data shown in Fig. 6.5a summarize predictions made with the Gates method for EOD conditions. The mean values range from 0.53 to 0.85 meaning the method underpredicts capacity by a factor of 0.53 to 0.85. The standard deviations range from 0.307 to 0.459 which correspond to a precision rating of good to fair.

The data shown in Fig. 6.5b are for BOR conditions. The mean value for BOR conditions is about 0.7, meaning the method underpredicts capacity. Use of BOR (instead of EOD) is seen to reduce the standard deviation but very slightly, and therefore, the precision for the method is unchanged.

In summary, the Gates formula underpredicts capacity and exhibits good precision. The method requires calibration to address the issue of underprediction. The precision for the Gates method is good – to - fair and use of BOR results do not improve the precision of the method.

WEAP Method of Analysis

The datasets used for assessing the WEAP method are restricted to the FHWA database only. The FHWA database is the only database in which predictions were made with WEAP. Values of mean and standard deviation for Q_p/Q_m are presented for two versions of the FHWA database in Table 6.5. The unfiltered database corresponds to any pile in which WEAP was used to predict capacity, and the filtered

database corresponds to loadtests in which capacities could be calculated using several predictive methods (EN, Gates, WEAP, ME, PDA, and CAPWAP). Resulting mean and standard deviation values are plotted in Figs. 6.6a and 6.6b.

The data shown in Fig. 6.6a summarize predictions made with WEAP for EOD conditions. The mean values range from 0.64 to 0.75 meaning the method underpredicts capacity. The standard deviations range from about 0.39 to 0.50 which correspond to an average precision rating of fair.

The data shown in Fig. 6.5b are for BOR conditions. The mean value for BOR conditions is about 1.1, meaning the method (on the average) overpredicts capacity by about ten percent. Use of BOR (instead of EOD) is seen to reduce the standard deviation slightly for the filtered database and significantly for the unfiltered database, resulting in good precision.

In summary, WEAP underpredicts capacity for EOD conditions and slightly (just by 10 percent) overpredicts capacity when using BOR. Precision is good when using BOR information, but only fair when using EOD information. It appears that WEAP predictions benefit significantly from using BOR data.

Measured Energy (ME) Method

The datasets used for assessing the ME method include the Paikowski database and the FHWA database. The two databases have some load tests in common with each other, so similar trends are seen for both. Values of mean and standard deviation for Q_p/Q_m are presented Table 6.6. The unfiltered FHWA database corresponds to any pile in which ME was used to predict capacity, and the filtered database corresponds to only load tests in which capacities could be calculated using several predictive methods (EN, Gates, WEAP, ME, PDA, and CAPWAP). Resulting mean and standard deviation values are plotted in Figs. 6.7a and 6.7b.

The data shown in Fig. 6.7a summarize predictions made with the ME approach for EOD conditions. The mean values are close to 1.0 and range from 0.93 to 1.06 meaning the method predicts capacity within ten percent. The standard deviations

range from about 0.30 to 0.46. The filtered database and the database by Paikowski exhibit good precision while the unfiltered FHWA database exhibits fair precision.

The data shown in Fig. 6.7b are for BOR conditions. The mean value for BOR conditions ranges from 1.25 to 1.41, meaning the method (on the average) overpredicts capacity. Use of BOR (instead of EOD) does not improve the precision for Paikowski's data. Precision improved for the unfiltered database, but degraded for the filtered database. However, all predictions using BOR data resulted in good precision.

In summary, the ME approach predicts capacity well for EOD conditions and overpredicts capacity when using BOR. Precision is good when using EOD and BOR information. It appears that EOD results are preferred with the ME approach for predicting capacity.

PDA Method

Three datasets (Davidson, FHWA (unfiltered), and FHWA (filtered)) are used for assessing the PDA method. The Davidson database contains only concrete piles driven in sands in Florida, while the FHWA includes all pile types. Values of mean and standard deviation for Q_p/Q_m are presented Table 6.7. The unfiltered FHWA database corresponds to any pile in which the PDA method was used to predict capacity, and the filtered database corresponds to load tests in which capacities could be calculated using all the predictive methods (EN, Gates, WEAP, ME, PDA, and CAPWAP). Resulting mean and standard deviation values are plotted in Figs. 6.8a and 6.8b.

The data shown in Fig. 6.8a summarize predictions made with the PDA for EOD conditions. The mean values range from 0.71 to 0.84 with an average mean value around 0.80. Accordingly, the method, on the average, underpredicts capacity for EOD conditions. The standard deviations range from about 0.30 to 0.45. The database by Davidson and the filtered FHWA database plot in the zone of good precision while the unfiltered FHWA database exhibits fair precision.

The data shown in Fig. 6.8b are for BOR conditions. The mean value for BOR conditions is higher than for EOD conditions and ranges from 0.90 to 1.07 with an average near unity. Use of BOR (instead of EOD) improves the precision for all three datasets. All predictions using BOR data resulted in precision rated as very good to good.

In summary, the PDA method predicts capacity very well for BOR conditions and with less precision for EOD conditions. There is a tendency to underpredict capacity by 20 – 30 percent with EOD results. Precision is very good to good when using BOR information and good to fair when using EOD results.

CAPWAP Method

Four datasets (Paikowski, Davidson, FHWA (unfiltered), and FHWA (filtered)) are used for assessing the CAPWAP method. Details of these databases are described in previous sections. Values of mean and standard deviation for Q_p/Q_m are presented Table 6.8. Resulting mean and standard deviation values are plotted in Figs. 6.9a and 6.9b.

The data shown in Fig. 6.9a summarize predictions made with the CAPWAP for EOD conditions. The mean values range from 0.58 to 0.75 with an average mean value around 0.70. Accordingly, the method, on the average, underpredicts capacity for EOD conditions. The standard deviations exhibit a wide range (0.38 to 0.59). The data from Davidson, Paikowski, and the filtered FHWA database plot in the zone of good precision while the unfiltered FHWA database exhibits poor precision.

The data shown in Fig. 6.9b are for BOR conditions. The mean value for BOR conditions is higher than for EOD conditions and ranges from 0.83 to 0.95. Use of BOR (instead of EOD) improves the precision for all four datasets. All predictions using BOR data resulted in precision rated as very good to good.

In summary, the CAPWAP method predicts capacity very well for BOR conditions and with less precision for EOD conditions. There is a tendency to underpredict

capacity by 20 – 40 percent with EOD results. Precision is very good to good when using BOR information and good to poor when using EOD results.

Static Method

Additional databases and predictive methods are included to provide a perspective on the accuracy and precision produced by methods using strengths determined in the field and in the laboratory to determine pile capacity. These predictive methods are identified as static methods. While it is not a focus of this effort to develop or evaluate static methods, it is instructive to provide, in a limited way, information on the ability of static methods to predict pile capacity. Accordingly, three datasets were collected: a dataset reporting results of predictions based on cone penetration tests (Eslami dataset), a dataset employing the SPT94 method (Davidson dataset) and a static method based on the FHWA manual for predicting pile capacity (FHWA dataset). Details of these databases are described in previous sections. Values of mean and standard deviation for Q_p/Q_m are presented Table 6.9. Resulting mean and standard deviation values are plotted in Figs. 6.10a and 6.10b.

The data shown in Fig. 6.10a summarize predictions made with the static method based on cone penetration results. The mean values range from 0.94 to 1.2. Each of the six cone methods represents a different method of analysis, however, it is interesting to note that the methods, on the average, predict capacity well. The standard deviations exhibit a wide range (0.28 to 0.45). The method by Eslami shows very good precision while the DeRuiter and Schmertmann methods exhibits fair precision.

The data shown in Fig. 6.10b are for static methods (other than cone). The mean value for the SPT94 (Davidson dataset) exhibits a mean of 0.53 and a standard deviation equal to 0.73. The result is a method that, on the average, underpredicts capacity greatly, and exhibits very poor precision. The static predictions for the

FHWA database (for filtered and unfiltered) tend to overpredict (mean values range from 1.15 to 1.38) and exhibit poor to very poor precision.

In summary, static methods based on cone results exhibit better accuracy and precision than the other static methods. The cone method proposed by Eslami predicts capacity with very good precision, but most of the other cone methods predict capacity with good to fair precision. The static methods exhibit poor to very poor precision.

MODIFIED GATES

Olson and Flaate (1969) identified the Gates method as an empirical formula that, with proper calibration, predicted capacity with precision similar to or better than the other dynamic methods available. The other dynamic formulas often required more measurement information and greater effort to calculate capacity than the Gates method. Olson and Flaate proposed a modified Gates formula to improve the relationship between measured and predicted capacity.

Data presented in this study also suggest the original Gates equation exhibits good precision (for a dynamic formula) but its predictive capabilities need to be improved. The mean value, as shown in Fig. 6.5 and reported in Table 6.4 shows the method underpredicts capacity ($\mu = 0.49$ to 0.85 , depending on the dataset). Plots of predicted versus measured capacity for the Gates method are shown in Fig. 6.11 for the datasets by Flaate, Fragaszy, FHWA (unfiltered), FHWA (filtered), and FHWA (where $E = W*H$). All datasets include only concrete and steel piles. All hammer types are included except gravity hammers. The FHWA (unfiltered) dataset include all piles in which the hammer energy could be determined, whether from the product of the weight of ram and height of drop ($E = W*H$), or from the rated energy. Energy calculated using $W*H$ was preferred. The FHWA (filtered) dataset includes all piles in which the capacity could be estimated using EN, Gates, WEAP, ME, PDA, and CAPWAP methods. The FHWA ($E=W*H$) method includes only piles in which the capacity could be determined using $W*H$.

It can be seen that, on the average, the Gates method underpredicts capacity for all datasets. All plots also show the underprediction is more severe for greater pile capacities. The trend is better illustrated in Fig. 6.12 as a plot of the ratio Q_p/Q_m versus measured pile capacity. Statistics for the values of Q_p/Q_m are given in Table 6.10. The average value for Q_p/Q_m using the original Gates formula is $\mu = 0.56$ and the standard deviation is $\sigma_{in} = 0.336$.

Dataset Created for Study of Gates Method

Datasets developed by Flaate, Fragaszy, and FHWA were combined to develop a single database of pile load tests for investigating the Gates formula and for determining if predictions with the Gates formula could be improved. The pile load tests included from each dataset require that the hammer energy be determined by $W*H$, the pile be steel or concrete. All hammer types were included except gravity hammers. A total of 108 load tests are in this database. The dataset is referred to as the Combined dataset. The relationship of predicted versus measured capacity is given in Fig. 6.13a and the relationship between the ratio Q_p/Q_m and measured capacity is given in Fig. 6.13b.

Modified Gates (with Linear Correction Factor)

Olson and Flaate (1969) modified the Gates formula to provide a better fit to the measured capacity for pile load tests in their collection. The correction was a simple modification of the original Gates formula following the form:

$$Q_{Gates(modified)} = A * Q_{Gates(original)} + B \quad (6.1)$$

where $Q_{Gates(modified)}$ is the modified pile capacity, $Q_{Gates(original)}$ is the pile capacity based on the original Gates equation, and A and B are constants. Olson and Flaate used their collection of load tests to determine the coefficients A and B that best fit the measured capacity. The constants were determined using a least squares fit through the plot of predicted versus measured capacity. Their findings were as follows:

$$Q_{Gates(modified)} = 1.62 * Q_{Gates(original)} - 54 \quad (6.2)$$

for concrete piling, and

$$Q_{Gates(modified)} = 2.34 * Q_{Gates(original)} - 166 \quad (6.3)$$

for steel piling. Pile capacities are in units of kips. If only one equation is to be used for both steel and concrete piles, then Olson and Flaate recommend averaging the coefficients, which results in the following equation:

$$Q_{Gates(modified)} = 1.98 * Q_{Gates(original)} - 110 \quad (6.4)$$

for both concrete and steel piling.

The same procedure (used by Olson and Flaate) was applied to determine the A and B coefficients for the load test data collected in this exercise. Load test data from Flaate, Fragaszy, and FHWA were compiled into one database and the constants A and B were determined from a least squares fit through the data. The resulting modified Gates formula is as follows:

$$Q_{Gates(modified)} = 2.47 * Q_{Gates(original)} - 154 \quad (6.5)$$

The agreement between predicted capacity (using the modified Gates formula as given in Eqn. 6.5) and measured capacity is shown in Fig. 6.14a. The general trend of the plotted points suggest that predicted capacity seems to agree with measured capacity for the entire range of capacity. This general trend is confirmed with the plot of Q_p/Q_m versus Q_m shown in Fig. 6.14b. Statistics for the values of Q_p/Q_m for the modified Gates formula are given in Table 6.10. The method is identified as the modified Gates method formula with a linear correction factor. The average value for Q_p/Q_m using the original Gates formula is $\mu = 1.01$ and the standard deviation is $\sigma_m = 0.347$.

However, a potential problem with using a linear correction factor (Eqns. 6.1 - 6.5) is that the coefficients A and B may result in predicting capacity less than zero. Accordingly, another form for the correction factor is explored below:

Modified Gates (with Power Function for Correction Factor)

The original Gates method clearly benefits from a correction factor that increases its predicted capacity; however, only slight correction is required for the lower capacities while a greater correction is required for the higher capacities. A correction factor in the form of a power function provides a means to accomplish this task without the risk of predicting a negative pile capacity (as can happen with the linear correction factor). Accordingly, the modified Gates formula using a power function was investigated. The form of the modified Gates formula is given below:

$$Q_{Gates(modified)} = A * Q_{Gates(original)}^B \quad (6.6)$$

The constants A and B were determined by plotting the ratio Q_p/Q_m versus Q_p on a log-log plot. A least squares fit through the data points resulted in determining the parameters $A = 0.25$ and $B = 1.35$. Thus, the resulting modified Gates formula is as follows:

$$Q_{Gates(modified)} = 0.25 * Q_{Gates(original)}^{1.35} \quad (6.7)$$

The agreement between predicted capacity (using the modified Gates formula as given in Eqn. 6.6) and measured capacity is shown in Fig. 6.15a. The general trend of the plotted points suggest that predicted capacity seems to agree with measured capacity for the entire range of capacity. This general trend is confirmed with the plot of Q_p/Q_m versus Q_m shown in Fig. 6.15b. Statistics for the values of Q_p/Q_m for the modified Gates formula (with a power function) are given in Table 6.10. The average value for Q_p/Q_m using the original Gates formula is $\mu = 0.98$ and the standard deviation is $\sigma_m = 0.337$.

The power function provides a slightly better fit with less scatter and Eqn. 6.7 will be used as the modified Gates method in this study.

H-PILES

The Flaate, Fragaszy, and FHWA databases were inspected to assess if there were differences in the predictions for H-piles versus the predictions for all piles. Plots of predicted capacity versus measured capacity for H-piles were compared with predicted versus measured capacity for all piles and statistics for Q_p/Q_m for each database were determined for all piles and compared with statistics for only H-piles.

Flaate Database

A plot of predicted versus measured capacity for all piles and for H-piles only is shown in Fig. 6.16 for the EN formula, Hiley formula, Janbu formula, and Gates formula. The data for “all piles” are designated with a hollow circle while the data for “H-piles” are designated with an “H.” There are 15 H-piles from a total of 54. The Flaate database was filtered to include only piles driven with air, steam, or diesel. No load tests for piles driven with gravity hammers were included.

The general trend observed for the H-pile data is similar to the trend for all piles, however, there are fewer H-piles in which pile capacity is severely underpredicted. Accordingly, one would expect the mean value of Q_p/Q_m for “H-piles” to be greater than “all piles.” The scatter for the H-pile data appears less than that observed for all piles.

Statistics for the Flaate database are given for all methods (EN, Hiley, Janbu, and Gates) in Table 6.11. Statistics are given for both “all piles” and for “H-piles” only. For the EN formula, the mean value of Q_p/Q_m for H-piles ($\mu = 3.45$) is significantly greater than the mean value for “all piles” ($\mu = 2.45$). The scatter, as quantified with the standard deviation for Q_p/Q_m , is less for the H-pile ($\sigma_{ln} = 0.441$) data than with all piles ($\sigma_{ln} = 0.790$). The other predictive methods also exhibited higher mean values, however, standard deviations for the H-pile data were slightly greater for the Janbu and Gates formulae.

Fragaszy Database

A plot of predicted versus measured capacity for all piles and for H-piles only is shown in Fig. 6.17 for the EN formula, Hiley formula, Janbu formula, and for the Gates formula. As before, the data for “all piles” are designated with a hollow circle while the data for “H-piles” are designated with an “H.” There are only 5 H-piles from a total of 63 pile load tests.

With only 5 H-pile load tests, general observations are limited. The trend observed for the H-pile data is similar to the trend for all piles, that is, the H-pile results plot within the results of the “all piles” data. Accordingly, one would expect the mean value of Q_p/Q_m for “H-piles” to be similar to that for “all piles.” Scatter for the H-pile data also appears similar to that observed for all piles.

Statistics for the Fragaszy database are given for all methods (EN, Hiley, Janbu, and Gates) in Table 6.12. Statistics are given for both “all piles” and for “H-piles” only. For the EN formula, the mean value of Q_p/Q_m for H-piles ($\mu = 1.62$) is significantly less than the mean value for “all piles” ($\mu = 2.41$). The scatter, as quantified with the standard deviation for Q_p/Q_m , is less for the H-pile ($\sigma_m = 0.474$) data than with all piles ($\sigma_m = 0.653$), however, this comparison has little value since only 5 load tests are available for the H-pile data.

Observations made with the EN formula were not similar to observations made with the Flaate database. While the Fragaszy database shows the mean value of Q_p/Q_m for H-piles to be significantly less than all piles, the Flaate database show the opposite trend. Furthermore, observations made with the EN formula (using the Fragaszy database) were not similar to observations made with the other predictive methods (using the Fragaszy database).

Mean values for Q_p/Q_m for H-piles and “all piles” were much closer for Hiley, Janbu, and Gates formulae. Mean values for H-piles were slightly higher than “all piles” for the Hiley formula, and slightly lower for the Janbu and Gates method. Standard deviations were less for H-piles than for all piles; however, detailed comparisons

between standard deviations are limited because the number of load tests are limited (only 5 H-pile load tests).

FHWA Database

A plot of predicted versus measured capacity for all piles and for H-piles only is shown in Fig. 6.18 for the EN formula, Gates formula, WEAP, ME approach, PDA, and CAPWAP. All predictions are based on driving resistance exhibited at the end of initial driving (EOD). A similar plot is shown in Fig. 6.19 for BOR conditions. Plots of predicted versus measured capacity contain all the piles in which a predictive method could be used to calculate capacity for both EOD and BOR conditions. Accordingly, the number of piles vary for each method and are given in Table 6.13.

The data for “all piles” are designated with a hollow circle while the data for “H-piles” are designated with an “H.” For all methods, the general trend observed for the H-pile data is similar to the trend for all piles. As observed earlier for the Flaate database and Fragaszy database, H-piles capacity is severely underpredicted less often than for “all piles.” Accordingly, one would expect the mean value of Q_p/Q_m for “H-piles” to be greater than for “all piles.” The scatter for the H-pile data is similar to the scatter observed for the EN, Gates, and ME methods, but appears to be less for WEAP, PDA, and CAPWAP methods.

Statistics for the FHWA database are given for all methods (EN, Gates, WEAP, ME, PDA, CAPWAP) in Table 6.13 for EOD and BOR conditions. Statistics are given for “all piles” and for “H-piles” so that mean values and standard deviation for Q_p/Q_m can be compared. For example, using the EN formula with EOD data, the mean value of Q_p/Q_m for H-piles ($\mu = 2.97$) is greater than the mean value for “all piles” ($\mu = 2.60$). However, the difference is not as great as observed for the Flaate database. The scatter, as quantified with the standard deviation for Q_p/Q_m , is less for the H-pile ($\sigma_{in} = 0.563$) data than with all piles ($\sigma_{in} = 0.675$), but these magnitudes of scatter indicate poor to very poor precision. A similar observation is made for H-piles using the EN formula with BOR data.

Statistics for Q_p/Q_m for EOD and BOR conditions are also listed for the other predictive methods in Table 6.13. The mean values for H-piles and “all piles” are similar for all the other predictive methods, indicating that the equations to predict capacity for H-piles are similar to the equations for all piles. The precision of the methods are also similar among H-piles and “all piles” for all methods except CAPWAP. The standard deviation for H-piles is lower ($\sigma_n = 0.372$) than for “all piles” ($\sigma_n = 0.591$); however, there are only 9 H-pile load tests in the CAPWAP (EOD) which is too few to draw ($\sigma_n = 0.372$) conclusions with certainty. The modified gates formula (as developed in the previous section of this chapter) yielded similar statistics for all piles and H-piles.

AGREEMENT OF JACKSONVILLE RESULTS WITH DATABASES

Two load tests were conducted in Jacksonville, Illinois as part of this research program. Details of the H-pile load tests are given in Appendix A, but the databases here are used to determine uniqueness of these load tests. Plots of predicted versus measured capacity for the two H-pile load tests conducted at Jacksonville Illinois are plotted in Fig. 6.18 (for EOD conditions) and 6.19 (for BOR conditions) for the FHWA database.

It can be seen in each of these cases that the results from the Jacksonville load tests fall in the middle of the data from both databases. This indicates the load tests conducted at Jacksonville yield typical results.

SUMMARY: BIAS AND SCATTER

The ability of EN, Gates, and ME methods to predict pile capacity accurately benefits little from using BOR data. WEAP, PDA, and especially CAPWAP benefit from the use of BOR data. Pile capacity using EOD data is shown to predict with about the same precision with Gates, WEAP, ME, PDA, and CAPWAP. The ME method appears provides the most precise measurements when only EOD data are used.

The database shows that use of CAPWAP with BOR data to predict capacity results in the greatest precision of all predictive methods investigated. For non-monitored methods, BOR results generally exhibited slightly less scatter than when using EOD data. The pile driving formulae exhibit greater precision than static methods although some methods that use cone penetrometer predicted capacity with similar precision. Specific observations are given below for each of the dynamic methods investigated.

The databases gave no indication there is a significant difference between predictions made for H-piles and predictions made for other piles. Accordingly, there is no strong evidence that capacity for H-piles should be predicted with different formulas. Additionally, the Jacksonville load test results indicate all the methods predicted capacity with reasonable precision, and are in general agreement with predictions of capacity studied in the load test databases.

EN formula

The ability of the EN formula to predict pile capacity is limited. The EN formula predicts capacity with poor precision for both EOD and BOR conditions. The method tends to overpredict capacity. All databases investigated (Flaate, Fragaszy, FHWA) identify the EN formula as predicting capacity with the least precision. There does not appear to be a fundamental difference in the ability for the EN formula to predict capacity for H-piles versus other piles.

Gates and Modified Gates

The Gates method, also a dynamic formula, predicts capacity with greater precision than the EN formula, although the method tends to underpredict capacity. Precision of the method was not influenced by use of EOD or BOR conditions. The Gates method predicts capacity with good – to – fair precision for all the databases investigated (Flaate, Fragaszy, FHWA). The original Gates method tends to underpredict capacity more severely as pile capacity increases, accordingly, a modified Gates method was developed. The modified method, on the average,

predicts capacity well, with good – to – fair precision (depending on the database investigated).

WEAP

The WEAP method of analysis models the pile and pile driving mechanism. WEAP analyses for capacity are generally considered superior to simple dynamic formulae such as EN and Gates. However, the FHWA database demonstrated that WEAP did not predict capacity with the same level of precision as Gates for EOD conditions. On the other hand, WEAP predicted capacity with greater precision than Gates for BOR conditions. WEAP, on the average, underpredicted capacity by 46 percent for EOD conditions and overpredicted capacity by 6 percent for BOR conditions. Accordingly, estimates of capacity using WEAP are enhanced greatly by using BOR information, and may be excessively conservative when using EOD information.

ME Approach

The ME approach for predicting pile capacity benefits little from using BOR data, thus EOD measurements provide results with the same accuracy. The accuracy and precision of predictions are generally good. The method requires pile monitoring, thus measured energy imparted to the pile and a more accurate measurement of pile set is used in estimating capacity. The basic equation for the ME approach is the EN formula; however, the method exhibits much better precision than the EN formula. The ME approach obviously benefits greatly from better assessment of energy imparted to the pile.

PDA Method

The PDA method of analysis uses simple models for the pile combined with measurements of the pile behavior during driving and energy delivered by the hammer. PDA estimates of capacity are better for BOR conditions than EOD conditions. PDA method generally underpredicts capacity (on the average of 44 percent) when using EOD conditions, but just slightly underpredicts capacity (by 7 percent) for BOR conditions. Precision of the method improves when BOR data are used.

CAPWAP Method

The CAPWAP method uses the most detailed modeling of the pile and hammer system and requires pile dynamic monitoring. Of the methods investigated in this report, it requires the greatest effort to determine pile capacity. However, the application of CAPWAP to EOD conditions results in underpredicting capacity (by 46 percent) with poor precision. However, when BOR information is used, the CAPWAP method predicts capacity well with very good precision, ranking as the best predictive method.

Table 6.1 Statistical parameters for Q_p/Q_m values from FHWA database for comparison of EOD versus BOR

Method	n	End of Driving (EOD)		Beginning of Restrike (BOR)	
		μ	σ_{ln}	μ	σ_{ln}
EN	116	2.66	0.661	4.61	0.514
Gates	116	0.54	0.405	0.72	0.392
WEAP	88	0.64	0.501	1.09	0.373
ME	60	0.91	0.426	1.38	0.403
PDA	67	0.66	0.426	0.93	0.323
CAPWAP	68	0.54	0.552	0.85	0.252

Table 6.2 Statistical parameters for Q_p/Q_m values using FHWA database. Load tests are filtered so that all tests are able to be predicted for either EOD or BOR

Method		n	μ	σ_{ln}
End of Driving (EOD)	EN	50	3.51	0.527
	Gates	50	0.63	0.340
	WEAP	50	0.75	0.392
	ME	50	1.06	0.309
	PDA	50	0.80	0.376
	CAPWAP	50	0.75	0.402
	Static	46	1.38	0.608
Beginning of Restrike (BOR)	EN	72	4.56	0.441
	Gates	72	0.68	0.327
	WEAP	72	1.10	0.361
	ME	72	1.36	0.300
	PDA	72	0.90	0.313
	CAPWAP	72	0.88	0.254
	Static	66	1.18	0.605

Table 6.3 Statistical parameters for Q_p/Q_m values for EOD and BOR conditions for all databases in which statistical values for EN formula could be determined

Database		n	μ	σ_{ln}
EOD	Flaate	54	2.45	0.523
	Fragaszy	57	2.58	0.610
	FHWA (unfiltered)	123	2.60	0.675
	FHWA (filtered)	50	3.51	0.527
BOR	FHWA (unfiltered)	116	4.62	0.514
	FHWA (filtered)	72	4.56	0.441

Table 6.4 Statistical parameters for Q_p/Q_m values for EOD and BOR conditions for all databases in which statistical values for Gates formula could be determined

Database		n	μ	σ_{ln}
EOD	Flaate	54	0.85	0.459
	Fragaszy	57	0.63	0.307
	FHWA (unfiltered)	123	0.53	0.410
	FHWA (filtered)	50	0.63	0.340
	FHWA (E=W*H)	51	0.49	0.323
BOR	FHWA (unfiltered)	116	0.72	0.392
	FHWA (filtered)	72	0.68	0.327

Table 6.5 Statistical parameters for Q_p/Q_m values for EOD and BOR conditions for all databases in which statistical values for WEAP could be determined

Database		n	μ	σ_{ln}
EOD	FHWA (unfiltered)	88	0.64	0.501
	FHWA (filtered)	50	0.75	0.392
BOR	FHWA (unfiltered)	114	1.11	0.385
	FHWA (filtered)	114	1.10	0.361

Table 6.6 Statistical parameters for Q_p/Q_m values for EOD and BOR conditions for all databases in which statistical values for ME formula could be determined

Database		n	μ	σ_{ln}
EOD	Paikowski	92	1.03	0.309
	FHWA (unfiltered)	73	0.93	0.462
	FHWA (filtered)	50	1.06	0.309
BOR	Paikowski	110	1.25	0.303
	FHWA (unfiltered)	92	1.41	0.363
	FHWA (filtered)	72	1.36	0.361

Table 6.7 Statistical parameters for Q_p/Q_m values for EOD and BOR conditions for all databases in which statistical values for PDA could be determined

Database		n	μ	σ_{ln}
EOD	Davidson	65	0.84	0.298
	FHWA (unfiltered)	77	0.71	0.454
	FHWA (filtered)	50	0.80	0.376
BOR	Davidson	62	1.07	0.266
	FHWA (unfiltered)	85	0.91	0.319
	FHWA (filtered)	72	0.90	0.300

Table 6.8 Statistical parameters for Q_p/Q_m values for EOD and BOR conditions for all databases in which statistical values for CAPWAP could be determined

Database		n	μ	σ_{ln}
EOD	Paikowski	91	0.73	0.398
	Davidson	49	0.70	0.375
	FHWA (unfiltered)	75	0.58	0.591
	FHWA (filtered)	50	0.75	0.402
BOR	Paikowski	109	0.83	0.304
	Davidson	70	0.95	0.317
	FHWA (unfiltered)	112	0.86	0.269
	FHWA (filtered)	72	0.88	0.254

Table 6.9 Statistical parameters for Q_p/Q_m values for static methods using cone results and other static formulas

Database		n	μ	σ_{ln}
Cone	Eslami (Schmertmann)	108	0.944	0.443
	Eslami (DeRuiter)	108	1.002	0.390
	Eslami (French)	108	0.939	0.447
	Eslami (Meyerhof)	55	1.258	0.391
	Eslami (Tumay)	33	1.153	0.374
	Eslami (Eslami)	108	1.197	0.276
Static	Davidson (SPT94)	71	0.53	0.734
	FHWA (unfiltered)	112	1.15	0.556
	FHWA (filtered for EOD)	46	1.38	0.608
	FHWA (filtered for BOR)	66	1.18	0.605

Table 6.10 Statistical parameters for Q_p/Q_m values for Original Gates method and the two modified Gates methods

Version of Gates Equation	n	μ	σ_{ln}
Gates (original)	108	0.56	0.336
Modified Gates $Q_{mod} = 2.47 * Q_{gates} - 154$	108	1.01	0.347
Modified Gates $Q_{mod} = 0.25 * (Q_{gates})^{1.35}$	108	0.98	0.337

Table 6.11 Statistical parameters for all piles compared with only H-piles using Olson and Flaate Data

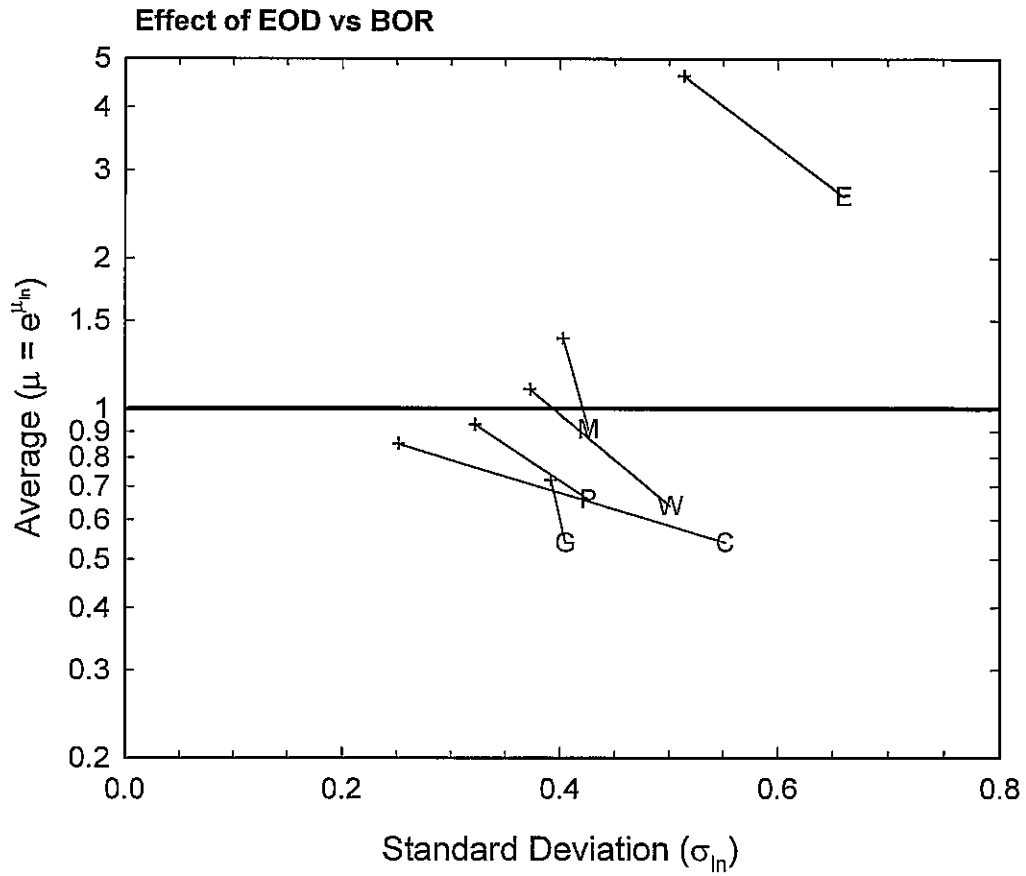
Hammer Type	Method	All pile types			H-piles only		
		n	μ	σ_{ln}	n	μ	σ_{ln}
All hammer types except gravity hammers	EN	54	2.45	0.790	15	3.45	0.441
	Hiley	54	0.74	0.499	15	1.09	0.448
	Janbu	54	1.08	0.307	15	1.44	0.527
	Gates	54	0.85	0.429	15	1.0	0.444

Table 6.12 Statistical parameters for all piles compared with only H-piles using load test data from Fragaszy

Method	All pile types			H-piles only		
	n	μ	σ_{ln}	n	μ	σ_{ln}
EN	63	2.41	0.653	5	1.62	0.474
Hiley	63	1.03	0.450	5	1.10	0.375
Janbu	63	0.87	0.659	5	0.77	0.313
Gates	63	0.64	0.322	5	0.62	0.132

Table 6.13 Statistical parameters for all piles compared with only H-piles using FHWA data

EOD/BOR	Method	All pile types			H-piles only		
		n	μ	σ_{ln}	n	μ	σ_{ln}
EOD	EN	123	2.60	0.675	18	2.97	0.563
	Gates	123	0.53	0.410	18	0.54	0.361
	Mod. Gates	108	0.98	0.337	12	0.95	0.386
	WEAP	88	0.64	0.501	13	0.57	0.460
	ME	73	0.93	0.462	13	1.11	0.442
	PDA	77	0.71	0.454	14	0.70	0.511
	CAPWAP	75	0.58	0.591	9	0.64	0.372
BOR	EN	116	4.62	0.514	15	6.00	0.529
	Gates	116	0.72	0.392	15	0.75	0.314
	WEAP	114	1.11	0.385	15	1.01	0.365
	ME	92	1.41	0.363	14	1.50	0.404
	PDA	85	0.91	0.319	15	0.99	0.318
	CAPWAP	112	0.86	0.269	17	0.91	0.268
Static		112	1.15	0.556	14	0.86	0.761



Symbol Legend

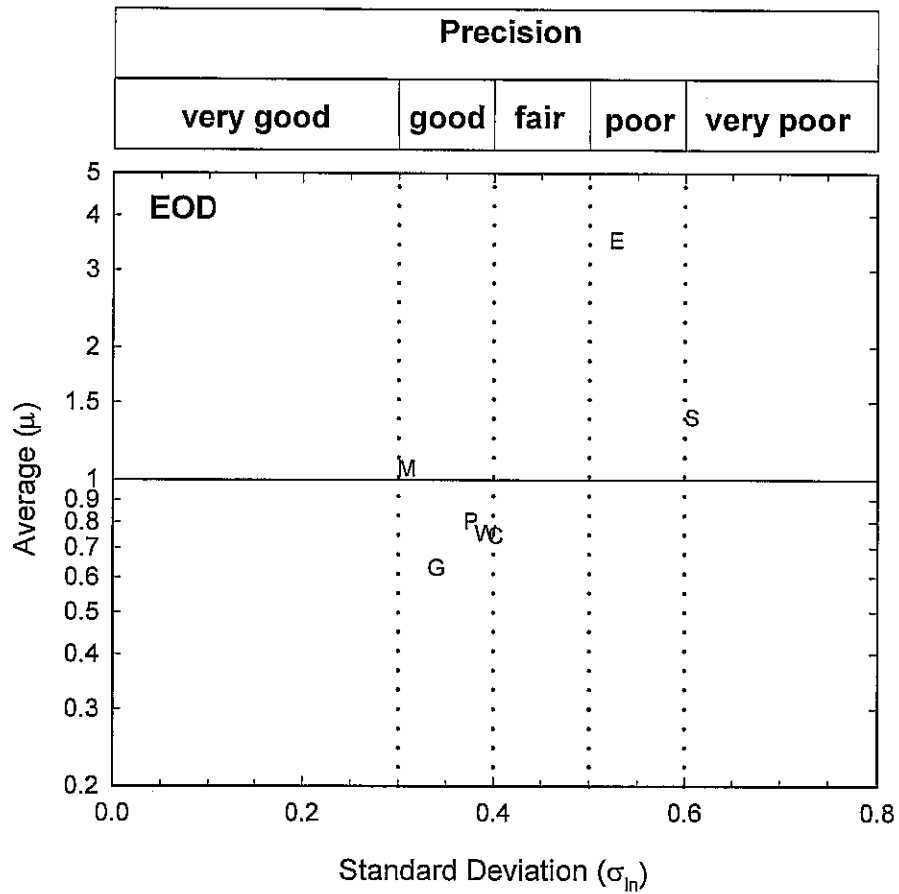
Engineering News formula
 Gates
 WEAP
 Measured Energy
 PDA
 CAPWAP

Graph Legend

Value for method using BOR → +

Value for method using EOD → w

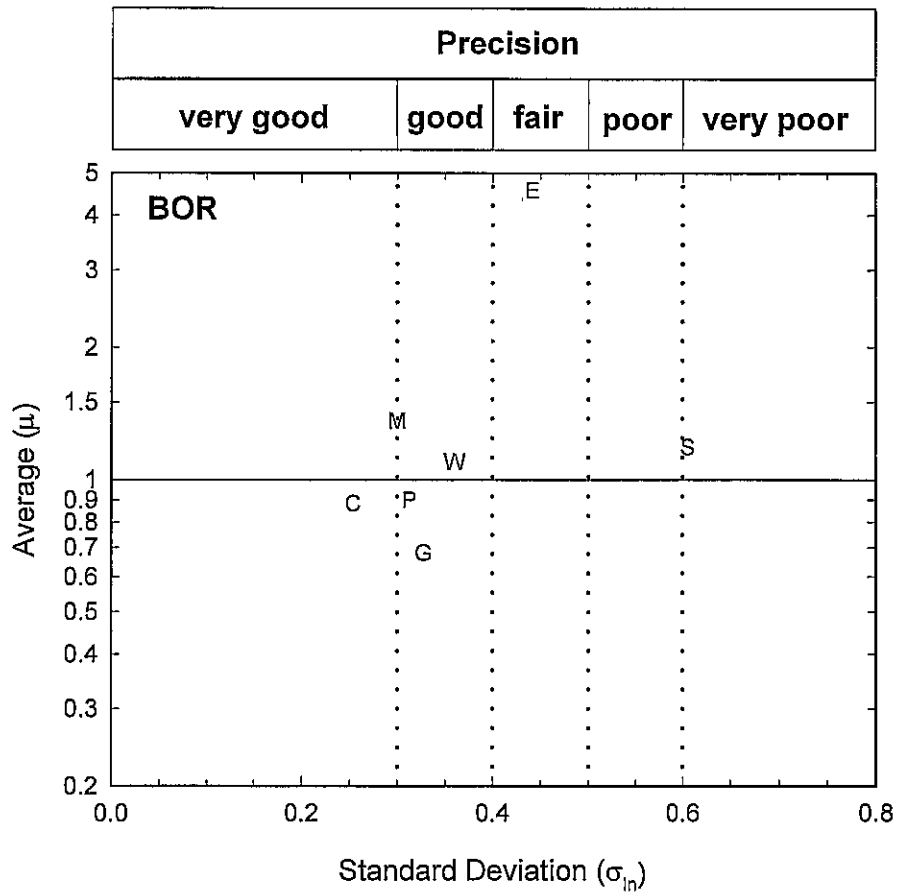
Figure 6.1 Average and standard deviation for all predictive methods in which each method could be used to predict capacity from both EOD and BOR results



Symbol Legend

- E - Engineering News Formula
- G - Gates formula
- W - WEAP
- M - Measured Energy Approach
- P - PDA
- C - CAPWAP
- S - Static method

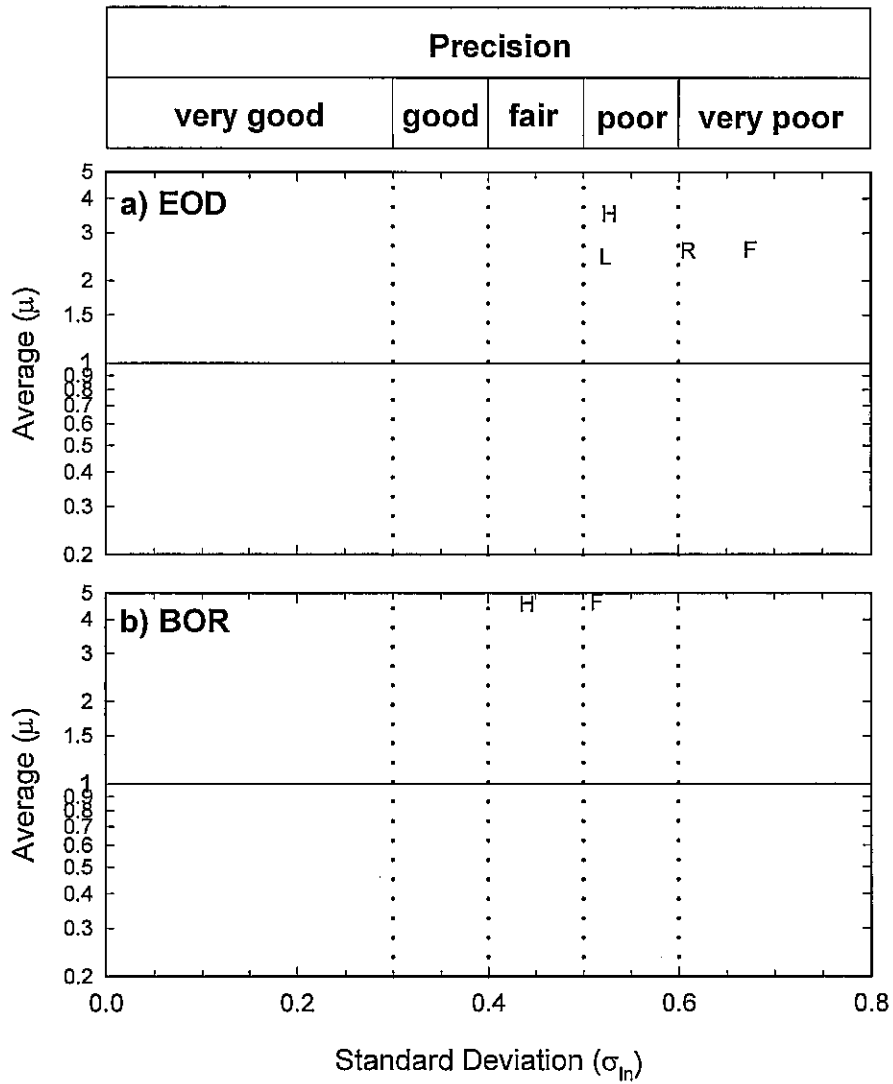
Figure 6.2 Average and standard deviation for all predictive methods in which each method could be used to predict capacity from EOD results



Symbol Legend

- E - Engineering News Formula
- G - Gates formula
- W - WEAP
- M - Measured Energy Approach
- P - PDA
- C - CAPWAP
- S - Static method

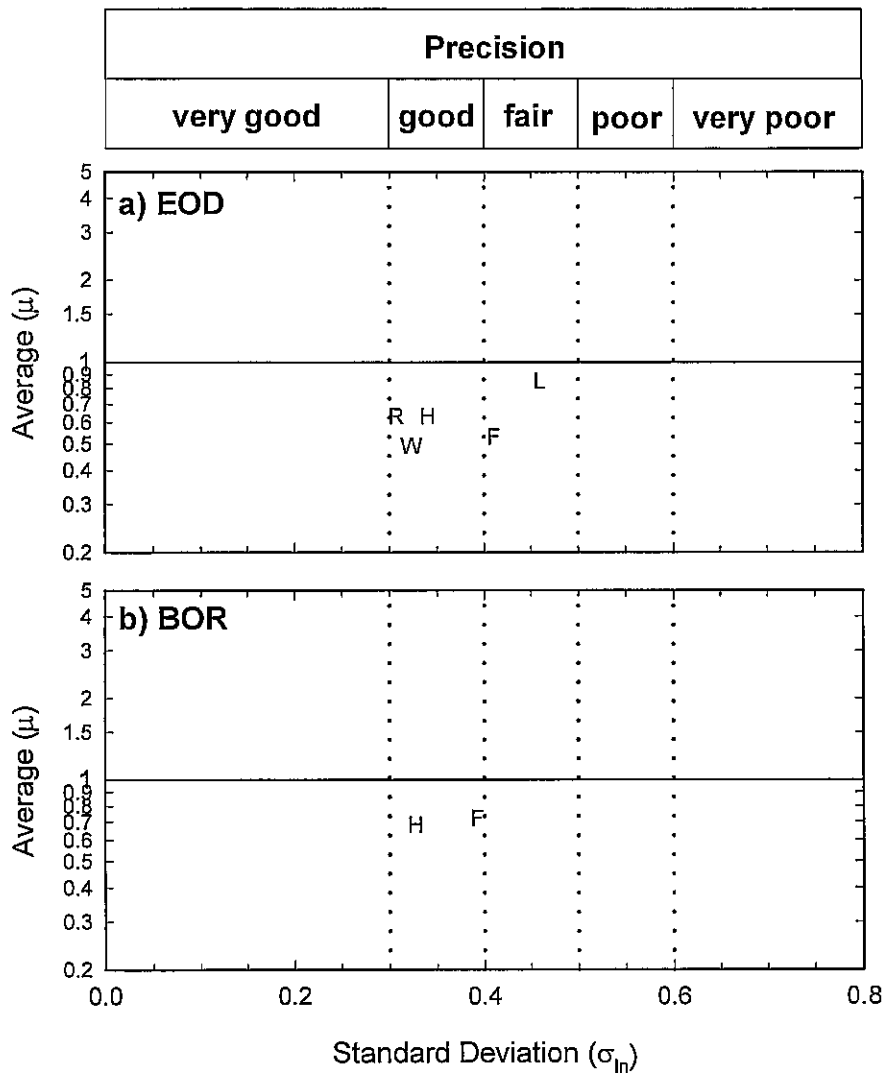
Figure 6.3 Average and standard deviation for all predictive methods in which each method could be used to predict capacity from BOR results



Symbol Legend

- L - Flaate
- R - Fragaszy
- F - FHWA (unfiltered)
- H - FHWA (filtered)

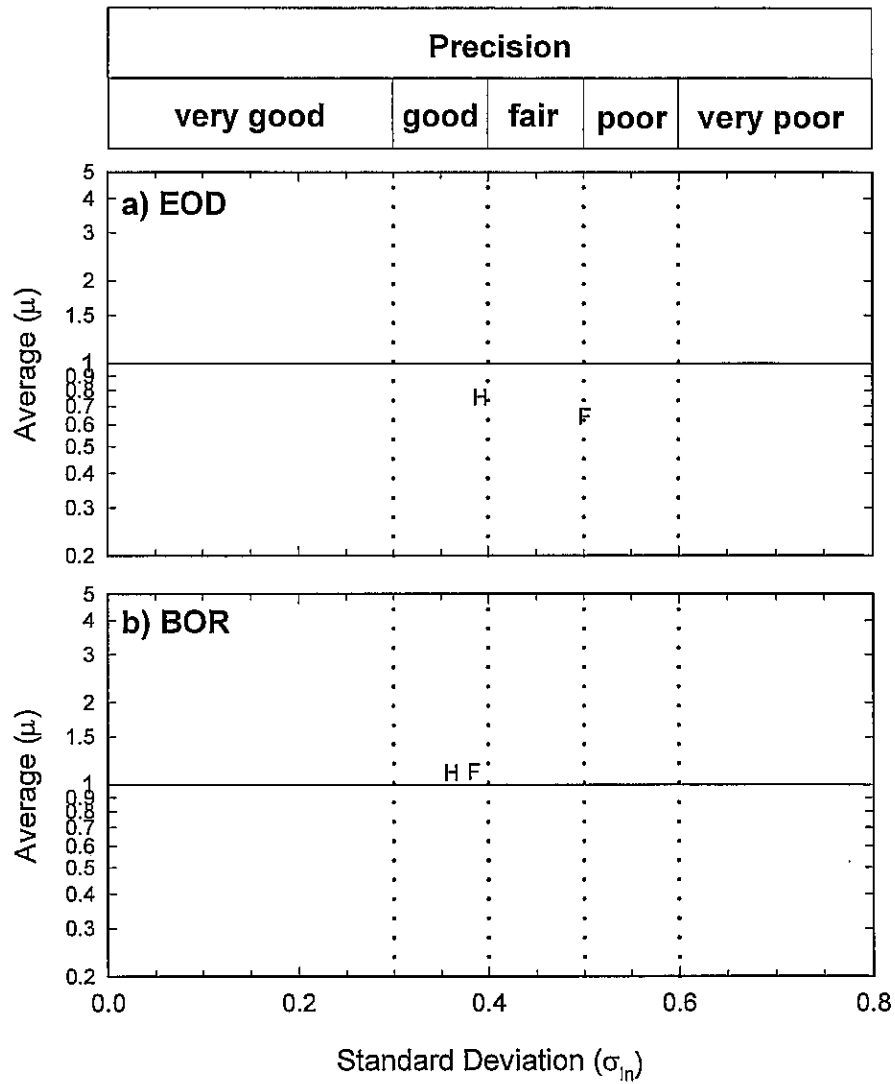
Figure 6.4 Average and standard deviation for datasets in which the EN formula could be used to predict capacity from EOD and BOR results



Symbol Legend

- L - Flaate
- R - Fragaszy
- F - FHWA (unfiltered)
- H - FHWA (filtered)
- W - FHWA ($E=W*H$)

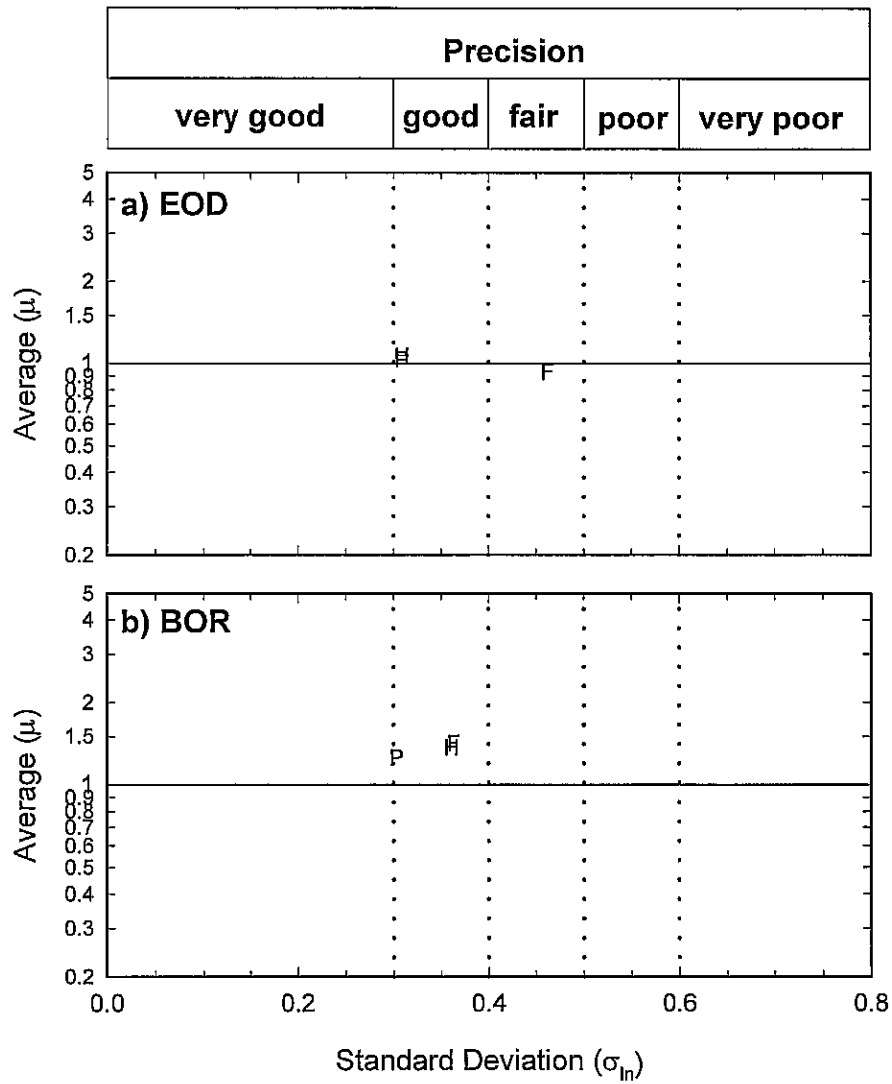
Figure 6.5 Average and standard deviation for datasets in which the Gates formula could be used to predict capacity from EOD and BOR results



Symbol Legend

- F - FHWA (unfiltered)
- H - FHWA (filtered)

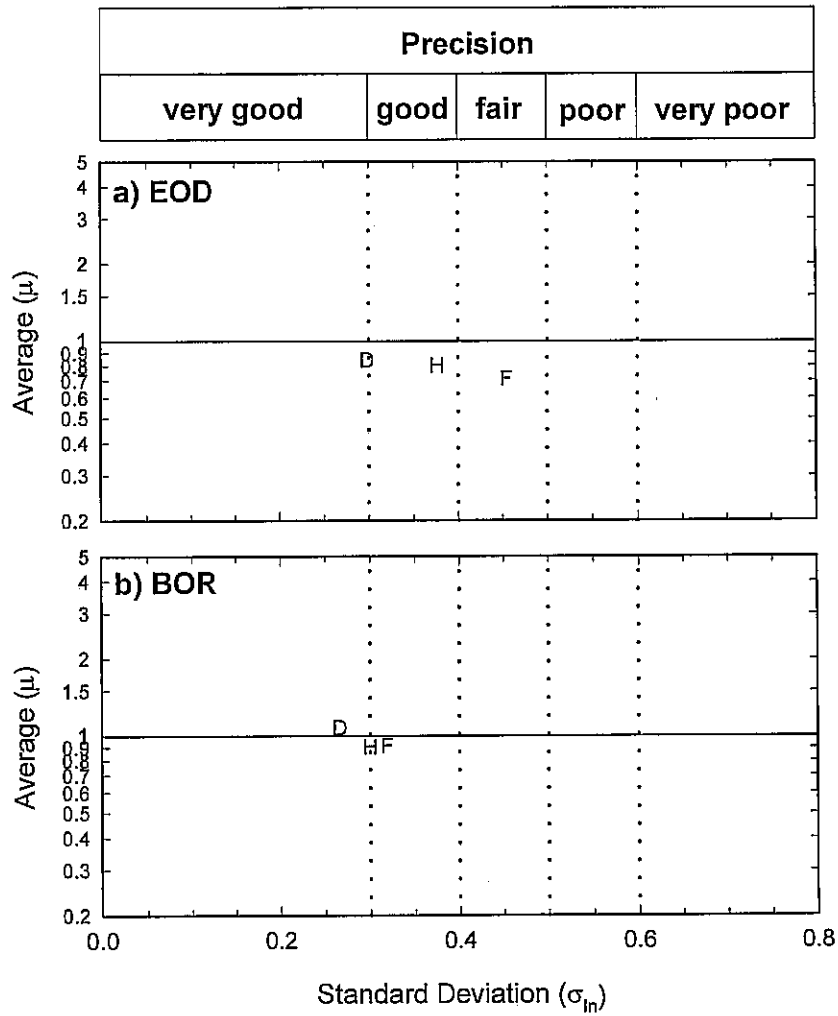
Figure 6.6 Average and standard deviation for datasets in which WEAP could be used to predict capacity from EOD and BOR results



Symbol Legend

- P - Paikowski
- F - FHWA (unfiltered)
- H - FHWA (filtered)

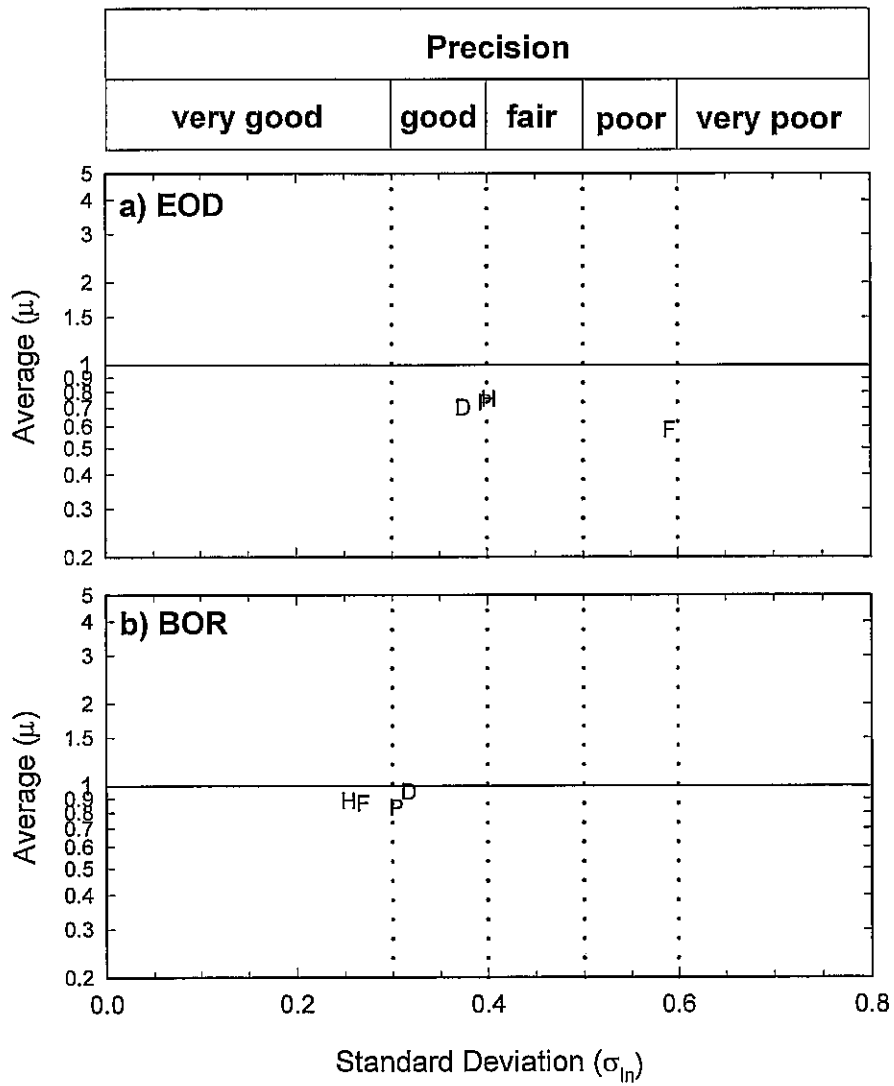
Figure 6.7 Average and standard deviation for datasets in which the ME method could be used to predict capacity from EOD and BOR results



Symbol Legend

- D - Davidson
- F - FHWA (unfiltered)
- H - FHWA (filtered)

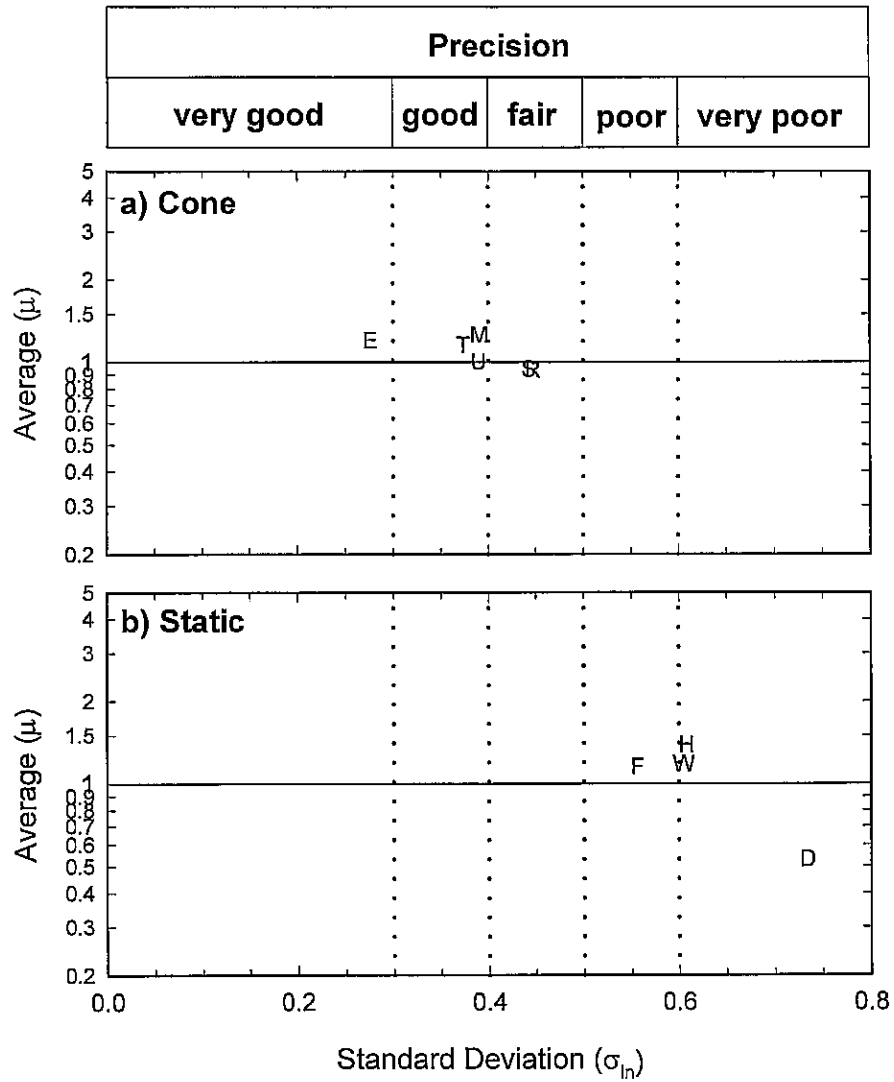
Figure 6.8 Average and standard deviation for datasets in which the PDA method could be used to predict capacity from EOD and BOR results



Symbol Legend

- P - Paikowski
- D - Davidson
- F - FHWA (unfiltered)
- H - FHWA (filtered)

Figure 6.9 Average and standard deviation for datasets in which CAPWAP could be used to predict capacity from EOD and BOR results



Symbol Legend

- S - Schmertmann (cone)
- U - DeRuiter (cone)
- R - French (cone)
- M - Meyerhof (cone)
- T - Tumay (cone)
- E - Eslami (cone)
- D - Davidson
- F - FHWA (unfiltered)
- H - FHWA (filtered for EOD data)
- W - FHWA (filtered for BOR data)

Figure 6.10 Average and standard deviation for datasets in which static formulae could be used to predict capacity from EOD and BOR results

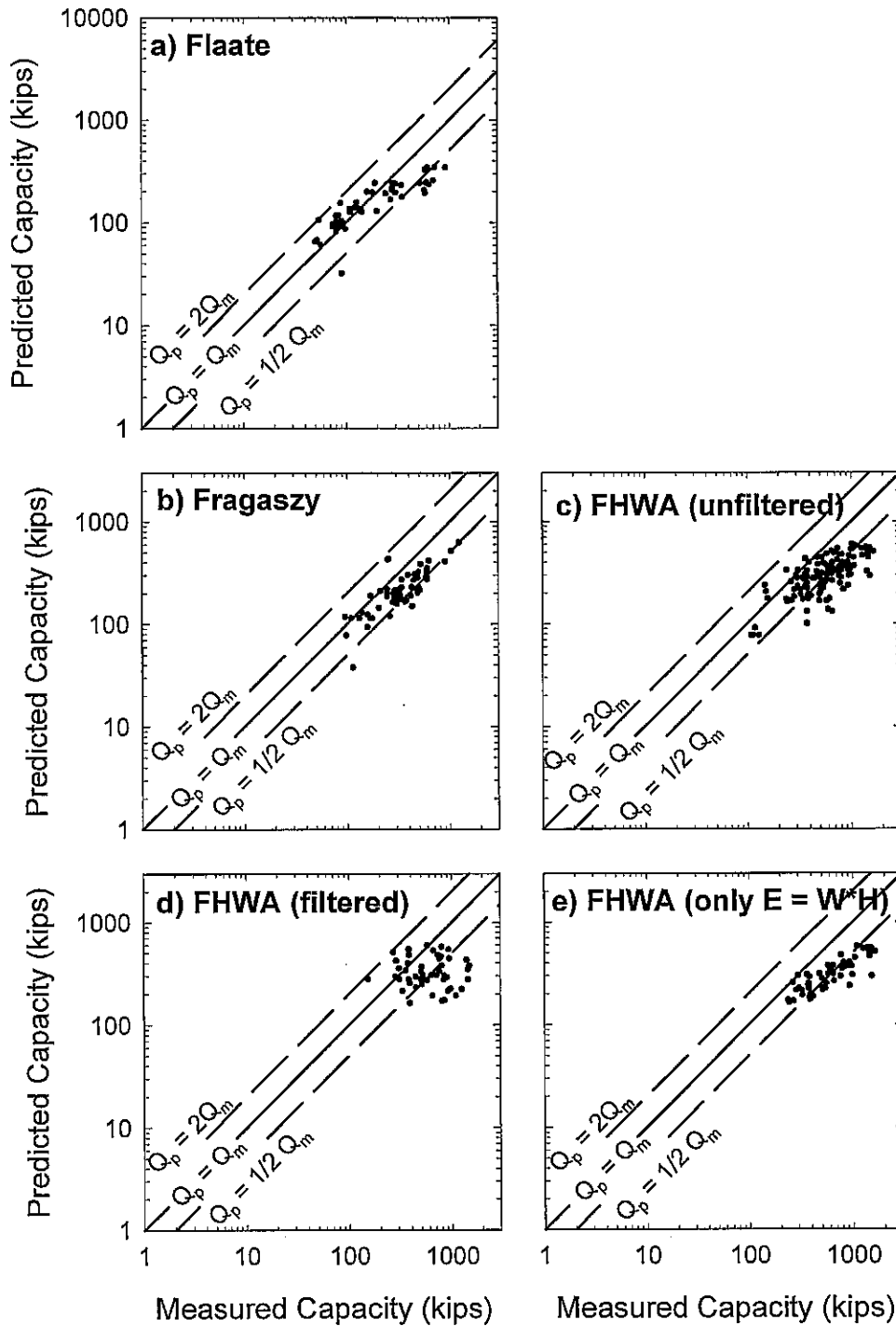


Figure 6.11 Predicted versus measured capacity for Gates method for the following databases: Flaate, Fragaszy, FHWA (unfiltered, filtered, and filtered for only cases where hammer energy could be determined as $W*H$)

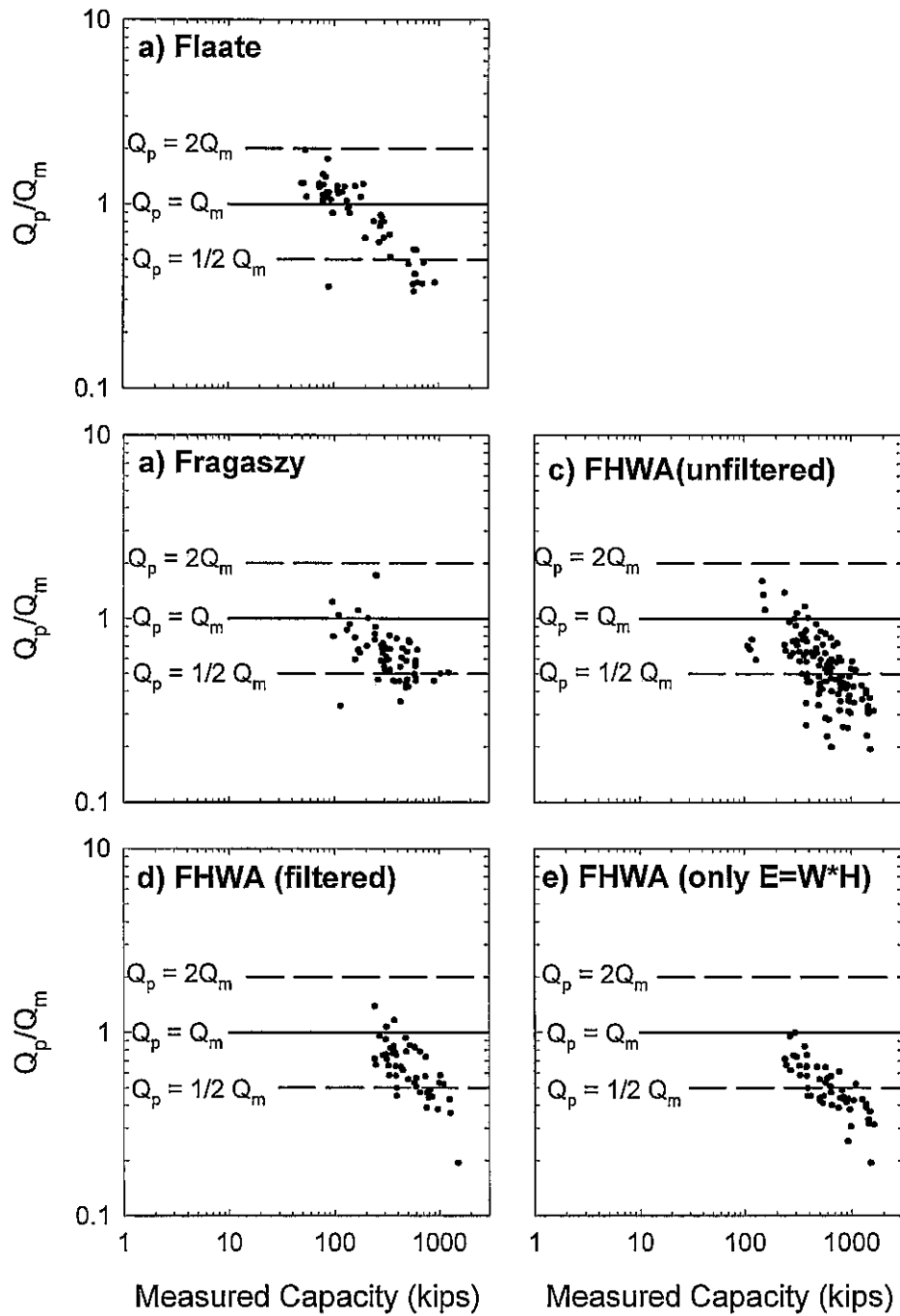


Figure 6.12 Ratio of Q_p/Q_m versus measured capacity for Gates method for the following databases: Flaate, Fragaszy, FHWA (filtered and unfiltered).

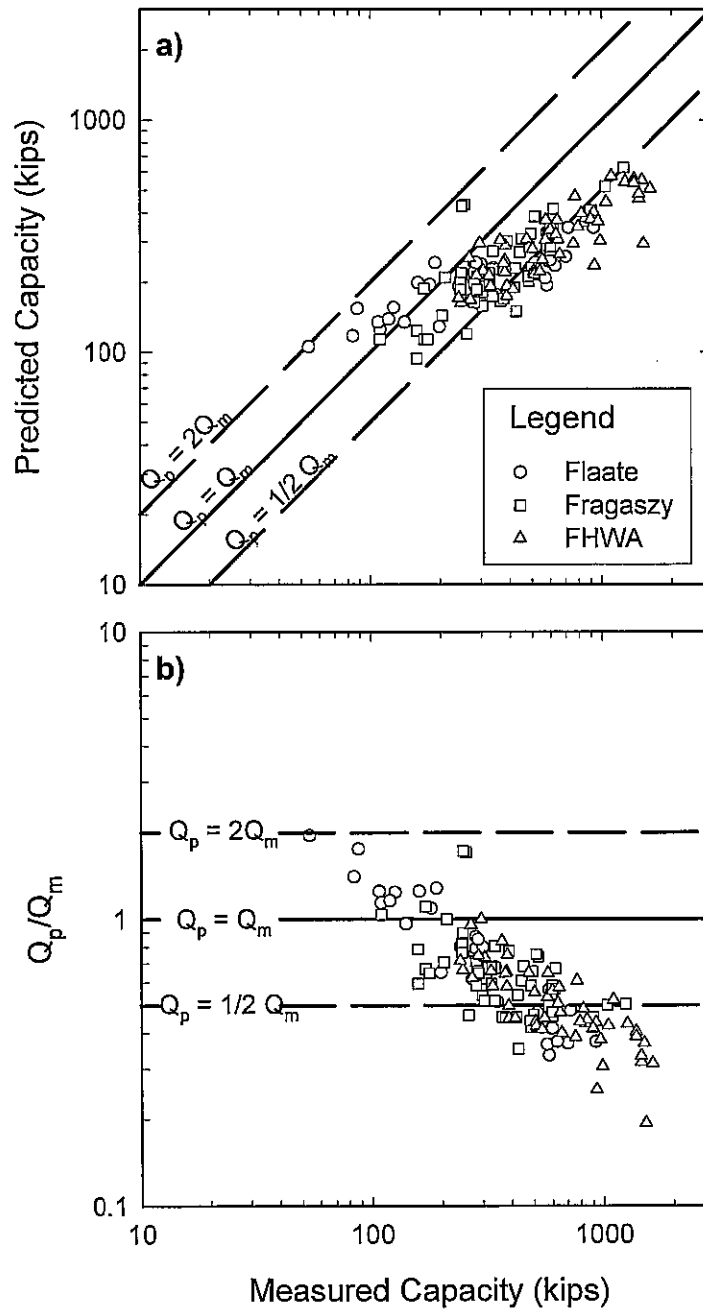
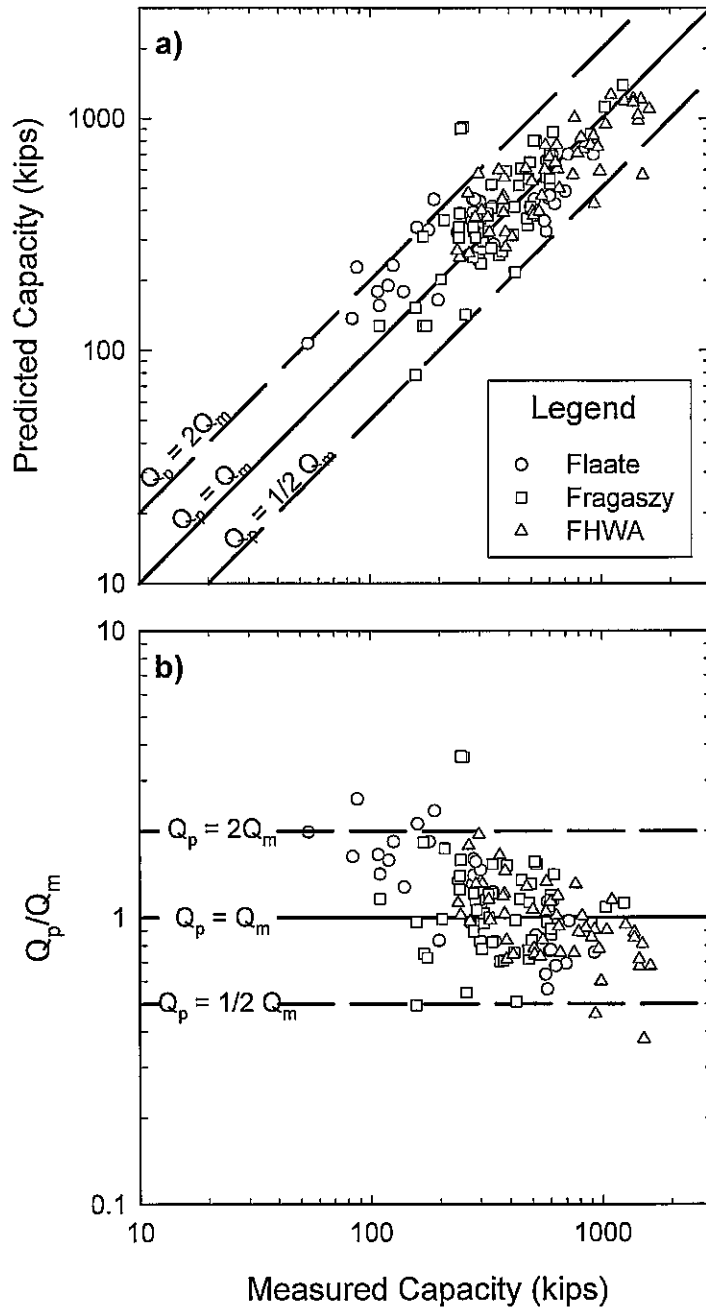


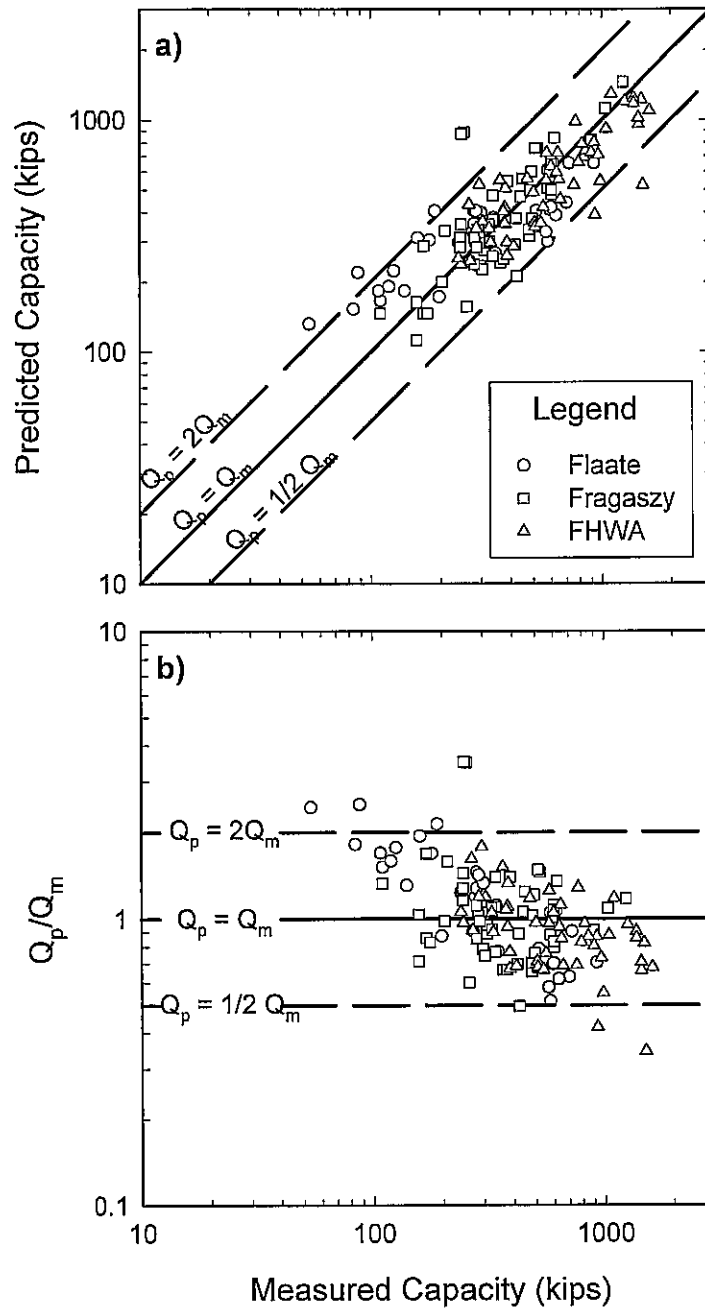
Figure 6.13 (a) Predicted versus measured and (b) Q_p/Q_m versus measured for Flaate, Fragaszy, and FHWA datasets using original Gates method



$$\text{Predicted Capacity} = Q_{\text{Gates(modified)}}$$

$$Q_{\text{Gates(modified)}} = 2.47 * Q_{\text{gates(original)}} - 154 \quad (\text{all numbers in kips})$$

Figure 6.14 (a) Predicted versus measured capacity and
 (b) Q_p/Q_m versus capacity for Flaate, Fragaszy and
 FHWA datasets using modified Gates formula
 (corrected with a linear function)



Predicted Capacity = $Q_{\text{Gates(modified)}}$
 $Q_{\text{Gates(modified)}} = 0.244 * (Q_{\text{gates(original)}})^{1.35}$ (all numbers in kips)
 Figure 6.15 (a) Predicted versus measured capacity and (b) Q_p/Q_m versus capacity for Flaate, Fragaszy, and FHWA dataset using modified Gates formula (corrected with a power function)

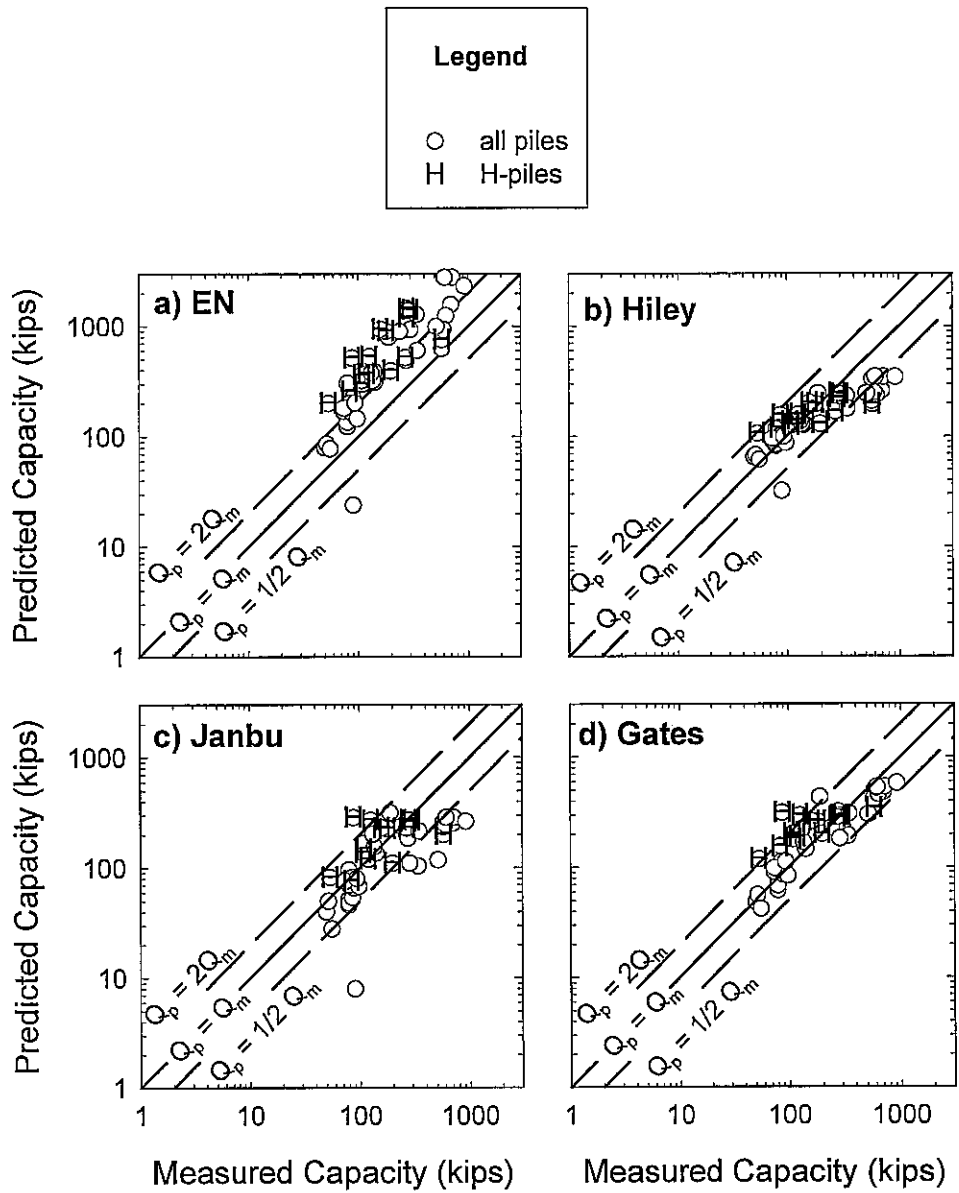


Figure 6.16 Comparison of predicted versus measured capacity for H-piles versus all piles (Flaate database)

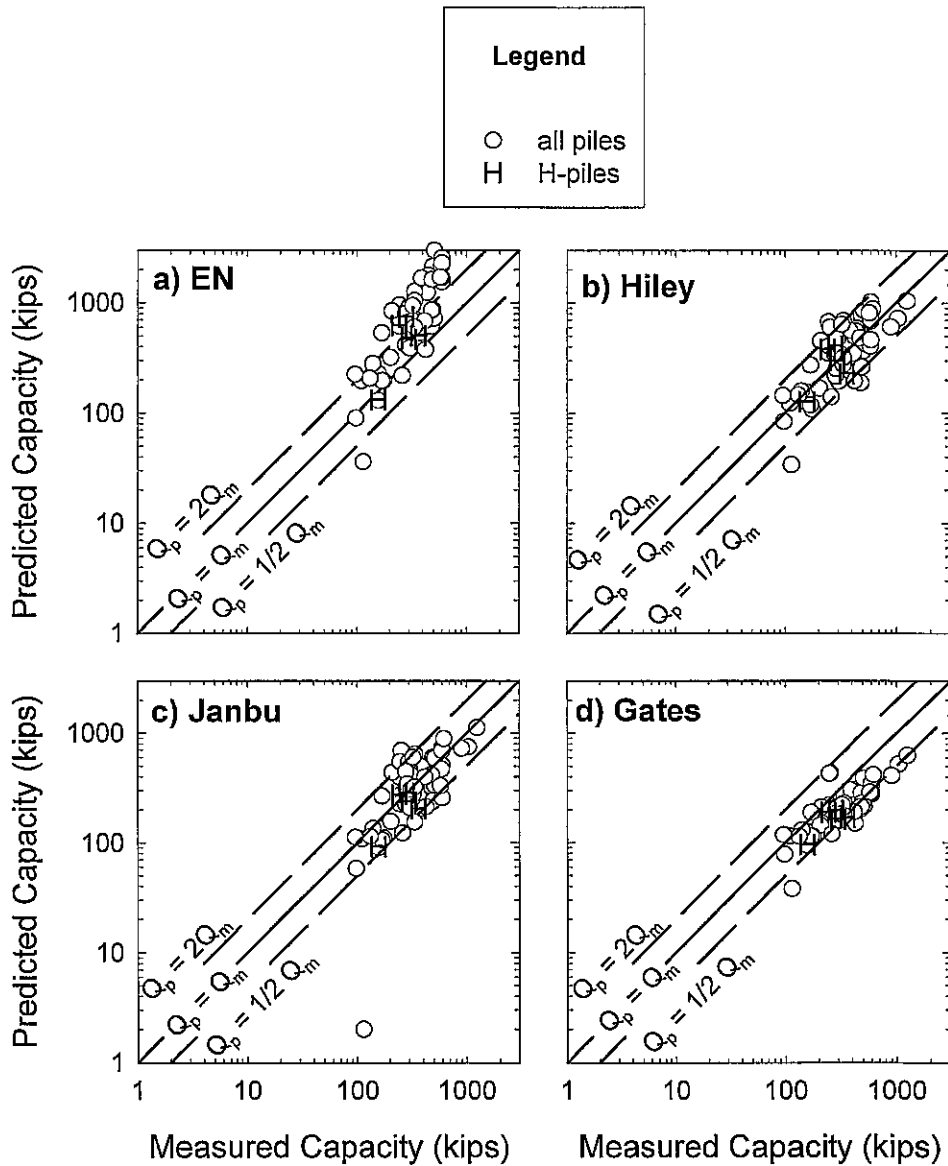


Figure 6.17 Comparison of predicted versus measured capacity for H-piles versus all piles (Fragaszy database)

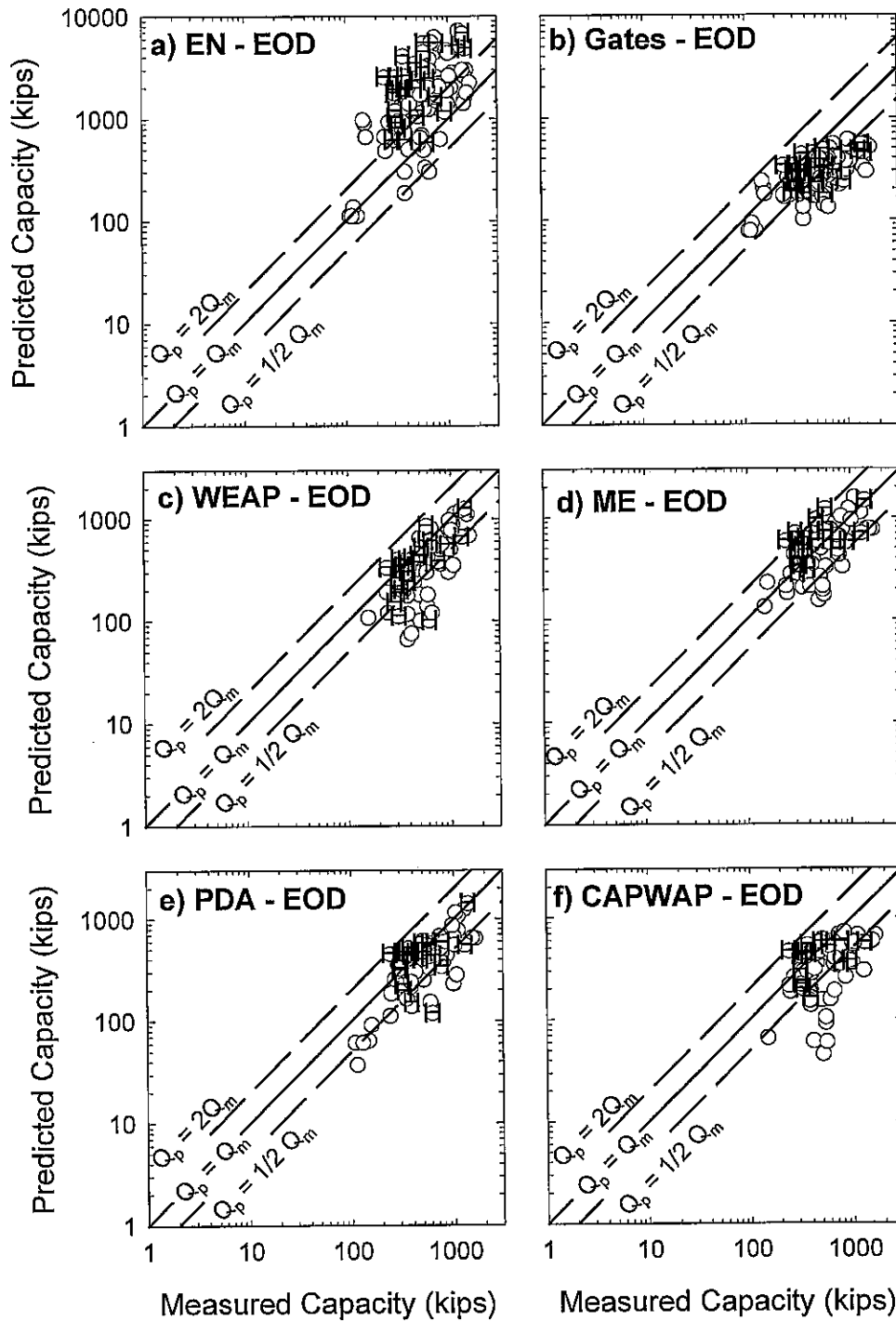


Figure 6.18 Comparison of predicted versus measured capacity for H-piles versus all piles (EOD - FHWA database)

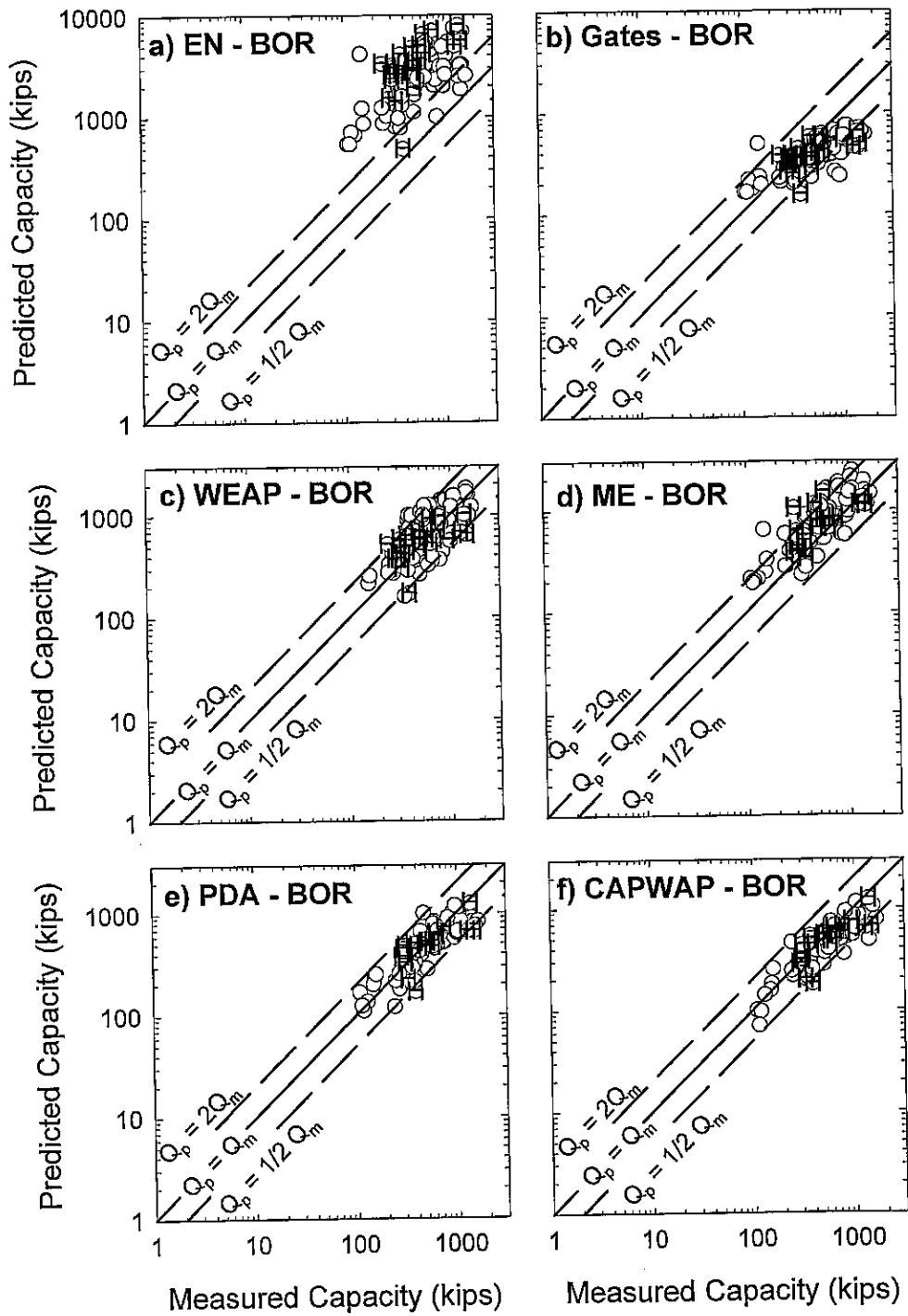


Figure 6.19 Comparison of predicted versus measured capacity for H-piles versus all piles (BOR - FHWA database)

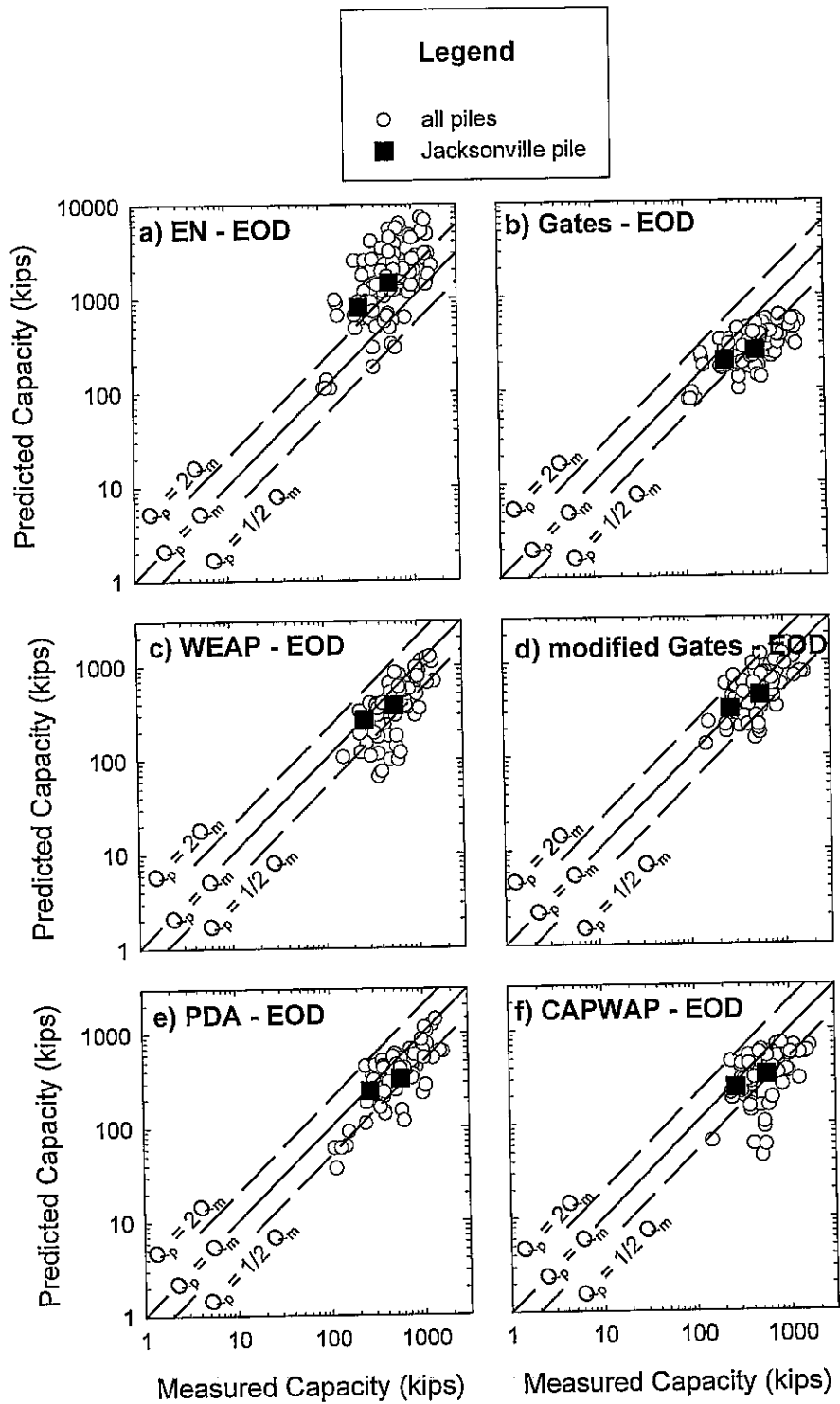


Figure 6.20 Comparison of predicted versus measured capacity for all piles (EOD - FHWA database) with emphasis on Jacksonville load test results

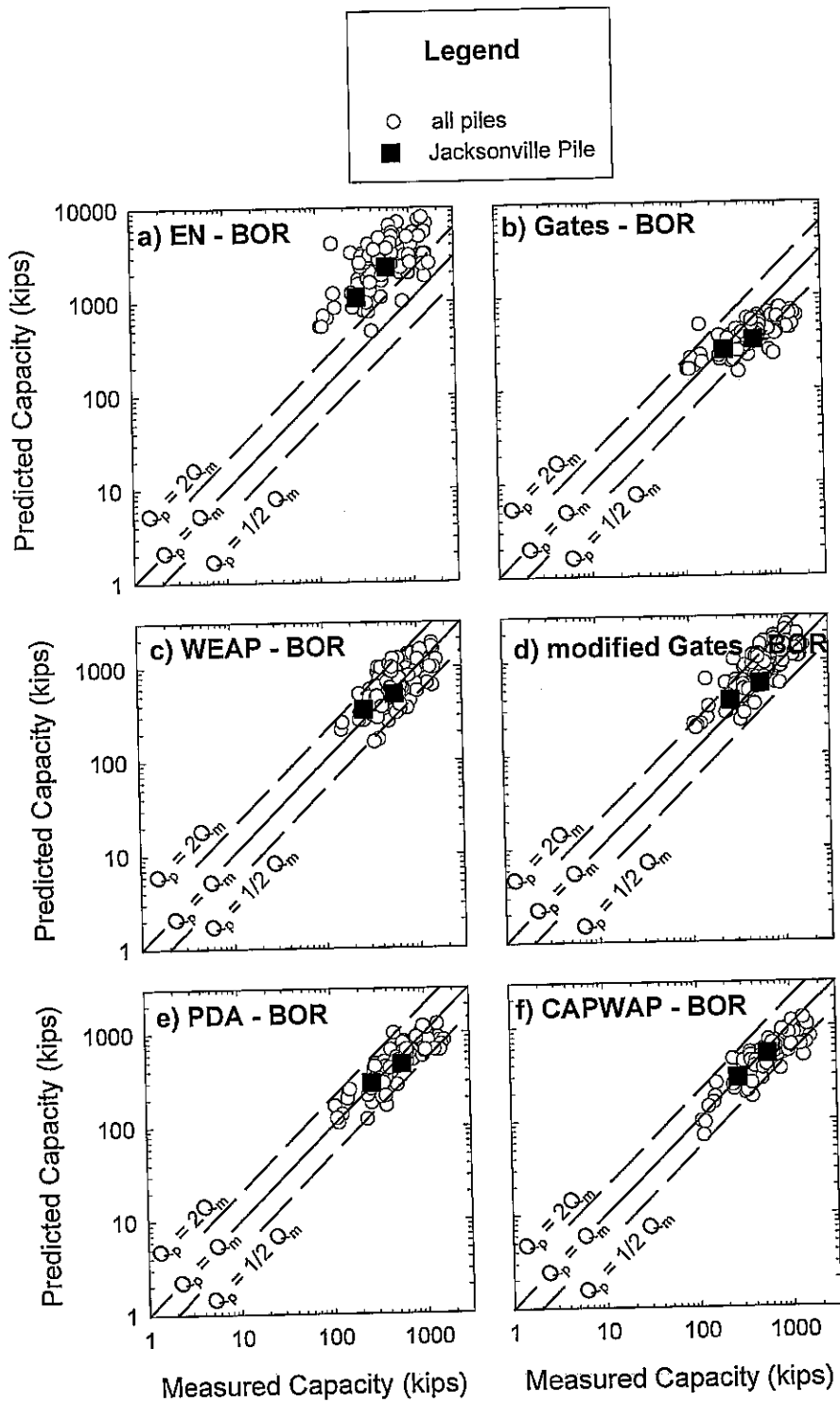


Figure 6.21 Comparison of predicted versus measured capacity for all piles (BOR - FHWA database) with emphasis on Jacksonville load test

SAFETY FACTORS AND WASTED CAPACITY

INTRODUCTION

Database results are used to determine factors of safety for a consistent level of reliability. The EN formula and load test results are used to determine reliability values for pile foundations. These reliability values are then used to calculate recommended factors of safety for each of the predictive methods. Finally, a measure of each method's efficiency is determined using a Wasted Capacity Index (WCI).

GLOBAL FACTOR OF SAFETY AND PILE RELIABILITY

It will be important, in the sections that follow, to establish a single value for a load factor, and a single value for the reliability of a single pile foundation. These values are necessary to determine the global factor of safety required for each of the different predictive methods (EN, Gates, modified Gates, WEAP, ME, PDA, CAPWAP) investigated in this report.

A Factor of Safety approach for sizing pile foundations is common practice. The approach requires the ratio of pile capacity divided by the design load to be greater than or equal to some factor (usually 2.0 to 4.0). The factor of safety is selected based on an assessment of the uncertainty with which the load can be predicted and the uncertainty with which the pile capacity can be predicted.

Uncertainties in load are different for dead loads and live loads. Load factors for dead load are generally lower than factors for live load because the magnitude of dead load can be estimated with more certainty than for live load. Factors of 1.3 and 1.7 have been reported (Barker, et al, 1991) for dead load and live load, respectively. For purposes of this report, a single value for the load factor is required. Axial loads

imposed on bridge foundations are dominated by dead loads, so an average load factor of 1.4 is used. The reliability of pile foundations is selected to be on the order of 95 percent.

CUMULATIVE DISTRIBUTION TO ASSESS LEVELS OF RELIABILITY

Statistical interpretations for predicted versus measured capacity, including the cumulative distribution, are introduced and discussed in Chapter 4. Cumulative distributions allow a relationship to be developed between the ratio of Predicted Capacity/Measured Capacity (Q_p/Q_m) and cumulative probability.

A cumulative distribution plot is constructed by sorting the ratio of Q_p/Q_m for each pile load test from smallest ratio to largest ratio. Simultaneously, each Q_p/Q_m value is assigned a cumulative probability value (CP) as discussed in Chapter 4. Values of Q_p/Q_m versus cumulative probability are plotted (Fig. 7.1) for the EN formula. The dataset corresponds to all piles in which EN formula could be used to predict capacity. The plot illustrates the relationship between cumulative probability (reliability) and Q_p/Q_m . For example, it can be seen that a cumulative probability of 50 percent corresponds to a Q_p/Q_m of 2.61. This means 50 percent of the time the predictive formula predicts capacity by a factor of 2.61 or less. In addition, a Q_p/Q_m factor of 6.0 corresponds to a cumulative probability of approximately 87 percent.

Accordingly, if a pile with a 87 percent reliability is desired (e.g. will carry an applied load without failing 87 percent of the time), the pile will require a predicted capacity 6.0 times greater than the applied load. Thus, the cumulative distribution provides a relationship between the ratio of predicted capacity/applied load and reliability. Each predictive method (EN, Gates, modified Gates, WEAP, ME, PDA, and CAPWAP) has its own cumulative distribution curve.

DETERMINING FACTOR OF SAFETY

The factor of safety is calculated for each predictive method by requiring a load factor equal to 1.4 and a pile reliability equal to 95 percent. The method uses the

cumulative distribution to determine the required ratio of predicted capacity/applied load and pile reliability. The ratio of predicted capacity/applied load will be termed as capacity factor. The procedure is conducted for each method.

Illustration of Methodology with EN Formula

Figure 7.1 illustrates the cumulative distribution for the EN formula and the FHWA dataset that includes all piles in which the EN formula could be applied. A pile reliability equal to 95 percent requires a capacity factor (Q_p/Q_m) equal to 7.9. The product of the load factor (1.4) and the capacity factor (7.9) equals to 11.1 for the overall factor of safety. While this factor appears unreasonably large, it is in agreement with the findings of others. For example, Flaate suggested a factor of safety of 12 for the EN formula. Fragaszy suggested a capacity factor equal to 7; however, the factor needs to be multiplied by the load factor (1.4) to obtain a factor of safety equal to 9.8.

Back-calculation of FS required for Load Test

Another method to confirm the proposed methodology is to back calculate the factor of safety when a load test is conducted. The axial capacity of piles driven at a site with the same soil conditions, the same hammer, and with load tests conducted should greatly reduce the uncertainty with which capacities can be predicted. Cumulative distributions were developed for several sites in which multiple load tests were conducted and statistics for each site were determined. The degree of scatter in Q_p/Q_m yielded standard deviations (σ_m) approximately 0.25. Accordingly, a 95 percent reliability corresponds to a capacity factor of 1.5. The product of the capacity factor (1.5) and the load factor (1.4) equals to a global factor of safety equal to 2.1. This factor is close to the traditional value of 2.0 used in practice and therefore provides some level of assurance that the methodology adopted herein to determine FS provides a consistent level of reliability and agrees with precedent.

Factors of Safety for Predictive Methods using EOD

Figure 7.1 illustrates the cumulative distribution for the EN formula using the FHWA dataset and including all piles in which the EN formula could be applied. In

the course of this report, however, we have used several filtered versions of the FHWA dataset as well as different datasets (Flaate, Fragaszy, FHWA) to investigate the EN formula. Each of these databases exhibit slightly different statistics and different cumulative distribution curves. Thus each variation will yield different capacity factors, and eventually, different factors of safety. Furthermore, several predictive methods are available (EN, Gates, modified Gates, WEAP, ME, PDA, CAPWAP) and each of these methods yield different capacity factors and global factors of safety. Values for the capacity factor and global factor of safety are presented in Table 7.1 for each database and each predictive method.

Capacity factors and global factors of safety for the EN formula were calculated for four databases (Table 7.1). Global factors of safety range from 8.1 for the Flaate database to 11.7 for the filtered FHWA database. Although the factors are quite high, the values correspond to the current practice (for driven H-piles, global FS = 9) of driving the piles to 50 percent greater bearing. A representative value for the capacity factor and the global factor of safety (Table 7.1) is based on the four datasets. The representative value of global factor of safety is equal to 9.8. There are two reasons why the method requires a high factor of safety: 1) the EN formula overpredicts capacity by a factor of about 2.6, and 2) the precision with which the EN formula can predict capacity is poor.

Capacity factors and global factors of safety for the Gates formula are given in Table 7.1 for five datasets. Calculated global factors of safety range from 1.2 to 2.5 with the Flaate database yielding a value of factor of safety significantly higher (2.5) than the four other datasets (1.2 to 1.5). A representative value for the capacity factor places more weight toward the four datasets resulting in a global factor of safety equal to 1.4. Although a factor of safety equal to 1.4 may raise concerns, the method, on the average underpredicts capacity by a factor of 0.57, thus, the capacity of the pile is required to be 2.5 ($= 1.4/0.57$) times the average value of Q_p/Q_m .

Capacity factors and global factors of safety for the modified Gates formula are given in Table 7.1 for only one dataset. The global factor of safety is calculated to be 2.4.

Capacity factors and global factors of safety for the WEAP method of analysis are given in Table 7.1 for two datasets. The global factor of safety is calculated to be 2.0 for both versions of the database yielding the same value.

The remaining three methods use pile dynamic monitoring as input for predicting capacity. Accordingly, the methods can better assess the energy being delivered to the pile. Three datasets were used to evaluate the ME approach. All three datasets result in similar values for factor of safety with a range of 2.4 to 2.8 with a representative factor of safety equal to 2.5.

Three datasets were used to investigate the PDA method. Global factors of safety for the Davidson database are 1.9 while the other two datasets yield a value of 2.1. A smaller factor of safety would be expected from the Davidson database since it contains only concrete piles driven in Florida. Accordingly, the predictions of capacity are more accurate and more precise because there is less diversity. The FHWA dataset contains several different pile types, driving conditions, and locations, thus, more weight is given to the factors of safety predicted with these datasets. The representative value for factor of safety is determined to be 2.1. While a factor of safety equal to 2.1 may seem low for the PDA method, the method tends to underpredict pile capacity by a factor of about 0.8. Thus, a factor of safety equal to 2.1 corresponds to a pile capacity of 2.6 ($=2.1/0.8$) times the design load.

Four datasets were used to investigate the CAPWAP method. Global factors of safety for the Davidson database are lowest (1.8) while the other three datasets range from 2.0 to 2.1. As described above, a smaller factor of safety would be expected for the Davidson database since it contains only concrete piles driven in Florida. The FHWA dataset contains several different pile types, driving conditions, and locations, thus, more weight is given to the factors of safety predicted with these datasets. The representative value for factor of safety is determined to be 2.1. The CAPWAP method tends to underpredict pile capacity by a factor of about 0.7. Thus, a factor of safety equal to 2.1 corresponds to a pile capacity of 3.0 ($=2.1/0.7$) times the design load.

Factors of Safety for Predictive Methods using BOR

Factor of safety were determined for several predictive methods (WEAP, ME, PDA, CAPWAP) using beginning of restrike (BOR) information. The use of BOR information combined with dynamic formulae (such as EN, Gates, and modified Gates) did not improve the precision of these methods significantly; therefore, factors of safety are not determined for these methods. However, the precision for the more rigorous and theoretical methods benefited from using BOR information. Accordingly, the EN, Gates, and modified Gates are not included in this section.

Capacity factors and global factors of safety for the WEAP method of analysis were calculated for two datasets (Table 7.2). Global factors of safety from both datasets are about 2.8 which are also considered to the representative values for WEAP analysis. A factor of 2.8 is at first glance rather large, and in fact, the factor is larger than WEAP for EOD conditions. However, WEAP tends to underpredict capacity for EOD (average $Q_p/Q_m = 0.75$) conditions while it tends to overpredict for BOR conditions (average $Q_p/Q_m = 1.1$).

Three datasets were used to evaluate the ME approach. The precision with which the ME approach calculates capacity is not improved by using BOR data. Furthermore, all three datasets show the method to overpredict capacity. As a result, the representative factor of safety equals to 3.2 (Table 7.2).

Three datasets were used to investigate the PDA method. The precision with which the PDA method calculates capacity is improved by using BOR data and the mean value of Q_p/Q_m also increases. The representative value for factor of safety is determined to be 2.3 (Table 7.2). While a factor of safety equal to 2.3 may seem higher for BOR conditions than EOD (FS = 2.1) conditions, it should be kept in mind that the PDA method underpredicts capacity for EOD conditions. A factor of safety equal to 2.3 for BOR conditions corresponds to a pile capacity of 2.3 (=2.3/1.0) times the design load while PDA estimates under EOD conditions corresponds to a pile capacity 2.6 times the design load.

Of all the methods investigated, the CAPWAP method benefited most from the use of BOR information. The representative value for factor of safety is determined to be 2.0 (Table 7.2). The CAPWAP method tends to underpredict pile capacity by a factor of about 0.9. Thus, a factor of safety equal to 2.1 corresponds to a pile capacity of 2.2 ($=2.0/0.9$) times the design load.

A summary of representative factors of safety for all predictive methods for EOD and BOR conditions is given in Table 7.3.

EFFICIENCY OF PREDICTIVE METHODS

It is important to quantify the cost effectiveness for a specific predictive method so that decisions can be made whether it is worth the investment to get better predictions. Methods that exhibit less scatter should require a smaller factor of safety to achieve a target foundation reliability, and therefore can provide better economy. However, additional costs may be associated with using methods that are more accurate. For example, dynamic monitoring may provide more accurate predictions of capacity and therefore can reduce the number of piles required at a site; however, can the savings due to a reduced number of piles compensate for the additional cost of monitoring?

Practically, it is impossible to compare the actual cost of these methods in a generally applicable way because the expense of conducting a load test or dynamic monitoring tests vary with location, availability and accessibility of equipment and personnel, time constraints, project scheduling, etc. Furthermore, the cost for acquiring additional capacity is impractical to estimate in general since it also site and project specific. Additional capacity may be obtained by requiring additional piling, or by driving the same pile a greater depth (or several other alternatives available to the engineer). The approach taken herein is to quantify the efficiency with which a method predicts capacity. This quantity will be termed "wasted capacity."

Wasted capacity refers to the extra capacity for which a foundation must be designed to account for uncertainties in load and pile capacity. The overall measure of wasted

capacity is quantified as the ratio of the global factor of safety divided by the average ratio of Q_p/Q_m for a specific predictive method.

$$WCI = FS / \mu \quad (7.1)$$

where WCI is the Wasted Capacity Index, FS is the representative value for factor of safety (Table 7.4) for the predictive method, and μ is the average ratio of Q_p/Q_m for the predictive method.

The WCI can be used to quantify wasted capacity associated with a method, and therefore allows comparisons of different methods. For example, compare the wasted capacity using PDA with the EN method. The WCI for the EN method is 3.76 while the WCI for the PDA is 2.60 for EOD conditions. Accordingly, the PDA method wastes less capacity than the EN formula to achieve the same level of pile reliability. In fact, the PDA method wastes only about 69 percent (=WCI for PDA divided by WCI for EN formula) as much capacity as is necessary for the EN formula. Furthermore, using PDA with BOR results in a smaller WCI (2.29) and wasting only 61 percent as much capacity as necessary for the EN formula.

The values of WCI can be inspected to identify which methods offer better efficiency. For EOD conditions, several methods are available that provide relatively low values for WCI. However, for EOD conditions, there is not a clear distinction between the effort needed to predict pile capacity and the benefit of using a more efficient design method. On the other hand, for BOR conditions, there does appear to be a relationship between effort and benefit of more precise predictions for pile capacity. When BOR conditions are used, CAPWAP provides the lowest WCI for all predictive methods.

Finally, for comparison, the WCI for a load test would be equal to about 2.1.

SUMMARY

The ability of EN, Gates, and ME methods to predict pile capacity accurately benefits little from using BOR data. WEAP, PDA, and especially CAPWAP benefit from the use of BOR data. Pile capacity using EOD data is shown to predict with about the same precision with WEAP, PDA, and CAPWAP. The ME and modified Gates methods appear to provide the more precise measurements when only EOD data are used.

Use of CAPWAP with BOR data results in the greatest precision of all predictive methods investigated. For non-monitored methods, BOR results generally exhibited slightly less scatter than when using EOD data.

The "cost" for using a method is expressed as a wasted capacity index. The WCI is a function of the reliability required for a foundation and the precision with which capacity can be determined, thus, significant reduction in WCI can result from using methods that are more accurate. While WCI and cost are related, the two are not directly proportional. Site specific details will govern whether requirements for extra capacity will be relatively expensive or inexpensive.

Table 7.1 Global Factors of Safety calculated for predictive methods using EOD

EOD BOR	Predictive Method	Database & Filter	n	μ	σ_{ln}	Capacity Factor	Global FS
End of Driving	EN	Flaate	54	2.45	0.523	5.8	8.1
		Fragaszy	57	2.58	0.610	7.0	9.9
		FHWA(all)	123	2.60	0.675	7.9	11.0
		FHWA(filtered)	50	3.51	0.527	8.4	11.7
		Representative		2.60	0.60	7.0	9.8
	Gates	Flaate	54	0.85	0.459	1.8	2.5
		Fragaszy	57	0.63	0.307	1.0	1.5
		FHWA(all)	123	0.53	0.410	1.0	1.5
		FHWA(filtered)	50	0.63	0.340	1.1	1.5
		FHWA(E=W*H)	51	0.49	0.323	0.8	1.2
		Representative		0.57	0.35	1.0	1.4
	Mod. Gates	Comb databases	108	0.98	0.337	1.7	2.4
		Representative		0.98	0.337	1.7	2.4
	WEAP	FHWA (unfiltered)	88	0.64	0.501	1.5	2.0
		FHWA (filtered)	50	0.75	0.392	1.4	2.0
		Representative		0.75	0.40	1.4	2.0
	ME	Paikowski	92	1.03	0.309	1.7	2.4
		FHWA (unfiltered)	73	0.93	0.462	2.0	2.8
		FHWA (filtered)	50	1.06	0.309	1.8	2.5
		Representative		1.00	0.35	1.8	2.5
	PDA	Davidson	65	0.84	0.298	1.4	1.9
		FHWA (unfiltered)	77	0.71	0.454	1.5	2.1
		FHWA (filtered)	50	0.80	0.376	1.5	2.1
		Representative		0.80	0.376	1.5	2.1
	CAPWAP	Paikowski	91	0.73	0.398	1.4	2.0
		Davidson	49	0.70	0.375	1.3	1.8
		FHWA (unfiltered)	75	0.58	0.591	1.5	2.1
		FHWA (filtered)	50	0.75	0.402	1.5	2.0
		Representative		0.70	0.45	1.5	2.1

Table 7.2 Global Factors of Safety calculated for predictive methods using BOR

EOD BOR	Predictive Method	Database & Filter	n	μ	σ_{ln}	Capacity Factor	Global FS
Beginning of Restrike	WEAP	FHWA (unfiltered)	114	1.11	0.385	2.1	2.9
		FHWA (filtered)	114	1.10	0.361	2.0	2.8
		Representative		1.10	0.37	2.0	2.8
	ME	Paikowski	110	1.25	0.303	2.1	2.9
		FHWA (unfiltered)	92	1.41	0.363	2.6	3.6
		FHWA (filtered)	72	1.36	0.361	2.5	3.4
		Representative		1.30	0.35	2.3	3.2
	PDA	Davidson	62	1.07	0.266	1.7	2.3
		FHWA (unfiltered)	85	0.91	0.319	1.5	2.2
		FHWA (filtered)	72	0.90	0.300	1.5	2.1
		Representative		1.00	0.3	1.6	2.3
	CAPWAP	Paikowski	109	0.83	0.304	1.4	1.9
		Davidson	70	0.95	0.317	1.6	2.2
		FHWA (unfiltered)	112	0.86	0.269	1.3	1.9
		FHWA (filtered)	72	0.88	0.254	1.3	1.9
		Representative		0.90	0.29	1.5	2.0

Table 7.3 Summary of Representative Factors of Safety

EOD/BOR	Predictive Method	Factor of Safety
EOD	EN	9.8
	Gates	1.4
	Modified Gates	2.4
	WEAP	2
	ME	2.5
	PDA	2.1
	CAPWAP	2.1
BOR	WEAP	2.8
	ME	3.2
	PDA	2.3
	CAPWAP	2.0

Table 7.4 Summary of Representative Factors of Safety and Wasted Capacity Index

EOD/BOR	Predictive Method	μ	Factor of Safety	Wasted Capacity Index (WCI)	Ratio of WCI/WCI for EN formula
EOD	EN	2.60	9.8	3.76	1.00
	Gates	0.57	1.4	2.49	0.66
	Mod. Gates	0.98	2.4	2.44	0.65
	WEAP	0.75	2	2.70	0.72
	ME	1.00	2.5	2.49	0.66
	PDA	0.80	2.1	2.60	0.69
	CAPWAP	0.70	2.1	2.93	0.78
BOR	WEAP	1.10	2.8	2.57	0.69
	ME	1.30	3.2	2.49	0.66
	PDA	1.00	2.3	2.29	0.61
	CAPWAP	0.90	2.0	2.26	0.60

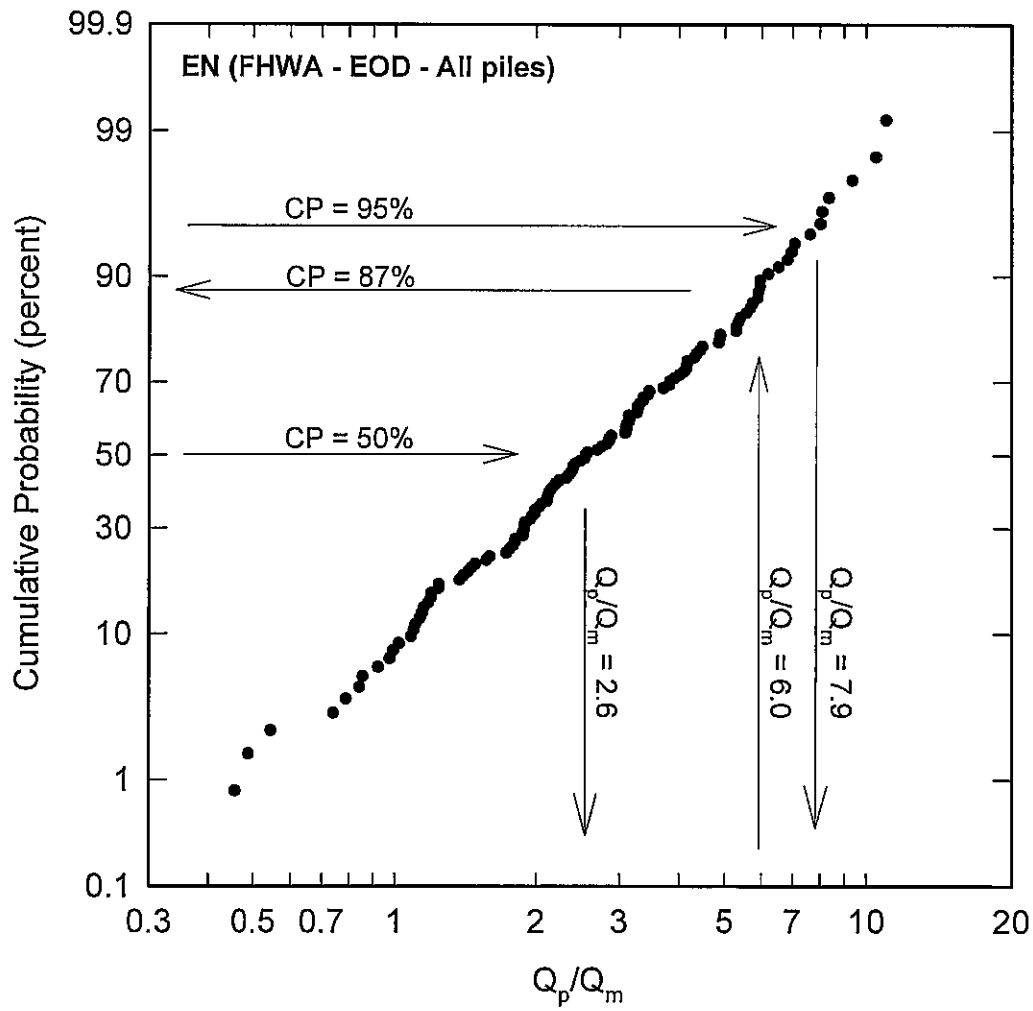


Figure 7.1 Cumulative distribution for EN formula for EOD conditions and using FHWA database with all piles

Chapter 8

SUMMARY AND CONCLUSIONS

SUMMARY

The ability of EN, Gates, and ME methods to predict pile capacity accurately benefits little from using BOR data. WEAP, PDA, and especially CAPWAP benefit from the use of BOR data. Pile capacity using EOD data is shown to predict with about the same precision with Gates, WEAP, ME, PDA, and CAPWAP. The ME method appears provides the most precise measurements when only EOD data are used.

The database shows that use of CAPWAP with BOR data to predict capacity results in the greatest precision of all predictive methods investigated. For non-monitored methods, BOR results generally exhibited slightly less scatter than when using EOD data.

The databases gave no indication there is a significant difference between predictions made for H-piles and predictions made for other piles. Accordingly, there is no strong evidence that capacity for H-piles should be predicted with different formulas. Additionally, the Jacksonville load test results indicate all the methods predicted capacity with reasonable precision, and are in general agreement with predictions of capacity studied in the load test databases.

The "cost" for using a method is expressed as a wasted capacity index (WCI) which is a function of the reliability required for a foundation and the precision with which capacity can be determined, thus, significant reduction in WCI can result from using methods that are more accurate. While WCI and cost are related, the two are not directly proportional. Site specific details will govern whether requirements for extra capacity will be relatively expensive or inexpensive.

Based on the results of this study, representative values for the factor of safety are given below for each method.

EOD/BOR	Predictive Method	Factor of Safety	Index for Wasted Capacity
EOD	EN	9.8	1.00
	Gates	1.4	0.66
	Modified Gates	2.4	0.65
	WEAP	2	0.72
	ME	2.5	0.66
	PDA	2.1	0.69
	CAPWAP	2.1	0.78
BOR	WEAP	2.8	0.69
	ME	3.2	0.66
	PDA	2.3	0.61
	CAPWAP	2.0	0.60

It is necessary for all pile foundations to be designed to resist greater than design loads so that they can account for uncertainties in the load and in the ability to predict pile capacity. The “cost” for using a method is expressed as a wasted capacity index and in the table above, it is normalized to be a value of 1.0 for the Engineering News formula. As can be seen, all the other methods have an index value less than the EN formula. For example, the index is 0.65 for the modified Gates method which means that, for the same pile reliability, the modified Gates method would waste only 65% as much pile capacity as the EN formula.

CONCLUSIONS OVERALL OBSERVATIONS OF BIAS AND SCATTER

EN formula

The ability of the EN formula to predict pile capacity is limited. The EN formula predicts capacity with poor precision for both EOD and BOR conditions. The method tends to overpredict capacity. All databases investigated (Flaate, Fragaszy, FHWA) identify the EN formula as predicting capacity with the least precision. There does not appear to be a fundamental difference in the ability for the EN formula to predict capacity for H-piles versus other piles.

Gates and Modified Gates

The Gates method, also a dynamic formula, predicts capacity with greater precision than the EN formula, although the method tends to underpredict capacity. Precision of the method was not influenced by use of EOD or BOR conditions. The Gates method predicts capacity with good – to – fair precision for all the databases investigated (Flaate, Fragaszy, FHWA). The original Gates method tends to underpredict capacity more severely as pile capacity increases, accordingly, a modified Gates method was developed. The modified method, on the average, predicts capacity well, with good – to – fair precision (depending on the database investigated).

WEAP

The WEAP method of analysis models the pile and pile driving mechanism. WEAP analyses for capacity are generally considered superior to simple dynamic formulae such as EN and Gates. However, the FHWA database demonstrated that WEAP did not predict capacity with the same level of precision as Gates for EOD conditions. On the other hand, WEAP predicted capacity with greater precision than Gates for BOR conditions. WEAP, on the average, underpredicted capacity by 46 percent for EOD conditions and overpredicted capacity by 6 percent for BOR conditions. Accordingly, estimates of capacity using WEAP are enhanced greatly by using BOR information, and may be excessively conservative when using EOD information.

ME Approach

The ME approach for predicting pile capacity benefits little from using BOR data, thus EOD measurements provide results with the same accuracy. The accuracy and precision of predictions are generally good. The method requires pile monitoring, thus measured energy imparted to the pile and a more accurate measurement of pile set is used in estimating capacity. The basic equation for the ME approach is the EN formula; however, the method exhibits much better precision than the EN formula. The ME approach obviously benefits greatly from better assessment of energy imparted to the pile.

PDA Method

The PDA method of analysis uses simple models for the pile combined with measurements of the pile behavior during driving and energy delivered by the hammer. PDA estimates of capacity are better for BOR conditions than EOD conditions. The PDA method generally underpredicts capacity (on the average of 44 percent) when using EOD conditions, but just slightly underpredicts capacity (by 7 percent) for BOR conditions. Precision of the method improves when BOR data are used.

CAPWAP Method

The CAPWAP method uses the most detailed modeling of the pile and hammer system and requires pile dynamic monitoring. Of the methods investigated in this report, it requires the greatest effort to determine pile capacity. However, the application of CAPWAP to EOD conditions results in underpredicting capacity (by 46 percent) with poor precision. However, when BOR information is used, the CAPWAP method predicts capacity well with very good precision, ranking as the best predictive method.

DISCUSSION AND LIMITATIONS

Several aspects of these databases need consideration. For example, the data only include load tests conducted to failure and all data are based on load tests conducted to failure. A more complete database should include all load tests whether they failed or not. Including unfailed load tests would serve to decrease the mean and standard deviation of Q_p/Q_m therefore, a database including only failed load tests is inherently conservative. Furthermore, the database reflects conditions where the pile hammer was monitored, thus ensuring proper operation and delivery of energy to the pile during driving. The plots and statistics are based on capacity developed during load tests, however, it is common for pile capacities to increase with time after the load tests were conducted. There are also inevitable limitations due to specific distributions of the load tests, soil types, and pile geometry in this study. This study neglects uncertainties in the measured load.

Pile reliabilities of 95 percent were used to determine capacity factors. These reliabilities require extrapolation with most of the current database since many only had 50 tests. Interpolation for 95 percent reliability would require 96 load tests or greater. The cumulative distribution used in this method provides a means to relate the ratio $(Q_p/Q_m)_{reqd}$ with reliability. Uncertainties associated with the design load were included by multiplying by a load factor. This provides a reasonable approach to a global factor of safety, but it will result in slight discrepancies in the reliability of the overall pile foundation system. The reliability of a foundation system depends on both the uncertainty in predicting capacity and in predicting the design load and there are means to determine this, but this is beyond the scope of work in this study.

Chapter 9

REFERENCES

- American Petroleum Institute, "Recommended Practice for Planning, Designing and Constructing Fixed Offshore Platforms, Section 1.6, Foundation Design," Sixteenth Edition, April 1, 1986.
- American Society for Testing Materials, "Practice for Preparing Precision Statements for Test Methods for Construction Materials, C670-90a, Annual ASTM Book of Standards, Vol. 04.08, 1990.
- Ang, A. and Tang, W. (1975) Probability Concepts in Engineering Planning and Design, Vol. I: Basic Principles, John Wiley & Sons, New York.
- Ang, A. and Tang, W. (1984) Probability Concepts in Engineering Planning and Design, Vol. II: Decision, Risk, and Reliability, John Wiley & Sons, New York.
- Barker, R.M., J.M. Duncan, K.B. Rojiani, P.S.K. Ooi, C.K. Tan, and S.G. Kim (1991), "Load Factor Design Criteria for Highway Structures, Appendix A," unpublished report to NCHRP, May, 143p.
- Briaud, J-L., and L.M. Tucker (1988), "Measured and Predicted Axial Response of 98 Piles," Journal of Geotechnical Engineering, ASCE, Vol. 114, No. 9, September, paper no. 22725, pp. 984-1028.
- Chao, L. L. (1969) Statistics: Methods and Analyses, McGraw-Hill, New York, 512p.
- Cheney, R.S. and R.G. Chassie (1982), "Soils and Foundations Workshop Manual," U.S. Department of Transportation, Federal Highway Administration.
- Cornell, C. A. (1969), "A Probability Based Structural Code," J. American Concrete Institute, Vol. 66, No.4, December, pp. 974-985.
- Davidson, J., and F.C. Townsend (1996), "Reliability and Limitations of Dynamic Methods for Predicting Capacity and Settlement of Driven Piles," Final report submitted to Florida Department of Transportation, June, 141p.
- Davisson, M. T. (1973), "High Capacity Piles," Innovations in Foundation Construction, Soil Mech. Div., Ill Section, ASCE, Chicago, pp. 81-112.

Dennis, N. D. and R. E. Olson (1983), "Axial Capacity of Steel Pipe Piles in Clay." Proceedings, ASCE Specialty Conference on Geotechnical Practice in Offshore Engineering, S. G. Wright, ed., April 27-29, Austin, Texas, 370-388.

Dennis, N. D. and R. E. Olson (1983), "Axial Capacity of Steel Pipe Piles in Sand." Proceedings, ASCE Specialty Conference on Geotechnical Practice in Offshore Engineering, S. G. Wright, ed., April 27-29, Austin, Texas, 389-402.

De Ruiter, J. (1971) "Electric Penetrometer for Site Investigations," J. Soil Mechanics and Foundation Engineering, ASCE, Vol. 97, SM2, p. 457.

FHWA, (1993), SPILE, A microcomputer Program for Determining Ultimate Vertical Static Pile Capacity, User's Manual, FHWA-SA-92-044, June, 172p.

Flaate, K. (1964), "An Investigation of the Validity of Three Pile-Driving Formulae in Cohesionless Material," Publication No.56, Norwegian Geotechnical Inst., Oslo, Norway: 11-22.

Fragaszy, R. J., D. Argo, and J. D. Higgins (1989), "Comparison of Formula Predictions with Pile Load Test," Transportation Research Board, 22-26 January.

Fragaszy, R. J., J. D. Higgins, and D. E. Argo (1988), "Comparison of Methods for Estimating Pile Capacity," Washington State Department of Transportation and in cooperation with U.S. Department of Transportation FHWA, August.

Gates, M. (1957), "Empirical Formula For Predicting Pile Bearing Capacity," Civil Engineering, Vol 27, No.3, March: 65-66.

Goble, G. G. and F. Rausche, "Wave Equation Analysis of Pile Driving - WEAP86 Program," U.S. Department of Transportation, Federal Highway Administration, Implementation Division, McLean, Va., Volumes I-IV. 1986.

Hannigan, P. J., "Dynamic Monitoring and Analysis of Pile Foundation Installations," Deep Foundations Institute Short Course Text, First Edition, 1990, 69p.

Issacs, D. V. (1931), "Reinforced Concrete Pile Formulas," Transactions, Institute of Engineers, Sydney, Australia, Vol. 12, pp. 305-323.

Kraft, L. M., Jr., R. P. Ray and T. Kagawa (1981), "Theoretical t-z Curves," Journal of the Geotechnical Engineering Division, Proceedings of the American Soc. of Civil Engineers, Vol. 107, No. GT11, November.

Long, J. H. and Shimel, S. (1989) "Drilled Shafts - A Database Approach," ASCE, Foundation Engineering Congress, Northwestern University, Evanston, IL.

Long, J.H., D. Bozkurt, J. Kerrigan, and M. Wysockey (1999), "Value of Methods for Predicting Axial Pile Capacity," 1999 Transportation Research Board, Transportation Research Record, Paper No. 99-1333, January, 1999.

Meyerhof, G. (1976) "Bearing Capacity and Settlement of Pile Foundations," J. Geotechnical Engineering Division, ASCE, Vol. 102, pp. 197-228.

Nordlund, R.L. (1963), "Bearing Capacity of Piles in Cohesionless Soils," ASCE, Journal of the Soil Mechanics and Foundations Division, No. SM-3.

Nordlund, R.L. (1979), "Point Bearing and Shaft Friction of Piles in Sand," 5th Annual Fundamentals of Deep Foundations Design, University of Missouri-Rolla.

Olson, R. E. and Dennis, N. D. (1983) "Reliability of Pile Foundations," Proc. ASCE Specialty Conference, Structures Congress, Houston, Texas.

Olson, R. E. and K. S. Flaate (1967), "Pile-Driving Formulas for Friction Piles in Sand," Journal of the Soil Mechanics and Foundations Division, ASCE, Vol.93, No.SM6, November:279-296.

Paikowsky, S. G., J. E. Regan, and J. J. McDonnell, "A Simplified Field Method For Capacity Evaluation Of Driven Piles," Publication No. FHWA-RD-94-042 , U.S. Department of Transportation, Federal Highway Administration, McLean, Virginia, September 1994.

Pile Dynamics, Inc., "Pile Driving Analyzer Manual; Model PAK," Cleveland, Ohio, 1996.

Rausche, F., G. Thendean, H. Abou-matar, G.E. Likins, and G.G. Goble (1996), Determination of Pile Driveability and Capacity from Penetration Tests, Final Report, U.S. Department of Transportation, Federal Highway Administration Contract DTFH61-91-C-00047.

Schmertmann, J. H. (1978) "Guidelines for Cone Penetration Test: Performance and Design," U.S. Dept. of Transportation, FHWA "TS" 78-209, Washington (DC).

Smith, E.A.L. (1960), "Pile driving by the wave equation," American Society of Civil Engineers, Journal of Soil Mechanics and Foundation Division, 86(4), pp. 35-61.

Terzaghi, K., R. B. Peck, and G. Mesri (1996), Soil Mechanics in Engineering Practice, Wiley, 549p.

Thurman, A. G. (1964), "Computed Load Capacity and Movement of Friction and End-Bearing Piles Embedded in Uniform and Stratified Soil," Phd. D. Thesis, Carnegie Institute of Technology.

Tomlinson, M. J. (1957), "The Adhesion of Piles Driven in Clay Soils." Proc. 4th Int. Conf. S.M. & F.E. vol. 2: 66-71.

Tomlinson, M. J. (1970), "Some Effects of Pile Driving on Skin Friction." Conf. on Beh. of Piles, Inst. Civ. Engrs., London: 59-66.

Tomlinson, M. J. (1985), Foundation Design and Construction. London: Pitman.

Tumay, M.Y., and M. Fakhroo (1981), "Pile Capacity in Soft Clays using Electric QCPT Data," American Society of Civil Engineers, ASCE, Proceedings of the Conference on Cone Penetration Testing and Experience, St. Louis, October 26-30, pp. 434-455.

U.S. Department of Transportation, FHWA (Federal Highway Administration), Research and Procurement, Design and Construction of Driven Pile Foundations. (Washington, D.C. :FHWA Contract No. DTFH61-93-C-00115, September 1995) I, II.

Vijayvergiya, V. N. & Focht, J. A. Jr. (1972), "A New Way to Predict the Capacity of Piles in Clay." 4th Annual Offshore Tech. Conf., Houston, vol. 2: 865-874.

Wellington, A. M. (1892) discussion of "The Iron Wharf at Fort Monroe, Va.," by J. B. Duncklee, Transactions, ASCE, Vol. 27, Paper No. 543, Aug., pp. 129-137.

Appendix A - Details of Jacksonville Site

Appendix A

DETAILS OF JACKSONVILLE SITE

INTRODUCTION

The primary purpose of the pile load test program was to evaluate the performance of several pile capacity predictive methods with static load test results. These methods included dynamic measurements, dynamic formulae, static analysis, and WEAP analyses. Secondary purpose included identifying and possibly quantifying the effects of time on pile capacity.

The pile load test program consisted of dynamically monitoring three test piles during initial driving and at selected re-strike intervals over a three-week period. In addition, static load tests were conducted on one of the driven piles. This appendix presents the pile installations and testing procedures and the results of the test program. The subsurface conditions present at the site are also included.

SITE LOCATION

The pile load test program was conducted at an Illinois D.O.T. construction project near Jacksonville, Illinois (Fig. A.1). The construction project consisted of the alignment of a proposed bridge over an existing southbound roadway [TR 187 Bridge over FA 310 (US 67) Section 69-1HB, S.N. 069-0079)] (see Fig. A.2). The site was located on the northwest corner of the original intersection.

SITE CHARACTERIZATION

Subsurface Investigation Program

The site investigation program included exploratory borings, soil sampling, and Standard Penetration Tests (SPT). Water contents and unconfined compressive strengths q_u (measured using both a modified Rimac tester and a pocket

penetrometer) were obtained from the recovered samples. In addition, a sample taken from the field exploration was laboratory tested for a grain-size analysis and Atterberg limits.

A total of four borings (designated as B-1 through B-4) were drilled at the test site: three along the alignment of the bridge and one along the southbound roadway. Figure A.4 shows the approximate locations of these borings within the site boundaries. Borings B-1, B-2, and B-3 were conducted in 1974 while boring B-4 was conducted in 1996. Boring depths ranged from 14.7 m to 16.7 m (48.2 ft to 54.8 ft) below the ground surface. The soil borings were carried out in accordance with ASTM D-1586. Copies of the boring logs are included at the end of this appendix.

Standard Penetration Tests (SPT's) were conducted as part of the soil exploration. Two types of mechanisms for raising and dropping the hammer were used: one by using a rope and rotating drum (or cathead) and the other by using an automatic trigger. SPT for borings B-1 through B-3 used the cathead mechanism whereas boring B-4 used the automatic trip hammer.

Soil Profile

Based on the results of the two field exploration programs, soil profiles delineating the specific subsoil conditions were obtained. The final soil profile (Fig. A.5) was developed using information from all the soil borings with particular emphasis given to boring B-4 due to its proximity to the load test site (Fig. A.4).

The subsoil can be divided into six layers. The top layer consists of a silty CLAY overlying 1.8 m of a silt LOAM, with a total thickness of about 3 m. Underlying this layer is an organic SILT approximately 1 m thick. Beneath is a 2.4 m silty clay LOAM layer (slightly organic) followed by a clay TILL of thickness equal to 0.75 m. At an elevation between 185 m and 186 m, a hard TILL was encountered which was overlain by 1.5 m of a medium SAND. The hard till layer was approximately 4 m thick and is the layer into which all of the test piles were driven. Results of grain size analyses from this layer indicate uniformity of particle sizes within the soil. The

median grain size is $D_{50} = 0.19$ mm and the material classifies as a silty SAND (SM) according to the Unified Soil Classification System. The soil has a fines content (% passing the # 200 sieve) of 29%. Results of Atterberg limit tests revealed the fines are non-plastic.

Soil Exploration Results

Plots of water content versus elevation for the four borings are shown in Fig. A.6. The water contents for the boring samples ranged from a low of about 6% to a high of about 120%. The majority of the water contents fell within the range of 6% to 30%. The average water content of the inorganic soil profile was found to be approximately 17% while that of the organic soil was approximately 110%.

Plots of Standard Penetration Resistance versus elevation for the four borings are shown in Fig. A.7. The SPT results from the borings were almost identical with depth and indicated similarity of the soil properties across the site (However, boring B-4 displayed significantly higher N-values between elev. 186 m and 182 m than from the other borings. Geologic variations in the soil properties may be a possible but unlikely explanation). The N-values remain fairly constant with depth (between 1 to 10 blows per 0.3 m) up to elev. 188m then begin to increase linearly to an equivalent of about 290 blows per 0.3 m) at elev. 184 m. The penetration resistance then decreases to 60 at Elev. 182m and remains constant to the depth of the boring at 179 m.

Plots of soil strength versus elevation for the four borings are shown in Fig. A.8. As noted previously, a limited number of pocket penetrometer tests were performed on the split spoon samples although the significant majority of strength tests were unconfined compressive tests. The undrained shear strengths s_u were obtained by dividing the unconfined compressive strengths q_u obtained in the field by a factor of two ($s_u = q_u/2$). Strengths ranged from 785+ kPa for some of the hard lower till layers to 10 kPa for the organic silt loams.

The groundwater table was encountered within the depths of the four borings. Water levels measured after 24 hrs of stabilization ranged from 0.21 m to 0.64 m (0.7 ft to 2.1 ft) below the ground surface.

The variation of water contents, STP, and undrained shear strength versus elevation are summarized in Fig. A.9. The undrained shear strengths s_u in Fig. A.9e were obtained by dividing the unconfined compressive strengths q_u by a factor of two ($s_u=q_u/2$) while s_u values in Fig. A.9d were obtained by multiplying the SPT blowcounts N by a value of six (s_u (kPa)=6N) (Terzaghi, et al., 1996). It should be noted that the dense till (EL 182 to 185 m) is a silty sand, and accordingly, estimates of undrained strength for this layer are inappropriate for determining static soil resistance for pile capacity.

PILE DRIVING

Installation and Equipment

A total of seven H-piles (12x53) were installed at the test site. Four of the piles were reaction piles. The three test piles were driven from west to east, spaced at 4 m (13 ft) intervals. The first test pile was designated as DTP-1 (dynamic test pile no.1), the second as SLTP (static load test pile), and the third as DTP-2 (dynamic test pile no. 2). The reaction piles were driven approximately 2.75 m (9 ft) north and south of the SLTP. A plan view of the pile layout is shown in Fig. A.10. All piles were driven in general accordance with current ASTM D 4945-89 procedures.

A Delmag D 19-32 single-acting diesel hammer was used to drive all the piles (Fig. A.11). The hammer has a ram weight of 18.64 kN (4190 lbs) and a manufacturer's maximum rated energy of 58028 N-m (42800 ft-lbs). Driving energies could be varied by adjusting the fuel settings (fuel settings ranged from 1 to 4 with 4 corresponding to the maximum setting).

The capblock assembly used for the hammer consisted of a striker plate, 43.18 cm (17.0 in) in diameter by 10.16 cm (4.0 in) in thickness and weighing 1.02 kN (230

lbs), a hammer cushion consisting of a 5.08 cm (2 in) thick plate of Blue Nylon, and a helmet weighing 8.45 kN (1900 lbs).

Pile Driving Criteria

All piles were driven to capacities predicted using the Engineering News formula. Thus, through a combination of final driving resistance and hammer stroke, an allowable load at the end of initial driving of 533.8 kN (60 tons) and at the end of restrike of 801 kN (90 tons) resulted.

The piles were reported to have a minimum yield strength of 404.7 MPa (58.7 ksi) and lengths at the time of driving of 15.24 m (50 ft).

Driving Schedule and Results

The test piles were installed on August 20, 1997. The driving order, from west to east, was DTP-1, SLTP, and DTP-2 (see Fig. A.10). DTP-1 was driven to a final driving resistance of 24 blows per 15cm [4 blows per inch (bpi)] with an observed hammer stroke of 1.98 m (6.5 ft). SLTP had a final driving resistance of 15 blows per 15 cm (3 bpi) with an observed hammer stroke of 2.10 m (6.9 ft). The last test pile driven, DTP-2, had a final driving resistance of 18 blows per 15 cm (3 bpi) and an observed hammer stroke of 2.06 m (6.75 ft). Final pile tip elevations on August 20, 1997 for DTP-1, SLTP, and DTP-2 were 185.14, 185.35, and 185.32 m respectively. All three piles were driven with a hammer fuel setting of 2. Penetration resistance for each test pile (DTP-1, DTP-2, and SLTP) are plotted in Figs. A.12, A.13, A.14.

DTP-1 was redriven one day later (on August 21, 1997) to assess the degree of setup after 24 hours. The pile was driven for 7.6 cm (3 inches) resulting in a total pile penetration of 10.97 m (36.0 ft). Driving resistances were measured for every inch of penetration and corresponded to 4, 5, and 7 blows per inch. The average observed hammer strokes for each inch of penetration were 2.41, 2.35, and 2.29 m (7.9, 7.7, and 7.5 ft).

A static load test was performed on test pile SLTP on August 27, 1997 (one week after initial driving). Results of the static load test are given later in this chapter.

After the static load test was performed, the load test frame was removed and piles DTP-1, SLTP, and DTP-2 were re-driven. All restrikes were performed on the same day (August 27, 1997). The restrike order was DTP-1, SLTP, and DTP-2. Upon re-driving, DTP-1 exhibited an initial driving resistance of 32 blows per 15 cm (5 bpi) and an observed hammer stroke of 2.32 m (7.6 ft). Re-driving the static load test pile (SLTP) resulted in an initial driving resistance of 32 blows per 15 cm (5 bpi) and an observed hammer stroke of 2.35 m (7.7 ft). DTP-2 had an initial driving resistance of 21 blows per 15 cm (4 bpi) and an observed hammer stroke of 2.39 m (7.7 ft). Driving resistances for the final 7.5 cm (3 inches) of driving for DTP-1, SLTP, and DTP-2 were 8, 14, and 24 blows per 7.5 cm (8, 14, and 24 blows per 3 inches), respectively. Their corresponding average stroke of the ram was 2.56 m (8.4 ft), 2.36 m (7.75 ft), and 2.68 m (8.8 ft). All three piles were driven to final tip elevations of approximately 183 m. The hammer fuel setting for SLTP and DTP-2 during the first three inches of re-strike was at 4 but then decreased to 3 during re-drive. Information regarding fuel setting for DTP-1 was unavailable.

The final day of driving occurred on September 11, 1997. The restrike order was SLTP, DTP-1, and DTP-2. DTP-1 and DTP-2 were re-driven an additional 10 cm (4 in) whereas SLTP was re-driven an additional 20 centimeters (8 inches). The restrike driving resistance for SLTP was 11, 13, 12, and 11 blows/inch for the first 10 cm (4 in) and 11, 11, 11, and 10 blows/inch for the final 10 cm (4 in). For DTP-1, restrike driving resistances for the 10 cm (4 inch) drive were 12, 10, 10, and 9 blows/inch and 16, 14, 14, and 14 blows/inch for DTP-2. Final pile penetrations for SLTP, DTP-1, and DTP-2, were 10, 9, and 14 blows per inch. All three piles were driven with the hammer fuel setting at 4.

Plots of penetration resistance versus depth for all three test piles DTP-1, DTP-2, and SLTP are shown in Figs. A.12, A.13, and A.14, respectively. A tabulation of the driving results for test piles DTP-1, DTP-2, and SLTP is presented in Tables 1, 2, and 3, respectively.

PILE TESTING PROGRAM

Static Load Test

Two static load tests were performed at the site on test pile SLTP. One static load test (SLT-1) was conducted on the morning of August 27, 1997 while the other (SLT-2) was performed on September 11, 1997.

The first test was conducted on a pile driven to a depth of 10.52 m (34.5 ft). A 1.14 m (3.75 ft) deep excavation was then dug around the test pile resulting in an embedded pile length equal to 9.38 m. The first static load test, SLT-1, was conducted on this pile. The pile was then redriven an additional 2.13 m (7.0 ft) before conducting the second load test (SLT-2). The pile had an embedded length equal to 11.54 m (37.86 ft). The embedded length includes the additional penetration of 32.94 mm that occurred due to permanent displacement of the pile during the first load test (SLT-1).

All static load tests were performed in general accordance with ASTM Standard D1143, "Quick Load Test Method for Individual Piles."

Equipment and Setup

A 2.67 MN (300 ton) hydraulic jack, resting on a steel plate, applied the load to the top of the pile (Fig. A.15 and A.16). The jack was connected to both an electric pump and a hand-operated pump equipped with a calibrated pressure gage (Fig. A.17 and A.18) that read to an accuracy of 5 psi (the hand pump was used to keep a constant load on the test pile). Above the jack rested a 3.34 MN (375 ton) calibrated load cell connected to a strain indicator. A spherical bearing was located under the reaction beam, between the load cell below and a steel plate above. This system was capable of obtaining a measurement resolution of approximately two percent of the applied load.

The jack/load cell exerted its force on two reaction beams (36WF328) placed between anchor piles (Fig. A.19). Two anchor piles were used at each end of the reaction beam. Two channel transfer beams (MC 18x58) were secured on each side of the

reaction piles to resist the force of the reaction beam. The test arrangement is shown in Fig. A.20.

Pile top displacements were recorded using two dial gages, placed on opposite sides of the test pile, whose measuring stems rested on angles welded to the test pile. These angles provided a flat, level surface on which the dial gages could rest. The dial gages in turn were supported by separate reference beams. A wire, mirror and scale system was also used during the load test for measurement of pile displacement (Fig. A.21).

Procedure

The test procedure was to load the pile in equal increments of 66.75 kN (7.5 tons). For SLT-1, the load was maintained for approximately five minutes prior to the next load increment. However, for SLT-2, the load was maintained for two and a half minutes for the first 15 tons and then increased to five minutes for the remainder of the test. During both tests, the deflections were recorded immediately after and at the end of the time interval following the application of the load. The loads were applied until the pile exhibited continuous movement with no increase in load. Upon reaching failure, the pile was unloaded in increments until no further load was recorded on the strain gage.

Results

Results of the load tests are presented graphically in Figs. A.22 and A.23. Tables A.4 and A.5 summarize the results of the static load tests SLT-1, and SLT-2, respectively.

Pile capacities were evaluated from the results of the load test by the method suggested by Davisson (Davisson, 1970). Based on this failure criteria, SLT-1 indicated an ultimate pile capacity of 1202 kN (135 tons) while SLT-2 indicated an ultimate pile capacity of 2537 kN (285 tons).

Dynamic Load Test

All test piles were dynamically monitored during initial installation and during restrikes. Dynamic test results were monitored with a Pile Driving Analyzer (PDA) and estimated of capacity were based on the Case Method. Subsequent analyses of

test results were conducted using the CAse Pile Wave Analysis Program (CAPWAP). A detailed description of the field equipment and analytical procedures are beyond the scope of this chapter, but additional information may be found in Gobel et al, 1997. A summary of test results is presented below.

PDA Results

Table A.6 summarizes the dynamic testing results of the PDA at selected pile penetration depths corresponding to final driving as well as the beginning and end of driving sequences.

It should be noted that the dynamic test data was averaged over every 10 hammer blows. In addition, data summaries were prepared per inch for the final 3 inches of initial driving, initial restrike, re-driving, and final restrike.

CAPWAP Results

Results from CAPWAP analysis include comparisons of measured with corresponding computed force/velocity curves. The pile is modeled numerically as a series of pile segments, and ultimate static resistance, soil quake and damping factors are determined. Also included in the results is a pile load-set curve from static test simulation. Results from CAPWAP analyses are given in Table A.7

CAPWAP analyses were performed on selected hammer blows obtained near the end of initial driving, near the beginning of the restrikes, and near the end of re-drive of the SLTP. The maximum Case Method equation was used to obtain estimates of the mobilized ultimate pile capacities during the driving of the piles. A Case damping factor of 0.8 was chosen for use with the maximum Case Method equation.

The average mobilized ultimate pile capacity of the SLTP over the final inch of initial driving was 240 kips (104 kips in skin friction and 136 kips in end bearing). Most of the skin friction (71%) was acting along the bottom 4.2 m (13.8 ft) of the pile.

Data representing the second blow of restrike was analyzed and indicated an average mobilized ultimate pile capacity of 284 kips (150 kips in skin friction and 134 kips in end bearing). As expected, all the capacity increase (46 kips) was added skin friction.

The SLTP was driven 2.13 m (7.0 ft) deeper during restrike and had an average mobilized ultimate pile capacity of 331 kips (180 kips in skin friction and 151 kips in end bearing). These results indicate an increase in total pile capacity of 47 kips.

For the SLTP, two additional blows, numbers 5 and 11, (in addition to blow number 2) were analyzed by CAPWAP. This was done in order to evaluate the sensitivity of the static capacity to repeated dynamic loading. For blow number 2, an average mobilized ultimate pile capacity of 515 kips (350 kips from skin friction and 165 kips in end bearing). An increase in pile capacity was almost entirely due to skin friction (170 kips). These values represent 1.5 times increase in total pile capacity and a doubling in skin friction from those at the end of driving. For blow numbers 5 and 11, the ultimate capacities quickly decreased to 476 kips and 452 kips, respectively. This reduction was due to skin friction losses (from 350 kips to 286 kips) while end bearing did not change at all.

OTHER LOAD CAPACITY PREDICTIONS

The ultimate pile capacities of the test piles were also predicted on the basis of dynamic formulae (the Engineering News (EN) and Gates formulae), and a Wave Equation analysis (WEAP). Each of these methods, along with their capacity predictions, is presented below.

Dynamic Formulae

As stated previously, a Delmag D 19-32, single-acting diesel hammer, with a maximum rated energy of 58028 N-m (42800 ft-lbs), was selected for the driving of the test piles. For this hammer, the ram has a weight of 18.64 kN (4190 lbs) with an equivalent fall of 3.11 m (10.21 ft). This information will be used in the analyses of the different dynamic formulae.

Engineering News (EN) formula

The Engineering News (EN) formula (as used by IDOT) is given by

$$R = \frac{2W_r h}{s + c} \quad (\text{A.1})$$

where R = allowable load (lbs), W_r = weight of ram (lbs), h = drop height of ram (ft), s = set per blow under final few blows (inches), c = constant (inches).

Specific values of c depend on the hammer type and may also depend on the weight of the pile and hammer ram. The Illinois Department of Transportation uses values of c according to the following criteria:

c = 1.0 (in) for gravity hammers

c = 0.1 (in) for air/steam and diesel hammers

c = 0.1 x W_p/W_r (in) for air/steam hammers in the case of very heavy steel and concrete piles, where W_p = weight of pile, and W_r = weight of ram

It is important to use to the specified units specified in Eq. A.1. If a consistent set of units are used, for example, all units of length are expressed in ft, then the right hand side of Eqn. A.1 should be replaced with (1/6)*WH/(s+c).

Dynamic load test results from the end-of-driving (EOD) and the beginning-of-restrike (BOR) of both SLTP-1 and SLTP-2 are summarized in Table A.2. For SLTP-1, a final penetration of 3 blows/inch and a hammer drop of 6.9 ft were recorded in the field at the EOD. For the BOR, an initial penetration of 4 blows/inch and a hammer drop of 7.7 ft were recorded. These values correspond to computed capacities of 133 kips for EOD and 184 kips for BOR, respectively. Similarly, for SLTP-2, a final penetration of 6 blows/inch and a hammer drop of 7.75 ft were recorded at the EOD while an initial penetration of 11 blows/inch and a hammer drop of 8.7 ft were recorded during the BOR. Capacities of 244 kips for EOD and 382 kips for BOR were calculated, respectively.

Gates formula

The Gates formula is given by

$$R_u = \left(\frac{3}{7}\right) \sqrt{e_h E_h} \log\left(\frac{10}{s}\right) \quad (\text{A.2})$$

where R_u = ultimate load (tons), e_h = efficiency of hammer, E_h = energy of hammer (ft-lbs), s = set per blow under final few blows (inches). Hammer efficiencies are assigned as follows:

$$e_h = 0.75 \text{ for drop hammers}$$

$$e_h = 0.85 \text{ for all other hammers}$$

$$e_h = \text{as specified by the manufacturer}$$

Referring again to the dynamic load test results (Table A.2), capacities of 198 kips and 227 kips were computed for the EOD and the BOR of SLTP-1 while for SLTP-2, capacities of 291 kips and 334 kips were calculated for the EOD and the BOR.

Thus, the Gates formula yields capacities much higher for both the EOD and BOR of SLTP-1 and the EOD of SLTP-2 than the Engineering News formula. However, the Gates formula yields a much lower capacity than the Engineering News Formula for the BOR of SLTP-2.

WEAP (Wave Equation Analysis of Pile Driving)

GRL's Wave Equation Analysis of Pile Driving is a program that simulates motions and forces in a pile when struck by a pile driving hammer. The program then computes the following: the blowcount (number of hammer blows/unit length of permanent set) of a pile; the axial stresses (both compressive and tensile) in a pile; and the energy transferred to a pile. Based on these results, the following can be indirectly derived: the pile's bearing capacity at the time of driving or restriking, given its resistance (blowcount); the stresses during pile driving; and the expected blowcount if the actual bearing capacity of the pile is known in advance (i.e., from a static load test).

By performing wave equation analyses over a wide range of ultimate capacities, a curve or “bearing graph” can be plotted which relates ultimate capacity to driving resistance.

The remaining section of this chapter will describe what input variables were assumed and present the results of several analyses.

Input Parameters

A summary of the input parameters used for WEAP analyses are shown in Table A.9. The input parameters were assigned according to information provided by actual data recorded during pile driving.

The stroke heights obtained by the IDOT and the PDA varied slightly for both pile tests at the EOD and the BOR. Thus, eight analyses were performed: two for the EOD and two for the BOR of each pile. For the EOD of SLTP-1, a fuel setting of 2 was used with hammer drop heights of 2.10 m (6.9 ft) (IDOT) and 2.07 m (6.8 ft) (PDA). For the BOR of SLTP-1, a fuel setting of 4 was used with hammer drop heights of 3.35 m (7.7 ft) (IDOT) and 2.26 m (7.4 ft) (PDA). For the EOD of SLTP-2, a fuel setting of 3 was used with hammer drop heights of 2.36 m (7.75 ft) (IDOT) and 2.16 m (7.1 ft) (PDA). For the BOR of SLTP-2, a fuel setting of 4 was used with a hammer drop of 2.65 m (8.7 ft) (IDOT and PDA).

To ensure a wide range of driving resistances (expressed in blows per meter), various combinations of the percent shaft resistance and the shaft resistance distribution (both triangular and linear) were analyzed. The procedure was as follows: for each hammer drop, significant shaft resistance was assumed to develop along the lower 40 percent, or 60 percent of the pile length. Furthermore, it was assumed that the shaft resistance accounted for 50, 70, and 90 percent of the total pile capacity. Finally, it was also assumed that the shaft resistance was either uniform along the length of the pile, or varied as a triangular distribution. The different assumptions result in twelve unique combinations of where the side resistance occurs (lower 40% or 60%), its distribution (triangular or uniform), and its percentage of total resistance (50%, 70%,

or 90%). A total of twelve bearing graphs were developed to cover each unique combination.

Results

The results of the analyses of each test pile for the EOD and the BOR are shown in Figures A.24, A.25, A.26, and A.27. Tables A.10 and A.11 summarizes the data for each test pile.

From the dynamic load test results (Table A.10), the driving resistance at the EOD of SLTP-1 was recorded as 3 blows per inch. From Figure A.24, this corresponds to an ultimate capacity of 267 kips (IDOT) and an ultimate capacity of 261 kips (PDA), with an average value of 264 kips. For the BOR, the recorded resistance was 4 blows per inch. From Figure A.25, this corresponds to an ultimate capacity of 354 kips (IDOT) and an ultimate capacity of 347 kips (PDA), with an average capacity of 350 kips. The driving resistance of SLTP-2 at the EOD was recorded as 6 blows per inch. From Figure A.26, this corresponds to an ultimate capacity of 400 kips (IDOT) and an ultimate capacity of 354 kips (PDA), with an average of 377 kips. The BOR driving resistance was found to be 11 blows per inch for both IDOT and PDA results. From Figure A.27, this corresponds to an ultimate capacity of 514 kips.

Table A.1 Pile Driving Record, Pile DTP-1

Tip Elev.	Penetration			Blows	Blows/6 in	Hammer Fall		Hammer Fall/3 in
	(m)	(m)	(ft)			(in)	(m)	
8/20/97 (1st drive-installation)								
186.133	9.906	32.5	390					
186.056	9.982	32.75	393	3				
185.980	10.058	33.00	396	3				
185.904	10.135	33.25	399	3.33	6.33			
185.828	10.211	33.50	402	3.33				
185.752	10.287	33.75	405	3.33	6.67			
185.675	10.363	34.00	408	6				
185.599	10.439	34.25	411	6.5	12.5			
185.523	10.516	34.50	414	6.5				
185.447	10.592	34.75	417	6.5	13			
185.371	10.668	35.00	420	6.5				
185.294	10.744	35.25	423	8	14.5			
185.218	10.820	35.50	426	10				
185.167	10.871	35.67	428	10				
185.142	10.897	35.75	429	4	24	1.98	6.5	6.5
8/21/97 (2nd drive-1st retap)								
185.142	10.897	35.75	0					
185.117	10.922	35.83	1		4	2.41	7.9	
185.091	10.947	35.92	2		5	2.35	7.7	
185.066	10.973	36.00	3		7	2.29	7.5	7.5
8/27/97 (3rd drive-2nd retap)								
185.066	10.973	36.00	0					
185.041	10.998	36.08	1			2.32	7.6	
185.015	11.024	36.17	2			2.32	7.6	
184.990	11.049	36.25	3			2.32	7.6	7.6
184.964	11.074	36.33	4			2.32	7.6	
184.939	11.100	36.42	5			2.32	7.6	
184.914	11.125	36.50	6			2.32	7.6	7.6
184.888	11.151	36.58	7			2.32	7.6	
184.863	11.176	36.67	8			2.32	7.6	
184.837	11.201	36.75	9	20		2.32	7.6	7.6
184.812	11.227	36.83	10	6		2.32	7.6	
184.787	11.252	36.92	11	6		2.32	7.6	
184.761	11.278	37.00	12	6	38	2.32	7.6	7.6
184.736	11.303	37.08	13	6		2.32	7.6	
184.710	11.328	37.17	14	6		2.32	7.6	
184.685	11.354	37.25	15	3		2.32	7.6	7.6
184.660	11.379	37.33	16	5		2.32	7.6	
184.634	11.405	37.42	17	6		2.32	7.6	
184.609	11.430	37.50	18	7	33	2.32	7.6	7.6

Table A.1 Pile Driving Record, Pile DTP-1 (cont'd)

Tip Elev.	Penetration			Blows	Blows/6 in	Hammer Fall		Hammer Fall/3 in
	(m)	(m)	(ft)			(in)	(m)	
184.583	11.455	37.58	19	5		2.32	7.6	
184.558	11.481	37.67	20	5		2.32	7.6	
184.533	11.506	37.75	21	5		2.32	7.6	7.6
184.507	11.532	37.83	22	5		2.32	7.6	
184.482	11.557	37.92	23	5		2.32	7.6	
184.456	11.582	38.00	24	5	30	2.32	7.6	7.6
8/27/97 (4th drive-redrive)								
184.456	11.582	38.00	0					
184.380	11.659	38.25	3			2.38	7.8	7.8
184.304	11.735	38.50	6	31	31	2.38	7.8	7.8
184.227	11.811	38.75	9			2.41	7.9	7.9
184.151	11.887	39.00	12	27	27	2.38	7.8	7.8
184.075	11.963	39.25	15			2.16	7.1	7.1
183.999	12.040	39.50	18	23	23	2.35	7.7	7.7
183.923	12.116	39.75	21			2.50	8.2	8.2
183.846	12.192	40.00	24	19	19	2.44	8	8
183.770	12.268	40.25	27			2.53	8.3	8.3
183.694	12.344	40.50	30	18	18	2.50	8.2	8.2
183.618	12.421	40.75	33			2.68	8.8	8.8
183.542	12.497	41.00	36	17	17	2.68	8.8	8.8
183.465	12.573	41.25	39			2.44	8	8
183.389	12.649	41.50	42	16	16	2.53	8.3	8.3
183.313	12.725	41.75	45			2.59	8.5	8.5
183.237	12.802	42.00	48	16	16	2.59	8.5	8.5
183.161	12.878	42.25	51			2.59	8.5	8.5
183.084	12.954	42.50	54	16	16	2.53	8.3	8.3
183.008	13.030	42.75	57			2.53	8.3	8.3
182.932	13.106	43.00	60	17	17	2.59	8.5	8.5
182.856	13.183	43.25	63			2.65	8.7	8.7
182.780	13.259	43.50	66	17	17	2.56	8.4	8.4
182.729	13.310	43.67	68	6				
182.703	13.335	43.75	69	3				
182.678	13.360	43.83	70	3				
182.653	13.386	43.92	71	3				
9/11/97 (5th drive-3rd retap)								
182.653	13.463	44.17	0					
182.628	13.488	44.25	1	12		2.65	8.7	
182.602	13.514	44.34	2	10		2.53	8.3	
182.577	13.539	44.42	3	10		2.59	8.5	8.5
182.551	13.565	44.50	4	9		2.53	8.3	

Table A.2 Pile Driving Record, Pile DTP-2

Tip Elev. (m)	Penetration			Blows	Blows/6 in	Hammer Fall		Hammer Fall/3 in (ft)
	(m)	(ft)	(in)			(m)	(ft)	
8/20/97 (1st drive-installation)								
186.689	8.84	29.00	348					
186.612	8.92	29.25	351	2				
186.536	8.99	29.50	354	3	5			
186.460	9.07	29.75	357	3				
186.384	9.14	30.00	360	3	6			
186.308	9.22	30.25	363	3				
186.231	9.30	30.50	366	3	6			
186.155	9.37	30.75	369	3				
186.079	9.45	31.00	372	4	7			
186.003	9.53	31.25	375	3.5				
185.927	9.60	31.50	378	3.5	7			
185.850	9.68	31.75	381	3				
185.774	9.75	32.00	384	3	6			
185.698	9.83	32.25	387	3				
185.622	9.91	32.50	390	3	6			
185.546	9.98	32.75	393	4				
185.469	10.06	33.00	396	6	10			
185.393	10.13	33.25	399	8				
185.342	10.19	33.42	401	7				
185.317	10.21	33.50	402	3	18	2.06	6.75	
8/27/97 (2nd drive-redrive)								
185.317	10.21	33.50	0					
185.292	10.24	33.58	1			2.35	7.7	
185.266	10.26	33.67	2			2.35	7.7	
185.241	10.29	33.75	3			2.35	7.7	7.7
185.165	10.36	34.00	6	21	21	2.44	8	8
185.088	10.44	34.25	9			2.47	8.1	8.1
185.012	10.52	34.50	12	31	31	2.41	7.9	7.9
184.936	10.59	34.75	15			2.38	7.8	7.8
184.860	10.67	35.00	18	38	38	2.41	7.9	7.9
184.784	10.74	35.25	21			2.44	8	8
184.707	10.82	35.50	24	41	41	2.53	8.3	8.3
184.631	10.90	35.75	27			2.56	8.4	8.4
184.555	10.97	36.00	30	36	36	2.56	8.4	8.4
184.479	11.05	36.25	33			2.56	8.4	8.4
184.403	11.13	36.50	36	37	37	2.53	8.3	8.3
184.326	11.20	36.75	39			2.62	8.6	8.6
184.250	11.28	37.00	42	39	39	2.65	8.7	8.7
184.174	11.35	37.25	45			2.65	8.7	8.7

Table A.2 Pile Driving Record, Pile DTP-2 (cont'd)

Tip Elev.	Penetration			Blows	Blows/6 in	Hammer Fall		Hammer Fall/3 in
	(m)	(ft)	(in)			(m)	(ft)	
184.098	11.43	37.50	48	42	42	2.65	8.7	8.7
184.022	11.51	37.75	51			2.65	8.7	8.7
183.945	11.58	38.00	54	28	28	2.65	8.7	8.7
183.869	11.66	38.25	57			2.65	8.7	8.7
183.793	11.73	38.50	60	28	28	2.68	8.8	8.8
183.717	11.81	38.75	63			2.59	8.5	8.5
183.641	11.89	39.00	66	16	16	2.59	8.5	8.5
183.564	11.96	39.25	69			2.47	8.1	8.1
183.488	12.04	39.50	72	18	18	2.47	8.1	8.1
183.412	12.12	39.75	75			2.44	8	8
183.336	12.19	40.00	78	19	19	2.53	8.3	8.3
183.260	12.27	40.25	81			2.62	8.6	8.6
183.183	12.34	40.50	84	26	26	2.74	9	9
183.158	12.37	40.58	85	6				
183.133	12.40	40.67	86	7				
183.107	12.42	40.75	87	8		2.68	8.8	8.8
183.082	12.45	40.83	88	8				
9/11/97 (3rd drive-retap)								
183.082	12.44	40.83	0					
183.057	12.47	40.91	1	16		2.71	8.9	
183.031	12.50	41.00	2	14		2.65	8.7	
183.006	12.52	41.08	3	14		2.71	8.9	8.8
182.980	12.55	41.16	4	14		2.68	8.8	

Table A.3 Pile Driving Record, Pile SLTP

Tip Elev. (m)	Penetration			Blows	Blows/6 in	Hammer Fall		Hammer Fall/3 in (ft)
	(m)	(ft)	(in)			(m)	(ft)	
8/20/97 (1st drive-installation)								
186.190	9.68	31.75	381					
186.114	9.75	32.00	384	2.5				
186.038	9.83	32.25	387	2.5				
185.962	9.91	32.50	390	3	5.5			
185.885	9.98	32.75	393	3				
185.809	10.06	33.00	396	3	6			
185.733	10.13	33.25	399	3.5				
185.657	10.21	33.50	402	4.5	8			
185.581	10.29	33.75	405	5.5				
185.504	10.36	34.00	408	6.5	12			
185.428	10.44	34.25	411	7				
185.377	10.49	34.42	413	5				
185.352	10.52	34.50	414	3	15	2.10	6.9	
8/27/97 (2nd drive-redrive)								
185.319	9.41	30.86	0					
185.294	9.43	30.94	1			2.35	7.7	
185.268	9.46	31.02	2			2.35	7.7	
185.243	9.48	31.11	3			2.35	7.7	7.7
185.167	9.56	31.36	6	32	32	2.35	7.7	7.7
185.090	9.63	31.61	9			2.35	7.7	7.7
185.014	9.71	31.86	12	25	25	2.35	7.7	7.7
184.938	9.79	32.11	15			2.32	7.6	7.6
184.862	9.86	32.36	18	28	28	2.41	7.9	7.9
184.786	9.94	32.61	21			2.50	8.2	8.2
184.709	10.02	32.86	24			2.50	8.2	8.2
184.633	10.09	33.11	27			2.62	8.6	8.6
184.557	10.17	33.36	30	40	40	2.59	8.5	8.5
184.481	10.24	33.61	33			2.50	8.2	8.2
184.405	10.32	33.86	36	22	22	2.47	8.1	8.1
184.328	10.40	34.11	39			2.62	8.6	8.6
184.252	10.47	34.36	42	23	23	2.50	8.2	8.2
184.176	10.55	34.61	45			2.53	8.3	8.3
184.100	10.62	34.86	48	21	21	2.47	8.1	8.1
184.024	10.70	35.11	51			2.50	8.2	8.2
183.947	10.78	35.36	54	29	29	2.38	7.8	7.8
183.871	10.85	35.61	57			2.41	7.9	7.9
183.795	10.93	35.86	60	28	28	2.38	7.8	7.8
183.719	11.01	36.11	63			2.35	7.7	7.7
183.643	11.08	36.36	66	30	30	2.35	7.7	7.7

Table A.3 Pile Driving Record, Pile SLTP (cont'd)

Tip Elev.	Penetration			Blows	Blows/6 in	Hammer Fall		Hammer Fall/3 in
	(m)	(m)	(ft)			(in)	(m)	
183.566	11.16	36.61	69			2.35	7.7	7.7
183.490	11.23	36.86	72	30	30	2.38	7.8	7.8
183.414	11.31	37.11	75			2.38	7.8	7.8
183.338	11.39	37.36	78	27	27	2.38	7.8	7.8
183.287	11.44	37.52	80	9		0.00		
183.262	11.46	37.61	81	5		2.38	7.8	7.8
183.236	11.49	37.69	82	5		0.00		
183.211	11.51	37.77	83	6		0.00		
183.185	11.54	37.86	84	6	31	2.36	7.75	7.75
9/11/97 (3rd drive-retap)								
183.149	11.58	37.98	0					
183.124	11.60	38.06	1	11		2.65	8.7	
183.098	11.63	38.14	2	13		2.71	8.9	
183.073	11.65	38.23	3	12		2.68	8.8	8.8
183.047	11.68	38.31	4	11		2.71	8.9	
183.022	11.70	38.39	5	11		2.56	8.4	
182.997	11.73	38.48	6	11	69	2.53	8.3	8.5
182.971	11.75	38.56	7	11		2.59	8.5	
182.946	11.78	38.64	8	10		2.50	8.2	

Table A.4 Load-displacement data for test 1 (SLT-1)

Time (min)	Nominal Load (tons)	Jack		Load Cell		Best Estimate		Dial Indicator		Wire & Mirror (in)
		Gage Pressure (psi)	Load (tons)	Rdg	Load (tons)	Load (tons)	Avg Settl (in)	1 (in)	2 (in)	
8:36 a.m.	0	0	0	0	0	0	0.000	2.000	2.000	1
0	7.5	225	7.4	14	7.1	7.2	0.010	1.990	1.990	1 1/16
5	7.5	225	7.4	14	7.1	7.2	0.011	1.989	1.989	
5	15	450	16.2	29	14.9	15.6	0.024	1.976	1.976	1 3/64
10	15	450	16.2	29	14.9	15.6	0.026	1.974	1.974	
10	22.5	650	24.1	44	22.8	23.4	0.040	1.960	1.960	1 3/64
15	22.5	650	24.1	44	22.8	23.4	0.041	1.959	1.959	
15	30	850	32.0	58	30.1	31.0	0.054	1.946	1.947	1 1/8
20	30	850	32.0	58	30.1	31.0	0.057	1.943	1.944	
20	37.5	1050	36.7	72	37.0	36.9	0.068	1.932	1.932	1 1/8
25	37.5	1050	36.7	72	37.0	36.9	0.071	1.930	1.929	
25	45	1275	45.0	86	44.6	44.8	0.086	1.913	1.916	1 1/8
30	45	1275	45.0	86	44.6	44.8	0.089	1.910	1.912	
30	52.5	1500	53.3	100	52.2	52.8	0.103	1.896	1.898	1 1/8
35	52.5	1500	53.3	100	52.2	52.8	0.107	1.892	1.894	
35	60	1700	60.6	114	59.9	60.2	0.122	1.877	1.880	1 5/32
40	60	1700	60.6	114	59.9	60.2	0.126	1.873	1.876	
40	67.5	1875	67.0	128	67.5	67.3	0.141	1.858	1.861	1 3/16
45	67.5	1875	67.0	128	67.5	67.3	0.146	1.853	1.856	
45	75	2100	75.3	142	75.2	75.2	0.160	1.839	1.842	1 7/32
50	75	2100	75.3	142	75.2	75.2	0.164	1.835	1.837	
50	82.5	2350	84.5	156	82.8	83.6	0.181	1.818	1.821	1 7/32
55	82.5	2350	84.5	156	82.8	83.6	0.187	1.812	1.815	
55	90	2500	90.0	169	89.9	89.9	0.201	1.797	1.801	1 1/4
60	90	2500	90.0	169	89.9	89.9	0.207	1.791	1.795	
60	97.5	2675	96.4	183	97.5	97.0	0.225	1.774	1.777	1 9/32
65	97.5	2675	96.4	183	97.5	97.0	0.234	1.765	1.768	
65	105	2900	104.7	197	105.2	104.9	0.251	1.747	1.752	1 5/16
70	105	2900	104.7	197	105.2	104.9	0.263	1.735	1.739	
70	112.5	3125	113.0	211	112.8	112.9	0.284	1.714	1.719	1 5/16
75	112.5	3125	113.0	211	112.8	112.9	0.308	1.690	1.695	
75	120	3300	119.4	225	120.5	119.9	0.332	1.666	1.671	1 3/8
80	120	3300	119.4	225	120.5	119.9	0.386	1.611	1.618	

Table A.4 Load-displacement data for test 1 (SLT-1) (cont'd)

Time (min)	Nominal Load (tons)	Jack		Load Cell		Best Estimate		Dial Indicator		Wire & Mirror (in)
		Gage Pressure (psi)	Load (tons)	Rdg	Load (tons)	Load (tons)	Avg Settl (in)	1 (in)	2 (in)	
80	127.5	3550	128.6	239	128.1	128.3	0.426	1.570	1.578	1 7/16
85	127.5	3550	128.6	239	128.1	128.3	0.540	1.457	1.464	
85	135	3700	134.1	252	135.2	134.6	0.591	1.405	1.413	1 5/8
90	135	3700	134.1	252	135.2	134.6	0.754	1.250	1.243	
90	142.5	3975	144.2	266	142.8	143.5	0.804	1.192	1.200	1 7/8
95	142.5	3975	144.2	266	142.8	143.5	1.052	0.943	0.953	
95	150	4175	151.5	280	150.5	151.0	1.104	0.892	0.901	2 1/8
100	150	4175	151.5	280	150.5	151.0	1.473	0.523	0.532	
100	(unloading)			200.5	107.1	107.1	1.432	0.564	0.572	2 13/32
105				201	107.4	107.4	1.429	0.566	0.576	
105				141.8	75.1	75.1	1.373	0.622	0.632	2 3/8
110				143.9	76.2	76.2	1.372	0.623	0.634	
110				73.4	37.7	37.7	1.299	0.697	0.706	2 5/16
115				75.8	39.0	39.0	1.296	0.699	0.709	
1:55 p.m.	(e.o.t.)			0	0.0	0.0				2 7/32

Table A.5 Load-displacement data for test 2 (SLT-2)

Time (min)	Nominal Load (tons)	Jack		Load Cell		Best Estimate		Dial Indicator		Wire & Mirror (in)
		Gage Pressure (psi)	Load (tons)	Rdg	Load (tons)	Load (tons)	Avg Settl (in)	1 (in)	2 (in)	
8:30 a.m.	0	0	0	0	0	0	0	1.971	1.951	1
0	7.5	250	8.4	14	7.1	7.7	0.009	1.962	1.942	
2.5	7.5	250	8.4	14	7.1	7.7	0.009	1.963	1.942	1
2.5	15	450	16.2	29	14.9	15.6	0.020	1.952	1.931	
5	15	450	16.2	29	14.9	15.6	0.019	1.953	1.931	1
5	22.5	600	22.1	44	22.8	22.5	0.031	1.941	1.919	
7.5	22.5	600	22.1	44	22.8	22.5	0.032	1.94	1.919	1 1/32
7.5	30	800	30.0	58	30.1	30.1	0.043	1.929	1.908	
10	30	800	30.0	58	30.1	30.1	0.043	1.929	1.907	1 1/32
10	37.5	1025	35.8	72	37.0	36.4	0.054	1.918	1.896	
12.5	37.5	1025	35.8	72	37.0	36.4	0.055	1.918	1.895	1 1/16
12.5	45	1250	44.1	86	44.6	44.3	0.066	1.906	1.884	
15	45	1250	44.1	86	44.6	44.3	0.066	1.906	1.884	1 1/16
15	52.5	1450	51.4	100	52.2	51.8	0.078	1.894	1.872	
20	52.5	1450	51.4	100	52.2	51.8	0.079	1.894	1.871	1 1/16
20	60	1650	58.8	114	59.9	59.3	0.090	1.882	1.86	
25	60	1650	58.8	114	59.9	59.3	0.091	1.882	1.859	1 3/32
25	67.5	1850	66.1	124	65.3	65.7	0.103	1.869	1.848	
30	67.5	1850	66.1	128	67.5	66.8	0.104	1.869	1.846	1 3/32
30	75	2075	74.4	142	75.2	74.8	0.115	1.857	1.835	
35	75	2075	74.4	142	75.2	74.8	0.116	1.856	1.834	1 3/32
35	82.5	2275	81.7	156	82.8	82.3	0.128	1.844	1.822	
40	82.5	2275	81.7	156	82.8	82.3	0.130	1.843	1.82	1 1/8
40	90	2475	89.1	169	89.9	89.5	0.141	1.832	1.809	
45	90	2475	89.1	169	89.9	89.5	0.143	1.83	1.806	1 1/8
45	97.5	2650	95.5	183	97.5	96.5	0.155	1.818	1.794	
50	97.5	2650	95.5	183	97.5	96.5	0.158	1.815	1.791	1 5/32
50	105	2860	103.2	197	105.2	104.2	0.170	1.803	1.779	
55	105	2860	103.2	197	105.2	104.2	0.173	1.801	1.776	1 5/32
55	112.5	3075	111.1	211	112.8	112.0	0.185	1.789	1.764	
60	112.5	3075	111.1	211	112.8	112.0	0.188	1.786	1.761	1 3/16
60	120	3290	119.0	225	120.5	119.7	0.199	1.774	1.75	
65	120	3290	119.0	225	120.5	119.7	0.203	1.771	1.746	1 3/16

Table A.5 Load-displacement data for test 2 (SLT-2) (cont'd)

Time (min)	Nominal Load (tons)	Jack		Load Cell		Best Estimate		Dial Indicator		Wire & Mirror (in)
		Gage Pressure (psi)	Load (tons)	Rdg	Load (tons)	Load (tons)	Avg Settl (in)	1 (in)	2 (in)	
65	127.5	3480	126.0	239	128.1	127.0	0.215	1.759	1.734	
70	127.5	3480	126.0	239	128.1	127.0	0.218	1.756	1.731	1 7/32
70	135	3660	132.6	252	135.2	133.9	0.230	1.744	1.719	
75	135	3660	132.6	252	135.2	133.9	0.233	1.741	1.716	1 7/32
75	142.5	3880	140.7	266	142.8	141.8	0.246	1.728	1.702	
80	142.5	3880	140.7	266	142.8	141.8	0.250	1.724	1.698	1 1/4
80	150	4125	149.7	280	150.5	150.1	0.263	1.711	1.685	
85	150	4125	149.7	280	150.5	150.1	0.267	1.708	1.68	1 1/4
85	157.5	4300	156.1	294	158.1	157.1	0.280	1.695	1.668	
90	157.5	4300	156.1	294	158.1	157.1	0.284	1.691	1.664	1 9/32
90	165	4490	163.1	307	165.2	164.2	0.295	1.679	1.653	
95	165	4490	163.1	307	165.2	164.2	0.299	1.675	1.649	1 9/32
95	172.5	4686	170.3	320	172.3	171.3	0.311	1.663	1.637	
100	172.5	4686	170.3	320	172.3	171.3	0.315	1.66	1.632	1 5/16
100	180	4890	177.8	334	179.9	178.9	0.328	1.647	1.62	
105	180	4890	177.8	334	179.9	178.9	0.334	1.641	1.614	1 5/16
105	187.5	5125	186.4	348	187.6	187.0	0.348	1.627	1.6	
110	187.5	5125	186.4	348	187.6	187.0	0.353	1.622	1.595	1 11/32
110	195	5340	194.3	361	194.7	194.5	0.365	1.61	1.582	
115	195	5340	194.3	361	194.7	194.5	0.371	1.605	1.576	1 11/32
115	202.5	5540	201.7	375	202.3	202.0	0.384	1.591	1.563	
120	202.5	5540	201.7	375	202.3	202.0	0.390	1.585	1.557	1 3/8
120	210	5760	209.8	389	209.9	209.9	0.404	1.571	1.544	
125	210	5760	209.8	389	209.9	209.9	0.410	1.565	1.537	1 3/8
125	217.5	5960	217.1	402	217.0	217.1	0.423	1.552	1.525	
130	217.5	5960	217.1	402	217.0	217.1	0.429	1.546	1.519	1 13/32
130	225	6170	224.8	416	224.7	224.7	0.443	1.532	1.504	
135	225	6170	224.8	416	224.7	224.7	0.452	1.524	1.495	1 7/16
135	232.5	6390	232.9	430	232.3	232.6	0.467	1.509	1.48	
140	232.5	6390	232.9	430	232.3	232.6	0.473	1.503	1.473	1 7/16
140	240	6560	239.1	443	239.4	239.3	0.486	1.49	1.461	
145	240	6560	239.1	443	239.4	239.3	0.496	1.48	1.451	1 15/32
145	247.5	6770	246.9	456	246.5	246.7	0.509	1.466	1.439	
150	247.5	6770	246.9	456	246.5	246.7	0.520	1.455	1.427	1 1/2

Table A.5 Load-displacement data for test 2 (SLT-2) (cont'd)

Time (min)	Nominal Load (tons)	Jack		Load Cell		Best Estimate		Dial Indicator		Wire & Mirror (in)
		Gage Pressure (psi)	Load (tons)	Rdg	Load (tons)	Load (tons)	Avg Settl (in)	1 (in)	2 (in)	
150	255	7000	255.3	469	253.6	254.5	0.534	1.441	1.413	
155	255	7000	255.3	469	253.6	254.5	0.547	1.428	1.4	1 17/32
155	262.5			482	260.7	260.7	0.562	1.413	1.385	
160	262.5			482	260.7	260.7	0.579	1.396	1.368	1 9/16
160	270	7440	271.5	496	268.3	269.9	0.596	1.379	1.352	
165	270	7440	271.5	496	268.3	269.9	0.624	1.351	1.324	1 19/32
165	277.5	7650	279.2	510	276.0	277.6	0.642	1.333	1.305	
170	277.5	7650	279.2	510	276.0	277.6	0.698	1.276	1.25	1 5/8
170	285	7970	290.9	523	283.1	287.0	0.720	1.254	1.229	
175	285	7970	290.9	523	283.1	287.0	1.031	0.94	0.92	2 1/16
180		7340	267.8	484.9	262.3	265.0	1.969	0.187	0.088	3 1/32
183	(unloading)			390	210.5	210.5	1.888	0.268	0.17	3 1/32
188				391.8	211.5	211.5	1.887	0.269	0.171	2 31/32
188				261.9	140.6	140.6	1.759	0.396	0.3	
193				264.8	142.2	142.2	1.759	0.395	0.3	2 27/32
193				137	72.4	72.4	1.627	0.526	0.433	
198				142.2	75.3	75.3	1.628	0.525	0.433	2 23/32
198				10.2	5.1	5.1	1.482	0.672	0.578	
203				11.2	5.6	5.6	1.476	0.678	0.584	2 9/16
11:53 p.m.	(e.o.t.)			0	0	0				2 9/16

**Table A.6 Summary of Dynamic Testing Field Results
Jacksonville Load Test Program, Jacksonville, Illinois**

Pile Number	Date Tested	Driving Status	Approximate Pile Penetration (feet)	Reported Pile Driving Resistances (blows / inch)	Average Calculated Hammer Stroke (ft)	Average Energy Transferred to Pile Head (ft.-kips)	Energy Transfer Ratio (%)	Average Hammer Operating Speed (blows / min)	Average Max. Pile Head Compression Stress (ksi)		Average Mobilized Case Method Capacity, RX8 (kips)	Range in Mobilized Case Method Capacity, RX8 (kips)
									Max. Pile Head Compression Stress	Average Mobilized Case Method Capacity, RX8		
SLT #1	8-20-97	EOD	34.25	4 / 1 in.	6.8	16	37	45.2	27.4	27.4	243	232 - 252
	8-27-97	BOR #1	34.25	4 / 1 in.	7.4	19	44	43.3	29.0	29.0	291	284 - 297
	8-27-97	EOR #1	42.50	14 / 3 in.	7.1	16	37	44.1	27.8	27.8	333	327 - 337
	9-11-97	BOR #2	42.50	11 / 1 in.	8.7	20	47	40.1	31.6	31.6	465	445 - 514
DTP #1	8-20-97	EOD	35.50	4 / 1 in.	6.2	14	33	47.0	26.5	26.5	289	270 - 297
	8-21-97	BOR #1	35.50	4 / 1 in.	7.5	20	46	43.1	29.4	29.4	307	296 - 310
	8-27-97	BOR #2	35.75	5 / 1 in.	7.5	18	42	43.1	29.4	29.4	332	327 - 335
	8-27-97	EOR #2	43.75	8 / 3 in.	7.5	18	42	43.0	28.8	28.8	285	284 - 286
8-11-97	BOR #3	43.75	12 / 1 in.	8.0	18	42	41.8	30.8	30.8	433	411 - 502	
DTP #2	8-20-97	EOD	33.50	3 / 1 in.	6.0	15	36	47.0	26.7	26.7	246	244 - 248
	8-27-97	BOR #1	33.50	3 / 1 in.	7.0	17	41	44.4	27.7	27.7	253	248 - 260
	8-27-97	EOR #1	40.92	24 / 3 in.	8.0	18	42	41.8	29.7	29.7	413	399 - 425
	9-11-97	BOR #2	40.92	16 / 1 in.	8.3	20	47	41.1	31.2	31.2	493	473 - 530

Notes: EOD = End of Initial Driving. BOR = Beginning of Restrike. EOR = End of Restrike. Summarized Data Represents Average Over Reported Driving Resistance Penetration Increment. Static Load Test Penetration Depths Referenced to Grade at End of Initial Driving. (Excavated 3.5 ft +/- After EOD)

Table A.7 Summary of CAPWAP Analysis Results
Jacksonville Load Test Program, Jacksonville, Illinois

Pile Number	Driving Status	Blow Number Analyzed	Approximate Pile Penetration Depth (ft)	Reported Driving Resistance (blows/in)	Mobilized CAPWAP Capacity (kips)		Soil Damping (sec/ft)		Soil Quake (inch)	
					Shaft	Toe	Shaft	Toe	Shaft	Toe
SLT #1	EOID	191	34.25	4/1 in.	104	136	0.19	0.10	0.10	0.51
	BOR #1	2	34.25	4/1 in.	150	134	0.16	0.10	0.10	0.43
	EOB #1	496	42.50	14/3 in.	180	151	0.18	0.15	0.10	0.34
	BOR #2	2	42.50	11/1 in.	350	165	0.26	0.22	0.09	0.12
	BOR #2	5	42.50	11/1 in.	311	165	0.24	0.18	0.11	0.20
BOR #2	11	42.50	42.50	11/1 in.	286	156	0.23	0.10	0.11	0.22
DTP #1	EOID	234	35.50	4/1 in.	120	165	0.19	0.07	0.10	0.39
	BOR #1	3	35.50	4/1 in.	137	164	0.18	0.07	0.10	0.57
	BOR #2	3	35.75	5/1 in.	169	156	0.18	0.06	0.10	0.34
	EOB #2	280	43.75	8/3 in.	157	140	0.18	0.09	0.08	0.44
	BOR #3	3	43.75	43.75	12/1 in.	305	185	0.26	0.09	0.08
DTP #2	EOID	174	33.50	3/1 in.	91	149	0.20	0.09	0.10	0.47
	BOR #1	3	33.50	3/1 in.	101	148	0.24	0.05	0.10	0.45
	BOR #2	441	40.92	24/3 in.	230	191	0.15	0.08	0.09	0.26
		3	40.92	16/1 in.	286	204	0.19	0.19	0.10	0.14

Notes: EOID = End of Initial Driving BOR = Beginning of Restrike EOR = End of Restrike

Table A.8 Dynamic load test results

Data set	SLTP-1				SLTP-2			
	EOD		BOR		EOD		BOR	
	Blowcount (bpi)	Stroke (ft)						
IDOT	3	6.9	4	7.7	14/3 in	7.75	11	8.7
PDA	3	6.8	4	7.4	14/3 in	7.1	11	8.7

Table A.9 Summary of WEAP input variables used in this study

Input		Value	Remark
Hammer	Hammer ID Number	38	Delmag D 19-32
	Stroke Option	-1	fixed stroke
	Fuel Setting	varies	see text
Pile	No. of Pile Segments	0	automatic
	No. of Splices	0	none
	Nonuniform Pile	0	uniform
	Pile Damping	1	steel piles
Shaft Resistance & Drivability	% Shaft Resistance	varies	see text
	Shaft Resistance Dist.	varies	see text
Helmet & Hammer Cushion	Helmet Weight	8.45 kN	
	Area	1464.5 cm ²	
	Elastic Modulus	1206.5 MPa	
	Thickness	50.8 mm	
	C.o.R.	0.92	
	Roundout	3 mm	default
	Stiffness	0	default
Pile Cushion	none		
Pile Information	Total Length	varies	see text
	Cross-sectional Area	100 cm ²	
	Elastic Modulus	210000 MPa	
	Specific Weight	78.5 kN/m ³	
	Circumference	0	
	Strenght/Yield	0	
	C.o.R.	0.85	steel piles
	Round Out	3 mm	default

Table A.9 Summary of WEAP input variables used in this study (cont'd)

Input		Value	Remark
Hammer Override Values	Stroke	varies	see text
	Efficiency	0	
	Pressure	0	
	Reaction Weight	0	
	ComDelay Ign. Vol.	0	
	Comb. Exp. Coeff.	0	
	Stroke Conv. Criteria	0	
Soil Parameters	Skin Quake	2.5 mm	cohesive cohesive
	Toe Quake	2.5 mm	
	Skin Damping	0.2 s/m	
	Toe Damping	0.15 s/m	
Ultimate Capacities		varies	see table
Extended Soil Model	none		
Radiation Damping	none		
Analysis Output	Output	0	automatic automatic
	Output Segment	0	
	Pile Input	0	
Hammer	Hammer Damping	0	default
Soil	Soil Damping	0	Standard Smith
	Damping Exponent	0	
	Residual Stress	0	
	Analysis		
Numeric	Time Increment Factor	0	default
	No. of Iterations	0	
	Max. Analysis Time	0	default

Table A.10 WEAP Output Data for test pile SLTP-1

	R_u (kN)	40/50t Blowcount (bpm)	40/70t Blowcount (bpm)	40/90t Blowcount (bpm)	60/50t Blowcount (bpm)	60/70t Blowcount (bpm)	60/90t Blowcount (bpm)	40/50l Blowcount (bpm)	40/70l Blowcount (bpm)	40/90l Blowcount (bpm)	60/50l Blowcount (bpm)	60/70l Blowcount (bpm)	60/90l Blowcount (bpm)	
EOD	600.8	26.9	27.8	28.8	26.7	27.6	28.5	27.1	28.1	29	26.9	27.8	28.7	
	901.1	58.6	60.1	62.2	58.1	60.1	62	58.6	60.8	62.8	58.6	60.1	62.1	
	961.2	65.1	67.4	69.9	64.8	67.1	69.4	65.7	68.4	70.9	65.5	67.4	70.8	
	1081.3	85.2	88.5	91.5	83.4	86.1	88.7	87.6	92.1	95.9	85.1	88.2	91	
	1201.5	104.2	108	111.5	101.9	105	107.8	108	113.3	116.7	103.9	107.5	110.7	
	1321.7	126.5	131.3	135.4	123.3	126.9	130.3	132	136.1	133.5	126.2	130.6	134.3	
	1501.9	170.1	174.2	177.3	165.7	169.7	172.9	175.8	172.3	169	168.9	172.4	174.6	
	1802.3	307.9	310.1	298.3	299.9	304.4	307.7	295.8	284.9	272.2	303.2	302.8	294	
	2102.6	713	744.7	704.1	660.9	710.2	749.6	673.8	624.7	555.4	711	734.6	664.2	
	2403	2076.3	2622.9	3001.2	1615.8	1914.6	2163.2	2698.9	3330.3	2780.6	2047.6	2458.6	2558.1	
	PDA	600.8	27.5	28.5	29.5	27.4	28.3	29.2	27.7	28.7	29.7	27.5	28.5	29.4
		901.1	60.2	61.8	63.9	59.7	61.7	63.7	60.2	62.5	64.6	60.2	61.8	63.8
		961.2	67	69.4	72	66.7	69.1	71	67.6	70.4	73.1	67	69.3	71.8
1081.3		87.6	90.9	94	85.7	88.5	91	90.3	94.7	98.5	87.4	90.6	93.3	
1201.5		107.2	111	114.7	104.8	108	100.8	111.1	116.6	118.2	106.9	110.5	113.8	
1321.7		130.5	135.3	139.5	127.2	130.7	134.1	136.2	138.2	136.8	130.1	134.5	138.2	
1501.9		175.9	180.1	183	171.7	175.5	178.7	179.2	177.5	173.9	174.7	178.1	180	
1802.3		325.5	320.6	312.3	317.2	321.4	324.5	309.6	297.8	283.4	320.6	318.4	303.4	
2102.6		760.1	815.3	774.2	699.4	755.1	798.7	735.8	679.3	598.7	752.6	784.7	724.6	
2403		2376.5	3116.5	3609.1	1811.3	2176.1	2493.7	3183.4	4069.1	3422	2356.7	2912.2	3017.6	
BOR		600.8	22.1	22.8	23.6	22	22.7	23.4	22.2	23	23.8	22.1	22.8	23.6
		901.1	47.8	49.5	51.2	47.4	49	50.6	48.3	50.1	51.7	47.8	49.5	51.1
		961.2	52.9	54.9	56.9	52.4	54.3	56.1	53.6	55.7	57.6	52.9	54.8	56.8
	1081.3	68.3	71.4	74.4	67.3	69.9	72.4	69.6	73.1	76.3	68.3	71.3	74.3	
	1201.5	85.1	88.4	91.4	83.2	85.9	88.4	88.1	92.5	95.2	84.9	88	90.8	
	1321.7	102	106.1	109.8	99.5	102.7	105.7	106.2	110.1	112.6	101.8	105.6	109	
	1501.9	133.9	139.3	140.4	129.8	133.8	137.7	138.2	140	138.4	133.4	138.2	140.7	
	1802.3	216.1	216.7	217.9	211.1	215.3	218.7	217.6	213.4	206.8	213.6	213.6	212.4	
	2102.6	423.6	413.4	399.6	420.2	432.5	416	397.2	377.7	350.9	413.4	400.2	381.8	
	2403	968.8	1092.7	1146.4	851.7	935.4	1001.4	1117.2	1037.7	850.6	959.8	1050.9	997	

Table A.10 WEAP Output Data for test pile SLTP-1 (cont'd)

		40/50t	40/70t	40/90t	60/50t	60/70t	60/90t	40/50l	40/70l	40/90l	60/50l	60/70l	60/90l
	R _u (kN)	Blowcount (bpm)											
BOR	PDA	23.4	24.2	25	23.3	24	24.8	23.5	24.4	25.2	23.4	24.2	25
		51.2	53.1	54.8	50.8	52.5	54.2	51.7	53.6	55.4	51.2	53	54.7
		56.9	59	61.2	56.3	58.3	60.3	57.6	59.8	62	56.9	59	61
		73.8	77.2	80.5	72.6	75.4	78.1	75.4	79.3	82.1	73.9	77.2	80.3
		91.3	94.8	97.9	89.3	92.1	94.8	94.6	98.2	101.8	91.1	94.3	97.2
		109.9	114.2	118.1	107.1	110.4	113.6	114.5	118.5	119.3	109.6	113.7	117.2
		145.6	150.4	151.3	141	145.2	148.9	149.4	150.2	148.1	145	149	149.5
		238.1	242.5	241.4	236.6	240.7	244.1	240.7	234.6	226.3	235.1	238	235.2
		505.4	493.9	474.5	492.8	508.9	510.2	466.9	441.9	406.5	497.4	478.8	452.6
		1198.8	1394.4	1511.7	1029.5	1150.1	1244	1433.6	1497.3	1162	1184	1325.1	1351.8

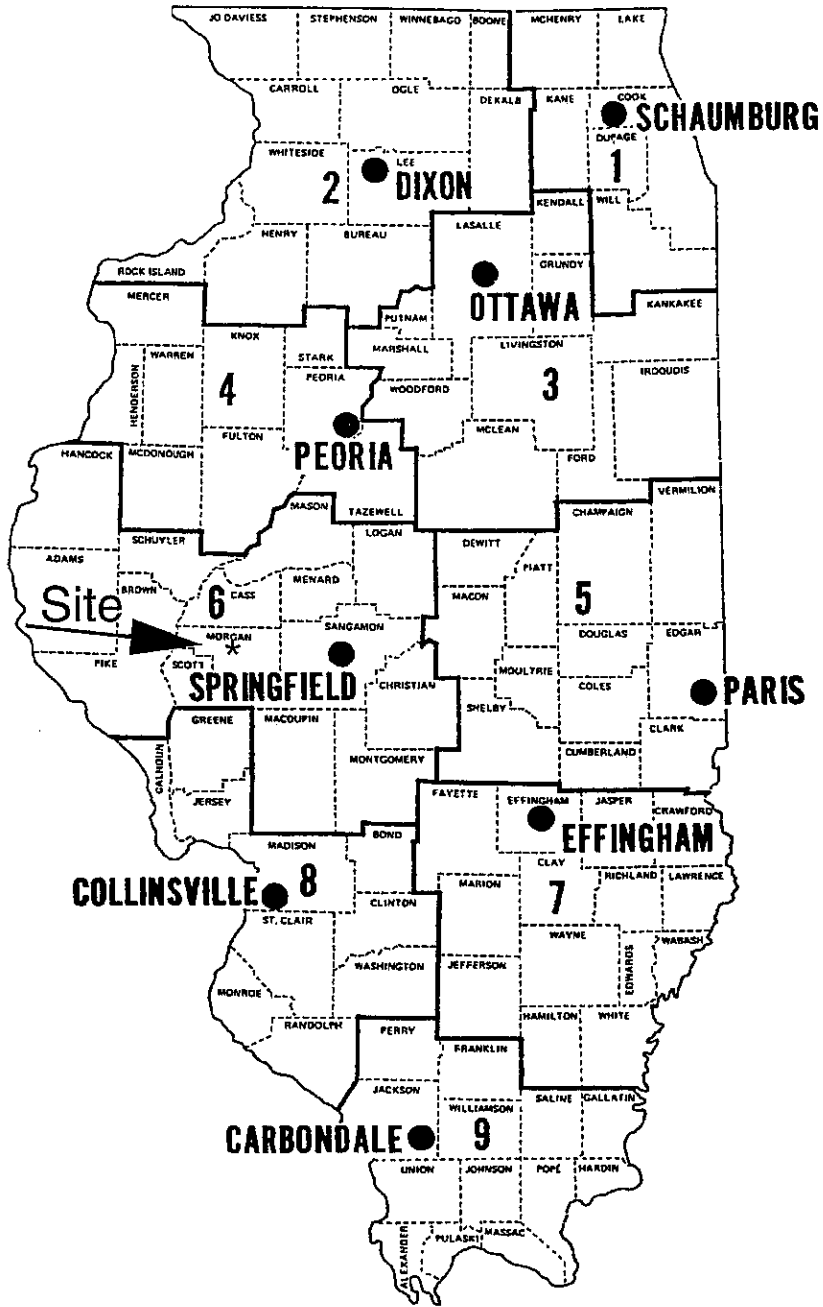


Figure A.1 General location map for Jacksonville load test site

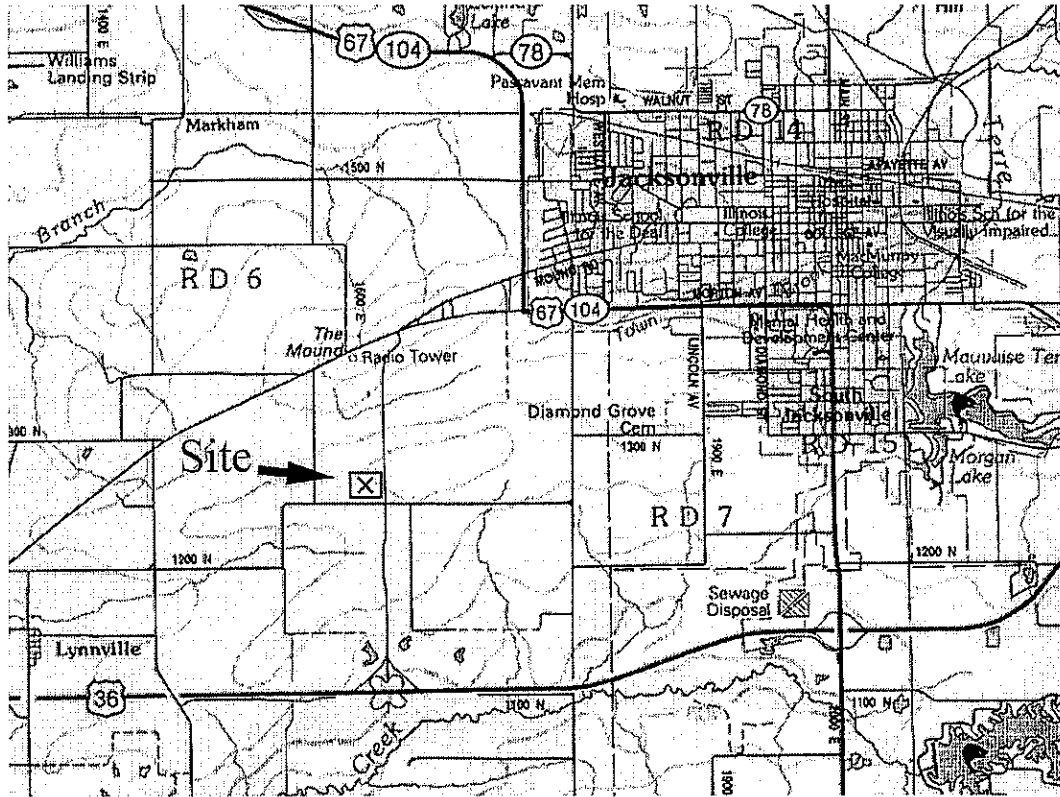


Figure A.2 Location map for load test site near Jacksonville, Illinois

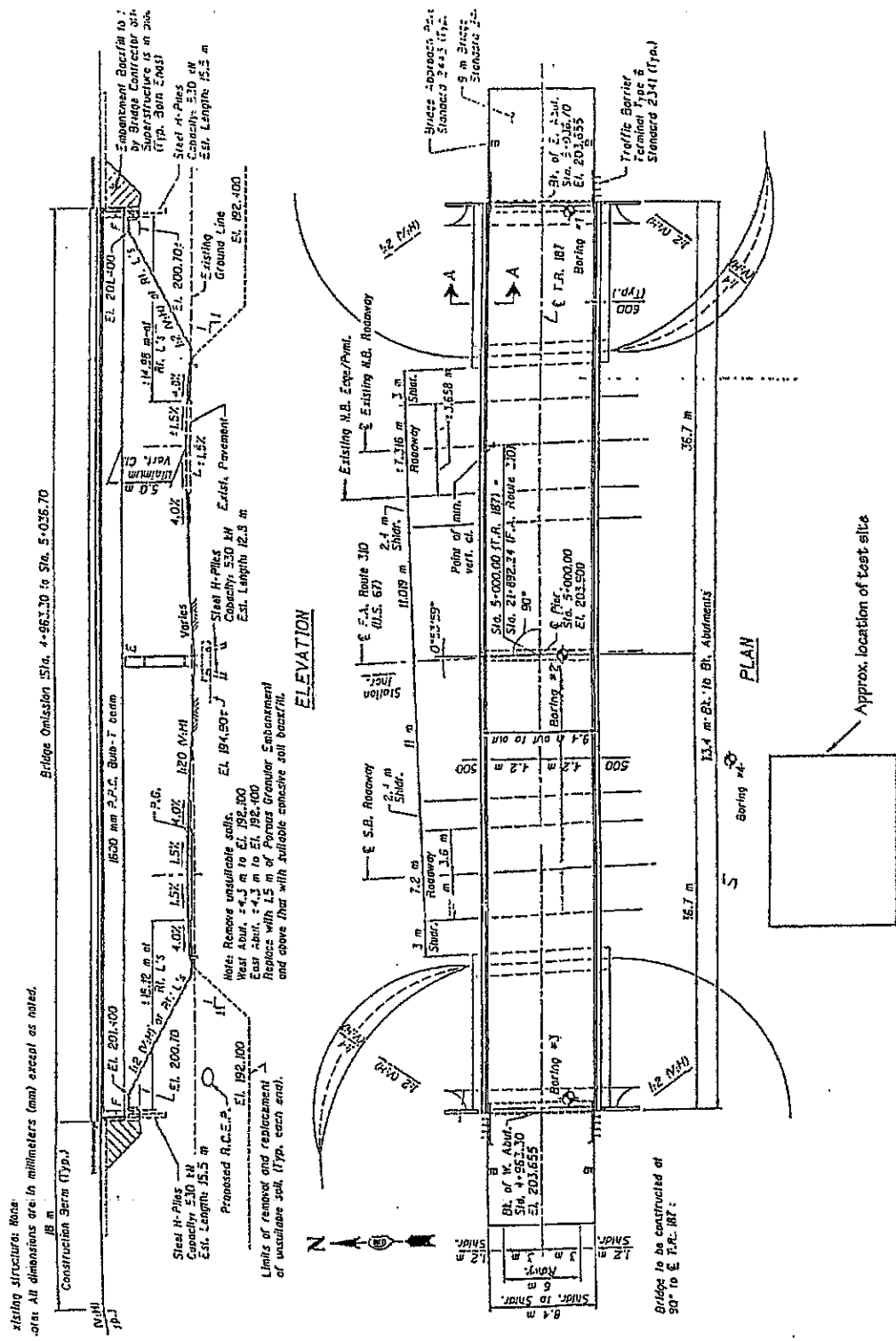


Figure A.3 Plan and profile views of overpass at Jacksonville load test site

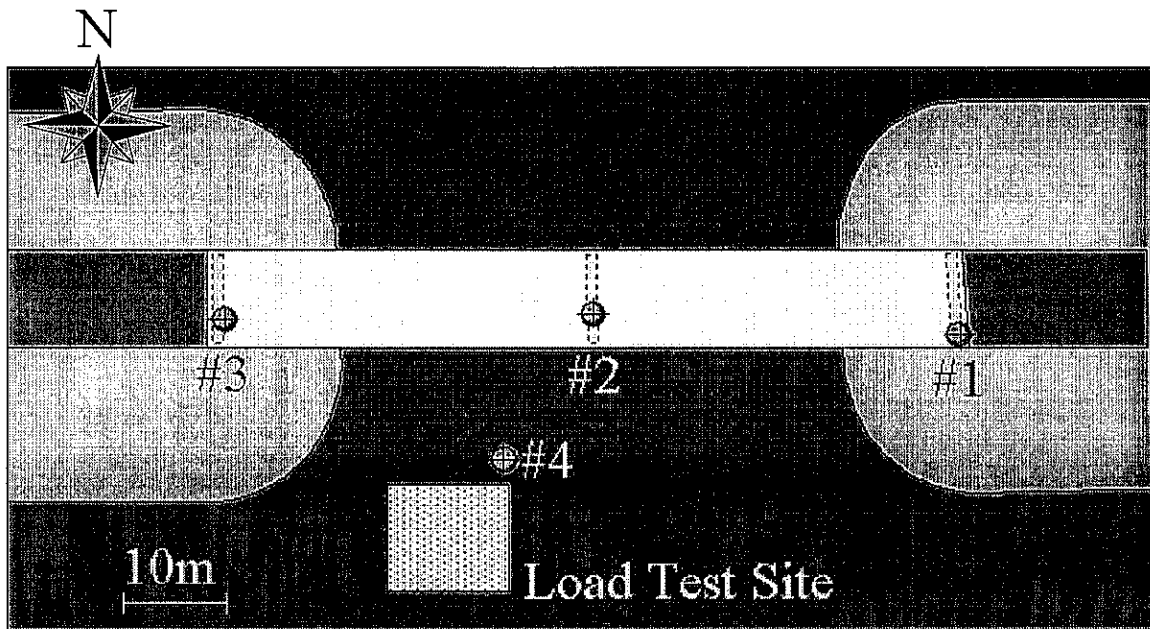


Figure A.4 Boring locations for Jacksonville load test site

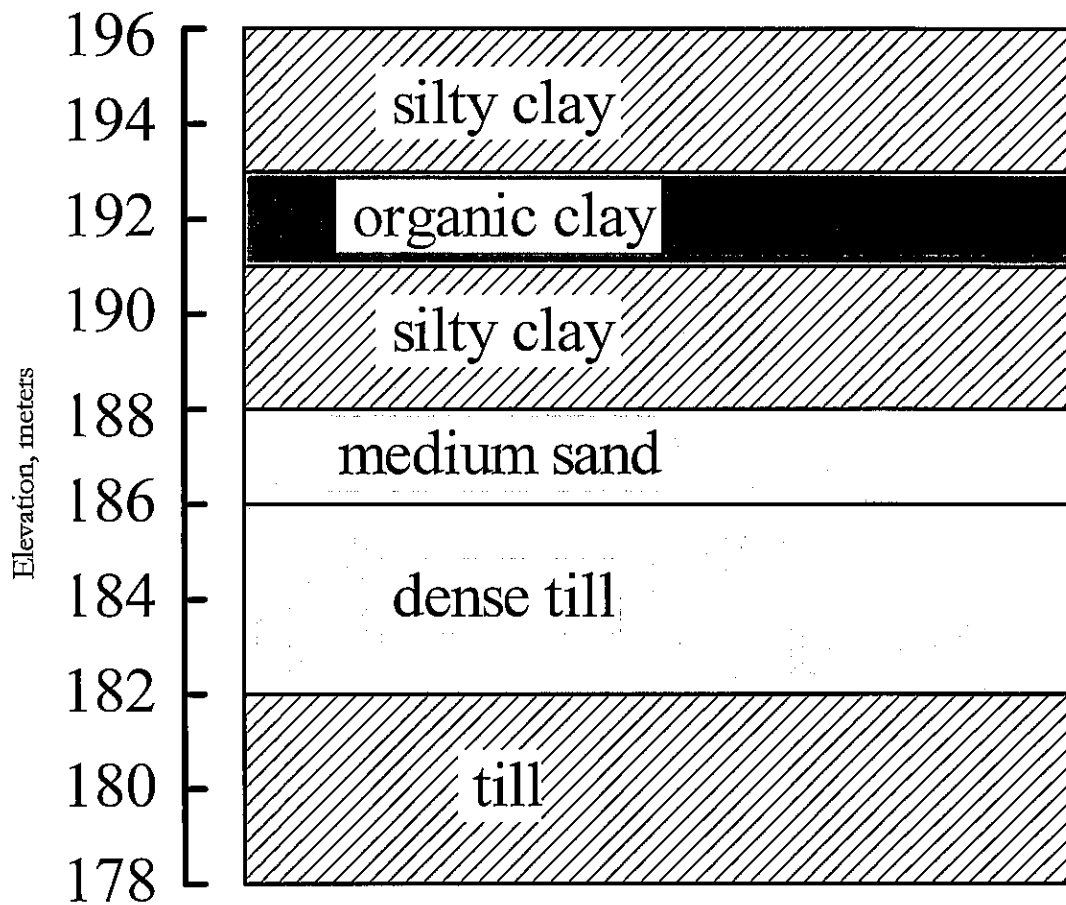


Figure A.5 Soil profile for Jacksonville load test site

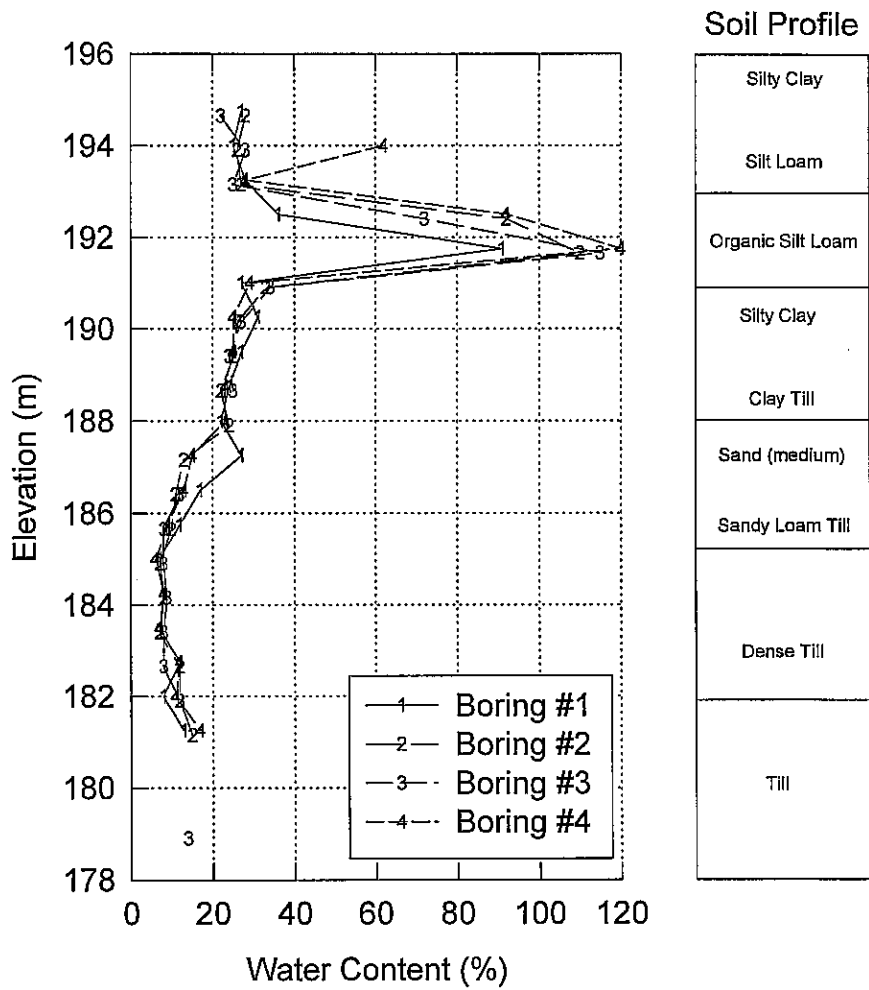


Figure A.6 Variation in water content with depth for soil profile at Jacksonville load test site

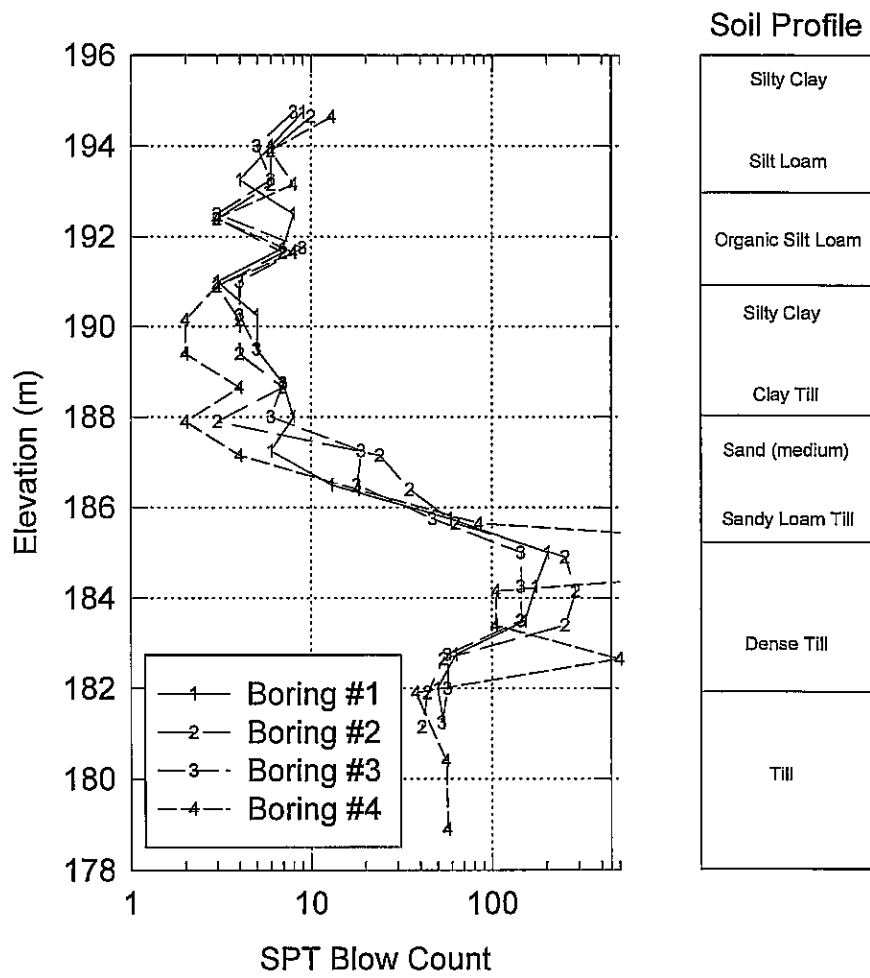


Figure A.7 Variation in Standard Penetration Resistance (blow count) with depth for soil profile at Jacksonville load test site

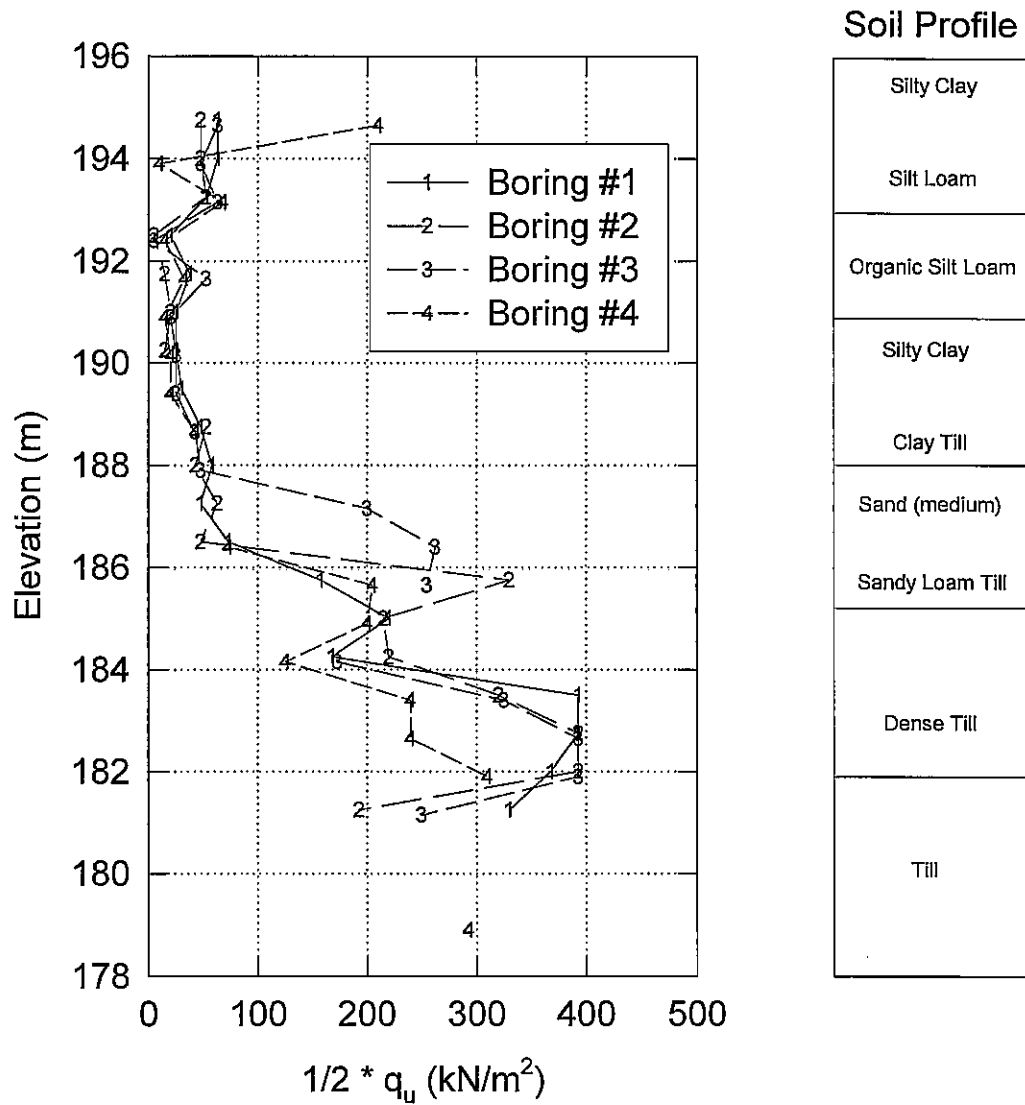


Figure A.8 Variation with depth of 1/2 the unconfined compressive strength for soil profile at Jacksonville load test site

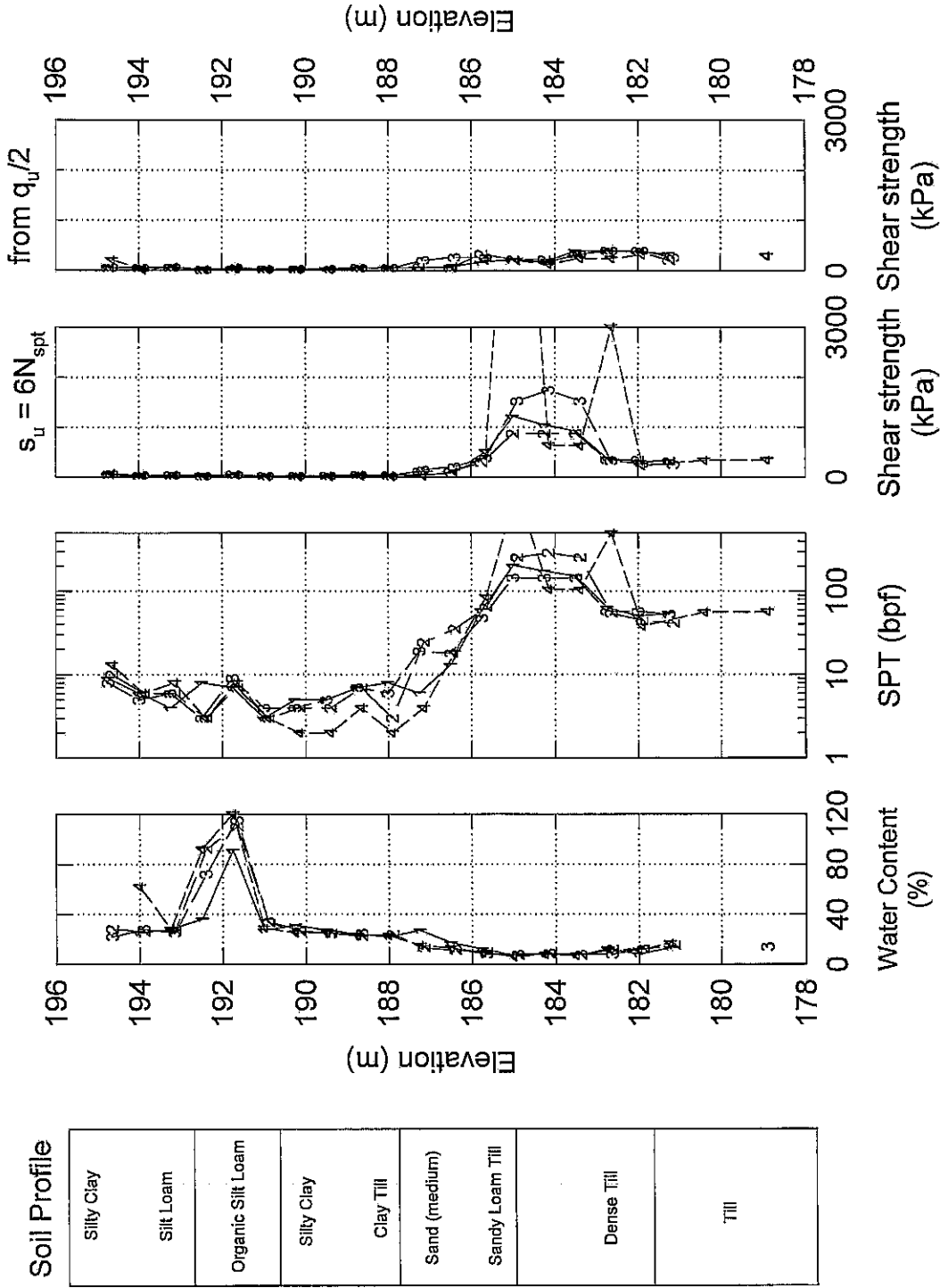


Figure A.9 Summary of water content, standard penetration resistance, and strength for Jacksonville load test site

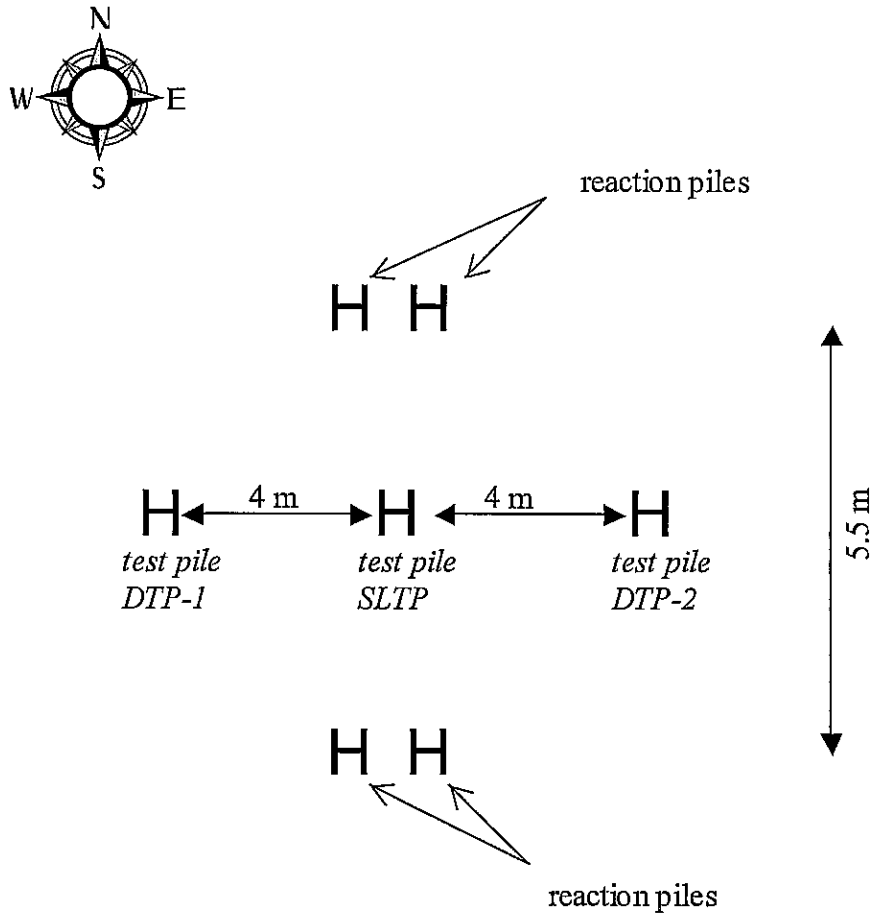


Figure A.10 Plan view of test and reaction piles at Jacksonville load test site

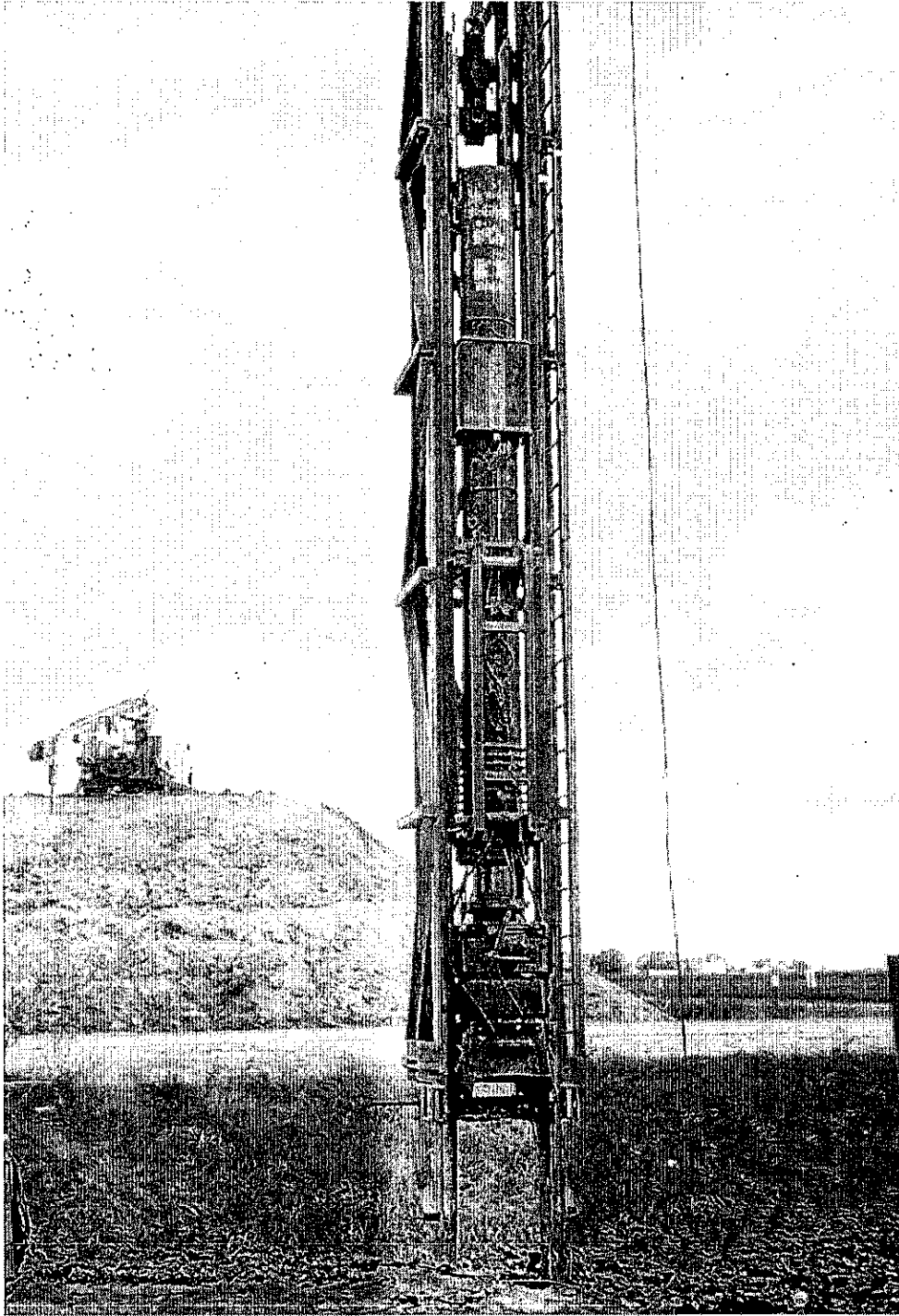


Figure A.11 Delmag D19-32 single acting diesel hammer used at Jacksonville load test site

DTP-1

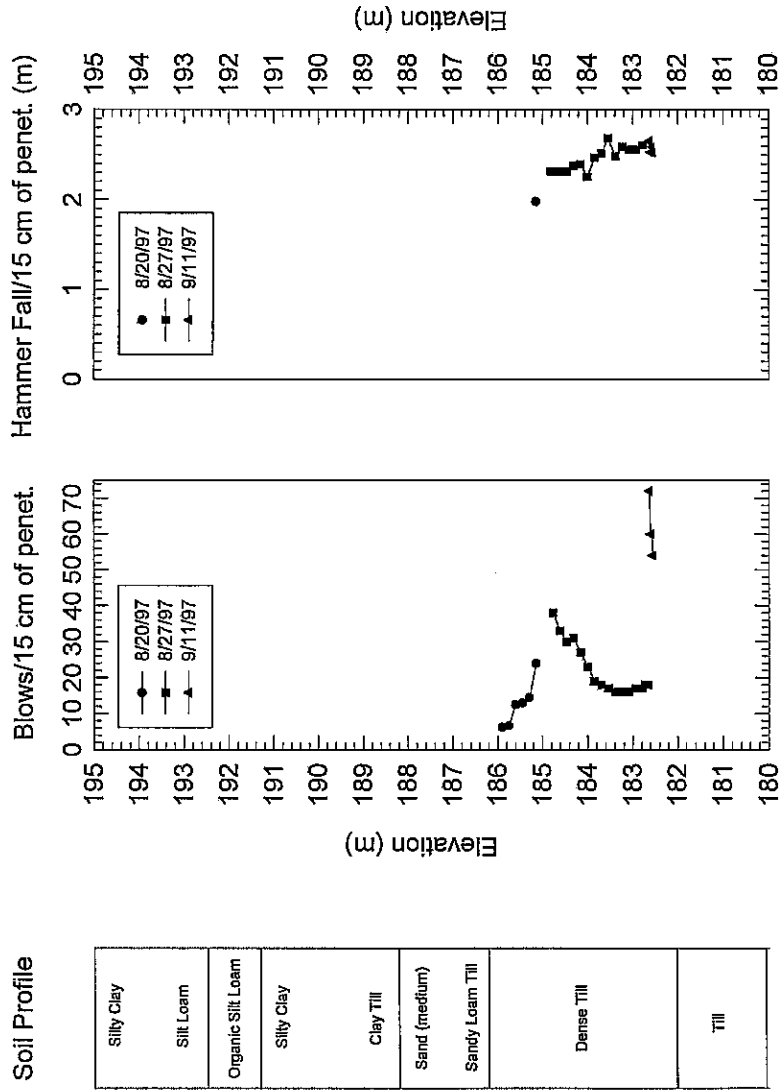


Figure A.12 Driving resistance of pile DTP-1 at Jacksonville load test site

DTP-2

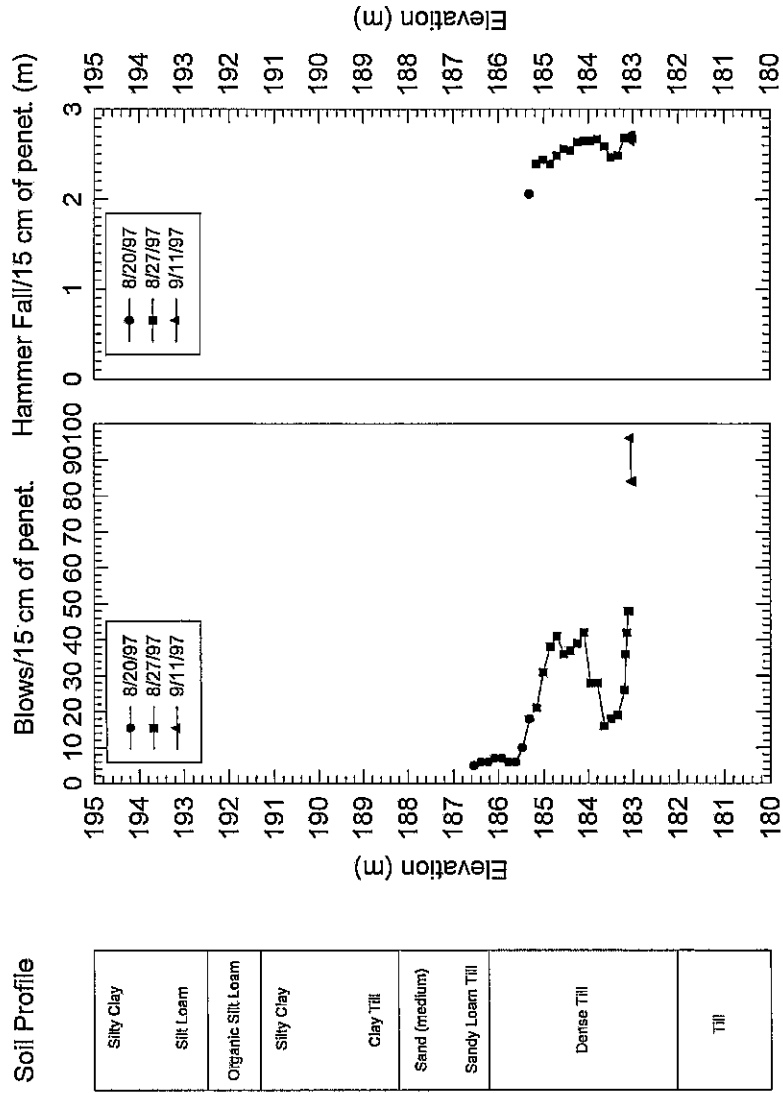


Figure A.13 Driving resistance of pile DTP-2 at Jacksonville load test site

SLTP

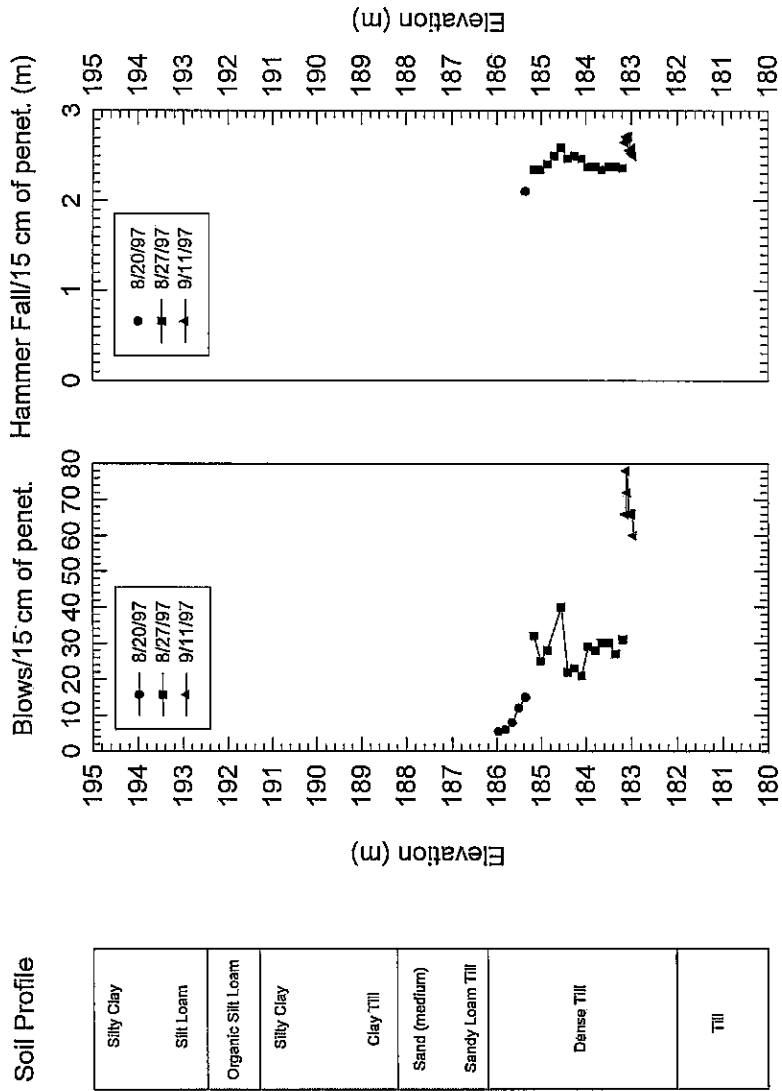


Figure A.14 Driving resistance of pile SLTP at Jacksonville load test site

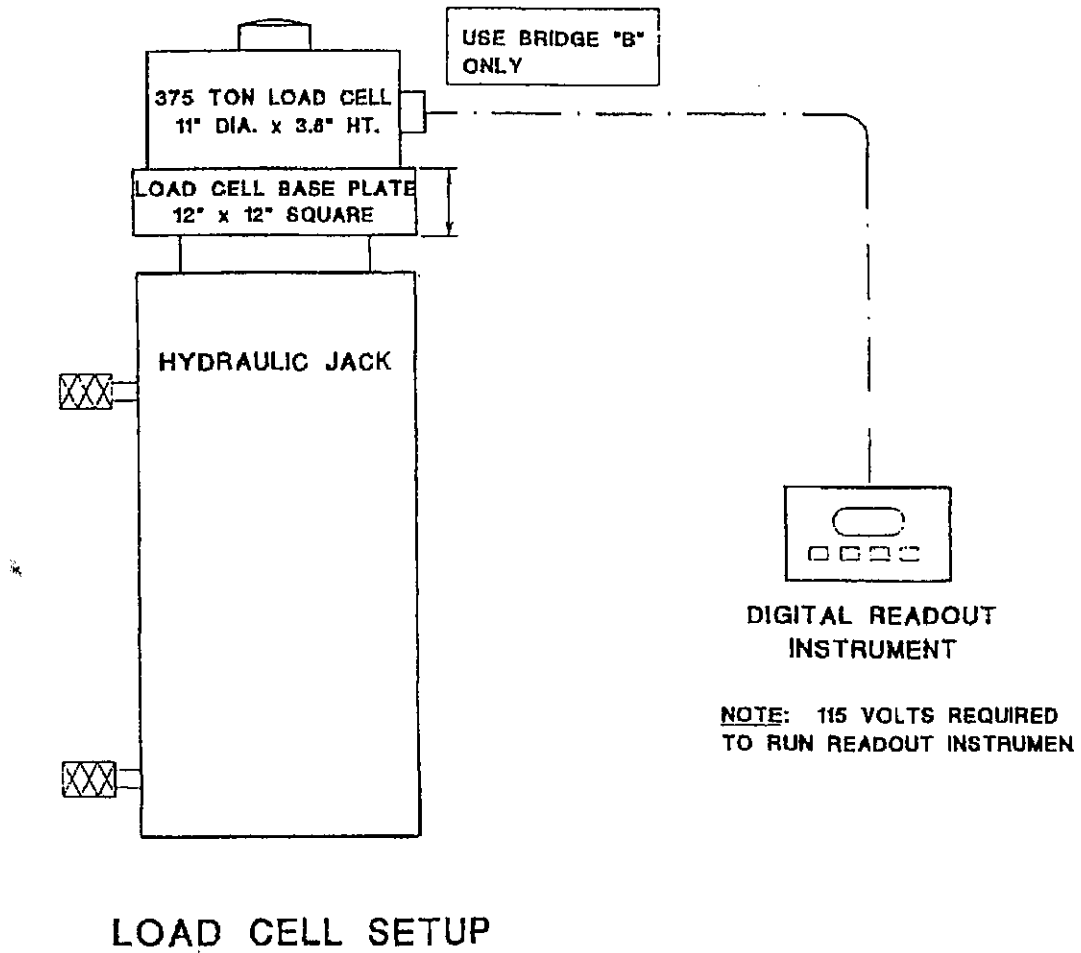


Figure A.15 Schematic view of hydraulic jack and load cell

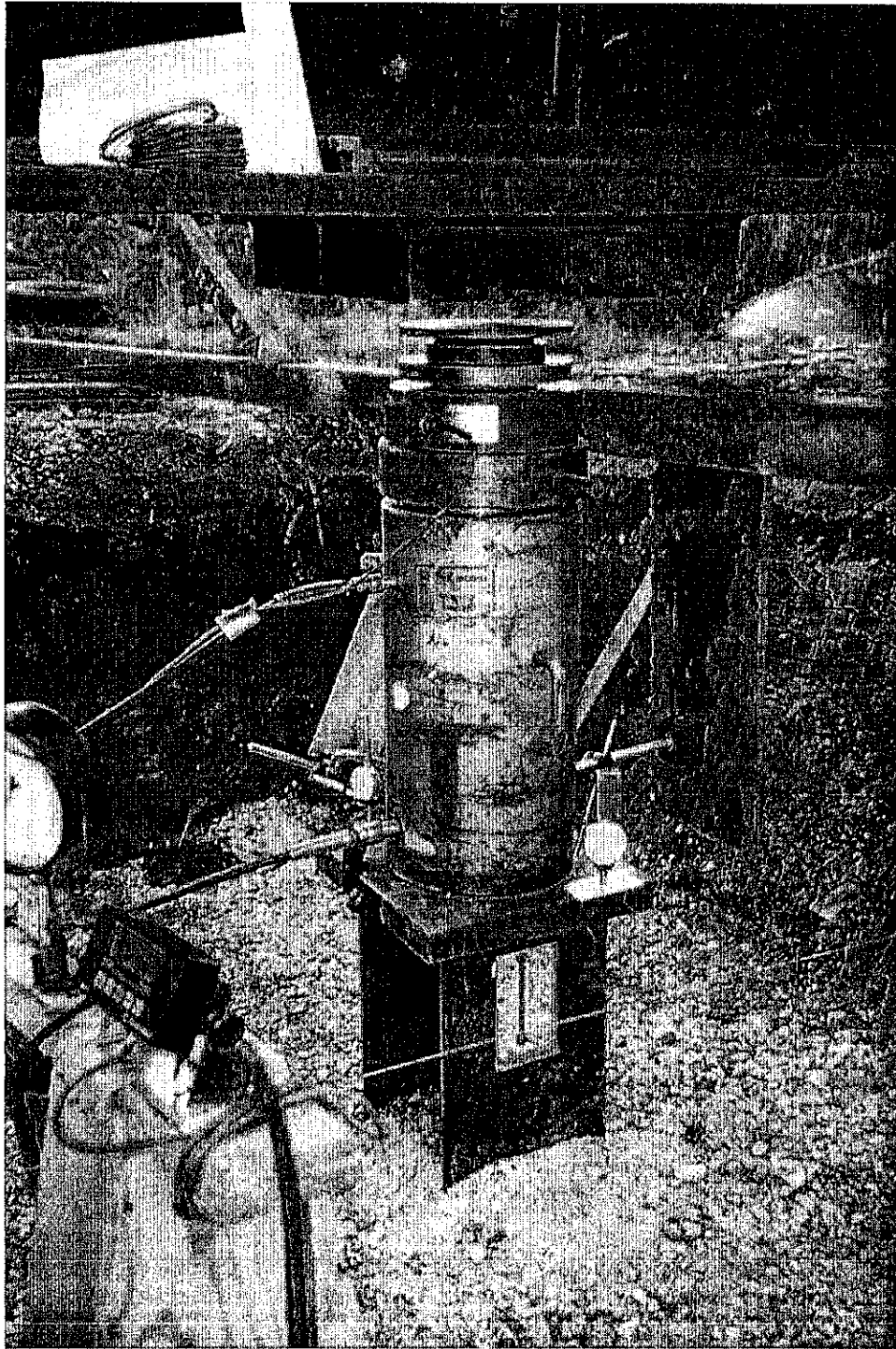


Figure A.16 Photograph of hydraulic jack and load cell

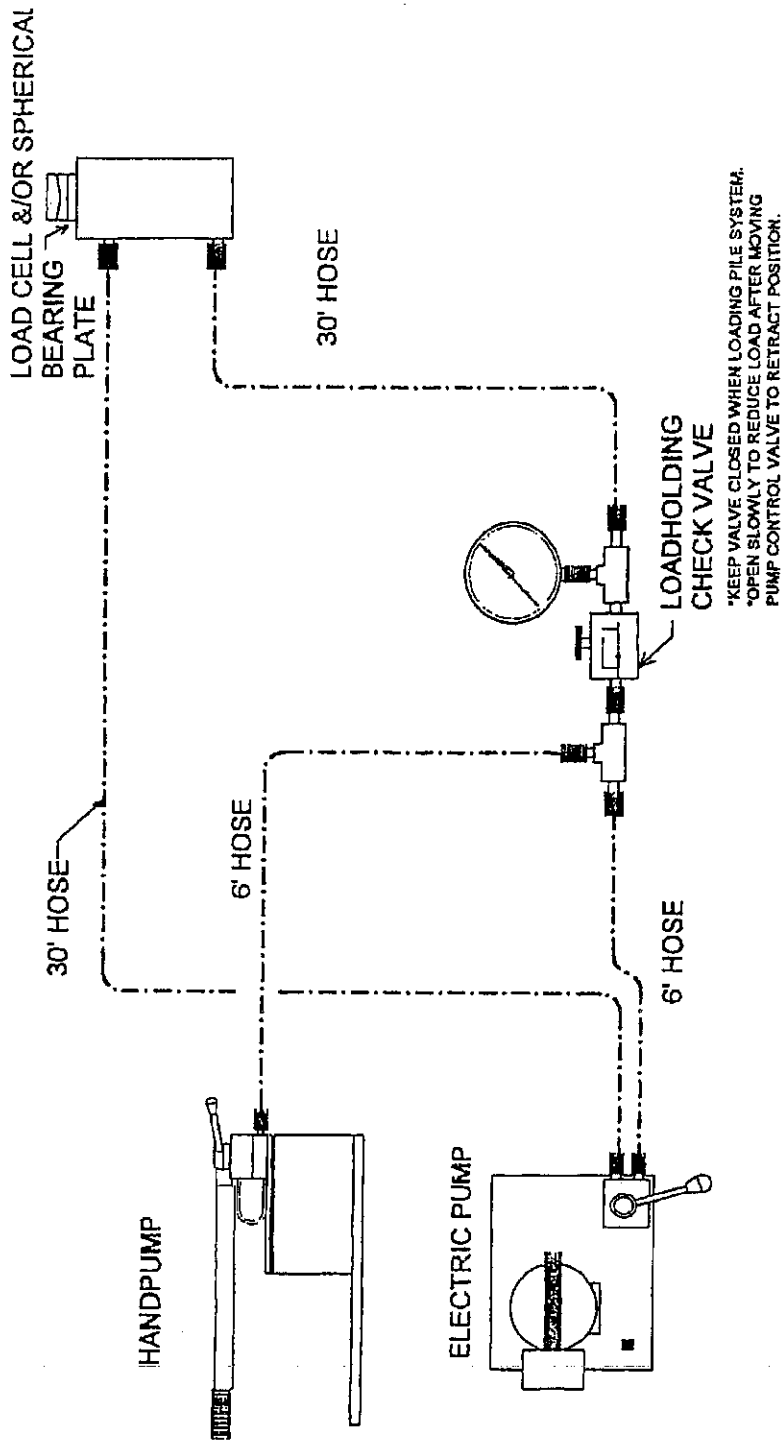


Figure A.17 Schematic view of hydraulic jack, electric pump, and hand pump for static load test

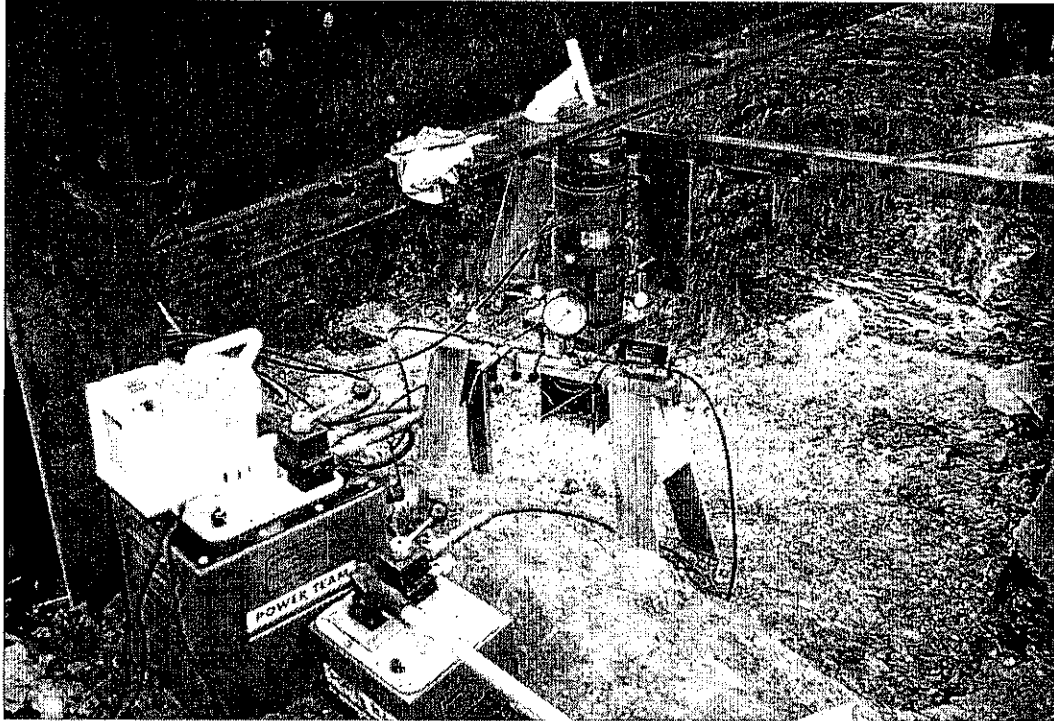


Figure A.18 Photograph of hydraulic jack, electric pump, and hand pump for static load test

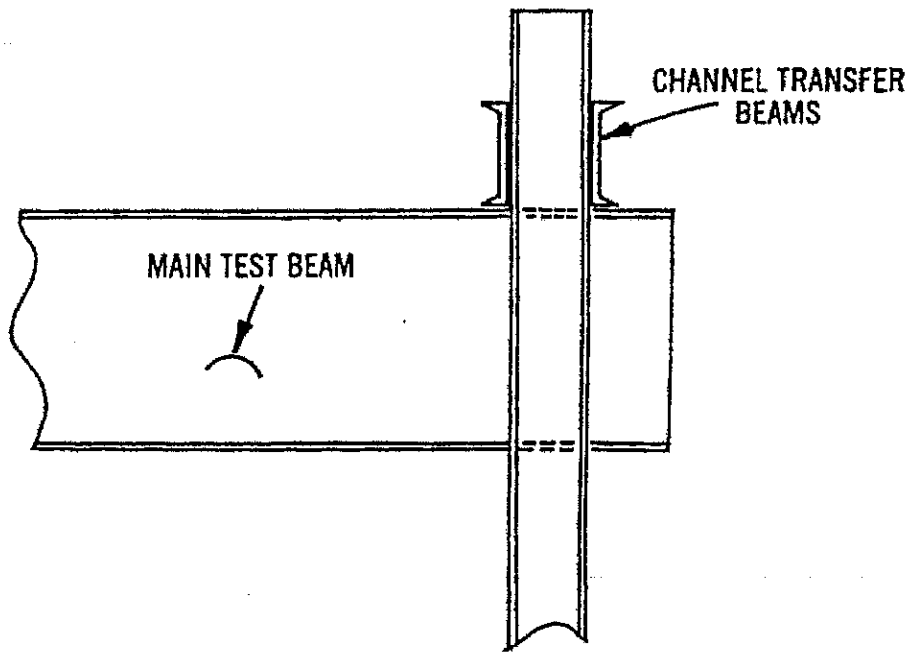
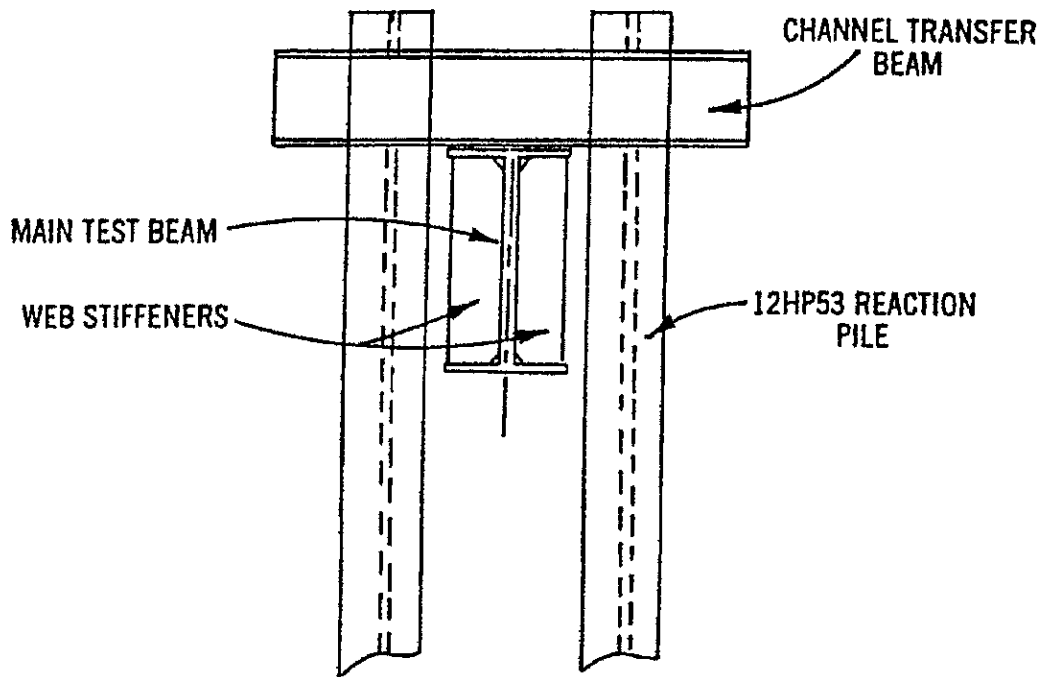


Figure A.19 Schematic view of reaction beam and two anchor piles

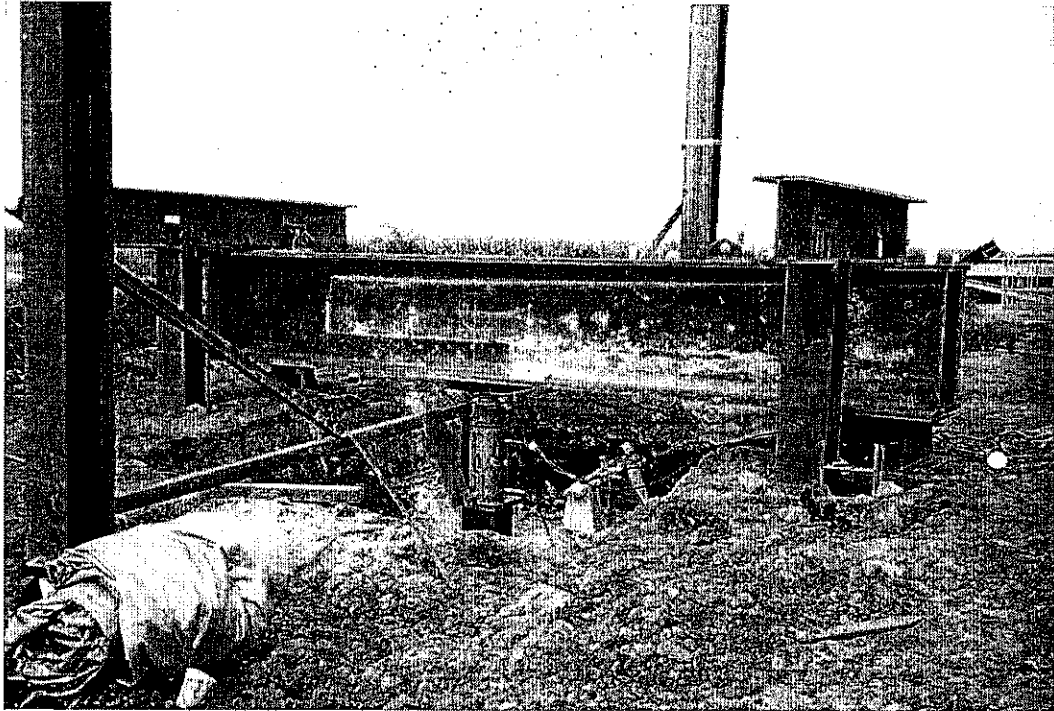


Figure A.20 Figure A.19 Photograph of reaction frame for load test. Two anchor piles are located on each end of the reaction frame. Test pile and hydraulic jack are in the center

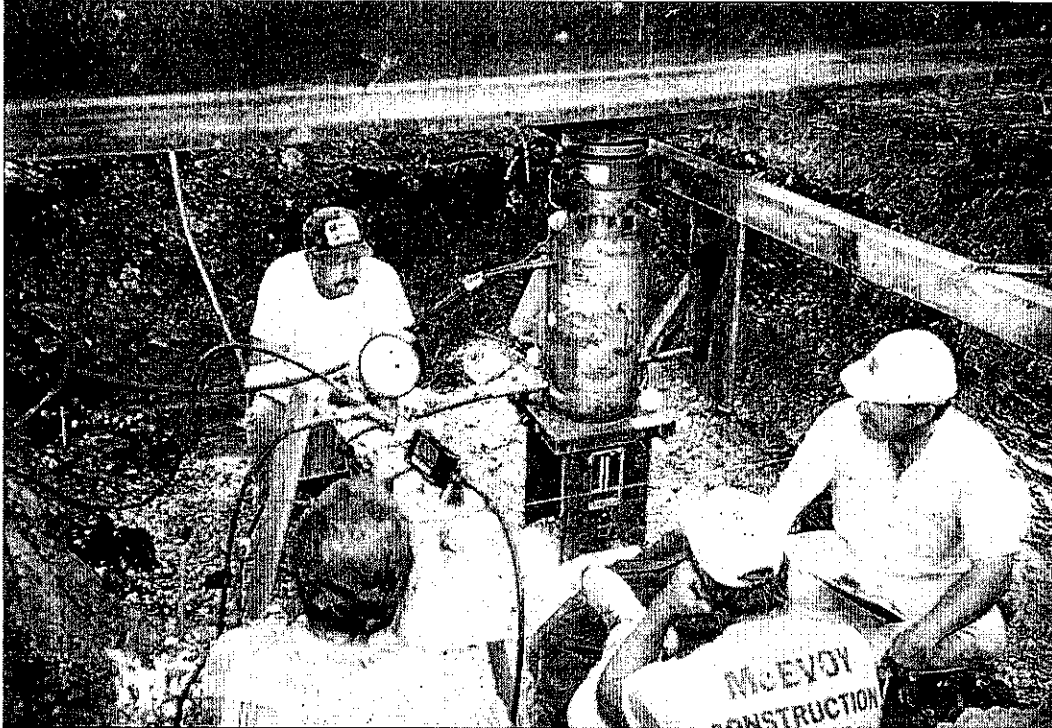


Figure A.21 Setup of dial gages and wireline, mirror, and scale system for measuring displacement during load test

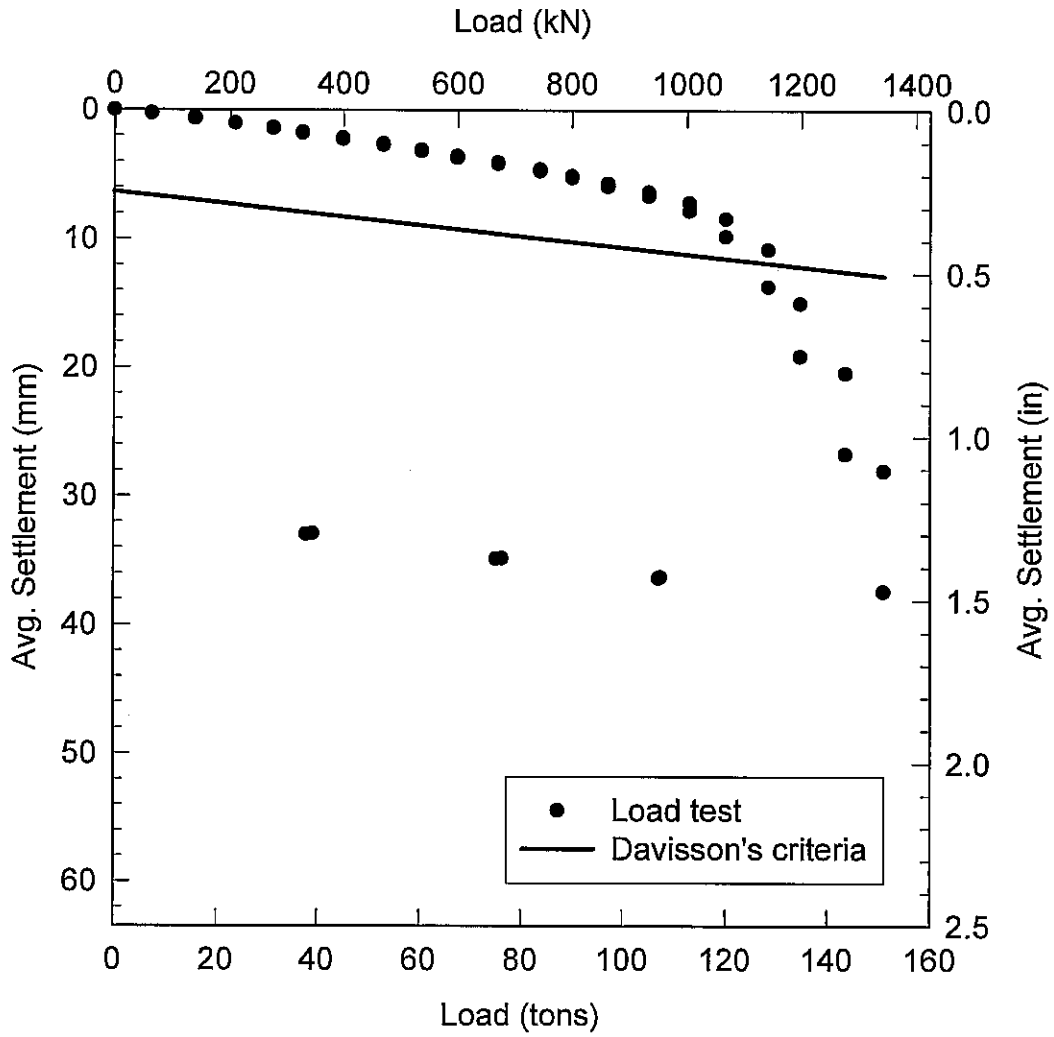


Figure A.22 Load-displacement relationship for the first static load test (SLT-1)

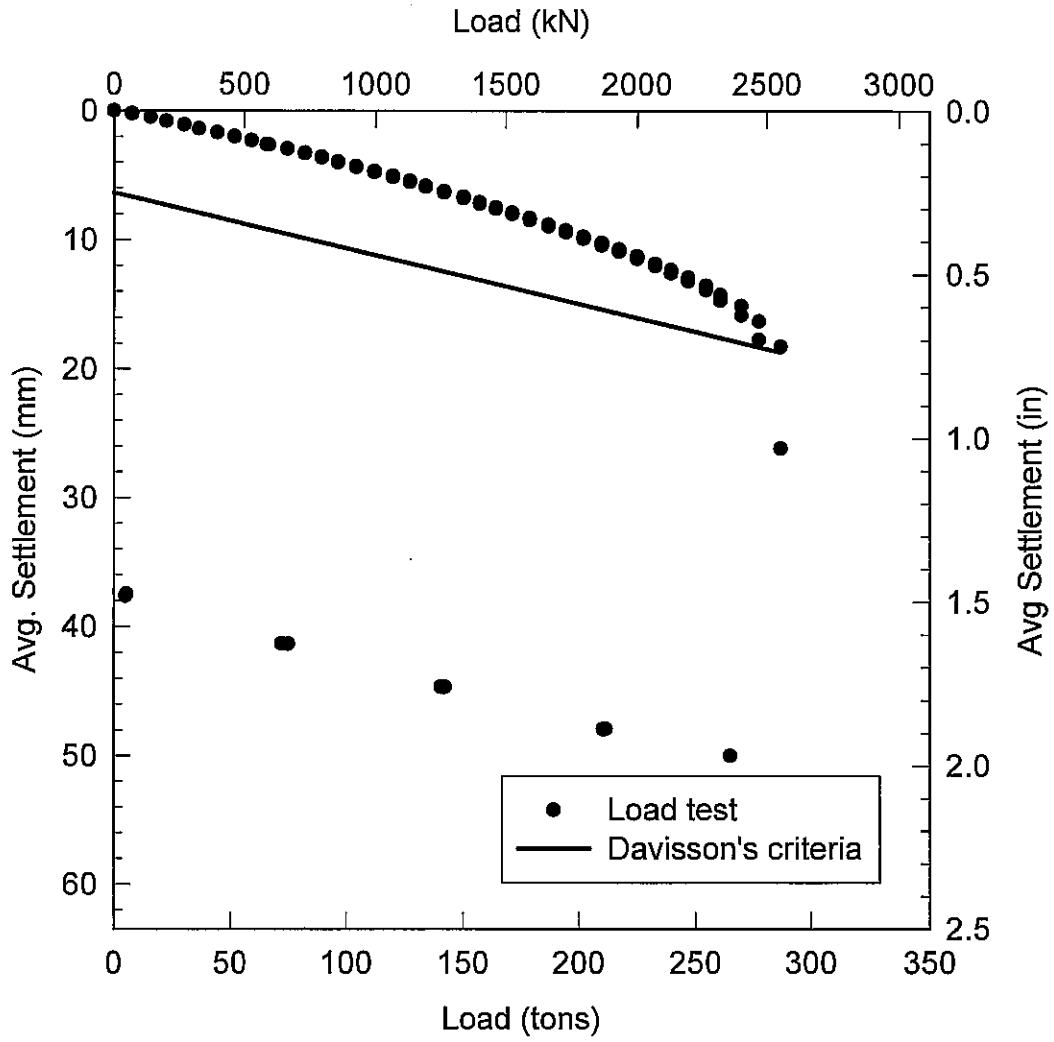


Figure A.23 Load-displacement relationship for the second static load test (SLT-2)

Ultimate Capacity vs Blowcount SLTP-1, EOD

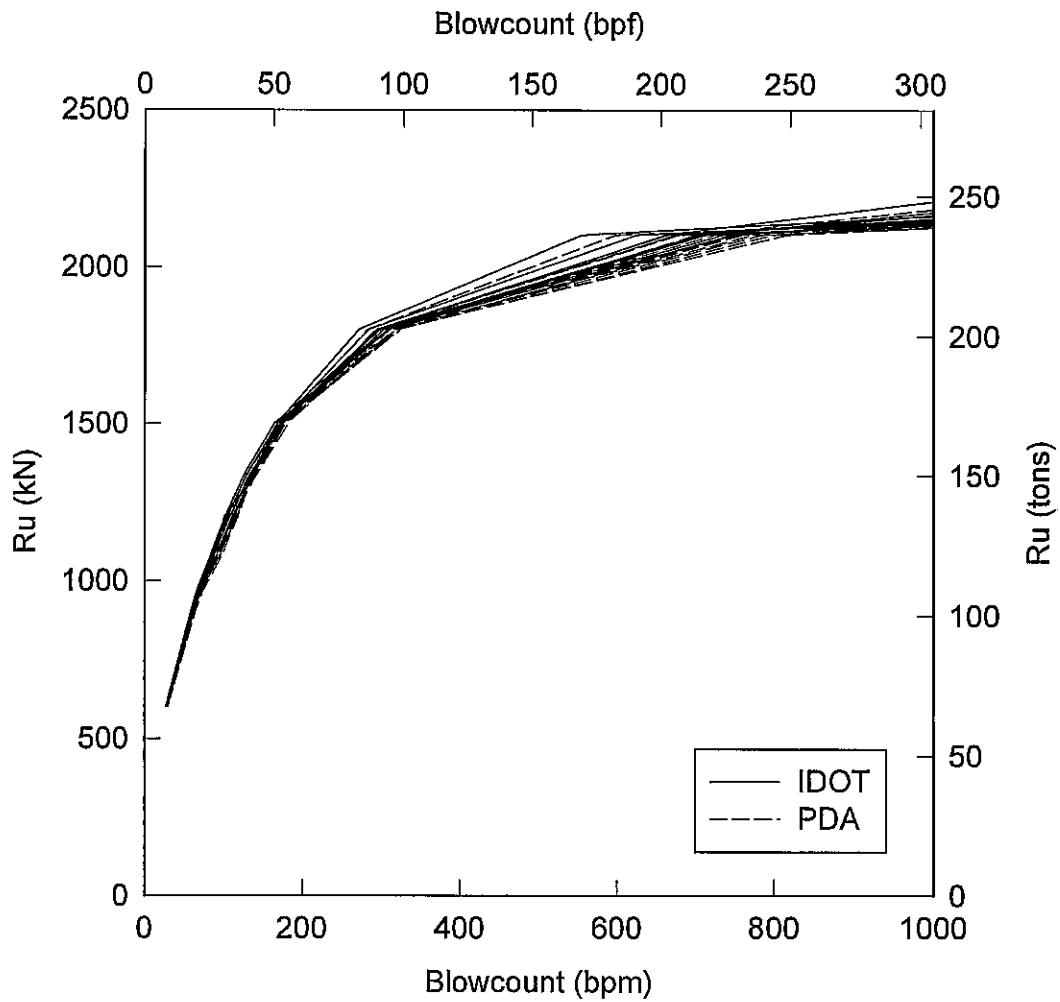


Figure A.24 Relationship between pile capacity and driving resistance based on penetration resistance at End-of-Driving (EOD) for comparison with first load test on pile SLT

Ultimate Capacity vs Blowcount SLTP-1, BOR

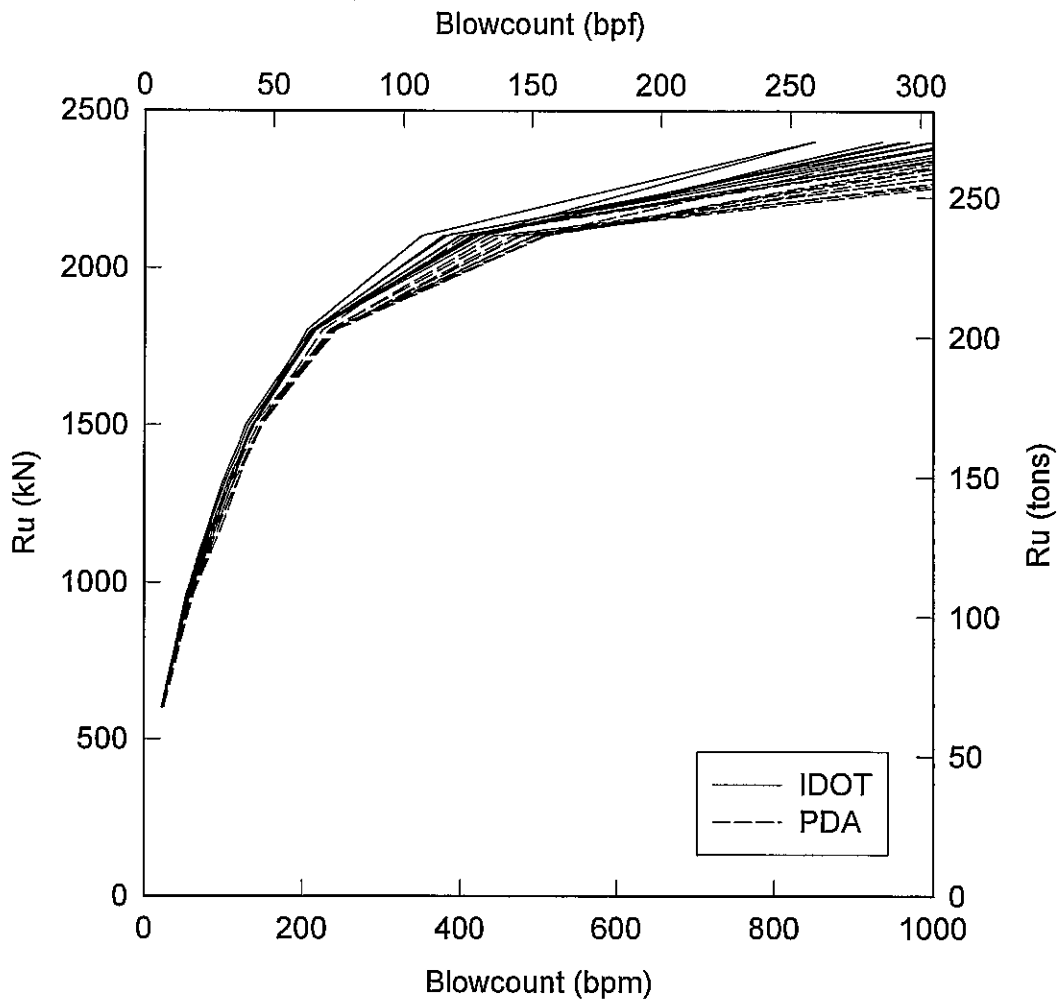


Figure A.25 Relationship between pile capacity and driving resistance based on penetration resistance at Beginning-of-Restrike (BOR) for comparison with first load test on pile SLT

Ultimate Capacity vs Blowcount SLTP-2, EOD

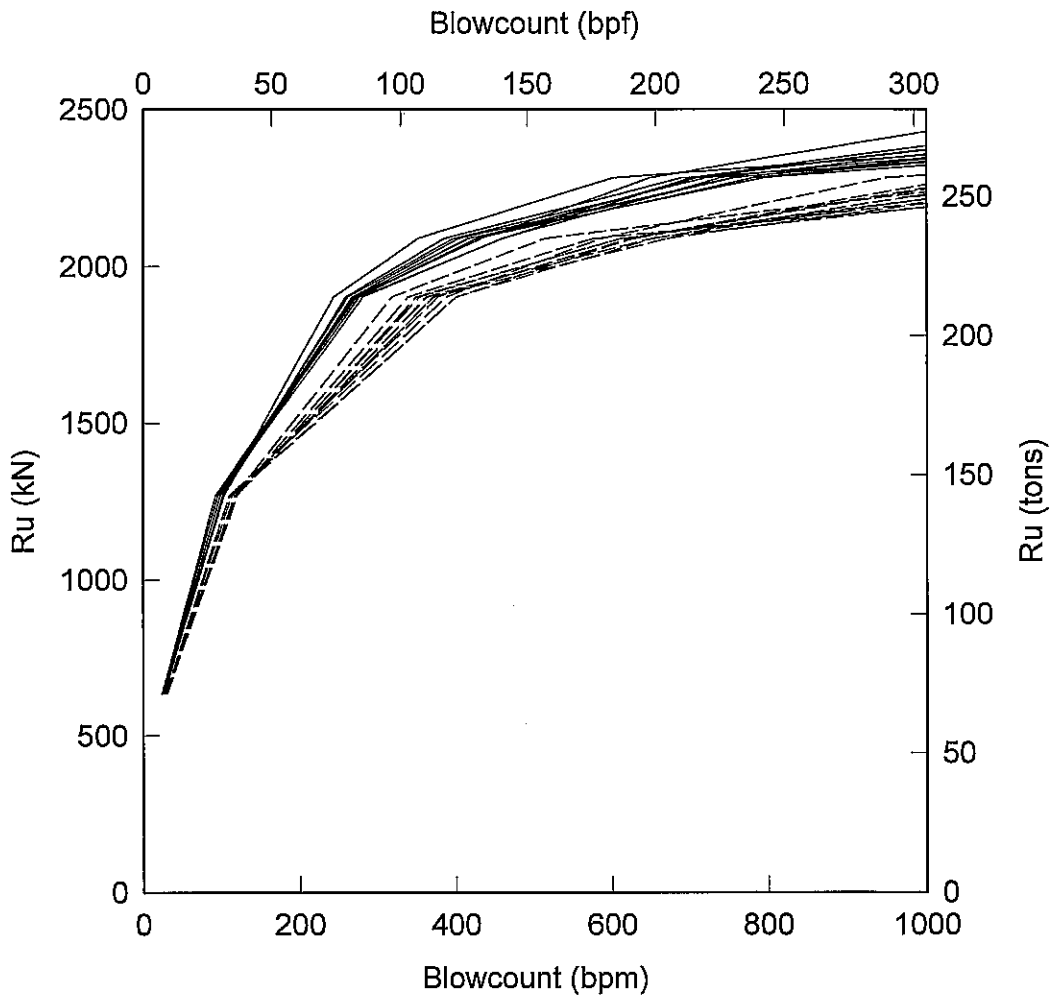


Figure A.26 Relationship between pile capacity and driving resistance based on penetration resistance at End-of-Driving (EOD) for comparison with second load test on pile SLT

Ultimate Capacity vs Blowcount SLTP-2, BOR

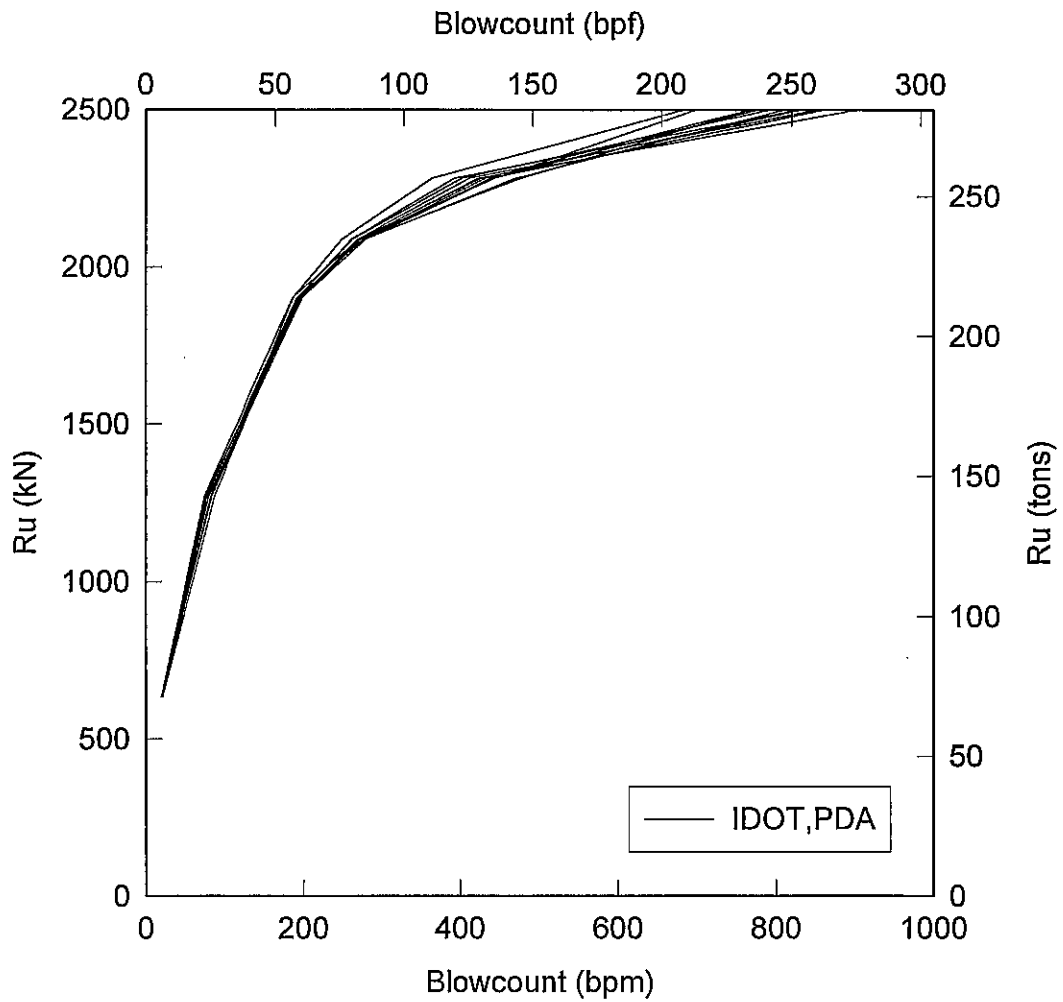


Figure A.27 Relationship between pile capacity and driving resistance based on penetration resistance at Beginning-of-Restrike (BOR) for comparison with second load test on pile SLT

Appendix B – Measured Time Effects for Axial Capacity of Driven Piling

Appendix B

MEASURED TIME EFFECTS FOR AXIAL CAPACITY OF DRIVEN PILING

INTRODUCTION

Pile capacities have been reported to both increase and decrease with time. The fact that the axial capacity of a pile in clay may change with time has been documented for nearly a century. As early as 1900, Wendel (1) conducted load tests on driven timber piles in clay and reported the axial capacity continued to increase for 2-3 weeks after driving. Other investigations have observed similar increases in pile capacity with time. Accordingly, Bjerrum, et al. (2) suggest conducting pile load tests about 1 month after driving.

The effects of time on pile capacity are believed affected by the type of soil into which the pile is being driven. An increase of pile capacity with time is known as setup while a decrease in capacity is referred to as relaxation. Piles driven into clay and sand generally experience setup. Percentage-wise, piles driven into soft clays tend to experience greater setup than piles driven into stiff clays. Piles driven into loose sands and silts generally experience a smaller magnitude of setup than for soft clays. Piles driven into saturated dense sands and silts or into shales may experience relaxation.

The results of a study to quantify effects of time on pile capacity are presented herein. This paper will present some background information for explaining time effects on pile capacity; however, the main focus is to present a database developed from various pile tests reported in the literature and present some observations based on the pile test data. Piles in primarily sand, primarily clay, and mixed soil profiles are shown to experience setup.

LITERATURE REVIEW

A brief review is presented to survey the current state of knowledge for time effects. It is commonly believed the increase in pile capacity with time is primarily a result of consolidation (or dissipation of excess porewater pressure). However, there is additional evidence that time dependent increase in

load continues after excess porewater pressure has dissipated. This additional increase in capacity is termed "aging."

The mechanisms contributing to the time dependent increase in pile capacity is presented in two parts: increase in capacity due to excess pore pressure dissipation, and increase in capacity due to soil aging. While these two mechanisms contribute to pile capacity and its change with time, it is difficult to quantify the contribution from each component.

Dissipation of Excess Pore Pressure

As a pile is driven, the soil adjacent to the pile is displaced outward and subjected to large strains (remolded). If the soil is saturated and positive excess pore pressures result, strength of the surrounding soil increases as pore pressures dissipate. The increase in pile capacity with time is called setup. If negative excess pore pressures occur due to driving, dissipation leads to a decrease in strength and the surrounding soil decreases in strength. The decrease in pile capacity with time is called relaxation.

Clays

When piles are driven into saturated soft-to-medium clays, the soil adjacent to the pile is remolded and pore pressure in the surrounding soil increases. The effect is to reduce temporarily the effective stress and strength of the clay. As these excess pore pressures dissipate, the surrounding clay increases in strength and significant gains in pile capacity can result (Fig. B.1).

After driving a pile, excess pore pressures in the soil surrounding the pile begin to dissipate. As pore pressures dissipate, the effective stress increases and the surrounding soil consolidates and gains strength. The concept of, and experimental evidence for, pore pressure dissipation as a mechanism to explain increase in pile capacity with time was proposed by Seed and Reese (3) and later by Bjerrum (2). Several authors have developed equations for estimating excess pore water pressures and their dissipation to explain the gain in pile capacity with time. Soderberg (4) proposed that dissipation of excess pore pressures can be predicted using the theory of radial consolidation. Soderberg suggested the increase in strength with time be related to the non-dimensional time factor T_h by

$$T_h = \frac{4c_h t}{B^2} \quad (\text{B.1})$$

where c_h is the coefficient of horizontal consolidation, t is time since the end of driving, and B is the pile width. Drainage of excess pore pressures occurs radially. Results of several load tests seem to confirm the trend predicted by Eqn. 1. The theory can be used to explain field observations that large diameter piles take longer to setup than smaller diameter piles and that setup occurs more quickly in more permeable soils.

Fellenius (5) and Eide et al. (6) use dissipation of excess pore pressures to explain field observations of soil adhering to the pile surface. When concrete and timber piles are driven into clays, excess pore pressures can dissipate into the pile causing excess pore water pressure in the soil adjacent to the pile surface to dissipate faster than soil a small distance away from the pile. As a result, the soil near the pile surface consolidates and gains strength more rapidly than the clay a small distance from the pile. When subjected to a load that causes failure, slippage will occur at some distance away from the pile wall rather than at the pile-soil interface. Greater soil resistance occurs along the length of the pile as the failure surface is forced outward. Eide suggests this mechanism (that results in a time dependent increase in pile capacity) will occur when the liquidity index is around 0.5-1.0).

Peck (7) presents three cases where setup occurred in soft and medium clays (soils with unconfined compressive strengths less than or equal to 100 kPa). The data show a general trend that piles driven into weaker clays experience a greater percentage of increase in capacity with time.

Sands

Yang (8, 9) states that relaxation is possible in dilative (dense to very dense) saturated fine sands. High resistance during driving may occur due to negative pore water pressures generated during driving, which temporarily increase the effective stress, and increase soil strength in the vicinity of the pile. After driving, excess pore pressures dissipate, and the effective stress and soil strength decrease, resulting in a reduction of pile capacity.

Skov and Denver (10) propose that setup in contractive fine sands can occur because positive excess pore pressures are generated during driving. After driving, dissipation of excess pore pressures result in stronger soil and greater pile capacity. Zai (11) also reports setup observed in sand.

Aging

Aging refers to a time dependent change in soil properties at a constant effective stress. The increase in pile capacity due to aging may be important in the economy for new structures, but aging effects may be more significant for rehabilitated or new structures using existing piling from a previous structure. Schmertmann (12) attributes aging to several mechanisms: thixotropy, secondary compression, particle interference, and clay dispersion. Schmertmann also identifies mechanisms for aging are active for both fine-grained and coarse-grained soils. Regardless of which specific mechanism(s) contribute to aging, the effect is to increase soil strength and modulus. Karlsrud and Haugen (13) conducted axial tension tests on over 20 piles in over-consolidated clay. Pore pressure instrumentation indicated dissipation of excess pore pressures 6 days after driving; however, pile capacities continued to increase another 22 percent over the next 30 days (Fig. B.2).

York (14) proposes that aging occurs in sand and can result in a measurable increase in axial pile capacity. Tavenas and Audy (15) state that setup continued in sand after excess water pressures have dissipated. They attribute the continued setup to time dependent changes in the sand structure around the pile. Chow et al. (16) also report on the increase in pile capacity with time for piles driven into sand. They attribute the increase in pile capacity to a time-dependent increase in effective stress along the pile shaft.

Empirical Relationships

Empirical relationships have been offered for quantifying setup. Skov and Denver (10) present an equation for setup based on a logarithmic increase of pile capacity with time. Svinkin (17) develops a formula for setup in sands based on load test data. They propose a semi-logarithmic empirical relationship to describe the increase in pile capacity with time after driving as

$$\frac{Q_t}{Q_0} = 1 + A \log \frac{t}{t_0} \quad (\text{B.2})$$

where Q_t is the axial capacity at time t after driving, Q_0 is the axial capacity of the pile at time t_0 , A is a constant depending on soil type, and t_0 is an empirical value measured in days. Table B.1 identifies recommended values for A and t_0 for different soil types.

Guang-Yu (18) presents an equation for capacity of piles driven into soft soils. The estimates are for capacity on the 14th day after driving and are based on the sensitivity of the fine-grained soil. Guang-Yu suggests that sands and gravels experience no increase in capacity after driving. Huang (19) presents a formula predicting the rate at which pile capacity is developed with time in the soft ground soil of Shanghai. Their formulas are presented in Table B.1.

Other Observations

York (14) proposes a mechanism for relaxation that may occur when driving a pile group into saturated sand. The effect of pile driving densifies the surrounding sand. Subsequent piles driven into dense saturated sand can dilate the densified and saturated sand, resulting in conditions associated with potential relaxation.

Parsons (20) reported relaxation of driven piles in the New York area. Pile penetration resistance dropped from 200 blows per quarter meter (20 blows per inch) at end of driving (EOD) to 40 blows per quarter meter (4 bpi) at beginning of restrike (BOR). Parsons concluded the relaxation was not caused by pore pressures but provided no alternative explanation for the observations.

Thompson and Thompson (21) propose relaxation can occur in highly jointed shale and limestone. Locked-in stresses are partially relieved due to soil/rock displacement and shear during driving. Over time, the effective stresses reduce in the shear zones displaced due to pile driving, reducing soil strength and causing relaxation in the pile. They also suggest that many false observations of relaxation may be explained when rated energy (instead of the product of weight of ram and measured stroke) is used with single-acting diesel hammers for calculating pile capacity. For example, a single acting diesel hammer tends to be more efficient on restriking than at the end of initial driving. A more efficient hammer would yield fewer blows per foot and result in a lower estimate of pile capacity than a less efficient hammer.

SUMMARY RELATIONSHIPS FOR DATABASE

A database containing both static and dynamic load tests was collected and sorted into three groups according to the primary subsurface profile: clays, sands, and mixed soil (Table B.2). The Table contains information about the test pile, soil conditions, and reference from which information was

obtained. Except where noted, each pile number refers to either a single pile or to similar piles at the same site that were tested for developing time-capacity relationships.

A graph of axial pile capacity versus time is shown for piles driven into clay (Fig. B.3). Estimates for pile capacity are based on static load tests, or reported from pile driving resistance. The axial pile capacity for piles driven in clay shows an increase in capacity with time. In some cases, the axial capacity increases by a factor of up to 6. The largest increase in axial capacity develops in the first 20 to 30 days after driving. This is probably increase in capacity due to dissipation of excess pore pressures. For times greater than 20 to 30 days, the capacity continues to increase (at a lesser rate) for about half the piles. The capacity appears to be constant with time for the other half of the piles.

Some Specific Observations

Some important facts regarding the data from these collections are presented in this section.

Pile #73. (15) The data include a combination of concrete piles and H-piles. These results are the only tests in which time dependent variations in load capacity were determined by performing static load tests (rather than dynamic load tests). The first static load test was conducted 12 hours after driving. The data for identifying the time dependent change in pile capacity was reported as a ratio of capacity at a given time to the capacity of the pile at 12 hours.

Pile #63. Pile 63 is actually 6 piles of the same area and depth.

Pile #s 12, 13, 14, 62, and 73. Low displacement piles were known to be used for piles 12, 13, and 14, 62, and 73. They are shown on the plots with dotted symbols.

Yang (8, 9) and Parsons (20) reported relaxation for piles in sand but did not provide actual load capacities. Parsons reported a reduction of blow count for the piles from around 20 blows/in to 4 blows/in on the second redrive. Yang reported a reduction in blow count ranging from 10 percent to over 50 percent.

Summary Relationships for Piles in each Soil Type

In an effort to look at the increase in capacity with time, axial capacity for the pile was normalized. Capacity at any time, t , was divided by a reference capacity (Q_t/Q_{ref}) and plotted versus time (Figs. B.4, B.5, and B.6) for piles in clay, sand, and mixed soil, respectively. The reference capacity was the

capacity from the first load test or load estimate carried out on the pile. Pile numbers on the plots correspond to the database pile numbers. If pile capacity was estimated at the end of driving by monitoring dynamic resistance (corresponding to end of driving), the time was taken to be .01 days.

Clay

The time-dependent increase of axial capacity for piles in clay varies considerably. Values of Q_t/Q_{ref} range from 1 to 6 times its original capacity. Low displacement piles exhibited setup within the range of all the other piles with similar Q_{mf} .

Effects of time on pile capacity level out around 100 days after driving (Fig. B.4). While restriking piles, or load testing piles, 100 days after driving is generally unfeasible in practice, these graphs provide evidence that piles continue to increase their load carrying capability with time.

Sand

Axial pile capacities for piles driven in sand show an increase in capacity with time (Fig. B.5). The increase in axial capacity is shown in several cases to increase by a factor of approximately two. This increase is smaller than exhibited by the piles in clay; however, the increase appears to continue for some piles tested up to 500 days after driving.

All cases in sand had at least 30 percent setup after about 10 days and some piles experienced as much as 100 percent. As mentioned earlier, no cases of relaxation in sand were found in which the axial capacities were reported.

Known low displacement piles had set-up factors in the same range of all piles, although the low displacement piles were on the lower boundary of set-up factors for piles in sand. Since only known low displacement piles were distinguished from the database, it is possible that other piles in the lower bound were also low displacement piles.

An empirical fit was established for setup in sand using a relationship presented by Mesri et al., (22) for the post-densification of sand. Their relationship was used to estimate the increase in cone resistance with time for clean sands that had been densified by blasting. Mesri et al, believe that post-densification of clean sands can increase the frictional resistance of the sand particles, which would increase cone penetration resistance over time. The strength increase would occur due to two

processes: during primary consolidation that occurs for a short time after blasting, and during secondary compression at a constant effective stress.

Relationships used by Mesri et al, were adapted to model the increase in pile capacity with time by replacing the increase in cone resistance with time to an increase in pile capacity with time. Using a log-log scale, the following equation is presented to give an empirical relationship for set-up in sand:

$$\frac{Q_t}{Q_{EOD}} = 1.1 \cdot t^\alpha \quad (B.3)$$

where Q_t is the pile capacity at time t (days), Q_{EOD} is the pile capacity at the end of driving, and α is the exponential coefficient. The following values of α were determined:

Lower bound = 0.05

Upper bound = 0.18

Average = 0.13

A plot of the data and the resulting empirical relationships are shown in Fig. B.7. The increase in capacity is believed to be a result of aging, but more data are needed to quantify the range of α . The proposed relationship should be considered tentative, and Eqn. 3 should be applied only for the first 100 days after driving. Using Eqn. B.4 (Table B.1) and the ranges of α , estimates of capacity increase suggest a lower bound increase in capacity of about 40 percent an upperbound increase of 200 percent, and an average increase of about 140 percent. Finally, aging may increase capacity with time, even in cases where relaxation has occurred. York (14) proposes that setup can occur after relaxation and result in a net increase for the final strength of the sand.

Mixed Soil Profile

Capacities for piles driven in mixed soil profiles (sand and clay) also show an increase in capacity with time (Fig. B.6) with increases up to a factor of 5 times the capacity at end of driving. The data illustrate capacity versus time behavior between those observed for piles driven in clay profiles and pile driven into sand profiles.

For piles driven into mixed soil profiles, all except one experienced an increase in pile capacity with time. One pile exhibited a 5 percent drop in capacity. The time dependent increase in pile capacity for piles in mixed-soil profiles are similar to increases seen for piles driven in clay. The magnitude of increase in pile capacity in mixed soil profiles is most likely related to the proportion of clay soil in the profile. Greater magnitudes of setup are expected in mixed-soil profiles with large percentages of clay.

The effect of small versus large displacement piles was investigated. There was no clear evidence provided by the data distinguishing a difference in the time dependent increase of capacity for small displacement piles driven into mixed soil profiles versus large displacement piles.

DISCUSSION

Pore pressure dissipation undoubtedly contributes to time effects; however, it is not the only mechanism responsible for time effects. Parsons experienced relaxation in sands with no significant pore pressure changes. Tavenas & Audy (15), and York (14) experienced setup in sand with very high permeabilities that would have undoubtedly dissipated excess pore pressure quickly. Seed and Reese (3), and Karlsrud and Haugen (13) present data showing the pile still gaining capacity after excess pore pressures were completely dissipated. These observations would indicate that changes in pile capacity are not explained completely by the effects of pore pressure.

Findings in this paper on the time-dependent increase in pile capacity are in general agreement with more fundamental observations on the time-dependent strength of soils. Mitchell and Solymar (23), Schmertmann (12) and Mesri et al. (22) report that strength of a soil increases at a constant effective stress after it has been disturbed. Mesri (22) and Schmertmann (12) contend the increase in strength is due to mechanical effects, such as an increase in soil friction or a change in effective stress with time. Mitchell and Solymar attribute that strength gain is due to cementation at inter-particle contacts. Regardless of the mechanism responsible, it is generally observed that sand is sensitive to disturbance and that an increase in strength is likely to occur over time.

SUMMARY AND CONCLUSIONS

A study was conducted on the subject of time effects on pile capacity. The study consisted of analyzing the change in pile capacity over time from load test information published in the literature. The data were grouped according to soil profiles into which the piles were driven: sand, clay and mixed. In addition, special attention was directed toward low displacement piles to observe the influence of pile type on magnitude of setup.

Setup in clay and mixed profiles varied from 1 to over 6 times the axial capacity estimated immediately after driving. Piles driven in mixed soil profiles exhibited time effects over a range between those for sand and those for clay. The gain in axial pile capacity with time is explained only partially by the dissipation of excess pore pressures. Aging can also contribute to the increase in capacity with time. No major difference in the development of pile capacity with time was observed for high and low displacement piles driven into the mixed and clay soil profiles.

Results showed that piles driven into sand experience setup. Axial pile capacity was found to increase from 30 to over 100 percent of the pile capacity immediately after driving. The increase in capacity is believed to be due to aging since excess pore water pressure dissipates quickly in sand. A time versus capacity relationship (Eqn. 4) is presented based on reported load test results. Since the pile capacity in sand is shown to increase with time, it is recommended that static load tests be performed at least 10 days after driving to take advantage of the increase with time. Pile capacities will continue to increase beyond 10 days but at a slower rate. There was not enough load test data to identify any difference in time effects for low- versus high- displacement piles.

While relaxation has been discussed in the literature, only two cases were recorded that presented sufficient numerical data to include in the database. One case had a 5 percent strength loss and the other a 15 percent loss. The loss in strength is relatively small and the paucity of cases would suggest that relaxation is a relatively rare occurrence.

ACKNOWLEDGMENTS

The research described in this report was performed as a part of Illinois Transportation Research Center (ITRC) contract IDOT ITRC 1-5-38911. The ITRC is a public-private-university joint cooperative transportation research unit underwritten by the Illinois Department of Transportation

(IDOT). The support and assistance of the IDOT office and field personnel is gratefully acknowledged.

REFERENCES

1. Wendel, E. (1900). "On the Test Loading of Piles and its Application to Foundation Problems in Gothenburg," *Tekniska Samf Goteberg handl.*, No. 7, 3-62.
2. Bjerrum, L., Hansen, J., and Sevaldson, R. (1958). "Geotechnical Investigations For a Quay Structure in Horten," *NGI Publication No. 28*, 1-17.
3. Seed, H.B., Reese, L.C. (1955). "The Action of Soft Clays Along Friction Piles," *Proceedings, ASCE*, Vol. 81, Paper No. 842, 842-1 -842-28.
4. Soderberg, L.O. (1962). "Consolidation Theory Applied to Foundation Pile Time Effects," *Geotechnique*, Vol. 12, No. 3, 217-225.
5. Fellenius, B. (1955). "Results of Tests on Piles at Gothenburg Railway Station," *Geotechnical Department, Swedish State Railways, Bulletin No. 5*.
6. Eide, O., Hutchinson, J.N., and Landva, A. (1961). "Short and Long-Term Testing of a Friction Pile in Clay," *Proc. of the 5th ICSMFE, Paris*, 45-53.
7. Peck, R.B (1958). *A Study of the Comparative Behavior of Friction Piles*. Highway Research Board, Special Report 36, National Academy of Sciences-National Research Council, Washington, D.C.
8. Yang, N. (1956). "Redriving Characteristics of Piles," *J. of the Soil Mech. and Found. Div., ASCE*, Vol. 96, Paper 1026, 1026-1 -1026-19.
9. Yang, N. (1970). "Relaxation of Piles in Sand and Inorganic Silt," *J. of the Soil Mech. and Found. Div., ASCE*, Vol. 96, SM2, 395-409.
10. Skov, R., and Denver, H. (1988). "Time Dependence of Bearing Capacity of Piles," *Proceedings of the 3rd Intl. Conf. on the Appl. of Stress Wave Theory to Piles, Ottawa, Canada*, B.H. Fellenius, ed., 879-889.
11. Zai, J. (1988). "Pile Dynamic Testing Experiences in Shanghai," *Proceedings of the 3rd Intl. Conf. on the Appl. of Stress Wave Theory to Piles, Ottawa, Canada*, B.H. Fellenius, ed., 781-792.
12. Schmertmann, J.H. (1991). "The Mechanical Aging of Soils," *J. of Geotechnical Engrg., ASCE*, Vol. 117, No. 9, 1288-1330.
13. Karlsrud, K. and T. Haugen (1991). "Axial Static Capacity of Steel Model Piles in Overconsolidated Clay," *Bull. No. 163, Norwegian Geot. Institute, Oslo, Norway*, 3.

14. York, D.L., Brusey, W.G., Clemente, F.M., and Law, S.K. (1994). "Setup and Relaxation in Glacial Sand," *J of Geotech. Engrg., ASCE*, Vol. 120, No. 9, 1498-1513.
15. Tavenas, F., and Audy, R. (1972). "Limitations of the Driving Formulas for Predicting the Bearing Capacities of Piles in Sand," *Canadian Geotech. J.*, Vol. 9, No. 47, 47-62.
16. Chow, F.C., R.J. Jardine, J.F. Nauroy, and F. Brucey (1997), "Time related increase in shaft capacities of driven piles in sand," *Geotechnique*, Vol. 47, No. 2, 353-361.
17. Svinkin, M. (1996). "Discussion on Setup and Relaxation in Glacial Sand," *J. Geotech. Engrg., ASCE*, Vol. 122, April 1996, 319-321. Yao,
18. Guang-Yu, Z. (1988). "Wave Equation Applications for Piles in Soft Ground," *Proceedings of the 3rd Intl. Conf. on the Appl. of Stress Wave Theory to Piles*, Ottawa, Canada, B.H. Fellenius, ed., 831-836.
19. Huang, S. (1988). "Application of Dynamic Measurement on Long H-Pile Driven into Soft Ground in Shanghai," *Proceedings of the 3rd Intl. Conf. on the Appl. of Stress Wave Theory to Piles*, Ottawa, Canada, B.H. Fellenius, ed., 635-643.
20. Parsons, J.D. (1966). "Piling Difficulties in the New York Area," *J. of the Soil Mech. and Found. Div., ASCE*, Vol. 92, No. 1, 43-64.
21. Thompson, C.D., and Thompson, D.E. (1985). "Real and Apparent Relaxation of Driven Piles," *J. of Geotech. Engrg., ASCE*, Vol. 111, No. 2, 225-237.
22. Mesri, G., Feng, T.W., and Benak, J.M. (1990). "Post-densification Penetration Resistance of Clean Sands," *J. of Geotech. Engrg., ASCE*, Vol. 116, No. 7, 1095-1115.
23. Mitchell, J. K. and Z.V. Solymar (1984). "Time-Dependent Strength Gain in Freshly Deposited or Densified Sand," *J. of Geotech. Engrg., ASCE*, Vol. 110, No. 11, 1559-1576.
24. Seidel, J.P., Haustorfer, I.J., and Plesiotis, S. (1988). "Comparison of Dynamic and Static Testing for Piles Founded in Limestone," *Proceedings of the 3rd Intl. Conf. on the Appl. of Stress Wave Theory to Piles*, Ottawa, Canada, B.H. Fellenius, ed., 717-723.
25. Housel, W.S. (1950). "Discussion on Effect of Driving Piles into Soft Clay," *Transactions, ASCE*, Vol. 115, 339-346.
26. Fellenius, B.H., Riker, R.E., O'Brien, A.J., and Tracy, G.R. (1989). "Dynamic and Static Testing in Soil Exhibiting Set-up," *J. of Geotech. Engrg., ASCE*, Vol. 115, No. 7, 984-1001.
27. Wong, P. (1988). "The Use of Pile Driving Analyzer at a Hospital Complex in Malaysia," *Proceedings of the 3rd Intl. Conf. on the Appl. of Stress Wave Theory to Piles*, Ottawa, Canada, B.H. Fellenius, ed., 762-770.

28. Yao, H.L., Shih, C.S., Kao, T.C., and Wang, R.F.(1988). Experiences of Dynamic Pile Loading Tests in Taiwan, " Proceedings of the 3rd Intl. Conf. on the Appl. of Stress Wave Theory to Piles," Ottawa, Canada, B.H. Fellenius, ed., 805-812.
29. Hunt, S.W., and Tarvin, P. (1993). "Piles for Marquette University Math Building," Design and Performance of Deep Foundations: Piles and Piers in Soil and Soft Rock, Geotech. Spec. Publ. No. 36, ASCE, 91-108.
30. Finno, R. (1989). *Predicted and Observed Axial Behavior of Piles*, Geotechnical Special Publication No. 23, ASCE
31. Vesic, A.S. (1977), *Design of Pile Foundations*, NCHRP, TRB, NRC, National Academy of Sciences, Washington, Synthesis of Highway Practice No. 42.

Table B.1 – Empirical Formulae for Predicting Pile Capacities with Time

Author	Equation	Comments									
Huang (1988) (19)	$Q_t = Q_{EOD} + 0.236(1 + \log(t))(Q_{max} - Q_{EOD})$ (4)	Q_t = pile capacity at time t (days) Q_{EOD} = pile capacity at EOD Q_{max} = maximum pile capacity									
Svinkin (1996) (17)	$Q_t = 1.4Q_{EOD}t^{0.1}$ (5)	upper bound									
	$Q_t = 1.025Q_{EOD}t^{0.1}$ (6)	lower bound									
Guang-Yu (1988) (18)	$Q_{14} = (0.375S_t + 1)Q_{EOD}$ (7)	Q_{14} = pile capacity at 14 days S_t = sensitivity of soil									
Skov and Denver (1988) (10)	$Q_t = Q_{EOD}[A \log(t/t_0) + 1]$ (8)	where <table border="1" style="display: inline-table; vertical-align: middle;"> <tr> <td></td> <td>t_0</td> <td>A</td> </tr> <tr> <td>sand</td> <td>0.5</td> <td>0.2</td> </tr> <tr> <td>clay</td> <td>1.0</td> <td>0.6</td> </tr> </table>		t_0	A	sand	0.5	0.2	clay	1.0	0.6
	t_0	A									
sand	0.5	0.2									
clay	1.0	0.6									

Table B.2 Load Test Database used for Time-Dependent Capacity

File #	Paper ref #	Paper pile #	Pile type	Soil type		Density	Strength (kPa)
1-8	(14)	T5-10, J5-4, LT2-172	mono 3 gage	sand	fine/med	30-50%	
9	(14)	TP-11	mono 5 gage	sand	fine/med	30-50%	
10	(14)	L-18-2	timber	sand	fine/med	30-50%	
11	(14)	PP3	pipe	sand	fine/med	30-50%	
12	(14)	P6	mono 3g hollow	sand	fine/med	30-50%	
13	(14)	TP5	mono 5g hollow	sand	fine/med	30-50%	
14	(14)	TP8	mono 3g hollow	sand	fine/med	30-50%	
15	(14)	TP4	mono 5g concrete	sand	fine/med	30-50%	
16	(14)	TP10	mono 5g concrete	sand	fine/med	30-50%	
17	(14)	TP7	mono concrete	sand	fine/med	30-50%	
18	(14)	TP9	mono concrete	sand	fine/med	30-50%	
19-23	(17)	CT1, CT2, CT3, CT4, CT5	prestressed concrete	sand	silty	dense	
36	(24)	pile 2	sq prestress concrete	sand		dense	
50-54	(11)	1, 4, 5, 2, 3	prestress conc. pipe	sand	fine		
62	(10)	case II	steel pipe-	sand	various		
63	(10)	case 4	precast concrete	sand	silt		
73	(15)	H-/concr		sand		med dense	
70	(3)		close-end pipe	clay	silty		15-35
71	(25)	pile	open-end pipe	clay	soft		
72	(6)		wood	clay			
101	(5)	E	timber	clay			16
102	(5)	F	timber	clay			16
103	(5)	1	reinf concrete	clay			16
104	(5)	2	reinf concrete	clay			16
105	(5)	3	reinf concrete	clay			16
106	(5)	4	NP30 steel grdr	clay			16
107	(5)	26	timber. box	clay			16
108	(5)	27	timber, box	clay			16
109	(5)	28	reinf concrete	clay			16
110	(5)	29	reinf concrete	clay			16
112-	(5)	1, 2, 2	capped pie-pile	clay			100
115	(5)	4.5	monotube	clay			23
24	(26)	A-2	thin wall pipe/concrete	mixed			
25	(26)	A-4	thin wall pipe/concrete	mixed			
26	(26)	B-2	12 HP63	mixed			
27	(26)	B-4	12 HP63	mixed			
29-32	(26)	F-1, G-1, H-1, I-1,	heavy wall pipe/concrete	mixed			
33	(26)	B-3	12 HP63	mixed			
34	(26)	E-4	heavy wall pipe/concrete	mixed			
35	(19)	none	HP 360x40x176	mixed			
37-42	(27)	TP5, TP6, TP7, TP11,	circl prestr concrete	mixed	soft clay/dense sand		
55-57	(28)	PC1, PC2, PC3	prestress concrete	mixed			
58	(28)	SP1	steel pipe -closed end	mixed			
59-61	(10)	P9/1, P5, P6	precast concrete	mixed			
64-67	(29)	TP-1, TP-2, TP-3, TP-4	pipe-close end	mixed			
68	(30)	HP	HP 14x73	mixed			
69	(30)	Pipe	close-end pipe	mixed			

Type	Dia.	Length ft.	Soil type	Location	Source
□ } steel H ■ }	14	{191} {219}	silt	Tappan Zee, N.Y.	Yang 1956
△ steel pipe	6	22	soft clay	San Francisco	Seed & Reese, 1957
▲ steel pipe	12	60	soft clay	Michigan	House1 1958
⊙ precast ○ concrete	14	{40} {56}	soft boulder clay	Horten Quay	Bjerrum et al., 1958
● steel ○ pipe	24	{242} {316} {300}	soft to stiff clay	Eugene Island	McClelland, 1969 Stevens, 1974 ----- (theoretical prediction)

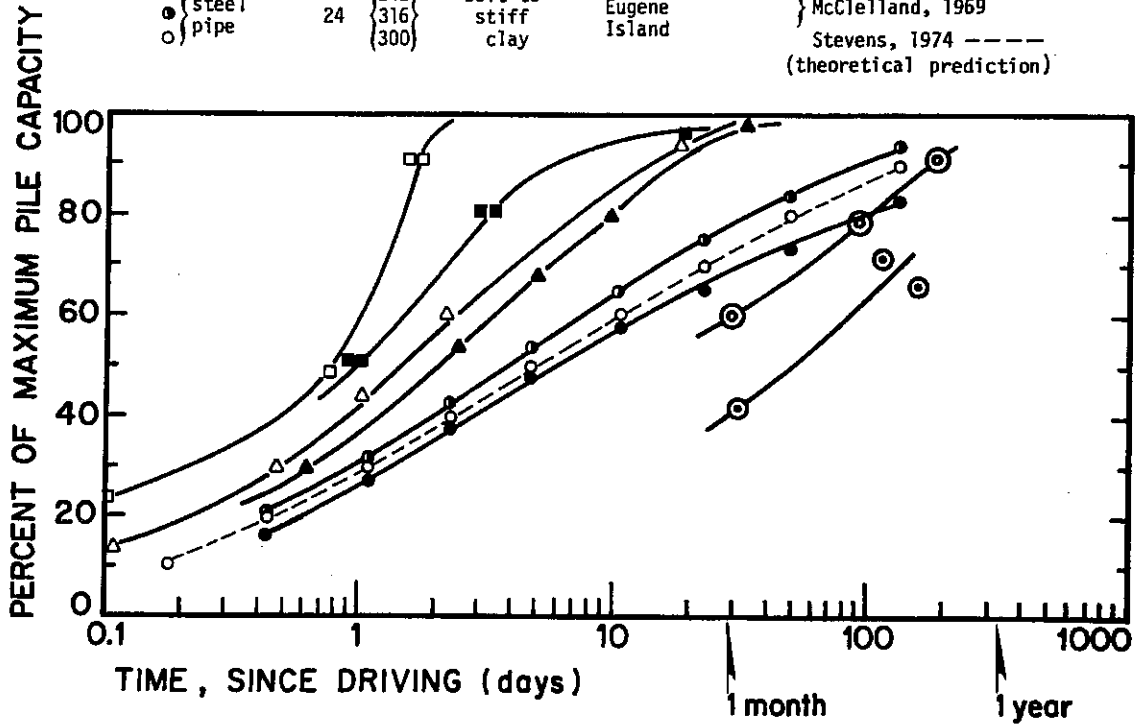


Figure B.1 Time dependent increase in pile capacity (31)

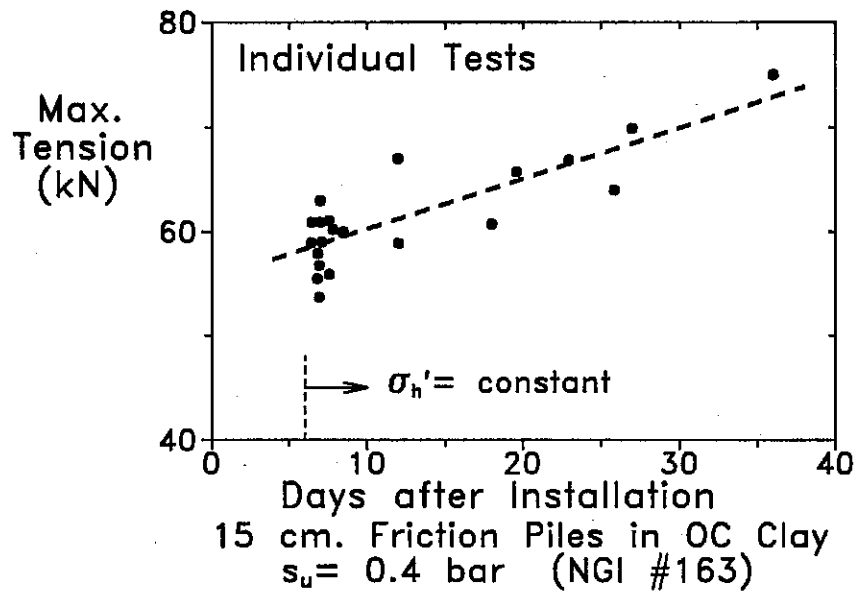


Figure B.2 Gain in capacity after dissipation of excess pore pressures

- | | | | | | |
|---------|----------|---------|----------|---------|----------|
| ---◇--- | Pile 70 | ---◆--- | Pile 104 | ---◇--- | Pile 110 |
| ---○--- | Pile 71 | ---●--- | Pile 105 | ---◇--- | Pile 111 |
| ---●--- | Pile 72 | ---○--- | Pile 106 | ---⊕--- | Pile 112 |
| ---■--- | Pile 101 | ---□--- | Pile 107 | ---⊕--- | Pile 113 |
| ---▲--- | Pile 102 | ---△--- | Pile 108 | ---△--- | Pile 114 |
| ---▼--- | Pile 103 | ---▽--- | Pile 109 | ---▽--- | Pile 115 |

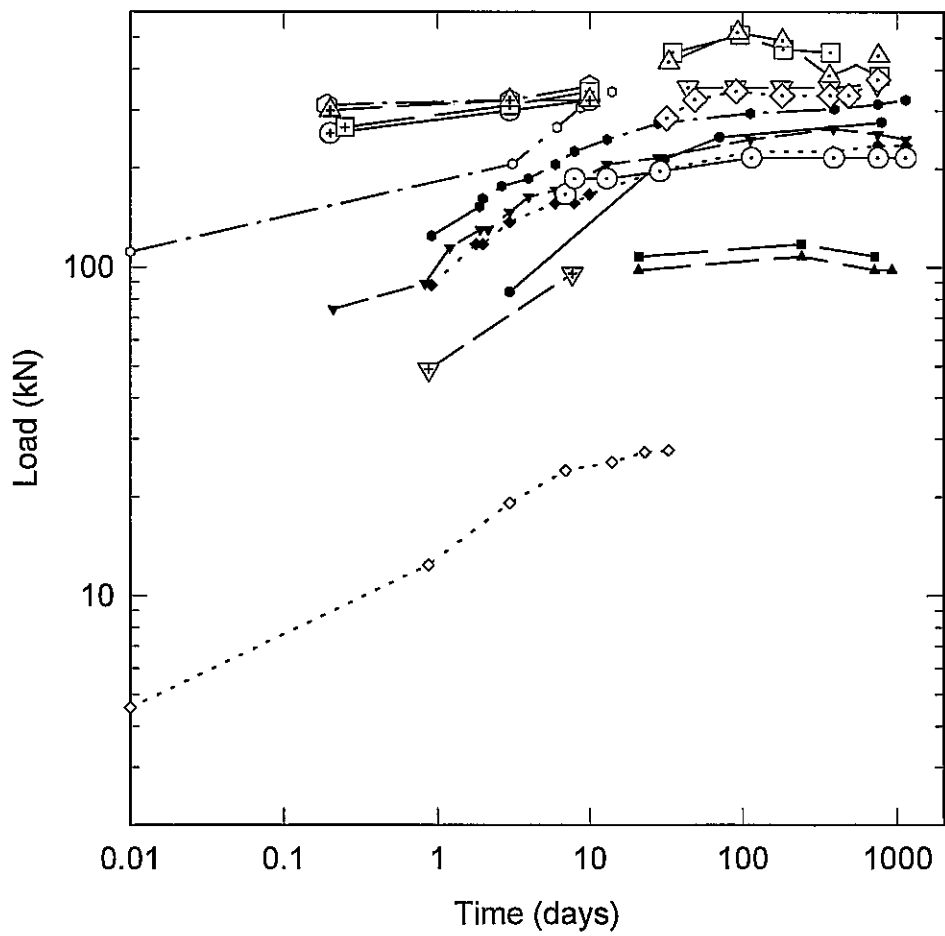


Figure B.3 Axial capacity for piles in clay

- | | | | | | |
|---------|----------|---------|----------|---------|----------|
| ---◇--- | Pile 70 | ---◆--- | Pile 104 | ---◇--- | Pile 110 |
| ---○--- | Pile 71 | ---●--- | Pile 105 | ---○--- | Pile 111 |
| ---●--- | Pile 72 | ---○--- | Pile 106 | ---⊕--- | Pile 112 |
| ---■--- | Pile 101 | ---□--- | Pile 107 | ---⊕--- | Pile 113 |
| ---▲--- | Pile 102 | ---△--- | Pile 108 | ---△--- | Pile 114 |
| ---▼--- | Pile 103 | ---▽--- | Pile 109 | ---▽--- | Pile 115 |

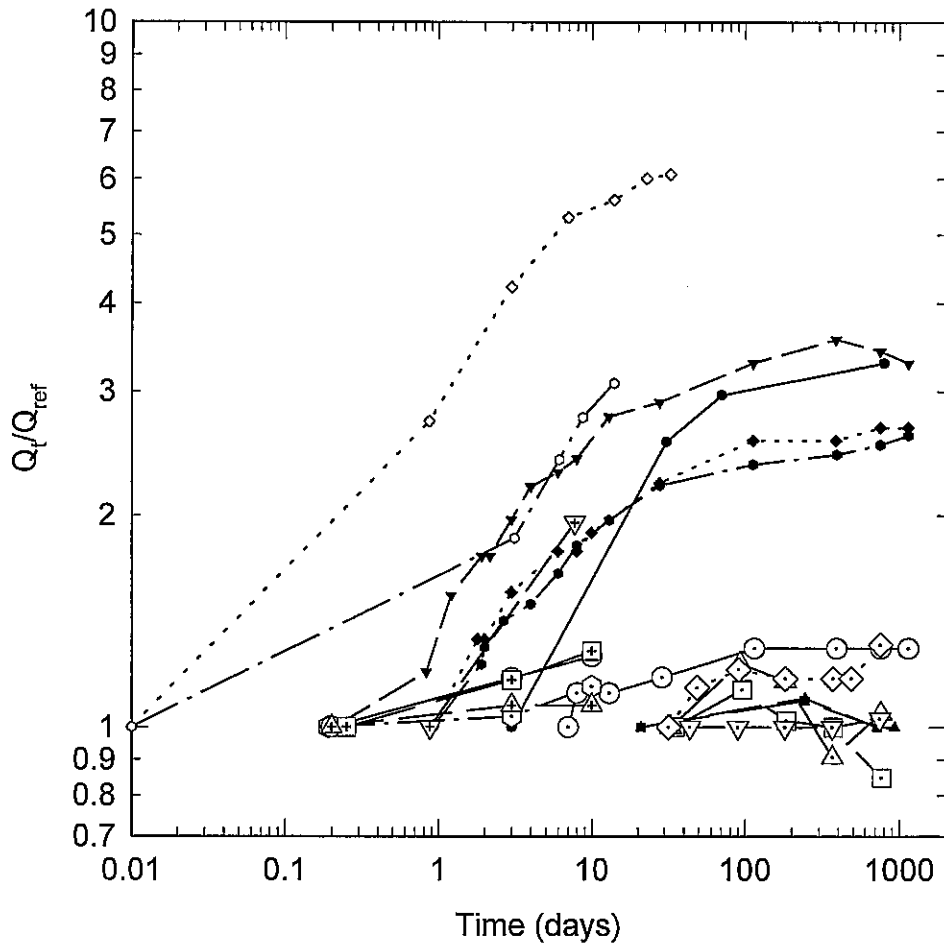


Figure B.4 Normalized capacity for piles in clay

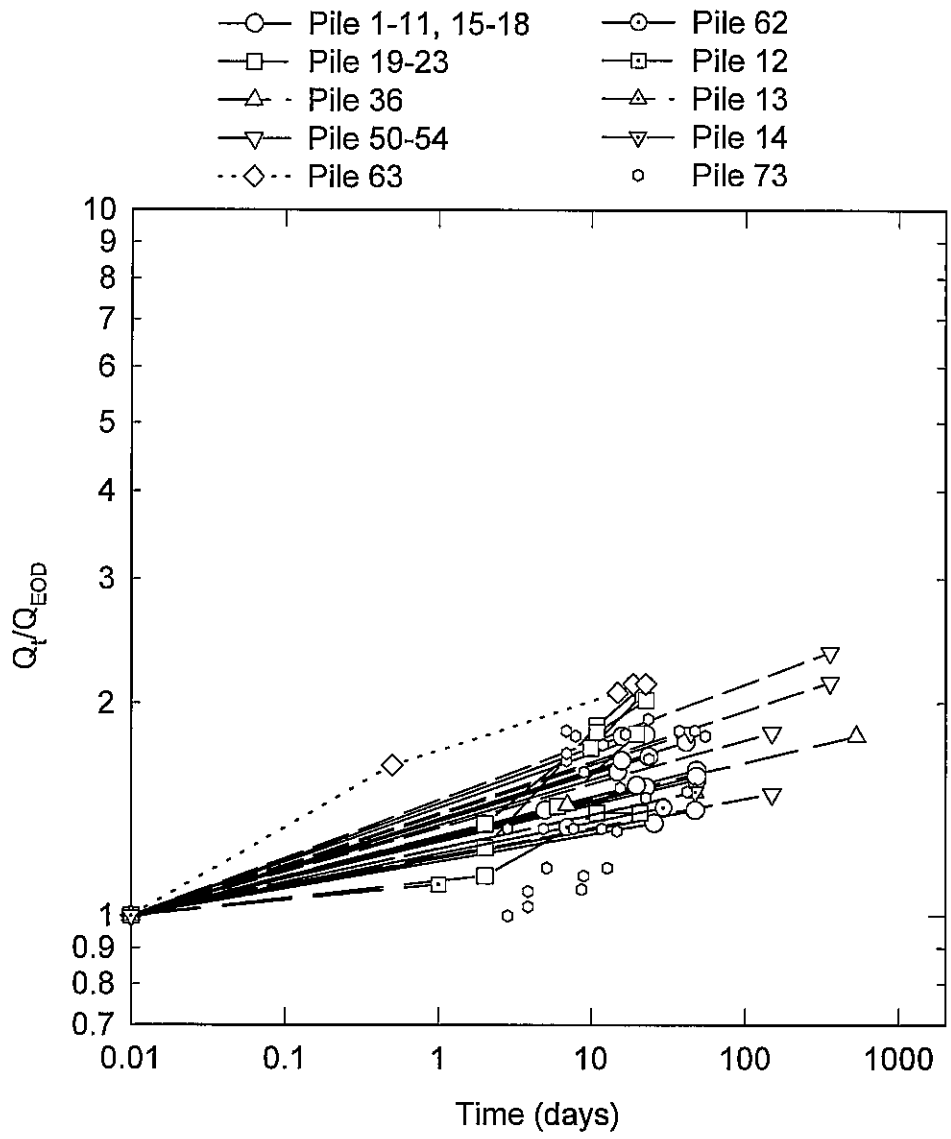


Figure B.5 Normalized capacity for piles in sand

- | | | |
|---------------|---------------|---------------|
| —○— Pile 24 | ··◆·· Pile 35 | —△— Pile 58 |
| —□— Pile 25 | —◆·· Pile 37 | —▽— Pile 59 |
| —△— Pile 26 | —○— Pile 38 | ··◇·· Pile 60 |
| —▽— Pile 27 | —□— Pile 39 | —⊕·· Pile 61 |
| ··◇·· Pile 29 | —△— Pile 40 | —●— Pile 64 |
| —○·· Pile 30 | —▽— Pile 41 | —■— Pile 65 |
| —●— Pile 31 | ··◇·· Pile 42 | —▲— Pile 66 |
| —■— Pile 32 | —⊕·· Pile 55 | —▽— Pile 67 |
| —▲— Pile 33 | —⊕— Pile 56 | —◆— Pile 68 |
| —▼— Pile 34 | —⊕— Pile 57 | |

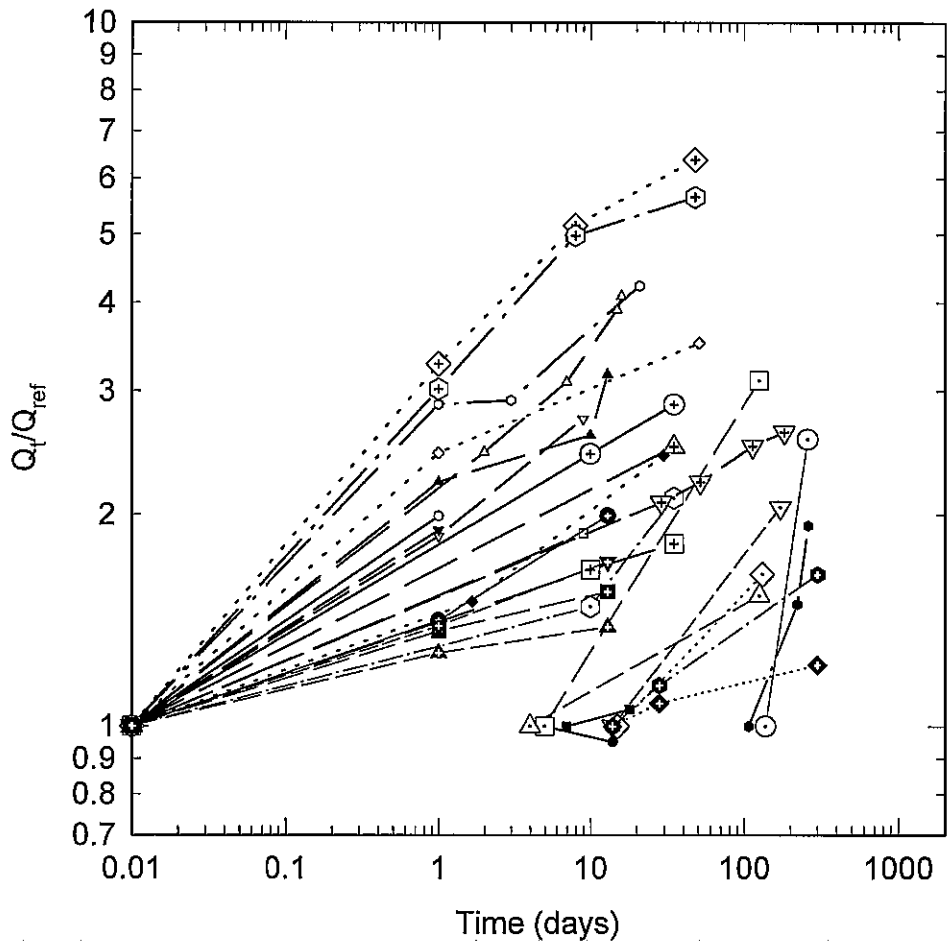


Figure B.6 Normalized capacity for piles in mixed soil profile

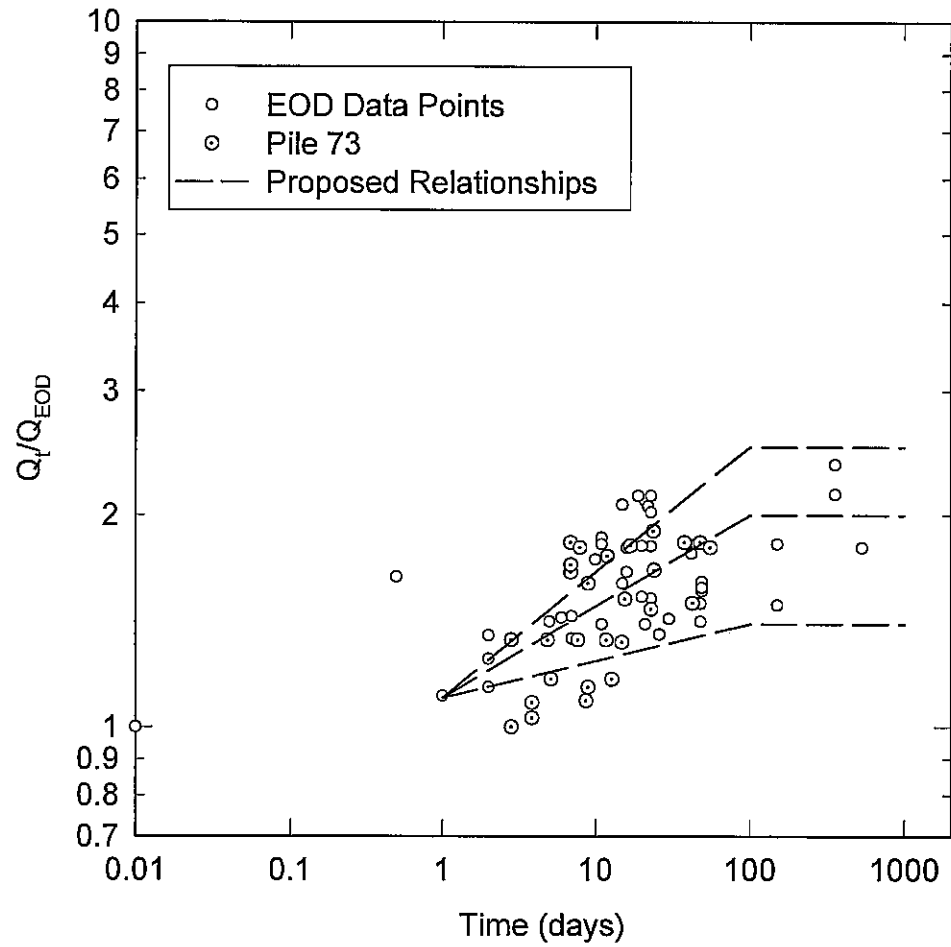


Figure B.7 Normalized capacity for sand with upper/lower bound

Appendix C - Statistics For Interpreting Q_p/Q_m Data

APPENDIX C

STATISTICS FOR INTERPRETING Q_p/Q_m DATA

INTRODUCTION

When working with any dataset (in our case, a Q_p/Q_m dataset), questions are raised concerning how the sample mean and standard deviation obtained from the dataset are representative of the population mean and standard deviation. This set of notes presents methods to address the following questions.

- a) How do we use the sample data to estimate the population mean?
- b) How can we show there is a (statistically significant) difference between the mean values of two datasets.
- c) How do we use the sample data to estimate the population variance?
- d) How can we show there is a (statistically significant) difference between the variance exhibited by two datasets.

Definitions

μ = population mean

σ = population standard deviation

\bar{x} = mean of sample dataset

\hat{s} = standard deviation of sample dataset

n = number of observations in sample dataset

ν = degrees of freedom ($\nu=n-1$)

CL = confidence level

$\alpha/2$ = mathematically, $\alpha/2 = (1-CL)/2$

$t_{(\nu, \alpha/2)}$ = t value for degrees of freedom (dof) and for $\alpha/2$.

$\chi^2_{(\nu, \alpha/2)}$ = chi squared value for dof and $\alpha/2$

$F_{(\nu_1, \nu_2, \alpha/2)}$ = F value for dof_1 , dof_2 , and $\alpha/2$

ESTIMATING THE POPULATION MEAN

(How do we use the sample data to estimate the population mean?)

Theory

Theoretically, calculating the population mean requires sampling of the total population, but such extensive sampling is rarely done due to limitations in resources and/or opportunities. Accordingly, we attempt to estimate the population mean based on a limited number of observations. A sample of the population may yield a mean value close to the population mean, but it is unlikely to yield the population mean exactly. So the data are used to estimate a range in which the population mean should fall (within some level of confidence). For example, you may use sample data to say *"I am 95 percent confident the population mean lies between this lower bound value and this upper bound value."*

The parameters and tools needed to identify the range for the population mean are:

- 1) the sample mean, \bar{x} ,
- 2) the sample standard deviation, \hat{s} ,
- 3) the number of observations, n ,
- 4) the degrees of freedom, v , ($v=n-1$)
- 5) a level of confidence (CL), and
- 6) a t value (from Table C.1)(The t distribution is also called student's t distribution and a more extensive discussion of this distribution can be found in any basic statistics textbook).

The results will be (for a chosen confidence level, say 95%):

- 1) a lower bound value for the population mean, and
- 2) an upper bound value for the population mean.

The upper value of the mean is estimated as:

$$x_{upperbound} = \bar{x} + t_{(v,\alpha/2)} \frac{\hat{s}}{\sqrt{n}} \quad (C.1)$$

and the lower value of the mean is estimated as

$$x_{lowerbound} = \bar{x} - t_{(v,\alpha/2)} \frac{\hat{s}}{\sqrt{n}} \quad (C.2)$$

The value of t is selected from Table C.1 based on the degrees of freedom, v , and the value of $\alpha/2$. The value of α is calculated as $(1-CL)$.

Example Problem

Given:

sample mean, $\bar{x} = 0.05187$

standard deviation of sample, $\hat{s} = 0.19110$

number of observations, $n = 14$

degrees of freedom, $v = 14-1 = 13$

Answer the following:

Estimate the range identifying the population mean with a 95 percent confidence level.

Determine t from Table C.1 (use $v=13$ and $\alpha/2 = (1-0.95)/2 = 0.025$).

$$x_{upperbound} = 0.05187 + 2.16 \frac{0.09110}{\sqrt{14}} = 0.1045 \quad (C.3)$$

$$x_{lowerbound} = 0.05187 - 2.16 \frac{0.09110}{\sqrt{14}} = -0.007 \quad (C.4)$$

Thus, we can say with 95 percent confidence that the value for the population mean is between -0.007 and 0.1045.

SIGNIFICANT DIFFERENCE BETWEEN TWO MEANS

(How can we show there is a statistically significant difference between the mean values of two datasets?)

Theory

We may need to compare the means between two different analyses or two different datasets, and answer the question “is the difference between these two means significant?” The answer is probabilistic rather than deterministic. In other words we cannot say “yes” or “no,” but rather we have to say “we have 95 percent confidence the two means are different.”

Parameters needed to help us identify the difference between two means are:

- 1) the mean for the two samples, \bar{x}_1, \bar{x}_2
- 2) the standard deviation for the two samples, $\hat{s}_1, \hat{s}_2,$

- 3) the number of observations for the two samples, n_1, n_2 ,
- 4) a level of confidence (CL), and
- 5) a t value (from a table with the "t" distribution).

The method is to determine a mean and standard deviation for the difference between the two samples. The absolute value of the difference between the two means (\bar{x}_{12}) is simply

$$\bar{x}_{12} = |\bar{x}_1 - \bar{x}_2| \quad (C.5)$$

The pooled estimate of standard deviation from the two samples is

$$\hat{s}_{12} = \sqrt{\frac{(n_1 - 1) \hat{s}_1^2 + (n_2 - 1) \hat{s}_2^2}{n_1 + n_2 - 2}} \sqrt{\frac{n_1 + n_2}{n_1 n_2}} \quad (C.6)$$

The t_{12} value is calculated as

$$t_{12} = \frac{\bar{x}_{12}}{\hat{s}_{12}} \quad (C.7)$$

The t_{12} value is compared with the t value for degrees of freedom v_{12} ($=n_1+n_2-2$) for a given α calculated as $(1-CL)$. Values of t are determined from Table C.1.

Example Problem

Given:

sample mean, $\bar{x}_1 = -0.17407$, $\bar{x}_2 = -0.04227$

standard deviation of sample, $\hat{s}_1 = 0.170813$, $\hat{s}_2 = 0.084288$

number of observations, $n_1 = 14$, $n_2 = 13$

Answer the following:

Is the difference between these two means significant? Can we say they are difference with a 95 percent degree of confidence?

Determine the standard deviation \hat{s}_{12} for the combined data

$$\hat{s}_{12} = \sqrt{\frac{(14-1) \cdot 0.170813^2 + (13-1) \cdot 0.084288^2}{14+13-2}} \sqrt{\frac{14+13}{14 \cdot 13}} = 0.0525 \quad (\text{C.8})$$

Determine the t_{12} value for the combined data

$$t_{12} = \left| \frac{-0.17407 - (-0.04227)}{0.0525} \right| = 2.5103 \quad (\text{C.9})$$

The value of t from Table C.1 (for $v_{12}=14+13-2=25$) and for a confidence level of 95 percent ($\alpha/2 = 0.025$) is

$$t_{(25,0.025)} = 2.060 \quad (\text{using Table C.1}) \quad (\text{C.10})$$

Because the computed t value (t_{12}) is greater than the t value in Table C.1, we conclude the two means are different with at least a 95 percent confidence level. In fact, the confidence level is slightly above 98 percent (you can confirm this using the column corresponding to $\alpha/2 = 0.01$ in Table C.1).

ESTIMATING THE POPULATION VARIANCE

(How do we use the sample data to estimate the population variance?)

Theory

We seldom know the variance (standard deviation²) for the total population. Theoretically, we need to sample the total population to determine the population variance. Since such a sampling effort is rarely feasible, we cannot estimate the exact standard deviation for a population.

The variance of the population is estimated from a limited set of observations. We define a sample variance and estimate a range in which the population variance should fall. We assign a degree of confidence with this range so you can say "there is 95 percent confidence the population variance lies between this lower bound value and this upper bound value." In these notes we will use standard deviation (which is the square root of variance).

The parameters and tools needed to identify the range for the true mean are:

- 1) the sample standard deviation, \hat{s} ,
- 2) the number of observations, n ,
- 3) the degrees of freedom, v ,
- 3) a level of confidence (CL), and

4) a χ^2 value (from a table with the χ^2 distribution). More extensive discussion of the χ^2 distribution can be found in most basic statistics textbooks.

The results will be for a chosen confidence level (say 95%):

- 1) a lower bound value for the population variance, and
- 2) an upper bound value for the population variance.

The upper bound value of the standard deviation is estimated as:

$$S_{upperbound} = \sqrt{\frac{(n-1) \hat{s}^2}{\chi^2_{(v, 1-\alpha/2)}}} \quad (C.11)$$

and the lower bound value of the standard deviation is estimated as

$$S_{lowerbound} = \sqrt{\frac{(n-1) \hat{s}^2}{\chi^2_{(v, \alpha/2)}}} \quad (C.12)$$

The value of α is calculated as (1-CL). Values of t are determined from Table C.2 based on the degrees of freedom (v) and the value of $\alpha/2$.

Example Problem

Given:

standard deviation of sample, $\hat{s} = 0.09110$

number of observations, $n = 14$

degrees of freedom, $v = 13$

Answer the following:

Determine the range identifying the population variance with a 95 percent confidence level.

Determine $\alpha/2 = (1-0.95)/2 = 0.025$. Determine the χ^2 value from Table C.2a using $v=13$ and $(1-0.025) = 0.975$ (χ^2 value = 5.00875).

$$S_{upperbound} = \sqrt{\frac{(14-1) \cdot 0.09110^2}{5.0087}} = 0.1353 \quad (C.13)$$

Determine the χ^2 value from Table C.2b using $v=13$ and $\alpha/2 = 0.025$ (χ^2 value = 24.7356)

$$S_{lowerbound} = \sqrt{\frac{(14-1) \cdot 0.09110^2}{24.7356}} = 0.0695 \quad (C.14)$$

Thus, we can say with 95 percent confidence that the values for the population standard deviation are in the range between 0.0695 and 0.1353.

SIGNIFICANT DIFFERENCE BETWEEN TWO VARIANCES

(How can we show there is a statistically significant difference between the variance exhibited by two datasets?)

Theory

We may need to compare the variances between two different analyses or two different datasets, and answer the question “is the difference between these two variances significant?” The answer is probabilistic rather than deterministic. In other words we cannot say “yes” or “no,” but we can say “we have 95 percent confidence the two variances are different.”

Parameters and tools needed to help us identify the difference between two means are:

- 1) the standard deviation for the two samples, \hat{s}_1 , \hat{s}_2 ,
- 2) the number of observations for the two samples, n_1 , n_2 ,
- 3) a level of confidence (CL), and
- 4) a table with the “F” distribution.

The F distribution is used to determine the significance of differences in sample variance, but also has other uses beyond the scope of this text. More extensive discussion of this distribution can be found in most basic statistics textbooks.

First determine the F value which is:

$$F = \frac{\hat{s}_1^2}{\hat{s}_2^2} \quad (C.15)$$

For simplicity, the values of “dataset 1” and “dataset 2” should be selected so that $F > 1$. The degree of confidence is selected, and the appropriate value of $\alpha/2$ is determined. An upper bound estimate for F is determined from Tables C.3a-C.3d using $v_1 = (n_1 - 1)$ and $v_2 = (n_2 - 1)$ and a confidence level of $\alpha/2$.

A lower bound estimate for F is determined by using $v_1 = (n_2 - 1)$ and $v_2 = (n_1 - 1)$ and a confidence level of $\alpha/2$. The lower bound value is then determined as $1/F$.

If the value of F is outside of the range of the upper and lower bound values, then it can be said that the variances are significantly different. However, if the F value falls within the range of upper and lower-bound values, then the values of variance are not significantly different within the degree of confidence specified.

Example Problem

Given:

standard deviation of sample, $\hat{s}_1 = 0.170813$, $\hat{s}_2 = 0.084288$

number of observations, $n_1 = 16$, and $n_2 = 13$

Answer the following:

Is the difference between these two variances significant? Can we say they are difference with a 95 percent degree of confidence?

Determine the F value

$$F = \frac{0.0170813^2}{0.084288^2} = 4.107 \quad (C.16)$$

Determine the upper bound F value for 2.5 percent (See Table C.3c for 2.5 percent confidence level, $v_1 = 16 - 1$, and $v_2 = 13 - 1$):

$$F_{upperbound} = 3.18 \quad (C.17)$$

Determine the lower bound F value for 2.5 percent (See Table C.3c for 2.5 percent confidence level, $v_1 = 13 - 1$, and $v_2 = 16 - 1$):

$$F_{lowerbound} = \frac{1}{2.96} = 0.3378 \quad (C.18)$$

Because the F value falls outside the range of the upper- and lower bound values, we conclude the two variances are different with a 95 percent confidence level. If we continue to increase our confidence level we can determine the two variances are different with greater than a 98 percent degree of confidence.

REFERENCES

- Ang, A. and Tang, W. (1975) Probability Concepts in Engineering Planning and Design, Vol. 1 - Basic Principles, John Wiley & Sons, New York, 409 p.
- Chao, L. L. (1969) Statistics: Methods and Analyses, McGraw-Hill, New York, 512p.

Table C.1. Student's t-distribution

dof v	Values of $\alpha/2$									
	0.4	0.25	0.1	0.05	0.025	0.01	0.005	0.0025	0.001	0.0005
1	0.3249	1.0000	3.0777	6.3137	12.7062	31.8210	63.6559	127.3211	318.2888	636.5776
2	0.2887	0.8165	1.8856	2.9200	4.3027	6.9645	9.9250	14.0892	22.3285	31.5998
3	0.2767	0.7649	1.6377	2.3534	3.1824	4.5407	5.8408	7.4532	10.2143	12.9244
4	0.2707	0.7407	1.5332	2.1318	2.7765	3.7469	4.6041	5.5975	7.1729	8.6101
5	0.2672	0.7267	1.4759	2.0150	2.5706	3.3649	4.0321	4.7733	5.8935	6.8685
6	0.2648	0.7176	1.4398	1.9432	2.4469	3.1427	3.7074	4.3168	5.2075	5.9587
7	0.2632	0.7111	1.4149	1.8946	2.3646	2.9979	3.4995	4.0294	4.7853	5.4081
8	0.2619	0.7064	1.3968	1.8595	2.3060	2.8965	3.3554	3.8325	4.5008	5.0414
9	0.2610	0.7027	1.3830	1.8331	2.2622	2.8214	3.2498	3.6896	4.2969	4.7809
10	0.2602	0.6998	1.3722	1.8125	2.2281	2.7638	3.1693	3.5814	4.1437	4.5868
11	0.2596	0.6974	1.3634	1.7959	2.2010	2.7181	3.1058	3.4966	4.0248	4.4369
12	0.2590	0.6955	1.3562	1.7823	2.1788	2.6810	3.0545	3.4284	3.9296	4.3178
13	0.2586	0.6938	1.3502	1.7709	2.1604	2.6503	3.0123	3.3725	3.8520	4.2209
14	0.2582	0.6924	1.3450	1.7613	2.1448	2.6245	2.9768	3.3257	3.7874	4.1403
15	0.2579	0.6912	1.3406	1.7531	2.1315	2.6025	2.9467	3.2860	3.7329	4.0728
16	0.2576	0.6901	1.3368	1.7459	2.1199	2.5835	2.9208	3.2520	3.6861	4.0149
17	0.2573	0.6892	1.3334	1.7396	2.1098	2.5669	2.8982	3.2224	3.6458	3.9651
18	0.2571	0.6884	1.3304	1.7341	2.1009	2.5524	2.8784	3.1966	3.6105	3.9217
19	0.2569	0.6876	1.3277	1.7291	2.0930	2.5395	2.8609	3.1737	3.5793	3.8833
20	0.2567	0.6870	1.3253	1.7247	2.0860	2.5280	2.8453	3.1534	3.5518	3.8496
21	0.2566	0.6864	1.3232	1.7207	2.0796	2.5176	2.8314	3.1352	3.5271	3.8193
22	0.2564	0.6858	1.3212	1.7171	2.0739	2.5083	2.8188	3.1188	3.5050	3.7922
23	0.2563	0.6853	1.3195	1.7139	2.0687	2.4999	2.8073	3.1040	3.4850	3.7676
24	0.2562	0.6848	1.3178	1.7109	2.0639	2.4922	2.7970	3.0905	3.4668	3.7454
25	0.2561	0.6844	1.3163	1.7081	2.0595	2.4851	2.7874	3.0782	3.4502	3.7251
26	0.2560	0.6840	1.3150	1.7056	2.0555	2.4786	2.7787	3.0669	3.4350	3.7067
27	0.2559	0.6837	1.3137	1.7033	2.0518	2.4727	2.7707	3.0565	3.4210	3.6895
28	0.2558	0.6834	1.3125	1.7011	2.0484	2.4671	2.7633	3.0470	3.4082	3.6739
29	0.2557	0.6830	1.3114	1.6991	2.0452	2.4620	2.7564	3.0380	3.3963	3.6595
30	0.2556	0.6828	1.3104	1.6973	2.0423	2.4573	2.7500	3.0298	3.3852	3.6460
35	0.2553	0.6816	1.3062	1.6896	2.0301	2.4377	2.7238	2.9961	3.3400	3.5911
40	0.2550	0.6807	1.3031	1.6839	2.0211	2.4233	2.7045	2.9712	3.3069	3.5510
45	0.2549	0.6800	1.3007	1.6794	2.0141	2.4121	2.6896	2.9521	3.2815	3.5203
50	0.2547	0.6794	1.2987	1.6759	2.0086	2.4033	2.6778	2.9370	3.2614	3.4960
55	0.2546	0.6790	1.2971	1.6730	2.0040	2.3961	2.6682	2.9247	3.2451	3.4765
60	0.2545	0.6786	1.2958	1.6706	2.0003	2.3901	2.6603	2.9146	3.2317	3.4602
70	0.2543	0.6780	1.2938	1.6669	1.9944	2.3808	2.6479	2.8987	3.2108	3.4350
80	0.2542	0.6776	1.2922	1.6641	1.9901	2.3739	2.6387	2.8870	3.1952	3.4164
90	0.2541	0.6772	1.2910	1.6620	1.9867	2.3685	2.6316	2.8779	3.1832	3.4019
100	0.2540	0.6770	1.2901	1.6602	1.9840	2.3642	2.6259	2.8707	3.1738	3.3905
110	0.2540	0.6767	1.2893	1.6588	1.9818	2.3607	2.6213	2.8648	3.1660	3.3811
120	0.2539	0.6765	1.2886	1.6576	1.9799	2.3578	2.6174	2.8599	3.1595	3.3734
∞	0.2533	0.6745	1.2816	1.6449	1.9600	2.3263	2.5758	2.8070	3.0902	3.2905

Table C.2a. Chi squared (χ^2) table for upper-bound estimate

dof v	Values of $1 - \alpha/2$						
	0.995	0.99	0.975	0.95	0.9	0.75	0.5
1	0.0000	0.0002	0.0010	0.0039	0.0158	0.1015	0.4549
2	0.0100	0.0201	0.0506	0.1026	0.2107	0.5754	1.3863
3	0.0717	0.1148	0.2158	0.3518	0.5844	1.2125	2.3660
4	0.2070	0.2971	0.4844	0.7107	1.0636	1.9226	3.3567
5	0.4118	0.5543	0.8312	1.1455	1.6103	2.6746	4.3515
6	0.6757	0.8721	1.2373	1.6354	2.2041	3.4546	5.3481
7	0.9893	1.2390	1.6899	2.1673	2.8331	4.2549	6.3458
8	1.3444	1.6465	2.1797	2.7326	3.4895	5.0706	7.3441
9	1.7349	2.0879	2.7004	3.3251	4.1682	5.8988	8.3428
10	2.1558	2.5582	3.2470	3.9403	4.8652	6.7372	9.3418
11	2.6032	3.0535	3.8157	4.5748	5.5778	7.5841	10.3410
12	3.0738	3.5706	4.4038	5.2260	6.3038	8.4384	11.3403
13	3.5650	4.1069	5.0087	5.8919	7.0415	9.2991	12.3398
14	4.0747	4.6604	5.6287	6.5706	7.7895	10.1653	13.3393
15	4.6009	5.2294	6.2621	7.2609	8.5468	11.0365	14.3389
16	5.1422	5.8122	6.9077	7.9616	9.3122	11.9122	15.3385
17	5.6973	6.4077	7.5642	8.6718	10.0852	12.7919	16.3382
18	6.2648	7.0149	8.2307	9.3904	10.8649	13.6753	17.3379
19	6.8439	7.6327	8.9065	10.1170	11.6509	14.5620	18.3376
20	7.4338	8.2604	9.5908	10.8508	12.4426	15.4518	19.3374
21	8.0336	8.8972	10.2829	11.5913	13.2396	16.3444	20.3372
22	8.6427	9.5425	10.9823	12.3380	14.0415	17.2396	21.3370
23	9.2604	10.1957	11.6885	13.0905	14.8480	18.1373	22.3369
24	9.8862	10.8563	12.4011	13.8484	15.6587	19.0373	23.3367
25	10.5196	11.5240	13.1197	14.6114	16.4734	19.9393	24.3366
26	11.1602	12.1982	13.8439	15.3792	17.2919	20.8434	25.3365
27	11.8077	12.8785	14.5734	16.1514	18.1139	21.7494	26.3363
28	12.4613	13.5647	15.3079	16.9279	18.9392	22.6572	27.3362
29	13.1211	14.2564	16.0471	17.7084	19.7677	23.5666	28.3361
30	13.7867	14.9535	16.7908	18.4927	20.5992	24.4776	29.3360
35	17.1917	18.5089	20.5694	22.4650	24.7966	29.0540	34.3356
40	20.7066	22.1642	24.4331	26.5093	29.0505	33.6603	39.3353
45	24.3110	25.9012	28.3662	30.6123	33.3504	38.2910	44.3351
50	27.9908	29.7067	32.3574	34.7642	37.6886	42.9421	49.3349
55	31.7349	33.5705	36.3981	38.9581	42.0596	47.6105	54.3348
60	35.5344	37.4848	40.4817	43.1880	46.4589	52.2938	59.3347
70	43.2753	45.4417	48.7575	51.7393	55.3289	61.6983	69.3345
80	51.1719	53.5400	57.1532	60.3915	64.2778	71.1445	79.3343
90	59.1963	61.7540	65.6466	69.1260	73.2911	80.6247	89.3342
100	67.3275	70.0650	74.2219	77.9294	82.3581	90.1332	99.3341
110	75.5498	78.4582	82.8671	86.7916	91.4710	99.6660	109.3341
120	83.8517	86.9233	91.5726	95.7046	100.6236	109.2197	119.3340

Table C.2b. Chi squared (χ^2) table for lower-bound estimate

dof v	$\alpha/2$						
	0.25	0.1	0.05	0.025	0.01	0.005	0.001
1	1.3233	2.7055	3.8415	5.0239	6.6349	7.8794	10.8274
2	2.7726	4.6052	5.9915	7.3778	9.2104	10.5965	13.8150
3	4.1083	6.2514	7.8147	9.3484	11.3449	12.8381	16.2660
4	5.3853	7.7794	9.4877	11.1433	13.2767	14.8602	18.4662
5	6.6257	9.2363	11.0705	12.8325	15.0863	16.7496	20.5147
6	7.8408	10.6446	12.5916	14.4494	16.8119	18.5475	22.4575
7	9.0371	12.0170	14.0671	16.0128	18.4753	20.2777	24.3213
8	10.2189	13.3616	15.5073	17.5345	20.0902	21.9549	26.1239
9	11.3887	14.6837	16.9190	19.0228	21.6660	23.5893	27.8767
10	12.5489	15.9872	18.3070	20.4832	23.2093	25.1881	29.5879
11	13.7007	17.2750	19.6752	21.9200	24.7250	26.7569	31.2635
12	14.8454	18.5493	21.0261	23.3367	26.2170	28.2997	32.9092
13	15.9839	19.8119	22.3620	24.7356	27.6882	29.8193	34.5274
14	17.1169	21.0641	23.6848	26.1189	29.1412	31.3194	36.1239
15	18.2451	22.3071	24.9958	27.4884	30.5780	32.8015	37.6978
16	19.3689	23.5418	26.2962	28.8453	31.9999	34.2671	39.2518
17	20.4887	24.7690	27.5871	30.1910	33.4087	35.7184	40.7911
18	21.6049	25.9894	28.8693	31.5264	34.8052	37.1564	42.3119
19	22.7178	27.2036	30.1435	32.8523	36.1908	38.5821	43.8194
20	23.8277	28.4120	31.4104	34.1696	37.5663	39.9969	45.3142
21	24.9348	29.6151	32.6706	35.4789	38.9322	41.4009	46.7963
22	26.0393	30.8133	33.9245	36.7807	40.2894	42.7957	48.2676
23	27.1413	32.0069	35.1725	38.0756	41.6383	44.1814	49.7276
24	28.2412	33.1962	36.4150	39.3641	42.9798	45.5584	51.1790
25	29.3388	34.3816	37.6525	40.6465	44.3140	46.9280	52.6187
26	30.4346	35.5632	38.8851	41.9231	45.6416	48.2898	54.0511
27	31.5284	36.7412	40.1133	43.1945	46.9628	49.6450	55.4751
28	32.6205	37.9159	41.3372	44.4608	48.2782	50.9936	56.8918
29	33.7109	39.0875	42.5569	45.7223	49.5878	52.3355	58.3006
30	34.7997	40.2560	43.7730	46.9792	50.8922	53.6719	59.7022
35	40.2228	46.0588	49.8018	53.2033	57.3420	60.2746	66.6192
40	45.6160	51.8050	55.7585	59.3417	63.6908	66.7660	73.4029
45	50.9849	57.5053	61.6562	65.4101	69.9569	73.1660	80.0776
50	56.3336	63.1671	67.5048	71.4202	76.1538	79.4898	86.6603
55	61.6650	68.7962	73.3115	77.3804	82.2920	85.7491	93.1671
60	66.9815	74.3970	79.0820	83.2977	88.3794	91.9518	99.6078
70	77.5766	85.5270	90.5313	95.0231	100.4251	104.2148	112.3167
80	88.1303	96.5782	101.8795	106.6285	112.3288	116.3209	124.8389
90	98.6499	107.5650	113.1452	118.1359	124.1162	128.2987	137.2082
100	109.1412	118.4980	124.3421	129.5613	135.8069	140.1697	149.4488
110	119.6084	129.3852	135.4802	140.9165	147.4143	151.9482	161.5815
120	130.0546	140.2326	146.5673	152.2113	158.9500	163.6485	173.6184

Table C.3a F-distribution values for the upper 10 percent

df2	df1																			
v2	1	2	3	4	5	6	7	8	9	10	12	15	20	24	30	40	60	120	∞	
1	39.9	49.5	53.6	55.8	57.2	58.2	58.9	59.4	59.9	60.2	60.7	61.2	61.7	62.0	62.3	62.5	62.8	63.1	63.3	
2	8.53	9.00	9.16	9.24	9.29	9.33	9.35	9.37	9.38	9.39	9.41	9.42	9.44	9.45	9.46	9.47	9.47	9.48	9.49	
3	5.54	5.46	5.39	5.34	5.31	5.28	5.27	5.25	5.24	5.23	5.22	5.20	5.18	5.18	5.17	5.16	5.15	5.14	5.13	
4	4.54	4.32	4.19	4.11	4.05	4.01	3.98	3.95	3.94	3.92	3.90	3.87	3.84	3.83	3.82	3.80	3.79	3.78	3.76	
5	4.06	3.78	3.62	3.52	3.45	3.40	3.37	3.34	3.32	3.30	3.27	3.24	3.21	3.19	3.17	3.16	3.14	3.12	3.10	
6	3.78	3.46	3.29	3.18	3.11	3.05	3.01	2.98	2.96	2.94	2.90	2.87	2.84	2.82	2.80	2.78	2.76	2.74	2.72	
7	3.59	3.26	3.07	2.96	2.88	2.83	2.78	2.75	2.72	2.70	2.67	2.65	2.59	2.58	2.56	2.54	2.51	2.49	2.47	
8	3.46	3.11	2.92	2.81	2.73	2.67	2.62	2.59	2.56	2.54	2.50	2.46	2.42	2.40	2.38	2.36	2.34	2.32	2.29	
9	3.36	3.01	2.81	2.69	2.61	2.55	2.51	2.47	2.44	2.42	2.38	2.34	2.30	2.28	2.25	2.23	2.21	2.18	2.16	
10	3.29	2.92	2.73	2.61	2.52	2.46	2.41	2.38	2.35	2.32	2.28	2.24	2.20	2.18	2.16	2.13	2.11	2.08	2.06	
11	3.23	2.86	2.66	2.54	2.45	2.39	2.34	2.30	2.27	2.25	2.21	2.17	2.12	2.10	2.08	2.05	2.03	2.00	1.97	
12	3.18	2.81	2.61	2.48	2.39	2.33	2.28	2.24	2.21	2.19	2.15	2.10	2.06	2.04	2.01	1.99	1.96	1.93	1.90	
13	3.14	2.76	2.56	2.43	2.35	2.28	2.23	2.20	2.16	2.14	2.10	2.05	2.01	1.98	1.96	1.93	1.90	1.88	1.85	
14	3.10	2.73	2.52	2.39	2.31	2.24	2.19	2.15	2.12	2.10	2.05	2.01	1.96	1.94	1.91	1.89	1.86	1.83	1.80	
15	3.07	2.70	2.49	2.36	2.27	2.21	2.16	2.12	2.09	2.06	2.02	1.97	1.92	1.90	1.87	1.85	1.82	1.79	1.76	
16	3.03	2.67	2.46	2.33	2.24	2.18	2.13	2.09	2.06	2.03	1.96	1.91	1.86	1.84	1.81	1.78	1.75	1.72	1.69	
17	3.01	2.62	2.42	2.29	2.20	2.13	2.08	2.04	2.00	1.98	1.93	1.89	1.84	1.81	1.78	1.75	1.72	1.69	1.66	
18	2.99	2.61	2.40	2.27	2.18	2.11	2.06	2.02	1.98	1.96	1.91	1.86	1.81	1.79	1.76	1.73	1.70	1.67	1.63	
19	2.97	2.59	2.38	2.25	2.16	2.09	2.04	2.00	1.96	1.94	1.89	1.84	1.79	1.77	1.74	1.71	1.68	1.64	1.61	
20	2.96	2.57	2.36	2.23	2.14	2.08	2.02	1.98	1.95	1.92	1.87	1.83	1.78	1.75	1.72	1.69	1.66	1.62	1.59	
21	2.95	2.56	2.35	2.22	2.13	2.06	2.01	1.97	1.93	1.90	1.86	1.81	1.76	1.73	1.70	1.67	1.64	1.60	1.57	
22	2.94	2.55	2.34	2.21	2.11	2.05	1.99	1.95	1.92	1.89	1.84	1.80	1.74	1.72	1.69	1.66	1.62	1.59	1.55	
23	2.94	2.54	2.33	2.19	2.10	2.04	1.98	1.94	1.91	1.88	1.83	1.78	1.73	1.70	1.67	1.64	1.61	1.57	1.53	
24	2.92	2.53	2.32	2.18	2.09	2.02	1.97	1.93	1.89	1.87	1.82	1.77	1.72	1.69	1.66	1.63	1.59	1.56	1.52	
25	2.91	2.52	2.31	2.17	2.08	2.01	1.96	1.92	1.88	1.86	1.81	1.76	1.71	1.68	1.65	1.61	1.58	1.54	1.50	
26	2.90	2.51	2.30	2.17	2.07	2.00	1.95	1.91	1.87	1.85	1.80	1.75	1.70	1.67	1.64	1.60	1.57	1.53	1.49	
27	2.89	2.50	2.29	2.16	2.06	2.00	1.94	1.90	1.87	1.84	1.79	1.74	1.69	1.66	1.63	1.59	1.56	1.52	1.48	
28	2.89	2.50	2.28	2.15	2.05	1.99	1.93	1.89	1.86	1.83	1.78	1.73	1.68	1.65	1.62	1.58	1.55	1.51	1.47	
29	2.88	2.49	2.28	2.14	2.04	1.98	1.93	1.88	1.85	1.82	1.77	1.72	1.67	1.64	1.61	1.57	1.54	1.50	1.46	
30	2.88	2.46	2.25	2.11	2.02	1.95	1.90	1.85	1.82	1.79	1.74	1.69	1.63	1.60	1.57	1.53	1.50	1.46	1.41	
35	2.85	2.46	2.25	2.11	2.02	1.95	1.90	1.85	1.82	1.79	1.74	1.69	1.63	1.60	1.57	1.53	1.50	1.46	1.41	
40	2.84	2.44	2.23	2.09	2.00	1.93	1.87	1.83	1.79	1.76	1.71	1.66	1.61	1.57	1.54	1.51	1.47	1.42	1.38	
45	2.82	2.42	2.21	2.07	1.98	1.91	1.85	1.81	1.77	1.74	1.70	1.64	1.58	1.55	1.52	1.48	1.44	1.40	1.35	
50	2.81	2.41	2.20	2.06	1.97	1.90	1.84	1.80	1.76	1.73	1.68	1.63	1.57	1.54	1.50	1.46	1.42	1.38	1.33	
55	2.80	2.40	2.19	2.05	1.95	1.88	1.83	1.78	1.75	1.72	1.67	1.61	1.55	1.52	1.49	1.45	1.41	1.36	1.31	
60	2.79	2.39	2.18	2.04	1.95	1.87	1.82	1.77	1.74	1.71	1.66	1.60	1.54	1.51	1.48	1.44	1.40	1.35	1.29	
70	2.78	2.38	2.16	2.03	1.93	1.86	1.80	1.76	1.72	1.69	1.64	1.59	1.53	1.49	1.46	1.42	1.37	1.32	1.27	
80	2.77	2.37	2.15	2.02	1.92	1.85	1.79	1.75	1.71	1.68	1.63	1.57	1.51	1.48	1.44	1.40	1.36	1.31	1.24	
90	2.76	2.36	2.14	2.01	1.91	1.84	1.78	1.74	1.70	1.67	1.62	1.56	1.50	1.47	1.43	1.39	1.35	1.29	1.23	
100	2.76	2.36	2.14	2.00	1.91	1.83	1.78	1.73	1.69	1.66	1.61	1.55	1.49	1.46	1.42	1.38	1.34	1.28	1.21	
110	2.75	2.35	2.13	2.00	1.90	1.83	1.77	1.73	1.69	1.66	1.61	1.55	1.49	1.45	1.42	1.37	1.33	1.27	1.20	
120	2.75	2.35	2.13	1.99	1.90	1.82	1.77	1.72	1.68	1.65	1.60	1.55	1.48	1.45	1.41	1.37	1.32	1.26	1.19	
∞	2.71	2.30	2.08	1.94	1.85	1.77	1.72	1.67	1.63	1.60	1.55	1.49	1.42	1.38	1.34	1.30	1.24	1.17	1.00	

Table C.3b F-distribution values for the upper 5 percent

df2	df1																			
v2	1	2	3	4	5	6	7	8	9	10	12	15	20	24	30	40	60	120	∞	
1	161.4	109.5	215.7	224.6	230.2	234.0	236.8	238.9	240.5	241.9	243.9	245.9	248.0	249.1	250.1	251.1	252.2	253.3	254.3	
2	18.51	19.00	19.16	19.25	19.30	19.33	19.35	19.37	19.38	19.40	19.41	19.43	19.45	19.45	19.46	19.47	19.48	19.49	19.50	
3	10.13	9.55	9.28	9.12	9.01	8.94	8.89	8.85	8.81	8.79	8.74	8.70	8.66	8.64	8.62	8.59	8.57	8.55	8.53	
4	7.71	6.94	6.59	6.39	6.26	6.16	6.09	6.04	6.00	5.96	5.91	5.86	5.80	5.77	5.75	5.72	5.69	5.66	5.63	
5	6.61	5.79	5.41	5.19	5.05	4.95	4.88	4.82	4.77	4.74	4.68	4.62	4.56	4.53	4.50	4.46	4.43	4.40	4.36	
6	5.99	5.14	4.76	4.53	4.39	4.28	4.21	4.15	4.10	4.06	4.00	3.94	3.87	3.84	3.81	3.77	3.74	3.70	3.67	
7	5.59	4.74	4.35	4.12	3.97	3.87	3.79	3.73	3.68	3.64	3.57	3.51	3.44	3.41	3.38	3.34	3.30	3.27	3.23	
8	5.32	4.46	4.07	3.84	3.69	3.58	3.50	3.44	3.39	3.35	3.28	3.22	3.15	3.12	3.08	3.04	3.01	2.97	2.93	
9	5.12	4.26	3.86	3.63	3.48	3.37	3.29	3.23	3.18	3.14	3.07	3.01	2.94	2.90	2.86	2.83	2.79	2.75	2.71	
10	4.96	4.10	3.71	3.48	3.33	3.22	3.14	3.07	3.02	2.98	2.91	2.85	2.77	2.74	2.70	2.66	2.62	2.58	2.54	
11	4.84	3.98	3.59	3.36	3.20	3.09	3.01	2.95	2.90	2.85	2.79	2.72	2.65	2.61	2.57	2.53	2.49	2.45	2.40	
12	4.75	3.89	3.49	3.26	3.11	3.00	2.91	2.85	2.80	2.75	2.69	2.62	2.54	2.51	2.47	2.43	2.38	2.34	2.30	
13	4.67	3.81	3.41	3.18	3.03	2.92	2.83	2.77	2.71	2.67	2.60	2.53	2.46	2.42	2.38	2.34	2.30	2.25	2.21	
14	4.60	3.74	3.34	3.11	2.96	2.85	2.76	2.70	2.64	2.59	2.52	2.46	2.39	2.35	2.31	2.27	2.22	2.18	2.13	
15	4.54	3.68	3.29	3.06	2.90	2.79	2.71	2.64	2.59	2.54	2.48	2.40	2.33	2.29	2.25	2.20	2.16	2.11	2.07	
16	4.49	3.63	3.24	3.01	2.85	2.74	2.66	2.59	2.54	2.49	2.42	2.35	2.28	2.24	2.19	2.15	2.10	2.06	2.01	
17	4.45	3.59	3.20	2.96	2.81	2.70	2.61	2.55	2.49	2.45	2.38	2.31	2.23	2.19	2.15	2.10	2.06	2.01	1.96	
18	4.41	3.55	3.16	2.93	2.77	2.66	2.58	2.51	2.46	2.41	2.34	2.27	2.19	2.15	2.11	2.06	2.02	1.97	1.92	
19	4.38	3.52	3.13	2.90	2.74	2.63	2.54	2.48	2.42	2.38	2.31	2.23	2.16	2.11	2.07	2.03	1.98	1.93	1.88	
20	4.35	3.49	3.10	2.87	2.71	2.60	2.51	2.45	2.39	2.35	2.28	2.20	2.12	2.08	2.04	1.99	1.95	1.90	1.84	
21	4.32	3.47	3.07	2.84	2.68	2.57	2.49	2.42	2.37	2.32	2.25	2.18	2.10	2.05	2.01	1.96	1.92	1.87	1.81	
22	4.30	3.44	3.05	2.82	2.66	2.55	2.46	2.40	2.34	2.30	2.23	2.15	2.07	2.03	1.98	1.94	1.89	1.84	1.78	
23	4.28	3.42	3.03	2.80	2.64	2.53	2.44	2.37	2.32	2.27	2.20	2.13	2.05	2.01	1.96	1.91	1.86	1.81	1.76	
24	4.26	3.40	3.01	2.78	2.62	2.51	2.42	2.36	2.30	2.25	2.18	2.11	2.03	1.98	1.94	1.89	1.84	1.79	1.73	
25	4.24	3.39	2.99	2.76	2.60	2.49	2.40	2.34	2.28	2.24	2.16	2.09	2.01	1.96	1.92	1.87	1.82	1.77	1.71	
26	4.23	3.37	2.98	2.74	2.59	2.47	2.39	2.32	2.27	2.22	2.15	2.07	1.99	1.95	1.90	1.85	1.80	1.75	1.69	
27	4.21	3.35	2.96	2.73	2.57	2.46	2.37	2.31	2.25	2.20	2.13	2.06	1.97	1.93	1.88	1.84	1.79	1.73	1.67	
28	4.20	3.34	2.95	2.71	2.56	2.45	2.36	2.29	2.24	2.19	2.12	2.04	1.96	1.91	1.87	1.82	1.77	1.71	1.65	
29	4.18	3.33	2.93	2.70	2.55	2.43	2.35	2.28	2.22	2.18	2.10	2.03	1.94	1.90	1.85	1.81	1.75	1.70	1.64	
30	4.17	3.32	2.92	2.69	2.53	2.42	2.33	2.27	2.21	2.16	2.09	2.01	1.93	1.89	1.84	1.79	1.74	1.68	1.62	
35	4.12	3.27	2.87	2.64	2.49	2.37	2.29	2.22	2.16	2.11	2.04	1.96	1.88	1.83	1.79	1.74	1.68	1.62	1.56	
40	4.08	3.23	2.84	2.61	2.45	2.34	2.25	2.18	2.12	2.08	2.00	1.92	1.84	1.79	1.74	1.69	1.64	1.58	1.51	
45	4.06	3.20	2.81	2.58	2.42	2.31	2.22	2.15	2.10	2.05	1.97	1.89	1.81	1.76	1.71	1.66	1.60	1.54	1.47	
50	4.03	3.18	2.79	2.56	2.40	2.29	2.20	2.13	2.07	2.03	1.95	1.87	1.78	1.74	1.69	1.63	1.58	1.51	1.44	
55	4.02	3.16	2.77	2.54	2.38	2.27	2.18	2.11	2.06	2.01	1.93	1.85	1.76	1.72	1.67	1.61	1.55	1.49	1.41	
60	4.00	3.15	2.76	2.53	2.37	2.25	2.17	2.10	2.04	1.99	1.92	1.84	1.75	1.70	1.65	1.59	1.53	1.47	1.39	
70	3.98	3.13	2.74	2.50	2.35	2.23	2.14	2.07	2.02	1.97	1.89	1.81	1.72	1.67	1.62	1.57	1.50	1.44	1.35	
80	3.96	3.11	2.72	2.49	2.33	2.21	2.13	2.06	2.00	1.95	1.88	1.79	1.70	1.65	1.60	1.54	1.48	1.41	1.32	
90	3.95	3.10	2.71	2.47	2.32	2.20	2.11	2.04	1.99	1.94	1.86	1.77	1.68	1.63	1.57	1.51	1.46	1.39	1.30	
100	3.94	3.09	2.70	2.46	2.31	2.19	2.10	2.03	1.97	1.93	1.85	1.76	1.67	1.62	1.56	1.50	1.44	1.38	1.28	
110	3.93	3.08	2.69	2.45	2.30	2.18	2.09	2.02	1.97	1.92	1.84	1.75	1.66	1.61	1.55	1.50	1.44	1.36	1.27	
120	3.92	3.07	2.68	2.45	2.29	2.18	2.09	2.02	1.96	1.91	1.83	1.75	1.66	1.61	1.55	1.50	1.43	1.35	1.25	
∞	3.84	3.00	2.60	2.37	2.21	2.10	2.01	1.94	1.88	1.83	1.75	1.67	1.57	1.52	1.46	1.39	1.32	1.22	1.00	

Table C.3c F-distribution values for the upper 2.5 percent

df2	df1																		
v2	1	2	3	4	5	6	7	8	9	10	12	15	20	24	30	40	60	120	∞
1	647.8	799.5	864.2	898.6	921.8	937.1	948.2	956.6	963.3	968.6	976.7	984.9	993.1	997.3	1001.4	1005.6	1009.8	1014.0	1018.3
2	38.51	39.00	39.17	39.25	39.30	39.33	39.36	39.37	39.39	39.40	39.41	39.43	39.45	39.46	39.46	39.47	39.48	39.49	39.50
3	17.44	16.94	15.44	15.10	14.88	14.73	14.62	14.54	14.47	14.42	14.34	14.25	14.17	14.12	14.08	14.04	13.99	13.95	13.90
4	12.22	10.65	9.98	9.60	9.36	9.20	9.07	8.98	8.90	8.84	8.75	8.66	8.56	8.51	8.46	8.41	8.36	8.31	8.26
5	10.01	8.43	7.76	7.39	7.15	6.98	6.85	6.76	6.68	6.62	6.52	6.43	6.33	6.28	6.23	6.18	6.12	6.07	6.02
6	8.81	7.26	6.60	6.23	5.99	5.82	5.70	5.60	5.52	5.46	5.37	5.27	5.17	5.12	5.07	5.01	4.96	4.90	4.85
7	8.07	6.54	5.89	5.52	5.29	5.12	4.99	4.90	4.82	4.76	4.67	4.57	4.47	4.41	4.36	4.31	4.25	4.20	4.14
8	7.57	6.06	5.42	5.05	4.82	4.65	4.53	4.43	4.36	4.30	4.20	4.10	4.00	3.95	3.89	3.84	3.78	3.73	3.67
9	7.21	5.71	5.08	4.72	4.48	4.32	4.20	4.10	4.03	3.96	3.87	3.77	3.67	3.61	3.56	3.51	3.45	3.39	3.33
10	6.94	5.46	4.83	4.47	4.24	4.07	3.95	3.85	3.78	3.72	3.62	3.52	3.42	3.37	3.31	3.26	3.20	3.14	3.08
11	6.72	5.26	4.63	4.28	4.04	3.88	3.76	3.66	3.59	3.53	3.43	3.33	3.23	3.17	3.12	3.06	3.00	2.94	2.88
12	6.55	5.10	4.47	4.12	3.89	3.73	3.61	3.51	3.44	3.37	3.28	3.18	3.07	3.02	2.96	2.91	2.85	2.79	2.72
13	6.41	4.97	4.35	4.00	3.77	3.60	3.48	3.39	3.31	3.25	3.15	3.05	2.95	2.89	2.84	2.78	2.72	2.66	2.60
14	6.30	4.86	4.24	3.89	3.66	3.50	3.38	3.29	3.21	3.15	3.05	2.95	2.84	2.79	2.73	2.67	2.61	2.55	2.49
15	6.20	4.77	4.15	3.80	3.58	3.41	3.29	3.20	3.12	3.06	2.96	2.86	2.76	2.70	2.64	2.59	2.52	2.46	2.40
16	6.12	4.69	4.08	3.73	3.50	3.34	3.22	3.12	3.05	2.99	2.89	2.79	2.68	2.63	2.57	2.51	2.45	2.38	2.32
17	6.04	4.62	4.01	3.66	3.44	3.28	3.16	3.06	2.98	2.92	2.82	2.72	2.62	2.56	2.50	2.44	2.38	2.32	2.25
18	5.98	4.56	3.95	3.61	3.38	3.22	3.10	3.01	2.93	2.87	2.77	2.67	2.56	2.50	2.44	2.38	2.32	2.26	2.19
19	5.92	4.51	3.90	3.56	3.33	3.17	3.05	2.96	2.88	2.82	2.72	2.62	2.51	2.45	2.39	2.33	2.27	2.20	2.13
20	5.87	4.46	3.86	3.51	3.29	3.13	3.01	2.91	2.84	2.77	2.68	2.57	2.46	2.41	2.35	2.29	2.22	2.16	2.09
21	5.83	4.42	3.82	3.48	3.25	3.09	2.97	2.87	2.80	2.73	2.64	2.53	2.42	2.37	2.31	2.25	2.18	2.11	2.04
22	5.79	4.38	3.78	3.44	3.22	3.05	2.93	2.84	2.76	2.70	2.60	2.50	2.39	2.33	2.27	2.21	2.14	2.08	2.00
23	5.75	4.35	3.75	3.41	3.18	3.02	2.90	2.81	2.73	2.67	2.57	2.47	2.36	2.30	2.24	2.18	2.11	2.04	1.97
24	5.72	4.32	3.72	3.38	3.15	2.99	2.87	2.78	2.70	2.64	2.54	2.44	2.33	2.27	2.21	2.15	2.08	2.01	1.94
25	5.69	4.29	3.69	3.35	3.13	2.97	2.85	2.75	2.68	2.61	2.51	2.41	2.30	2.24	2.18	2.12	2.05	1.98	1.91
26	5.66	4.27	3.67	3.33	3.10	2.94	2.82	2.73	2.65	2.59	2.49	2.39	2.28	2.22	2.16	2.09	2.03	1.95	1.88
27	5.63	4.24	3.65	3.31	3.08	2.92	2.80	2.71	2.63	2.57	2.47	2.36	2.25	2.19	2.13	2.07	2.00	1.93	1.85
28	5.61	4.22	3.63	3.29	3.06	2.90	2.78	2.69	2.61	2.55	2.45	2.34	2.23	2.17	2.11	2.05	1.98	1.91	1.83
29	5.59	4.20	3.61	3.27	3.04	2.88	2.76	2.67	2.59	2.53	2.43	2.32	2.21	2.15	2.09	2.03	1.96	1.89	1.81
30	5.57	4.18	3.59	3.25	3.03	2.87	2.75	2.65	2.57	2.51	2.41	2.31	2.20	2.14	2.07	2.01	1.94	1.87	1.79
35	5.48	4.11	3.52	3.18	2.96	2.80	2.68	2.58	2.50	2.44	2.34	2.23	2.12	2.06	2.00	1.93	1.86	1.79	1.70
40	5.42	4.05	3.46	3.13	2.90	2.74	2.62	2.53	2.45	2.39	2.29	2.18	2.07	2.01	1.94	1.88	1.80	1.72	1.64
45	5.38	4.01	3.42	3.09	2.86	2.70	2.58	2.49	2.41	2.35	2.25	2.14	2.03	1.96	1.90	1.83	1.76	1.68	1.59
50	5.34	3.97	3.39	3.05	2.83	2.67	2.55	2.46	2.38	2.32	2.22	2.11	1.99	1.93	1.87	1.80	1.72	1.64	1.55
55	5.31	3.95	3.36	3.03	2.81	2.65	2.53	2.44	2.36	2.29	2.19	2.08	1.97	1.90	1.84	1.77	1.69	1.61	1.51
60	5.29	3.93	3.34	3.01	2.79	2.63	2.51	2.41	2.33	2.27	2.17	2.06	1.94	1.88	1.82	1.74	1.67	1.58	1.48
70	5.25	3.89	3.31	2.97	2.75	2.59	2.47	2.38	2.30	2.24	2.14	2.03	1.91	1.85	1.78	1.71	1.63	1.54	1.44
80	5.22	3.86	3.28	2.95	2.73	2.57	2.45	2.35	2.28	2.21	2.11	2.00	1.88	1.82	1.75	1.66	1.58	1.48	1.37
90	5.20	3.84	3.26	2.93	2.71	2.55	2.43	2.34	2.26	2.19	2.09	1.98	1.86	1.80	1.73	1.66	1.56	1.46	1.35
100	5.18	3.83	3.25	2.92	2.70	2.54	2.42	2.32	2.24	2.18	2.08	1.97	1.85	1.78	1.71	1.64	1.54	1.45	1.33
110	5.16	3.82	3.24	2.90	2.68	2.53	2.40	2.31	2.23	2.17	2.07	1.96	1.84	1.77	1.70	1.63	1.54	1.45	1.33
120	5.15	3.80	3.23	2.89	2.67	2.52	2.39	2.30	2.22	2.16	2.05	1.94	1.82	1.76	1.69	1.61	1.53	1.43	1.31
∞	5.02	3.69	3.12	2.79	2.57	2.41	2.29	2.19	2.11	2.05	1.94	1.83	1.71	1.64	1.57	1.48	1.39	1.27	1.00

Table C.3d F-distribution values for the upper 1 percent

df1	v2	v1																		
		1	2	3	4	5	6	7	8	9	10	12	15	20	24	30	40	60	120	∞
1	4052	4959	5104	5024	5164	5859	5928	5981	6022	6055	6107	6157	6209	6244	6286	6339	6366	6399	6430	6460
2	98.50	99.80	99.16	99.25	99.30	99.33	99.36	99.38	99.39	99.40	99.42	99.43	99.45	99.46	99.47	99.48	99.48	99.49	99.50	99.50
3	34.12	30.82	29.46	28.71	28.24	27.91	27.67	27.49	27.34	27.05	26.87	26.87	26.69	26.60	26.50	26.41	26.32	26.22	26.13	26.13
4	21.20	18.00	16.69	15.98	15.52	15.21	14.98	14.80	14.66	14.55	14.37	14.20	14.02	13.93	13.84	13.75	13.65	13.56	13.46	13.46
5	16.26	13.27	12.06	11.39	10.97	10.67	10.46	10.29	10.16	10.05	9.89	9.72	9.55	9.47	9.38	9.29	9.20	9.11	9.02	9.02
6	13.75	10.92	9.78	9.15	8.75	8.47	8.26	8.10	7.98	7.87	7.72	7.56	7.40	7.31	7.23	7.14	7.06	6.97	6.88	6.88
7	12.25	9.55	8.45	7.85	7.46	7.19	6.99	6.84	6.72	6.62	6.47	6.31	6.16	6.07	5.99	5.91	5.82	5.74	5.65	5.65
8	11.26	8.65	7.59	7.01	6.63	6.37	6.18	6.03	5.91	5.81	5.67	5.52	5.36	5.28	5.20	5.12	5.03	4.95	4.86	4.86
9	10.56	8.02	6.99	6.42	6.06	5.80	5.61	5.47	5.35	5.26	5.11	4.96	4.81	4.73	4.65	4.57	4.48	4.40	4.31	4.31
10	10.04	7.56	6.55	5.99	5.64	5.39	5.20	5.06	4.94	4.85	4.71	4.56	4.41	4.33	4.25	4.17	4.08	4.00	3.91	3.91
11	9.65	7.21	6.22	5.67	5.32	5.07	4.89	4.74	4.63	4.54	4.40	4.25	4.10	4.02	3.94	3.86	3.78	3.69	3.60	3.60
12	9.33	6.93	5.95	5.41	5.06	4.82	4.64	4.50	4.39	4.30	4.16	4.01	3.86	3.78	3.70	3.62	3.54	3.45	3.36	3.36
13	9.07	6.70	5.74	5.21	4.86	4.62	4.44	4.30	4.19	4.10	3.96	3.82	3.66	3.59	3.51	3.43	3.34	3.25	3.17	3.17
14	8.86	6.51	5.56	5.04	4.69	4.46	4.28	4.14	4.03	3.94	3.80	3.66	3.51	3.43	3.35	3.27	3.18	3.09	3.00	3.00
15	8.68	6.36	5.42	4.89	4.56	4.32	4.14	4.00	3.89	3.80	3.67	3.52	3.37	3.29	3.21	3.13	3.05	2.96	2.87	2.87
16	8.55	6.23	5.29	4.77	4.44	4.20	4.03	3.89	3.78	3.69	3.55	3.41	3.26	3.18	3.10	3.02	2.93	2.84	2.75	2.75
17	8.40	6.11	5.19	4.67	4.34	4.10	3.93	3.79	3.68	3.59	3.46	3.31	3.16	3.08	3.00	2.92	2.83	2.75	2.66	2.66
18	8.29	6.01	5.09	4.58	4.25	4.01	3.84	3.71	3.60	3.51	3.37	3.23	3.08	3.00	2.92	2.84	2.75	2.66	2.57	2.57
19	8.18	5.93	5.01	4.50	4.17	3.94	3.77	3.63	3.52	3.43	3.30	3.15	3.00	2.92	2.84	2.76	2.67	2.58	2.49	2.49
20	8.10	5.85	4.94	4.43	4.10	3.87	3.70	3.56	3.46	3.37	3.23	3.09	2.94	2.86	2.78	2.69	2.61	2.52	2.42	2.42
21	8.02	5.78	4.87	4.37	4.04	3.81	3.64	3.51	3.40	3.31	3.17	3.03	2.88	2.80	2.72	2.64	2.55	2.46	2.36	2.36
22	7.95	5.72	4.82	4.31	3.99	3.76	3.59	3.45	3.35	3.26	3.12	2.98	2.83	2.75	2.67	2.58	2.50	2.40	2.31	2.31
23	7.88	5.66	4.76	4.26	3.94	3.71	3.54	3.41	3.30	3.21	3.07	2.93	2.78	2.70	2.62	2.54	2.45	2.35	2.26	2.26
24	7.82	5.61	4.72	4.22	3.90	3.67	3.50	3.36	3.26	3.17	3.03	2.89	2.74	2.66	2.58	2.49	2.40	2.31	2.21	2.21
25	7.77	5.57	4.68	4.18	3.85	3.63	3.46	3.32	3.22	3.13	2.99	2.85	2.70	2.62	2.54	2.45	2.36	2.27	2.17	2.17
26	7.72	5.53	4.64	4.14	3.82	3.59	3.42	3.29	3.18	3.09	2.96	2.81	2.66	2.58	2.50	2.42	2.33	2.23	2.13	2.13
27	7.68	5.49	4.60	4.11	3.78	3.56	3.39	3.26	3.15	3.06	2.93	2.78	2.63	2.55	2.47	2.38	2.29	2.20	2.10	2.10
28	7.64	5.45	4.57	4.07	3.75	3.53	3.36	3.23	3.12	3.03	2.90	2.75	2.60	2.52	2.44	2.35	2.26	2.17	2.06	2.06
29	7.60	5.42	4.54	4.04	3.73	3.50	3.33	3.20	3.09	3.00	2.87	2.73	2.57	2.49	2.41	2.33	2.23	2.14	2.03	2.03
30	7.56	5.39	4.51	4.02	3.70	3.47	3.30	3.17	3.07	2.98	2.84	2.70	2.55	2.47	2.39	2.30	2.21	2.11	2.01	2.01
35	7.42	5.27	4.40	3.91	3.59	3.37	3.20	3.07	2.96	2.88	2.74	2.60	2.44	2.36	2.28	2.19	2.10	2.00	1.89	1.89
40	7.31	5.18	4.31	3.83	3.51	3.29	3.12	2.99	2.89	2.80	2.66	2.52	2.37	2.29	2.20	2.11	2.02	1.92	1.80	1.80
45	7.23	5.11	4.25	3.77	3.45	3.23	3.07	2.94	2.83	2.74	2.61	2.46	2.31	2.23	2.14	2.05	1.96	1.85	1.74	1.74
50	7.17	5.06	4.20	3.72	3.41	3.19	3.02	2.89	2.78	2.70	2.56	2.42	2.27	2.18	2.10	2.01	1.91	1.80	1.68	1.68
55	7.12	5.01	4.16	3.68	3.37	3.15	2.98	2.85	2.75	2.66	2.53	2.38	2.23	2.15	2.06	1.97	1.87	1.76	1.64	1.64
60	7.08	4.98	4.13	3.65	3.34	3.12	2.95	2.82	2.72	2.63	2.50	2.35	2.20	2.12	2.03	1.94	1.84	1.73	1.60	1.60
70	7.01	4.92	4.07	3.60	3.29	3.07	2.91	2.78	2.67	2.59	2.45	2.31	2.15	2.07	1.98	1.89	1.78	1.67	1.54	1.54
80	6.96	4.88	4.04	3.56	3.26	3.04	2.87	2.74	2.64	2.55	2.42	2.27	2.12	2.03	1.94	1.85	1.75	1.63	1.49	1.49
90	6.93	4.85	4.01	3.53	3.23	3.01	2.84	2.72	2.61	2.52	2.39	2.24	2.09	2.00	1.92	1.82	1.72	1.60	1.46	1.46
100	6.90	4.82	3.98	3.51	3.21	2.99	2.82	2.69	2.59	2.50	2.37	2.22	2.07	1.98	1.89	1.80	1.69	1.57	1.43	1.43
110	6.87	4.80	3.96	3.49	3.19	2.97	2.81	2.68	2.57	2.49	2.35	2.21	2.05	1.96	1.88	1.78	1.67	1.55	1.40	1.40
120	6.85	4.79	3.95	3.48	3.17	2.96	2.79	2.66	2.56	2.47	2.34	2.19	2.03	1.95	1.86	1.76	1.66	1.53	1.38	1.38
∞	6.83	4.61	3.78	3.32	3.02	2.80	2.64	2.51	2.41	2.32	2.18	2.04	1.88	1.79	1.70	1.59	1.47	1.32	1.00	1.00